FINAL REPORT

Risk Evaluation of Potential Environmental Hazards From Low Frequency Electromagnetic Field Exposure Using Sensitive *in vitro* Methods

A project funded by the European Union
under the programme
Quality of Life and Management of Living Resources
Key Action 4 "Environment and Health"
Contract: QLK4-CT-1999-01574
Start date: 01 February 2000
End date: 31 May 2004
Acronym: REFLEX

Table of contents

FOREWORD 1

LIST OF PARTICIPANTS 5

1.0 INTRODUCTION 7

2.0 MATERIAL AND METHODS 9

2.1 Exposure setups (Participant 10) 9
2.1.1 ELF-EMF exposure setup 9
2.1.2 RF-EMF exposure setup 10

2.2 Experiments with human fibroblasts, lymphocytes, monocytes, melanocytes and muscle cells and with granulosa cells of rats (Participant 3) 12
2.2.1 ELF and RF-EMF exposure setups 12
2.2.2 Cell culture and exposure conditions 12
2.2.3 Comet assay 13
2.2.4 Micronucleus assay 13
2.2.5 Chromosomal aberrations 13
2.2.6 Fluorescence in situ hybridisation (FISH) 14
2.2.7 Changes in mitochondrial membrane potential (JC-1 staining) 14
2.2.8 Statistical analysis 15

2.3 Experiments with human HL-60 cells (Participant 2) 15
2.3.1 RF-EMF exposure setup 15
2.3.2 Cell culture and exposure conditions 15
2.3.3 in vitro genotoxicity tests 16
2.3.4 in vitro cytotoxicity testing 17
2.3.5 Preparation of nuclei suspensions from cells for flow cytometry analysis 17
2.3.6 Flow cytometric exclusion of apoptosis via Annexin V assay and TUNEL assay 18
2.3.7 Reactive oxygen species (ROS) and antioxidant enzyme activity 18
2.3.8 Analysis of cellular growth behaviour 20
2.3.9 Statistics 20
2.3.10 Proteomics 20
2.3.11 Gene expression profiling 21

2.4. Experiments with the human neuroblastoma cell line NB69 (Participant 5) 21
2.4.1 ELF-EMF exposure setup 21
2.4.2 RF-EMF exposure setup 22
2.4.3 Cell culture and EMF-Exposure 22
2.4.4 Immunocytochemical characterisation of NB69 Cells 23
2.4.5 Immunocytochemical characterisation of neural stem cells (NSC) 24
2.4.6 Immunocytochemical staining for the Cell Nuclear Antigen (PCNA). 24
2.4.7 5-bromo-2'-deoxyuridine (BrdU) labelling for identification of cells synthesising DNA. 24

2.4.8 Flow cytometry assay 24
2.4.9 Apoptosis assay 24
2.4.10 Immunocytochemical staining for the expression p-CREB 25
2.4.11 Indirect immunocytochemistry 25
2.4.12 Hybridisation histochemistry 26
2.4.13 Nucleic acid probes 26
2.4.14 Analysis of inmunocytochemical data 26

2.5 Experiments with human lymphocytes and thymocytes and embryonic stem cells of mice during cardiac differentiation (Participant 8) 26
2.5.1 ELF-EMF exposure setup 26
2.5.2 RF-EMF exposure setup 27
2.5.3 Cell proliferation by 3H-TdR incorporation test 27
2.5.4 Cell proliferation by flow cytometry 27
2.5.5 Cell cycle analysis by flow cytometry 27
2.5.6 Expression of membrane receptors on T lymphocytes by flow cytometry 28
2.5.7 Spontaneous and induced apoptosis by flow cytometry 28
2.5.8 MMP modifications in induced and spontaneous apoptosis 28
2.5.9 Cytokine production by ELISA 29
2.5.10 Hsp70 levels in induced and spontaneous apoptosis by flow cytometry 29
2.5.11 Thymocyte development and apoptosis by HTOC and flow cytometry 29
2.5.12 T lymphocyte gene expression by microarray technology 30
2.5.13 Cell culture of embryonic stem cells and EMF-Exposure 30
2.5.14 Analysis of mRNA expression 30
2.5.15 Transcriptional analysis in isolated nuclei 30

2.6 Experiments with brain cells of different origin and human monocytes and endothelial cells (Participant 9) 31
2.6.1 Exposure setup and exposure conditions 31
2.6.2 Cell culture and RF-EMF exposure 32
2.6.3 Chemicals and other treatments 34
2.6.4 Detection of apoptosis 34
2.6.5 Western Blot analysis 35
2.6.6 Griess reaction 35
2.6.7 Hsp immunolabelling and image analysis 35
2.6.8 RNA extraction and cDNA array hybridisation 35

2.7 Experiments with embryonic stem cells of mice (Participant 4) 36
2.7.1 Exposure setups 36
2.7.2 Cell culture and EMF exposure 36
2.7.3 Detection of mRNA levels by semi-quantitative RT-PCR analysis 38
2.7.4 Detection of mRNA levels by quantitative RT-PCR (Q-RT-PCR) 39
2.7.5 Single cell gel electrophoresis (Comet assay) 39
2.7.6 Analysis of cardiac differentiation 40
2.7.7 Flow cytometric analysis of cell cycle phases 40

2.8 Experiments with the human neuroblastoma cell line SY5Y (Participant 11) 40
2.8.1 ELF-EMF -exposure setup 40
2.8.2 Cell culture and exposure conditions 41
2.8.3 RNA preparation and Northern blot analysis 41
2.8.4 Radioligand assay with 125I-a Bungarotoxin and 3H-Epibatidine 41

2.8.5 Protein preparation and Western blot analysis 42

2.9 Experiments with Xenopus laevis oocytes, granulosa cells of rats, HeLa cells, Chinese Hamster Ovary (CHO) cells and human fibroblasts (Participant 7) 42
2.9.1 ELF-EMF-exposure setup 42
2.9.2 ELF-EMF exposure, expression in Xenopus oocytes and RNA preparation of rCx46 42
2.9.3 Electrophysiological recordings of single and paired oocytes 43
2.9.4 Vvoltage-jump current-relaxation and membrane conductance of hemi-channels 43
2.9.5 Cell cultures 44
2.9.6 Measurement of [Ca2+]I 44
2.9.7 Comet assay 44
2.9.8 Measurement of cell volume regulation 44

2.10 Experiments with the human endothelial cell lines EA.hy926 and EA.hy926v1 (Participant 6) 45
2.10.1 RF-EMF 900 MHz GSM signal exposure system dosimetry 45
2.10.2 Cell cultures and exposure 46
2.10.3 ^{32}P-othophosphate metabolic labelling 46
2.10.4 2D-electrophoresis - for protein phosporylation studies 46
2.10.5 ^{32}P-autoradiography 47
2.10.6 2D-electrophoresis - protein expression screening 47
2.10.7 Western blotting 47
2.10.8 Immunoprecipitation 48
2.10.9 cDNA Expression Arrays 48
2.10.10 Cell cycle analysis 48
2.10.11 Caspase-3 activity 49
2.10.12 Immunhistochemistry 49
2.10.13 Image analysis 49
2.10.14 cICAT method 49

2.11 Effects of ELF-EMF and RF-EMF on gene expression in human cells analysed with the cDNA array (Participant 12) 50
2.11.1 ELF-EMF and RF-EMF exposure setups 50
2.11.2 Cell cultures and RNA isolation 50
2.11.3 RZPD cDNA arrays 50
2.11.4 Hybridisation of global cDNA arrays and image analysis 51
2.11.5 Pre-processing (data cleaning) and Modified SAM method (and Selective SAM method) 51
2.11.6 Biostatistics (Dr. Daniel Remondini, Participant 8) 52
2.11.7 Data mining 53

3.0 RESULTS 55

3.1 Results in ELF-EMF research 55

3.1.1 Genotoxic effects 55
3.1.1.1 Human fibroblasts, lymphocytes, monocytes, melanocytes and muscle cells and granulosa cells of rats (Participant 3) 55
Intermittent ELF-EMF exposure, but not continuous ELF-EMF exposure induced DNA strand breaks in human fibroblasts. 55

ELF-EMF 50 Hz sinus generated a higher rate of DNA strand breaks in human fibroblasts than ELF-EMF powerline. *57*
Genotoxic effects were frequency dependent. *58*
Increase in DNA strand breaks in human fibroblasts after ELF-EMF exposure was dependent on exposure time. *58*
Increase in DNA strand breaks in human fibroblasts after ELF-EMF exposure was dependent on the age of the donors. *59*
Increase in DNA strand breaks in human fibroblasts after ELF-EMF exposure was accompanied by a rise in micronuclei frequencies. *60*
ELF-EMF exposure did not diminish the number of fibroblasts in culture. *60*
ELF-EMF exposure induced DNA strand breaks in human fibroblasts in a dose dependent way. *61*
DNA strand breaks in human fibroblasts after ELF-EMF exposure were rapidly repaired. *62*
DNA repair deficient cells react differently to ELF-EMF exposure. *63*
Generation of DNA strand breaks through ELF/EMF was cell type specific. *63*
Generation of DNA strand breaks in human fibroblasts through ELF-EMF and their repair were modified by UVC or heat stress. *64*
ELF-EMF generated chromosomal aberrations in human fibroblasts. *67*
ELF-EMF did not alter the mitochondrial membrane potential in human fibroblasts. *67*
3.1.1.2 Granulosa cells of rats, Chinese hamster ovary cells (CHO) and HeLa cells (Participant 7) 67
ELF-EMF exposure caused a significant increase of DNA strand breaks in cultured rat granulosa cells, CHO cells and HeLa cells. *67*
3.1.1.3 Embryonic stem cells (ES) of mice (Participant 4) 69
Lack of effects on single and double strand break induction 0, 18, 24 and 48 hours after completion of a 6 or 48 hours ELF-EMF exposure. *69*
3.1.1.4 Summary (Participant 1) 69

3.1.2 Cell proliferation and differentiation **70**
3.1.2.1 Human neuroblastoma cell line NB69 (Participant 5) 70
ELF-EMF promoted the growth rate of NB69 neuroblastoma cells. *70*
A growth-promoting effect of ELF-EMF in NB69 neuroblastoma cells was not observed after an extended exposure period. *71*
ELF-EMF did not counteract the retinoic acid-induced inhibition of cell proliferation in NB69 neuroblastoma cells. *71*
ELF-MF enhanced the cellular proliferation rate NB69 neuroblastoma cells as revealed through analysis of cell proliferation markers (PCNA). *72*
ELF-EMF increased the DNA synthesis in NB69 neuroblastoma cells. *73*
ELF-EMF affected the cell cycle in NB69 neuroblastoma cells. *74*
ELF-EMF diminished the spontaneous apoptosis in NB69 neuroblastoma cells. *74*
ELF-EMF altered the activation of the phosphorylated cyclic adenosine monophosphate response-element binding protein (p-CREB). *75*
3.1.2.2 Embryonic stem cells of mice during cardiac differentiation (Participant 8) 76
ELF-EMF accelerated the cardiac differentiation of embryonic stem cells through enhanced expression of cardiac genes. *76*
3.1.2.3 Human lymphocytes (Participant 8) 76
ELF-EMF exposure did not have any influence on proliferation, cell cycle and functionality of human lymphocytes. *76*
3.1.2.4 Embryonic stem cells of mice (Participant 4) 76
ELF-EMF did not have any influence on the growth and neuronal differentiation of embryonic stem cells of mice. *76*
3.1.2.5 Summary (Participant 1) 76

3.1.3 Apoptosis **77**
3.1.3.1 Embryonic stem cells of mice (Participant 4) 77
ELF-EMF at a flux density of 2 mT up-regulated the transcript levels of the anti-apoptotic gene bcl2 and the growth arrest and DNA damage inducible gene GADD45 and down-regulated bax in ES cell-derived neural progenitor cells. This may indirectly influence the apoptotic process in neural progenitor cells. *77*
3.1.3.2 Neuroblastoma cell line NB69 (Participant 5) 77
ELF-EMF at a flux density of 100 µT inhibited the spontaneous apoptosis in NB69 neuroblastoma cells. *77*
3.1.3.3 Human fibroblasts (Participant 3) 77
No differences in cell count between ELF-EMF exposed and sham exposed human fibroblasts at any exposure duration could be detected. Therefore a possible elimination of cells by apoptosis and cell death can probably be ruled out. *77*
3.1.3.4 Summary (Participant 1) 77

3.1.4 Gene and protein expression **77**
3.1.4.1 Embryonic stem cells of mice (Participant 4) 77
ELF-MF exposure resulted in up-regulation of egr-1, c-jun and p21 transcript levels in p53-deficient, but not in wild type ES cells. *77*
ELF-MF exposure of p53-deficient cells induced only short-term and transient effects on gene expression levels. *78*
ELF-MF effects on transcript levels of regulatory genes in p53-deficient cells were dependent on intermittence cycles (on/ off cycle duration). *79*
ELF-EMF exposure up-regulated the transcript levels of bcl-2, the growth arrest and DNA damage inducible gene (GADD45) and down-regulates bax in ES cell-derived neural progenitor cells. *79*
3.1.4.2 Human neuroblastoma cell line SY5Y (Participant 11) 82
ELF-EMF did not affect the expression of nicotinic acetylcholine receptors (nAchRs) which represent the neuronal nicotinic system in human neuroblastoma cells. *82*
ELF-EMF did not affect the expression of markers of the cathecolaminergic system in neuroblastoma cells. *86*
3.1.4.3 Embryonic stem cells of mice during cardiac differentiation (Participant 8) 88
ELF-EMF affected the expression of cardiogenic genes in murine embryonic stem cells (GTR1). *88*
Exposure of GTR1 ES cells to ELF-EMF after LIF removal and throughout 4 days of puromycin selection for an overall period of 10 days from LIF withdrawal was able to increase the yield of ES-derived cardiomyocytes: the number of beating colonies reached 170.44 ± 28.0 % of the control value, estimated in cardiomyocytes selected from untreated cells (mean ± SEM of 4 separate experiments). *91*
3.1.4.4 Membrane currents of oocytes of Xenopus laevis expressing rCx46 (Participant 7) 92
ELF-EMF did not significantly affect the leak-current of oocytes of Xenopus laevis expressing hemi-channels of rCx46. *92*
No significant influence of ELF-EMF on the number of expressed and conducting hemi-channels composed of rCx46 in oocytes. *93*
No significant influence of ELF-EMF on the voltage-dependent gating properties of rCx46 expressing oocytes *93*
No significant influence of ELF-EMF on the reversal potential of rCx46-mediated membrane current in oocytes. *96*
A slight but not significant influence of ELF-EMF on the gating properties of hemi-channels expressed in Xenopus oocytes dependent on the external calcium concentration was observed. *97*
ELF-EMF did not significantly affect the results of electrophysiological recordings of paired Xenopus oocytes. *98*

No significant influence of ELF-EMF on gap junctional coupling of rat granulosa cells was observed. *99*
An effect of ELF-EMF on cytoplasmic free calcium of cultured human fibroblasts and granulosa cells of rats was not observed. *100*
The volume regulatory response of granulosa cells appeared not to be influenced by ELF-EMF. *102*
3.1.4.5 Whole-genome analysis of various cell lines exposed to ELF-EMF (Participant 12) 102
3.1.4.6 Summary (Participant 1) 106

3.2 Results in RF-EMF research **107**

3.2.1 Genotoxic effects **107**
3.2.1.1 Human HL-60 cell line (Participant 2) 107
A. Direct genotoxicity 107
RF-EMF increased the micronucleus frequency and the number in DNA strand breaks in HL-60 cells dependent on the energy of radiation as determined by the cytokinesis-block in vitro micronucleus assay and the Comet assay. *107*
RF-EMF increased the micronucleus frequency and the number of DNA strand breaks in HL-60 cells dependent on the exposure time as determined by the cytokinesis-block in vitro micronucleus assay and the Comet assay. *110*
The effects of RF-EMF on genomic integrity of HL-60 cells were exposure-signal-dependent as determined by the cytokinesis-block in vitro micronucleus assay and the Comet assay. *111*
As shown by flow cytometric analysis RF-EMF increased the micronuclei frequency, but did not affect cell cycle. *113*
RF-EMF did not affect apoptosis as demonstrated by the Annexin V and TUNEL assay. *115*
RF-EMF did not exert a cytotoxic effect on HL-60 cells. *117*
B. Indirect genotoxicity (by reactive oxygen species) 119
RF-EMF induced formation of reactive oxygen species as shown by flow cytometric detection of oxyDNA and rhodamine fluorescence. *119*
RF-EMF did not affect antioxidant enzyme activities of HL-60 cells (SOD and GPx activity). *123*
The generation of genotoxic effects through RF-EMF was inhibited by ascorbic acid. *124*
3.2.1.2 Human fibroblasts and granulosa cells of rats (Participant 3) 125
RF-EMF generated DNA strand breaks in human fibroblasts and in granulosa cells of rats. *125*
RF-EMF generated chromosomal aberrations in human fibroblasts. *128*
RF-EMF induced micronuclei in human fibroblasts. *128*
Results on the influence of RF-EMF on the mitochondrial membrane potential were inconsistent. *129*
3.2.1.3 Mouse embryonic stem cells (Participant 4) 129
RF-EMF affected double-strand DNA break induction in ES cell derived neural progenitors immediately after exposure. *129*
3.2.1.4 Summary (Participant 1) 129

3.2.2 Cell proliferation and cell differentiation **130**
3.2.2.1 Human neuroblastoma cell line NB69 and neural stem cells (NSC) (Participant 5) 130
RF-EMF did not affect growth or viability of NB69 neuroblastoma cells and neural stem cells (NSC). *130*
RF-EMF may affect the expression of FGF receptors in NB69 human neuroblastoma cells and in neural stem, potentially influencing cellular differentiation. *131*
RF-EMF affected the differentiation of neural stem cells (NSC), but not of neuroblastoma cells (NB69). *131*
3.2.2.2 Human lymphocytes and thymocytes (Participant 8) 133

RF-EMF did not affect proliferation, cell cycle and activation of human lymphocytes. *133*
RF-EMF (DTX) may inhibit the production of IL-1beta in human lymphocytes, but did not affect the production of IL 6. *134*
RF-EMF did not affect thymocyte differentiation. *135*
3.2.2.3 Human promyelocytic cell line HL-60 (Participant 2) 135
RF-EMF did not affect the cell cycle of HL-60 cells as shown by flow cytometric analysis. *135*
RF-EMF did not affect the growth behaviour of HL-60 cells with respect to growth velocity and DNA synthesis. *135*
3.2.2.4 Mouse embryonic stem cells (Participant 4) 137
RF-EMF did not induce cardiac differentiation of R1 ES cells and cardiac differentiation and proliferation of P19 EC cells, but may affect the bcl-2 mediated apoptotic pathway in ES-cell derived neural progenitors and neuronal differentiation by inhibiting nurr-1 and TH transcription. *137*
3.2.2.5 Summary (Participant 1) 137

3.2.3 Apoptosis **137**
3.2.3.1 Brain cells of different origin and human monocytes (Participant 9) 137
RF-EMF did not affect apoptosis in neuronal cells. *137*
RF-EMF did not affect apoptosis in astrocytic cells. *139*
RF-EMF did not influence apoptosis in immune cells. *140*
RF-EMF did not influence chemically-induced apoptosis in immune cells. *142*
3.2.3.2 Human lymphocytes (Participant 8) 142
RF-EMF did not affect apoptosis in human lymphocytes. *142*
RF-EMF did not increase the Hsp70 level in human lymphocytes after induction of apoptosis. *142*
RF-EMF did not affect apoptosis in thymocytes. *143*
3.2.3.3 Human promyelocytic cell line HL-60 (Participant 2) 143
RF-EMF did not affect apoptosis in HL-60 cells as shown by flow cytometric analysis and the Annexin V and TUNEL assay. *143*
3.2.3.4 Embryonic stem cells of mice (Participant 4) 143
RF-EMF exposure may influence the bcl-2 mediated apoptotic pathway in ES-cell derived neural progenitors. *143*
3.2.3.5 Human endothelian cell lines (Participant 6) 143
The RF-EMF-induced enhancement of hsp27 phosphorylation as well as the concomitantly RF-EMF-induced down-regulation of proteins of Fas/TNFα suggest that the anti-apoptotic pathway in RF-EMF exposed cell systems may be modified. *143*
3.2.3.6 Summary (Participant 1) 143

3.2.4 Gene and protein expression **144**
3.2.4.1 Mouse embryonic stem cells (Participant 4) 144
Loss of p53 function rendered pluripotent ES cells sensitive to RF-EMF after prolonged exposure. *144*
RF-EMF did not influence cardiac differentiation and gene expression levels in R1 ES cells. *145*
RF-EMF did not induce cardiac differentiation and gene expression and the proliferation of P19 EC cells. *145*
RF-EMF exposure may affect the bcl-2 mediated apoptotic pathway in ES-cell derived neural progenitors and neuronal differentiation by inhibiting nurr-1 and TH transcription. *146*
3.2.4.2 Human neuroblastoma cell line NB69 and neural stem cells (NSC) (Participant 5) 148
RF-EMF (GSM-CW and GSM-Basic) interfered with the expression of FGF receptors in NB69 human neuroblastoma cells. *148*
RF-EMF affected the expression of FGF receptors in neural stem cells (NSC). *150*

RF-EMF did not affect gene expression of FGF Receptor-1 in NB69 neuroblastoma cells and in neural stem cells (NSC) *151*
3.2.4.3 Human promyelocytic cell line HL-60 (Participant 2) 152
RF-EMF exposure reproducibly up- and down-regulated protein expression in HL-60 cells (41 proteins showed to be up-, 1 protein to be down-regulated and 14 proteins appeared to be de-novo expressed). *152*
3.2.4.4 Human lymphocytes (Participant 8) 158
RF-EMF did not affect gene expression in human lymphocytes. *158*
3.2.4.5 Brain cells of different origin (Participant 9) 159
RF-EMF exposure did not affect expression and activity of the inducible nitric oxide synthase (iNOS or NOS2) in nerve cells. *159*
RF-EMF (GSM-900 signals) did not affect heat shock protein expression in nerve cells. *161*
GSM-900 microwave exposure did not affect hsp27 expression in human endothelial cell line EA.hy926. *162*
No conclusive data was obtained on the effect of RF-EMF exposure on Hsp27 expression in rat brain. *163*
RF-EMF (GSM-900) exposure weakly affected gene expression in immune cells. *164*
3.2.4.6 Human endothelial cell lines EA.hy926 and EA.hy926v1 (Participant 6) 164
A. The 5-step feasibility study 165
B. Genotype-dependent cell response to 900 MHz GSM radiation 171
C. Comparison of the effect of CW and modulated RF-EMF on protein expression 177
3.2.4.7 Whole-genome analysis of various cell lines exposed to RF-EMF (Participant 12) 179
3.2.4.8 Summary (Participant 1) 182

4.0 DISCUSSION **183**

4.1 Results obtained after ELF-EMF exposure **183**

4.1.1 Genotoxic effects **183**
4.1.1.1 Human fibroblasts, lymphocytes, monocytes, melanocytes and muscle cells and granulosa cells of rats (Participant 3) 183
Intermittent ELF-EMF exposure generated DNA strand breaks in various but not all cell lines. *183*
Genotoxic effects of ELF-EMF varied with exposure time. *183*
ELF-EMF produced DNA strand breaks in human fibroblasts in a dose dependent way. *184*
Generation of DNA strand breaks in human fibroblasts through ELF-EMF was related to the age of the donors. *184*
Effects of ELF-EMF were cell type specific. *184*
Generation of DNA strand breaks in human fibroblasts through ELF-EMF and their repair were modified by UVC or heat stress. *185*
Generation of DNA strand breaks in human fibroblasts through ELF-EMF was dependent on the genetic background of cells. *185*
Generation of DNA strand breaks in human fibroblasts by ELF-EMF was dependent on the frequency of ELF-EMF. *185*
ELF-EMF generated chromosomal aberrations in human fibroblasts. *185*
ELF-EMF did not influence the mitochondrial membrane potential. *186*
4.1.1.2 Human fibroblasts and granulosa cells of rat (Participant 7) 186
The genotoxic effects induced by ELF-EMF are not reflected by physiological functions like volume regulation and free cytoplasmic Ca2+-concentration. *186*
4.1.1.3 Mouse embryonic stem cells (Participant 4) 187

ELF-EMF did not induce the formation of DNA strand breaks in embryonic stem cells. *187*
4.1.1.4 Summary (Participant 1) 188

4.1.2 Cell proliferation and differentiation **189**
4.1.2.1 Human neuroblastoma cells (NB69 cell line) (Participant 5) 189
ELF-EMF enhanced proliferation and reduces spontaneous apoptosis of NB69 neuroblastoma cells. *189*
The mechanism of interaction between ELF-EMF and NB69 neuroblastoma cells is not known yet. *189*
4.1.2.2 Mouse embryonic stem cells (Participant 4) 190
ELF-EMF did not exert any influence on neuronal differentiation of embryonic stem cell. *190*
4.1.2.3 Human lymphocytes and embryonic stem cells (Participant 8) 190
ELF-EMF did not affect proliferation, cell cycle and activation of lymphocytes. *190*
ELF-EMF activated the expression of cardiac genes in embryonic stem cells thus enhancing their cardiac differentiation. *190*
4.1.2.4 Summary (Participant 1) 190

4.1.3 Apoptosis **191**
4.1.3.1 Mouse embryonic stem cells (Participant 4) 191
ELF-EMF altered the expression of bcl-2, bax and GADD45 gene in ES-cell derived neural progenitor cells. *191*
4.1.3.2 Neuroblastoma cells (NB69 cell line) (Participant 5) 191
ELF-EMF inhibited spontaneous apoptosis in neuroblastoma cells. *191*
4.1.3.3 Human fibroblasts (Participant 3) 193
ELF-EMF may not affect the apoptotic process in human fibroblasts after intermittent exposure for 24 hours at a flux density of 1 mT. *193*
4.1.3.4 Summary (Participant 1) 193

4.1.4 Gene and protein expression **193**
4.1.4.1 Mouse embryonic stem cells (Participant 4) 193
Short-term high intensity exposure to ELF-EMF signals may cause a transient up-regulation of immediate early response and regulatory genes in p53-deficient ES cells. *193*
The nature of gene-expression responses to ELF-EMF was short-term only. *194*
There is some indication that threshold of field flux density exists for ELF-EMF biological effects. *194*
ELF-EMF effects in p53-deficient cells were dependent on intermittency cycles (on/off cycle duration). *194*
The mechanism of action induced by ELF-EMF exposure of living cells is not yet known. *194*
4.1.4.2 Neuroblastoma cells (SY5Y cell line) (Participant 11) 194
ELF-EMF did not affect the expression of neuronal genes such as nAchRs, DβH, Phox2a and Phox2b, either at mRNA or protein level. *195*
4.1.4.3 Embryonic stem cells of mice during cardiac differentiation (Participant 8) 196
ELF-EMF up-regulated the expression of cardiac specific genes thus promoting cardiogenesis. *196*
4.1.4.4 rCx46 in oocytes of Xenopus laevis (Participant 7) 196
4.1.4.5 Whole-genome analysis of various cell lines exposed to ELF-EMF (Participant 12) 197
4.1.4.6 Summary (Participant 1) 197

4.2 Results obtained after RF-EMF exposure **198**

4.2.1 Genotoxic effects **198**

4.2.1.1 Human promyelocytic cell line HL-60 (Participant 2) 198
RF-EMF exposure for different SAR and different exposure times (1800 MHz, continuous wave) led to the induction of single and double DNA strand breaks. *198*
RF-EMF exposure for different SAR and different exposure times (1800 MHz, continuous wave) led to an increase in micronuclei. *199*
RF-EMF-associated increase of DNA strand breaks and micronuclei (1800 MHz, 1.3 W/kg, 24h) in HL-60 cells was signal-independent. *199*
RF-EMF induced formation of reactive oxygen species as shown by flow cytometric detection of oxyDNA and rhodamine fluorescence. *199*
Co-administration of ascorbic acid, a free radical scavenger, inhibited the effects of RF-EMF on HL-60 cells and may, thus, decrease DNA damage without affecting cellular growth. *200*
4.2.1.2 Human fibroblasts and granulosa cells of rats (Participant 3) 200
RF-EMF generated DNA strand breaks in granulosa cells of rats and DNA strand breaks and chromosomal aberrations in human fibroblasts. *200*
4.2.1.3 Mouse embryonic stem (ES) cells (Participant 4) 201
RF-EMF exposure of ES-derived neural progenitor cells induced a low transient increase of double DNA strand breaks measured by the neutral Comet assay. *201*
4.2.1.4 Summary (Participant 1) 201

4.2.2 Cell proliferation and differentiation **202**
4.2.2.1 NB69 neuroblastoma cells and neural stem cells (NSC) (Participant 5) 202
RF-EFM did not affect cell growth of NB69 and neural stem cells. *202*
4.2.2.2 Human lymphocytes and thymocytes (Participant 8) 202
RF-EMF may not affect proliferation, cell cycle, apoptosis and activation of human lymphocytes and thymocytes. *202*
4.2.2.3 Human promyelocytic cell line HL-60 (Participant 2) 203
RF-EMF generated genotoxic effects in HL-60 cells within a narrow energy window without affecting cell proliferation, cell progression and apoptosis. *203*
4.2.2.4 Mouse embryonic stem (ES) cells (Participant 4) 203
RF-EMF exerted no influence on ES-derived cardiogenesis and did not affect DMSO-induced cardiac differentiation, proliferation and expression of regulatory genes in P19 EC cells. *203*
The differentiation process in cells is affected by RF-EMF exposure, when applied at the neural progenitor stage. *204*
4.2.2.5 Summary (Participant 1) 204

4.2.3 Apoptosis **205**
4.2.3.1 Brain cells of different origin and human monocytes (Participant 9) 205
There is no indication that apoptosis is affected in nerve and immune cells after exposure to GSM-like RF-EMF. *205*
4.2.3.2 Human lymphocytes (Participant 8) 206
RF-EMF may not affect apoptosis in human lymphocytes. *206*
4.2.3.3 Human promyelocytic cell line HL-60 (Participant 2) 206
4.2.3.4 Mouse embryonic stem (ES) cells (Participant 4) 207
RF-EMF affected the bcl-2 –mediated anti-apoptotic pathway in differentiating embryonic stem cells. *207*
4.2.3.5 Human the endothelial cell lines EA.hy926 and EA.hy926v1 (Participant 6) 207
RF-EMF may affect the hsp27 mediated anti-apoptotic pathway in human endothelial cells. *207*
4.2.3.6 Summary (Participant 1) 207

4.2.4 Gene and protein expression **208**
4.2.4.1 Mouse embryonic stem (ES) cells (Participant 4) 208

The genetic constitution of early differentiating embryonic stem cells may play a role on their responsiveness to differently modulated RF-EMF. *208*
The response of early differentiating cells to RF-EMF is dependent mainly on the carrier frequency of the modulation schemes. *208*
The exposure duration may also influence the biological responses to RF-EMF. *209*
4.2.4.2 NB69 neuroblastoma cells and neural stem cells (NSC) (Participant 5) 209
RF-EMF reduced the expression of the receptor FGFR1 of fibroblast growth factor (FGF) in the human neuroblastoma NB69 cell line and in neural stem cells from rat embryonic nucleus striatum. *209*
The changes in FGFR1 induced by RF-EMF is dependent mainly on the carrier frequency. *210*
4.2.4.3 Human promyelocytic cell line HL-60 (Participant 2) 210
RF-EMF modulates the gene and protein expression in HL-60 cells. *210*
4.2.4.4 Human lymphocytes (Participant 8) 210
RF-EMF did not affect gene expression in human lymphocytes. *210*
4.2.4.5 Brain cells of different origin, human immune cells and human endothelial cell lines (Participant 9) 211
There is no indication that expression and activity of the inducible Nitric Oxide Synthase (iNOS or NOS2) is affected in nerve cells after exposure to RF-EMF. *211*
There is no indication that expression of heat shock proteins is affected in nerve cells after exposure to RF-EMF. *211*
We failed to independently confirm that expression of heat shock proteins is affected in EA-hy926 cells after exposure to GSM-like RF-EMF. *211*
There is some indication that gene expression is affected in immune cells after exposure to RF-EMF. *212*
4.2.4.6 Human endothelial cell lines EA.hy926 and EA.hy926v1 (Participant 6) 212
RF-EMF induced cellular stress response. *212*
5-step feasibility study of applying proteomics/transcriptomics to mobile phone research. *214*
Use of HTST to determine genotype-dependent and modulation-dependent cellular responses. *215*
4.2.4.7 Effects of RF-EMF on gene expression in human cells analysed with the cDNA array (Participant 12) 215
4.2.4.8 Summary (Participant 1) 216

5.0 CONCLUSIONS **219**

5.1 Conclusions based on the findings obtained in ELF-EMF research **219**
5.1.1 Human fibroblasts, human lymphocytes, human monocytes, human melanocytes, human muscle cells and granulosa cells of rats (Participant 3) 219
5.1.2 Human neuroblastoma cell line NB69 and human hepatocarcinoma cell line HepG2 (Participant 5) 219
5.1.3 Human lymphocytes (Participant 8) 220
5.1.4 Mouse embryonic stem cells (Participant 4) 220
5.1.5 Experiments with embryonic stem cells of mice during cardiac differentiation (Participant 8) 220
5.1.6 Experiments with the human neuroblastoma cell line SY5Y (Participant 11) 220
5.1.7 Xenopus laevis oocytes, human fibroblasts and granulosa cells of rats (GFSHR-17 cell line) (Participant 7) 221
5.1.8 Effects of ELF-EMF on gene expression in human cells analysed with the cDNA array (Participant 12) 221
5.1.9 Summary (Participant 1) 222

5.2 Conclusions based on the findings obtained in RF-EMF research 222
5.2.1 Human promyelocytic cell line HL-60 (Participant 2) 222
5.2.2 Human fibroblasts and granulosa cells of rats (Participant 3) 223
5.2.3 Human lymphocytes and thymocytes (Participant 8) 224
5.2.4 Human neuroblastoma cell line NB69 and neural stem cells (Participant 5) 224
5.2.5 Brain cells of different origin and human monocytes (Participant 9) 224
5.2.6 Mouse embryonic stem cells (Participant 4) 224
5.2.7 Human the endothelial cell lines EA.hy926 and EA.hy926v1 (Participant 6) 225
5.2.8 Effects of RF-EMF on gene expression in human cells analysed with the cDNA array (Participant 12) 225
5.2.9 Summary (Participant 1) 226

6.0 EXPLOITATION AND DISSEMINATION OF RESULTS 227

6.1 Coordination (Participant 1) 227
6.2 Experiments with the human promyelocytic cell line HL-60 (Participant 2) 228
6.3 Experiments with human fibroblasts, human lymphocytes, human monocytes, human melanocytes, human muscle cells and granulosa cells of rats (Participant 3) 228
6.4 Embryonic stem cells (Participant 4) 230
6.5 Experiments with the human neuroblastoma cell line NB69 and neural stem cells (Participant 5) 230
6.6 Human the endothelial cell lines EA.hy926 and EA.hy926v1 (Participant 6) 231
6.7 rCx46 in oocytes of Xenopus laevis and human fibroblasts and granulosa cells of rats (Participant 7) 232
6.8 Experiments with human lymphocytes and thymocytes and with mice embryonic stem cells during cardiac differentiation (Participant 8) 233
6.9 Experiments with brain cells of different origin and human monocytes (Participant 9) 234
6.10 Provision of exposure setups and technical quality control (Participant 10) 235
6.11 Experiments with the human neuroblastoma cell line SY5Y (Participant 11) 236
6.12 Effects of EMF on gene expression in human cells analysed with the cDNA array (Participant 12) 237

7.0 POLICY RELATED BENEFITS 239

7.1 Studies on the human promyelocytic cell line HL-60 (Participant 2) 239
7.2 Studies on human fibroblasts, human lymphocytes, human monocytes, human melanocytes, human muscle cells and granulosa cells of rats (Participant3) 239
7.3 Studies on mouse embryonic stem cells (Participant 4) 239
7.4 Studies on the human neuroblastoma cell line NB69 and neural stem cells (Participant 5) 239
7.5 Studies on the human endothelial cell lines EA.hy926 and EA.hy926v1 (Participant 6) 240
7.6 Studies on rCx46 in oocytes of Xenopus laevis and human fibroblasts and granulosa cells of rats Participant 7) 240
7.7 Studies on embryonic stem cells during cardiac differentiation and human lymphocytes and thymocytes (Participant 8) 240
7.8 Studies on brain cells of different origin and human monocytes (Participant 9) 241
7.9 Provision of exposure set-ups and technical quality control (Participant 10) 241
7.10 Studies on the human neuroblastoma cell line SY5Y (Participant 11) 241
7.11 cDNA array analysis (Participant 12) 241

7.12 Summary (Participant 1) 241

8.0 REFERENCES **243**

ANNEX I

ANNEX II

FOREWORD

Prof. William Ross Adey, who made fundamental contributions to the emerging science of the biological effects of electromagnetic fields (EMFs), died on May 20, 2004, in Redlands, California, USA. He was scheduled to deliver his personal views of EMF research at a REFLEX workshop held in Bologna in October 2002. But by then he was already too frail to travel. Dr. Adey who was an informal advisor of the REFLEX consortium sent us his talk in written form. In memory of his achievements as a scientist and in recognition of his support of the REFLEX work, the consortium decided that his message would be an inspiration to all those scientists who are willing to accept the challenges posed by EMF research, and in addition, make a fitting introduction to the final report.

THE FUTURE OF FUNDAMENTAL RESEARCH IN A SOCIETY SEEKING CATEGORIC ANSWERS TO HEALTH RISKS OF NEW TECHNOLOGIES

The Challenge to Conventional Wisdom

The history of bioelectromagnetics epitomizes a range of problems that arise whenever a community of sciences is confronted with a frontier that delves deeply into the established orthodoxies of biology, the physical sciences and engineering. These conflicts have become even more sharply defined when emerging new knowledge in bioelectromagnetics research has challenged the conventional wisdom in each part of this trinity.

Thirty-five years ago, we, who first voiced our observations of physiological responses to a spectrum of environmental EMFs at levels below thresholds for significant tissue heating, were promptly challenged by acolytes of orthodoxies in the biological and physical sciences. At best, we were euphemistically described as “controversial,” a designation that persists to this day. A Yale physicist recently added the charming term “crackpot” to describe a highly qualified biophysicist investigator.

What is the basis of this deep thorn of discontent? Historically, excitation in biological systems has been modeled and tested in terms of equilibrium thermodynamics. In this classic tradition, it was assumed that the potential effectiveness of an exciting agent could be assessed by its ability to transfer energy to the receptor in excess of its random thermal atomic and molecular collisions. Thus, the physical expression kT, the union of the Boltzmann constant and temperature, has been regarded as an expression of an immutable threshold below which an exciting agent would not be physiologically effective. In like fashion from the quantum realm of the physicist, photon energies of low-frequency magnetic fields, now known to act as effective physiological stimuli, would also fall below this thermal barrier.

Here is one example: The human auditory threshold involves a hair cell vibration of 10-11 meters, or about the diameter of a single hydrogen atom. But, by an as-yet-unknown mechanism, the ear suppresses the vastly larger noise of its thermal atomic and molecular collisions, functioning as an almost “perfect” amplifier close to 0°K.

Clearly, we face a profound paradox, with answers to be sought in cooperative states and nonequilibrium thermodynamics, as first suggested in a biological context almost 60 years ago by Herbert Fröhlich.

The lesson is clear. The awesome complexity of biological organization demands our most careful consideration.

The Recent History of Technology Applications

We also find the heat of controversy in the recent history of technological applications in western societies. At no point in the last 20 years has public school education ensured that a majority of citizens has even a basic understanding of sophisticated communication devices and systems, such as telephones, radio and television. Similarly, automotive engineering remains a sea of vast ignorance for most users. Nor is such knowledge considered appropriate or necessary.

In summary, we have become superstitious users of an ever-growing range of technologies, but we are now unable to escape the web that they have woven around us.

Media reporters in general are no better informed. Lacking either responsibility or accountability, they have created feeding frenzies from the tiniest snippets of information gleaned from scientific meetings or from their own inaccurate interpretation of published research. In consequence, the public has turned with pleading voices to government legislatures and bureaucracies for guidance.

Public Concerns and the Evolving Pattern of Research Funding

We face the problem brought on by the blind leading the blind. Because of public pressure for rapid answers to very complex biological and physical issues, short-term research programs have been funded to answer specific questions about certain health risks.

Participating scientists have all too often accepted unrealistic expectations that, in a matter of a few years, they will provide answers to pivotal questions in cell and molecular biology that can only be achieved slowly, painstakingly and collaboratively over a decade or more.

Using EMFs as tools, we have launched our ship on a vast, uncharted ocean, seeking a new understanding of the very essence of living matter in physical processes at the atomic level. This is an awesome and humbling prospect, surely not to be ignored or forgotten in the pragmatic philosophies of most risk research.

In many countries, and particularly in the USA, the effects of such harassing and troublesome tactics on independent, careful fundamental research have been near tragic. Beguiled by health hazard research as the only source of funding, accomplished basic scientists have diverted from a completely new frontier in physical regulation of biological mechanisms at the atomic level. Not only have governments permitted corporate interests in the communications industry to fund this research, they have even permitted them to determine the research questions to be addressed and to select the institutions performing the research.

These policies overlook the immutable needs of the march of science. In their hasty rush to judgment, they have sought a scientific consensus where none can yet exist. Such a consensus will occur only after experimental convergence emerges from a spectrum of related but certainly not identical experiments.

Defining the Role of Epidemiology in Current Controversies

Much in the fashion of ancient Romans, standing four-square and reading the auguries of future events by noting flight patterns of passing birds, the modern-day epidemiologist has become the high priest in the search for correlates of disease processes with a constellation of environmental observables. It is rare for them to be competent in delving into questions of causality, particularly where no exposure metric has been established for a suspected environmental factor. Nevertheless, in courts of law, in legislatures, and among a concerned public, epidemiological opinions have become a gold standard, typically outranking evidence based on a balanced and often cautionary review of current medical science.

We should remind ourselves that their professional tool is biostatistics —they build endless Byzantine edifices of levels of statistical risk, with little or no commitment to the underlying science or medicine. Their mutual discussions have produced the technique of meta-analysis, the pooling of statistical analyses from a series of epidemiological studies. The method ignores the nuances of both experimental design and epidemiological findings in the separate studies, and blinds us to options for further research based on the possible uniqueness of these separate observations.

It appears reasonable that there should be no more large epidemiological studies on human EMF exposures until essential exposure metrics are established, based on mechanisms of field interactions in tissues.

Repairing the Body Politic of Science: Some Personal Reflections

The passage of time across the years has not diminished in any way the importance, even the urgency, that one feels towards the growing edifice of science. We must not fail to engender in younger minds a passionate curiosity and an imagination sufficient to kindle their commitment to all that is great and good in the scientific method.

As I reflect on major changes wrought in the U.S. national research scene over the past 40 years, I sense a deep and growing concern that research training and the culture of research accomplishment have stifled

the burning thorn of personal discontent that should be the creative option of all young minds entering on a research career.

Graduate students are assigned a project that is typically a segment of their advisor's grand vista. They may not deviate to ask creative “what if?” questions. They emerge from the chrysalis of their training, bearing a parchment for the professional market place, affirming proficiency in certain techniques, but in no way proclaiming the arrival of that precious citadel of a creative mind.

Please allow me to conclude with an urgent proposal that comes from my own research experience. Formal instruction in physics, theoretical and applied, has become the weakest link for those entering on a career in medical research. Bioelectromagnetics research has opened the door to a new understanding of the very essence of living matter in physical regulation at the atomic level, beyond the realm of chemical reactions in the exquisite fabric of biomolecules. Without versatility in biophysics that matches their typical knowledge in molecular biology and biochemistry, none of these students may cross this threshold to the cutting edge of in future medical research. Let us not see this opportunity lost prematurely through prostitution of mechanistic research in the market place of possible health risks.

Thank you for the great privilege of offering these personal reflections.

LIST OF PARTICIPANTS

1. VERUM - Stiftung für Verhalten und Umwelt, München, Germany
   (Scientific person in charge of the project: Prof. Franz Adlkofer)
2. Institut für Klinische Chemie, Universitätsklinikum Benjamin Franklin, Berlin, Germany
   (Scientific person in charge of the project: Prof. Rudolf Tauber)
3. Abteilung für Arbeitsmedizin, Universitätsklinik für Innere Medizin, Wien, Austria
   (Scientific person in charge of the project: Prof. Hugo W. Rüdiger)
4. Institut für Pflanzengenetik und Kulturpflanzenforschung, Gatersleben, Germany
   (Scientific person in charge of the project: Prof. Anna M. Wobus)
5. Insalud, Ramon y Cajal Hospital, Madrid, Spain
   (Scientific person in charge of the project: Dr. Angeles Trillo)
6. STUK - Radiation and Nuclear Safety Authority, Helsinki, Finland
   (Scientific person in charge of the project: Prof. Dariusz Leszczynski)
7. Institut für Biophysik, Universität Hannover, Germany
   (Scientific person in charge of the project: Prof. H. Albert Kolb)
8. Laboratoire PIOM, ENSCPB, Bordeaux, France
   (Scientific person in charge of the project: Dr. Isabelle Lagroye)
9. Universita degli Studi di Bologna, Italy
   (Scientific person in charge of the project: Prof. Fernando Bersani)
10. Institut für Integrierte Systeme, ETH Zentrum, Zürich, Switzerland
    (Scientific person in charge of the project: Prof. Niels Kuster)
11. Cattedra di Farmacologia, Universita degli Studi di Milano, Italy
    (Scientific person in charge of the project: Prof. Francesco Clementi)
12. Ressourcenzentrum für Genomforschung GmbH (RZPD), Heidelberg, Germany
    (Scientific person in charge of the project: Dr. Christian Maercker)

1.0 INTRODUCTION

Based on the state of knowledge acquired during the last 50 years of research on possible biological effects of electromagnetic fields (EMF), the majority of the scientific community is convinced that exposure to EMF below the existing security limits does not cause a risk to the health of the general public. However, this position is questioned by others, who are of the opinion, that the available research data are contradictory or inconsistent and therefore, unreliable. As a consequence, it is necessary that the methodology applied in EMF research to be considerably improved and complemented by the most recent molecular biological techniques. In the REFLEX project, biological effects of extremely low frequency electromagnetic fields (ELF-EMF) and radio frequency electromagnetic fields (RF-EMF) are studied using sophisticated and diverse research methodologies separately since it is assumed that the generation of effects, if verifiable at all, may be based on different mechanisms.

Many laboratory investigations have been performed to test the hypothesis that ELF-EMF exposure may constitute a risk to the health of people. This hypothesis is almost entirely based on epidemiological studies, some of which indicate that ELF-EMF may contribute to the development of leukaemia in children, and other cancers in adults chronically exposed in residential environments or occupational settings (NRPB 2001; California EMF Program 2002; IARC Monographs 2002). The existing uncertainty is a source of increasing concern for the public, the health authorities and also the industry. *In vitro* studies have shown that ELF-EMF induces significant biological alterations in a variety of cells and tissues. These changes concern the up-regulation of several early response genes, including c-myc (Jin et al. 2000), c-fos (Rao and Henderson 1996) and hsp70 mRNA (Goodman and Blank 1998), thus increasing the production of stress inducible heat shock proteins (Goodman and Henderson 1988; Tokalov and Gutzeit 2003). In spite of this, it is still an unsolved issue whether or not exposure to ELF-EMF may promote pathological processes such as carcinogenesis and if so, whether or not the field effects are exerted through mechanisms influencing the genome of cells, cell proliferation, differentiation or programmed cell death (apoptosis). Results from several studies have indicated that ELF-EMF does not exert any direct genotoxic effect, but may promote carcinogenesis indirectly by interfering with the signal transduction pathways of cells (Blackman et al. 1985; Liburdy et al.1993). Of course, the present uncertainty could considerably be diminished by increasing our knowledge on the parameters of the electromagnetic field which are critical for the generation of biological effects and of the biological systems which are crucial for the occurrence of pathological cellular events.

As with ELF-EMF, several epidemiological and animal studies also cast suspicion on RF signals to promote cancer and other diseases in chronically exposed individuals (Stewart Report 2000; Hardell et al. 2003). Because of its overwhelming presence in our society, the potential influence of RF-EMF exposure on the development of adverse health effects has become a major topic of interest for all concerned, including the government, the general public, and the industry. Putatively non-thermal, immediate and reversible responses have been described in the literature for several years (Roschke and Mann 1997; Wagner et al.1998; Borbely et al.1999; Preece et al. 1999; Koivisto et al. 2000; Huber et al. 2000; Krause et al. 2000). However, these effects, because of their unspecific nature have been regarded as indications of potential biological responses to electrical excitation, rather than harmful effects able to produce permanent damage to health. To date, several *in vitro* studies have been carried out to investigate the disease causing potential of RF radiation. While most of these studies using different cell systems, exposure set-ups and molecular-biological and toxicological methodologies did not show any biological effect, increasing numbers of studies have come up with contradicting results (Moulder et al. 1999; Vescovic et al. 2002).

As stated above, although investigations of possible biological effects of EMF have been conducted for decades, reliable answers are still missing. Extensive epidemiological and animal studies commonly expected to provide the answer as to whether or not EMF might be hazardous are in progress. However, this approach alone might not be able to provide certain evidence whether EMF can or cannot contribute to the pathogenesis of diseases such as cancer or neurodegenerative disorders. The low sensitivity of the epidemiological methodology in detecting low risk associations is probably insufficient to reliably identify any risk to health caused by EMF. Therefore, although epidemiological studies will be needed to ultimately validate the extent of any potential health hazard of EMF, such research must be supplemented and supported by data from animal and *in vitro* studies. Therefore, *in vitro* studies using the most modern molecular biological techniques such as. genomics and proteomics are urgently needed in order to create at least a hypothetical basis for the understanding of disease development through EMF-exposure. If it can be determined that such a basis exists, it becomes even more important, to search for marker

substances which are specific for EMF exposure. Such marker substances could considerably increase the accuracy of epidemiological studies, so that even a low health risk due to EMF exposure would not escape epidemiological detection.

The main goal of the REFLEX project is to investigate the effects of EMF on single cells *in vitro* at the molecular level below the energy density reflected by the present safety levels. Most, if not all chronic diseases, including cancer and neurodegenerative disorders, are of diverse and heterogeneous origins. This variability is to a great extent generated by a relatively small number of critical events, such as gene mutations, deregulated cell proliferation and suppressed or exaggerated programmed cell death (apoptosis). Gene mutations, cell proliferation and apoptosis are caused by or result in an altered gene and protein expression profiles. The convergence of these critical events is required for the development of all chronic diseases. The REFLEX project is, therefore, designed to answer the question whether or not any of these disease-causing critical events could occur in living cells after EMF exposure. Failure to observe the key critical events in living cells *in vitro* after EMF exposure would suggest that further research efforts in this field could be suspended and financial resources should be reallocated for the investigation of more important issues.

2.0 MATERIAL AND METHODS

2.1 Exposure setups (Participant 10)

In order to compare the results of investigations carried out in the different laboratories and to ensure the conclusiveness of the data obtained in the studies, it is of the utmost importance that the conditions of exposure to EMF be strictly controlled. It was the task of Participant 10 to evaluate and modify already existing setups, to develop new optimised exposure systems and to provide technical quality control during the entire period of exposure. The latter was realised by (1) the conduct of a thorough dosimetry including an analysis of possible artefacts, (2) the continuous monitoring of exposure and environmental parameters and (3) blinded exposure protocols. Details about this work can be found in the appendix.

2.1.1 ELF-EMF exposure setup

A novel ELF setup was developed, and four copies were installed in the laboratories of Participants 3, 4, 7 and 11. The setup consists of two four-coil systems, each of which is placed inside a µ-metal shielding box. The coils produce a linearly polarised B-field over the area of the Petri dishes with a B-field vector perpendicular to the dish plane. The shielded design of the chamber guarantees non-interference between the two units, such that they can be kept close to each other inside the same incubator in order to guarantee identical ambient conditions for the cell dishes. Two fans per coil system ensure fast atmospheric exchange between the chambers and incubator. The airflow temperature is monitored with accurate Pt100 probes fixed inside the exposure chamber.

The signal is generated by a computer-controlled arbitrary function generator. A custom-designed current source allows arbitrary field variations in the range from MHz to 1.5 kHz. The maximum achievable magnetic flux density for a sinusoidal with a frequency of less than 80 Hz is 3.6 mT RMS. Sinusoidal signals with a frequency range from 3 Hz up to 1000 Hz can be applied, controlled and monitored. A powerline signal was defined which represents a worst-case scenario with respect to spectral content and corresponds to the maximum accepted distortions for power systems by the International Electrotechnical Commission (IEC 1995) (Figure 1). In addition to these waveforms, arbitrary field on/off intermittently in the range from seconds to hours can be applied.

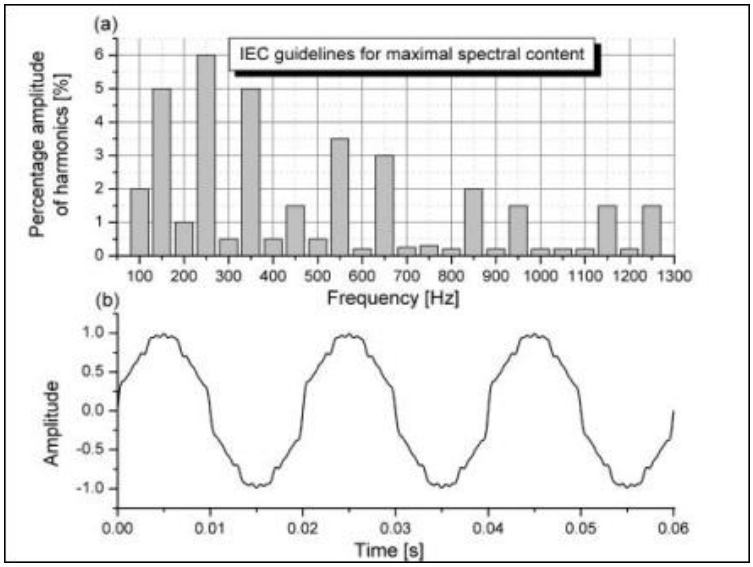

Figure 1. (a) Frequency composition of the powerline signal, corresponding to the maximum allowed spectral content according the IEC guidelines for low and medium voltage power networks (IEC 1995). Shown are the spectral amplitudes of the harmonics in relation to the main 50 Hz component. (b) The resulting powerline signal in the time domain.

The coil current and consequently the magnetic field is quasi-continuously (10s intervals) recorded and regulated using resistors providing low-temperature sensitivity. The currents in the bifilar coils can be randomly switched parallel for field exposure or nonparallel for sham control by the computer. This procedure is used to apply blind protocols and additionally to avoid temperature artefacts between exposed and control coils, since they are heated by the same current.

The evaluation and optimisation of the coil configuration was performed using numerical techniques (Mathematica V4.1) and experimental methods (3-axis Hall meter, FH49 Magnet Physik, Germany). A non-uniformity of less than 1% for the magnetic field over the exposure area of 16 cm x 16 cm x 23 cm is achieved. An uncertainty of 4.3% for the B-field assessment and a B-field variability of 1.6% were found. The average deviation of 2.9% between simulation and measurement is integrated in the uncertainty assessment. Parasitic electric fields generated by the coil system are reduced to less than 1 V/m by a grounded, metallic shielding box between the coil and Petri dishes. The temperatures inside the cell media have been analysed and no temperature differences due to field or sham exposures could be detected (i.e., temperature differences were below 0.1°C). The induced electric fields resulting from a sinusoidal exposure can be expressed as $E = 3.2*f*B*r$ [V/m] and for the powerline exposure as $E = 664*B*r$ [V/m], whereby f is the frequency of the sinusoidal [Hz], B is the average B-field [T] and r is the radial distance from the dish centre [m]. The estimated vibration of the exposed cells is less than 1 m/s^2 (= 0.1 g), which is a factor of 20 above the minimal background level for sham. If an elastically damped dish holder is used (as provided for Participant 4) the vibration load can be further reduced by a factor 12 to 0.1 m/s^2.

In addition to the newly developed exposure systems, it was decided to use two existing setups (Participants 5, 8).

The ELF setup of Participant 5 is based on a pair of Helmholtz coils placed inside a μ-metal shield; exposure and sham are kept in different incubators (no blinded protocols); and sinusoidal B-fields (50 Hz) up to 0.1 mT can be applied.

The ELF setup of Participant 8 is based on two unshielded 4-coil systems arranged in the same incubator; B-fields up to 1 mT (50 Hz) can be applied under non-blinded exposure conditions.

2.1.2 RF-EMF exposure setup

A novel RF setup (GSM) was developed, and four copies were installed in the laboratories of Participants 2, 5, 6, and 8. The system enables EMF exposure of cells under defined conditions with respect to field strengths, polarisation, modulation and temperature and is operated within the GSM DCS mobile frequency band. The setup consists of two single-mode resonator cavities for 1.8 GHz that are placed within an CO_2 incubator. Up to six 35 mm diameter Petri dishes can be exposed in one waveguide resonator. A dish holder guarantees that the dishes are placed exactly in the H-field maximum of the standing wave inside the waveguide.

Each waveguide is equipped with a fan for rapid environmental atmospheric exchange. In order to ensure stable exposure independent of the loading and drifts, monopole antennas are integrated to monitor and control the incident field. The system enables the exposure of monolayers of cells with a non-uniformity of SAR of less than 30% and an efficiency of better than 20 W/kg per W input power.

Much care has been taken to avoid artefacts due to temperature differences between exposed and sham exposed cells. The temperature response of the medium has been assessed by measurements in terms of the incident field strength, cell medium volume and air flow. A temperature load of less than 0.03°C per W/kg SAR was found. The air flow temperature is monitored with accurate Pt100 probes, resulting in differences of less than 0.1°C between the air flow temperature of the exposed and sham waveguides. A numerical heat flow analysis has shown that the possibility of temperature hot spots inside the medium can be excluded.

Field strengths, temperatures and fan currents as well as all commands are continuously logged to encrypted files which are evaluated after the experiments in order to ensure studies under 'blind' conditions (exposure and sham conditions are blindly assigned to the two waveguides by the computer-controlled signal unit).

Field, SAR and temperature characterisations were performed with numerical methods (FDTD simulation platform SEMCAD, SPEAG, Switzerland) and were experimentally verified using the near field scanner DASY3 (SPEAG, Switzerland) equipped with dosimetric field and temperature probes. An uncertainty and variability analysis resulted in an absolute uncertainty for the SAR assessment of 20% and a variability of 5%. The average deviation of 15% between SAR measurement and simulation is within the range of the uncertainty and therefore verifies the reliability of the numerical dosimetry.

The signal unit allows the application of the following five different exposure signals (Figure 2):

- Continuous Wave (CW): An unmodulated CW signal can be applied as a reference (same thermal load, but no ELF modulation components).
- GSM-217Hz: GSM signals are amplitude modulated by rectangular pulses with a repetition frequency of 217 Hz and a duty cycle of 1:8 (pulse width 0.576 ms), corresponding to the dominant modulation component of GSM. The ratio between slot average SAR and time average SAR is 8.
- GSM-Basic: In addition to this basic GSM-217Hz TDMA frame, every 26th frame is idle, which adds an 8 Hz modulation component to the signal. The ratio between slot average SAR and time average SAR is 8.3.
- GSM-DTX: The discontinuous transmission mode (DTX) is active during periods without speaking into the phone. To save battery power, the transmission is reduced to 12 frames per intermediate multiframe of 104 frames (compared to 100 frames for GSM Basic). The frame structure of the DTX signal results in 2, 8 and 217 Hz components. The ratio between slot average SAR and time average SAR is 69.3.
- GSM-Talk: GSM-Talk generates temporal changes between GSM-Basic and GSM-DTX and simulates a conversation with an average duration of 97s and 50s for Basic and DTX, respectively. The ratio between slot average SAR and time average SAR is 11.9. Furthermore, arbitrary field on/off intermittence in the range from seconds to hours can be applied.

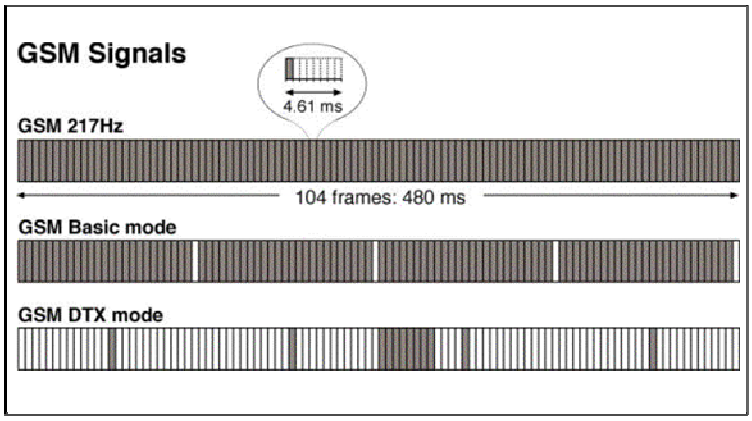

Figure 2. Pulse structure of the applied GSM signals. The basic frame has a period of 4.61 ms and contains a 576 µs burst including 15 µs rising and falling edges. 26 frames make up a GSM multiframe (MF) and 104 frames a GSM intermediate multiframe (IMF). GSM-217Hz is composed of a repetition of basic frames (104 bursts per IMF), whereby every 26th frame is blanked for the GSM-Basic signal (100 burst per IMF). The GSM DTX mode is active during periods of silence and transmission is reduced to 12 bursts per IMF.

In addition to the newly developed exposure systems, it was decided to use three existing setups (Participants 4, 6, 9) and to modify and improve the two setups of Participants 4 and 9.

The RF setup of Participant 4 is based on two R14 waveguides operated at 1710 MHz (Schönborn et al. 2000). Eight 60 mm diameter Petri dishes are exposed with the same concept as for the RF setup (GSM). An identical signal unit is applied, and similar performance is achieved. However, different settings for GSM-Talk were used: Average duration of Basic and DTX was 50s and 97s (instead of 97s and 50s). Therefore the ratio between slot average SAR and time average SAR is 19.8 (instead of 11.9).

The existing RF setup of Participant 6 is based on a R9 resonator cavity operated at 900 MHz. Active water cooling of the Petri dishes is integrated; for details see Toivo et al. (2001). The signal unit can apply GSM-217Hz. Blinded exposure protocols are not possible. In the course of the project, Participant 6 was additionally equipped with the standard RF-setup (GSM).

The RF setup of Participant 9 is based on the Wire-Patch cell and is operated at 900 MHz (Laval et al. 2000). The system was equipped with a new signal unit, allowing the full spectrum of GSM signals. However, also this setup does not allow for computer-controlled blinded exposure conditions. On the other hand, Participant 9 assures that exposure using this system was done blinded (see 2.6.2 below)

2.2 Experiments with human fibroblasts, lymphocytes, monocytes, melanocytes and muscle cells and with granulosa cells of rats (Participant 3)

2.2.1 ELF and RF-EMF exposure setups

See 2.1

2.2.2 Cell culture and exposure conditions

Human diploid fibroblasts (obtained from healthy donors) and SV40 transformed GFSH-R17 rat granulosa cells (Keren-Tal 1993) (provided by Participant 7) were cultivated in Dulbecco´s modified Eagle's medium (DME) supplemented with 10% fetal calf serum (FCS), 20 mM Hepes buffer, 40 µg/ml neomycin, 2 mM L-glutamine, 100 IU/ml penicillin and 100 µg/ml streptomycin. Human melanocytes (male, 3 years old) and skeletal muscle cells (male, 63 years old) were received from Promocell (Heidelberg, Germany) and cultured according to the supplied protocol. Cells were incubated at 37°C in an atmosphere of 5% CO_2 and at 90-100% relative humidity and supplied with fresh culture medium every 48h.

Leukocytes from a healthy donor (female, 31 years old) were isolated from venous blood using Ficoll Paque gradient centrifugation. Cells were washed twice with PBS, resuspended in DME medium with additives and seeded into 35 mm Petri dishes. After 2 hours monocytes had become completely attached on the bottom surface and were separated from lymphocytes by decantation. Monocytes were washed twice with PBS and taken up in 3 ml DME medium.

Lymphocytes from a healthy donor (female, 27 years old) were isolated from venous blood with Ficoll Paque gradient centrifugation. Cells were resuspended in fresh culture medium (DME, 25% FCS, 20 mM Hepes buffer, 40 µg/ml neomycin, 2 mM L-glutamine, 100 IU/ml penicillin and 100 µg/ml streptomycin) with or without stimulation with phytohemagglutinine (1%). The cells were seeded into 35 mm Petri dishes at a density of 2×10^5 cells/3 ml, 24 hours prior to ELF-EMF exposure.

The cells mentioned above were exposed or sham-exposed in suitable waveguides connected with an ELF-EMF generation system provided by Participant 10 within a Heraeus incubator (model Kendro BBD 6220). After exposure cells were detached with trypsin and suspended in fresh culture medium for Comet assay analysis or maintained in culture for cytogenetic testing. Each exposure level was tested in duplicate. In another series of experiments human fibroblasts (cell strain ES-1) and SV40 transformed GFSH-R17 rat granulosa cells (Keren-Tal 1993) (provided by Participant 7) were exposed or sham-exposed in suitable waveguides connected with a RF-EMF generation system (RF 1800 MHz) provided by Participant 10 within a Heraeus incubator (model Hera cell 150l). These experiments were first performed by E. Diem in the laboratories of Participant 2 and later on continued in our own laboratories with a comparable RF-EMF exposure setup, but a RF of 1950 MHz. After exposure cells were detached with trypsin and suspended in fresh culture medium for Comet assay analysis or maintained in culture for cytogenetic testing. Each exposure level was tested in duplicate.

Combined exposures to UVC and ELF-EMF were performed on ice using a germicidal lamp (60 W, Desaga, Heidelberg, Germany), the output of which predominantly contains UVC (253.7 nm). Exposure to UVC prior to ELF-EMF was carried out at an intensity of 2 W/m^2 (measured with a radiometer, Blak-

ray®, Ultra-violet products. Inc., model J225, San Gabriel, USA) for 10 minutes, which equals 1.2 kJ/m^2. Exposure to UVC post to ELF-EMF exposure was performed at an intensity of 2.5 W/m^2 for 30 minutes, which equals 4.5 kJ/m^2.

For thermal exposure cells were incubated at 38.5°C for 4 hours in a commercial incubator (BBD 6220, Kendro, Vienna, Austria). To study repair kinetics, cells were further incubated at 37°C for up to 24 hours.

2.2.3 Comet assay

We followed the technique described by Östling and Johanson (1984) with minor modifications by Singh et al. (1988, 1991). EMF-exposed and sham-exposed cells (10,000 – 30,000) were mixed with 100 µl low melting agarose (0.5%, 37°C) to form a cell suspension, pipetted onto 1.5% normal melting agarose pre-coated slides, spread using a cover slip, and maintained on a cold flat tray for about 10 minutes to solidify. After removal of the cover slip the third layer of 0.5% low melting agarose was added and solidified. The slides were immersed in freshly prepared cold lysis solution (2.5 M NaCl, 100 mM Na_2EDTA, 10 mM Tris, pH 10, 1% sodium sarcosinate, 1% Triton X-100, 10% DMSO, pH 10) and lysed for 90 minutes at 4°C. Subsequently, the slides were drained and placed in a horizontal gel electrophoresis tank side by side, nearest the anode. The tank was filled with fresh electrophoresis buffer (1mM Na_2EDTA, 300 mM NaOH, pH>13 or pH=12.1 in case of alkaline Comet Assay and 100 mM Tris, 300 mM sodium acetate, 500 mM sodium chloride, pH 8.5 in case of neutral Comet Assay) to a level approximately 0.4 cm above the slides. For both, alkaline and neutral Comet assay, slides were left in the solution for 40 minutes for equilibration and unwinding of the DNA before electrophoresis. Electrophoresis conditions (25 V, 300 mA, 4°C, 20 min, field strength: 0.8 V/cm) were the same for neutral and alkaline Comet assay. All steps were performed under dimmed light to prevent the occurrence of additional DNA damage. After electrophoresis the slides were washed 3 times with Tris buffer (0.4 M Tris, pH 7.5) to neutralise, then air-dried and stored until analysis. Comets were visualised by ethidium bromide staining (20 µg/ml, 30 seconds) and examined at 400 X magnification using a fluorescence microscope (Axiophot, Zeiss, Germany). One thousand DNA spots from each sample were classified into 5 categories corresponding to the amount of DNA in the tail according to Anderson et al. (1994) with modifications. The proposed classification system provides a fast and inexpensive method for genotoxic monitoring. Due to the classification to different groups by eye, no special imaging software is required. The different classification groups are not weighted equally, due to the fact that they do not represent equal grades of damage. Moreover, the technique becomes more sensitive, because many cells can be scored in a short time (1000 cells instead of 50-100 cells with image analysing). The subsequent calculation of a "Comet tailfactor" allows quantifying DNA damage as a single figure, which makes it easier to compare results. Due to the scoring of 1000 cells in one experiment, which are tenfold the cells processed with image analysing, standard deviations are very low. Reproducibility has been thoroughly checked. Results expressed as "Comet tailfactors" were calculated according to Diem et al. (2002). All experiments were performed in duplicate by the same investigator.

2.2.4 Micronucleus assay

Micronucleus (MN) assay was performed according to Fenech and Morley (1985) and Fenech (1993). Fifty thousand cells were seeded into slide flasks (Nunc, Roskilde, Denmark) and exposed to ELF-EMF. In order to block cytokinesis, cytochalasin B (3 µg/ml, Sigma, St. Louis, USA) was added four hours before the first round of replication. After termination of the culture, fibroblasts were treated with hypotonic KCl solution (0.075 M, 30 min.) and fixed with a mixture of methanol : aqua bidest. (7:3) for 10 min. Slides were air-dried and stained with 4,6-diamidino-2-phenylindole (DAPI, Sigma, St. Louis, USA) for 3 minutes. MNs were visualised under a fluorescence microscope and 2000 binucleated cells were scored according to criteria published by Lasne et al. (1984). The results are expressed as MN events/500 binucleated cells.

2.2.5 Chromosomal aberrations

For evaluation of chromosomal aberrations 2 x 10^5 cells were seeded into 35 mm petri dishes (Nunc, Roskilde, Denmark) and exposed to EMF at conditions producing maximum effects in the Comet assay.

After EMF exposure, fibroblasts were trapped at metaphase by incubation with colcemid (0.2 µg/ml, Invitrogen Corporation, Paisely, Scotland) for the last 4h prior to harvesting. Subsequently, the cells were detached with trypsin (Invitrogen Corporation, Paisely, Scotland) and subjected to a hypotonic treatment (0.075 M KCl, 37°C, 30 min.). Thereafter, cold fixative (methanol : acetic acid 3 : 1) was slowly added and cells were collected by centrifugation. Fixation procedure was repeated twice. Finally, the cells were resuspended in 0.5 ml of fixative, dropped on clean slides, air dried, stained for 12 minutes with 4% GIEMSA, prepared in Sorensen's buffer (38 mM KH_2PO_4, 60 mM Na_2HPO_4 x 12 H_2O, pH=7) and rinsed with aqua bidest. Chromosomal aberrations were evaluated in 10,000 well-spread and complete (46 chromosomes) metaphases (5,000 ELF-exposed, 5,000 sham-exposed). The identification of chromosome aberrations was carried out following the criteria recommended by the WHO (1985). Different types of aberrations (chromosome gaps, chromosome breaks, ring chromosomes, dicentric chromosomes and acentric fragments) were scored separately. Five independent experiments were performed. Results are expressed as percent chromosomal aberrations per cell.

2.2.6 Fluorescence *in situ* hybridisation (FISH)

For evaluation of stable translocations, cells were seeded into 35 mm petri dishes at cell density of 2 x 10^5/3ml. After ELF-EMF exposure and an additional repair time of one replication round, fibroblasts were trapped at metaphase by incubation with colcemid (0.2 µg/ml, Invitrogen Corporation, Paisely, Scotland) for the last 4h prior to harvesting. Subsequently, the cells were detached with trypsin (Invitrogen Corporation, Paisely, Scotland) and subjected to a hypotonic treatment (0.075 M KCl, 37°C, 30 min.). Thereafter, cold fixative (methanol : acetic acid 3 : 1) was slowly added and cells were collected by centrifugation. Fixation procedure was repeated twice. Finally, the cells were resuspended in 0.5 ml of fixative, dropped on clean slides and air-dried. Subsequently, slides were denatured (70% formamide/2×SSC pH 7, 72°C, 2 min) and immediately dehydrated through a cold (-20°C) ethanol series (70%, 80%, 90%). The rhodamine-labelled whole chromosome probes (chromosome 1-22, X, Y) were prepared according to the recommendation of the manufacturer (Appligene Oncor Q-biogene, Illkirch, France). Aliquots of 30 µl were applied to the metaphase preparations, the slides were covered with a cover slip and incubated overnight in a moist chamber at 37°C. The following day, slides were immersed in 0.5×SSC at 72°C for 5 min, transferred to 1×PBD at room temperature for 2 min and counterstained with DAPI (4,6-diamidino-2-phenylindole, 0.02 µg/ml, Sigma, St. Louis, USA). Fluorescence signals were evaluated using a fluorescence microscope equipped with filters capable of simultaneously passing DAPI/Rhodamine. 1,000 well spread and complete (46 chromosomes) metaphases were scored for translocations for each labelled chromosome.

2.2.7 Changes in mitochondrial membrane potential (JC-1 staining)

Changes in the mitochondrial membrane potential ($\Delta\Psi_m$) upon ELF-EMF exposure were assessed by staining mitochondria with 5,5',6,6'-tetrachloro-1,1',3,3'-tetraethyl-benzimidazolcarbo-cyanine iodide (JC-1, Molecular Probes, Leiden, The Netherlands), a fluorescent dye with high sensitivity to $\Delta\Psi_m$ in intact cells (Cossarizza et al. 1993b; Salvioli et al. 1997). This lipophilic cation forms J-aggregates in the matrix of intact mitochondria (emitting at 590 nm) or is released in a monomeric form (527 nm) from depolarised mitochondria. A good correlation between the J-aggregate fluorescence of JC-1 and $\Delta\Psi_m$ has been reported previously (Smiley et al. 1991). Immediately after exposure to ELF-EMF (50 Hz, 1 mT, 15h, intermittent 5 min on/10 min off) or RF-EMF (GSM basic 1950 MHz, SAR=1 W/kg, 15h, intermittent 5 min on/10 min off), cells were trypsinated, centrifuged (700 g, 5 min) and resuspended in medium (RPMI 1640 with 10% fetal calf serum). Subsequently, the cells were incubated in triplicates at a density of 0.45 x 10^6 cells/ml in complete medium for 15 min at 37°C in the dark with 10 µg/ml JC-1. After incubation with JC-1 the fibroblasts were washed twice with phosphate buffered saline (Gibco, Vienna, Austria) and adjusted to 2.15 x 10^5 cells/ml. From each of the three stained samples per ELF-EMF exposure and sham exposure, respectively, 8 x 250 µl cell suspension have been transferred to a 96 well sample plate. Measurement of red fluorescence (excitation 540 nm, emission 590 nm) and green fluorescence (excitation 485 nm, emission 535 nm) was done on a Wallac Victor 2 fluorescence plate reader (EG&G Wallac, Turku, Finland). Results were expressed as ratios of red/green fluorescence. For positive controls cell cultures were treated for 18h with 20 µM camptothecin (Sigma-Aldrich, Vienna, Austria), a well known inducer of apoptosis.

2.2.8 Statistical analysis

Statistical analysis was performed with STATISTICA V. 5.0 package (Statsoft, Inc., Tulsa, USA) and SPSS 10.0 package (SPSS Inc., Illinois, USA). All data are presented as mean ± standard deviation (SD). The differences between exposed and sham-exposed, as well as between different exposure conditions were tested for significance using independent Student's t-test or one-factorial ANOVA with post hoc Student´s t-test Bonferroni-correction. A difference at $p<0.05$ was considered statistically significant. Correlation was assessed by multiple regression analysis using linear regression.

2.3 Experiments with human HL-60 cells (Participant 2)

2.3.1 RF-EMF exposure setup

See 2.1.2

2.3.2 Cell culture and exposure conditions

Human HL-60 cells (ATCC, Rockville, MD, USA) were cultured in RPMI 1640 medium supplemented with 10% fetal calf serum (Promocell, Heidelberg, Germany), 1% L-glutamine, 1% HEPES buffer and 2% penicillin/ streptomycin (Gibco BRL Life Technologies, Rockville, MD, USA) under temperature- and pH-control conditions. The cell line was maintained in logarithmic growth phase at 37°C in a 5% CO_2 atmosphere. For radio-frequency (RF) exposure experiments the initial seeding density per 35 mm petri dish was 7.5 x 10^5 cells. In addition to sham-exposed cells, cells incubated under these normal cell culture conditions without the waveguides being connected to the generator system (see below) were examined as incubator controls. In positive control cells DNA breakage was induced either by incubation of cells for 60 min in cell culture medium containing hydrogen peroxide at a final concentration of 100 µmol/l or by 6 MeV γ-irradiation (0.5 Gy, exposure time: 5.2 s). In case of assessing indirectly the generation of reactive oxygen species and directly the modulation of detoxifying capacities of HL-60 cells, culture medium was supplemented with ascorbic acid (10 µmol/l) prior to RF-exposure.

The following exposure conditions were examined with respect to direct and indirect genotoxic effects in HL-60 cells using the alkaline Comet assay, the cytokinesis-block micronucleus assay, the flow cytometric measurement of micronuclei induction and DNA alterations, cytotoxicity testing, assessment of cell viability and cell growth:

- 1800 MHz, continuous wave (C.W.) exposure, 24 hours, SAR=0.2 W/kg, 1.0 W/kg, 1.3 W/kg, 1.6 W/kg, 2.0 W/kg and 3.0 W/kg, compared with the corresponding sham exposed cells, incubator control cells and positive controls.
- At 1800 MHz, SAR 1.3 W/kg, C.W., different periods of exposure, ranging from 2h up to 72h exposure.
- 1800 MHz, SAR of 1.3 W/kg different RF-signals: C.W., 5 min on/10 min off; GSM-217Hz; GSM-Talk were examined.
- 1800 MHz, GSM-DTX, 24 hours, 5 min on/5 min off, SAR 1.0 W/kg, compared with the corresponding sham exposed cells, for gene expression profiling studies.
- 1800 MHz, C.W., 24 hours, SAR1.3 W/kg, compared with the corresponding sham exposed cells and incubator controls for gene expression profiling studies.

Cells were exposed or were sham-exposed in waveguides connected with a RF-generator system in a Heraeus incubator (Model Hera Cell). After each run the cells were immediately taken out of the incubator for subsequent analyses unless otherwise stated. Experiments were performed under blinded conditions in the following way: after the cells were placed in the two waveguides, and the incubator chamber was closed, the selection which of the two waveguides was connected to the RF generator and which remained disconnected, i.e. served as a sham control, was controlled by the computer system provided by Participant 10 and remained concealed to the experimentalists until analyses by the Comet assay and the micronucleus assay were completed and results documented. For decoding which of the two waveguides was connected to the RF-generator or remained disconnected, respectively, and for control of

the experimental conditions of each run, technical data were mailed independently to Participant 10 and returned electronically with electronic documentation of the time points of dispatching and return. Temperature within the waveguides was monitored during each run for as well sham-exposed and RF-field exposed cells and documented electronically. Additionally, at the end of the experiment pH values were controlled within the cell culture medium of sham-exposed, RF-field exposed and control cells.

An independent experiment consisted of 6 exposed and 6 sham-exposed petri dishes (35 mm diameter) with an initial seeding density of 7.5 x 10^5 cells per petri dish. In order to rule out potential differences of the six positions within the waveguide, the cells from the six exposed petri dishes and of the six sham-exposed dishes, respectively, were pooled prior to further analysis. Differences between exposed cells and corresponding controls were tested for significance, employing the Student´s t-test at a level of $p \leq 0.05$.

2.3.3 *in vitro* genotoxicity tests

The cytokinesis-block in vitro micronucleus (MN) assay

The MN assay was carried out as described by Natarajan and Darroudi (1991) according to the guidelines developed by Fenech (1993, 2000), Fenech and Morley (1985, 1986), Fenech and Rinaldi (1995), Fenech et al. (1994) and Garriott et al. (2002). In order to evaluate the frequency of MN in binucleated (BN) human HL-60 cells, cytochalasin B (final concentration 3.0 µg/ml) was added to the growth medium after exposure and washing. Cytochalasin B prevents the cells from completing cytokinesis resulting in the formation of multinucleated cells (Fenech and Morley 1985). The cells were fixed after 24 hours. For fixation the cells were washed and treated with cold hypertonic KCl solution (5.6 g/l). Then the cells were fixed 3 times with a solution of acetic acid/methanol (1:3) and subsequently air dried preparations were made. For the detection of MN in binucleated cells (BNC) the slides were stained with 2.0% Giemsa solution. To determine the frequency of MN of RF-exposed, sham-exposed or control cultures the number of MN in 1000 BNC cells were scored microscopically at 400 fold magnification by one person in 2 slides for each experimental point. All particles about the size smaller than one-third that of the main nuclei, round-shaped with similar staining characteristics as the main nuclei were counted as micronuclei. In particular after high doses of γ-irradiation (2 and 3 Gy, respectively), it was sometimes difficult to distinguish between "true" micronuclei and apoptotic bodies that occurred also in BN cells. Experiments were repeated at least three times independently.

To study the effects of RF-EMF on cell division, the number of BNC relative to the number of mono-, bi-, tri- and tetranucleated cells (% BNC) was determined according to Fenech (2000). Furthermore, apoptotic cells can be recognised by a characteristic pattern of morphological changes, which may be broadly defined as cell shrinkage, cell shape change, condensation of cytoplasm, nuclear envelope changes, nuclear fragmentation and loss of cell surface structures.

Alkaline single cell gel electrophoresis assay (SCGE, Comet assay)

The alkaline SCGE assay was carried out as described by Singh et al. (1988) according to the guidelines developed by Tice et al. (1990, 2000), Fairbairn et al. (1995) and Klaude et al. (1996). After exposure and washing, a single cell suspension of 1 x 10^4 cells was mixed with 100 µl of 0.7% LMP agarose in PBS and transferred to the fully frosted slides precoated first with 1% and then with 0.5% NMP agarose in PBS. Finally, a covering layer (0.7% LMP agarose) was transferred to the slide. All procedures were performed under dimmed light. Subsequently, the slides were covered with a coverslip and allowed to solidify in the refrigerator. Then the coverslips were removed and the slides were immersed for 1 hour at 4°C in lysing solution (2.5 M NaCl, 100 mM Na_2EDTA, 10 mM Tris, pH 10) containing 1% Triton-X 100 and 10% DMSO added just before use. Thereafter, the slides were exposed to 0.3 M NaOH for 20 min to allow the DNA to unwind. After this, the slides were placed in a horizontal gel electrophoresis tank containing freshly prepared cold electrophoresis buffer (1 mM Na_2EDTA and 300 mM NaOH, pH 13.5) following electrophoresis at 0.8 V/cm (25 V, 300 mA) for 20 min. After electrophoresis, the slides were rinsed 2x with 400 mM Tris, pH 7.5 and were stained with 80 µl ethidium bromide (0.02% in water), covered with a coverslip. To prevent additional DNA damage all steps described above were conducted under dimmed light or in the dark. 50 randomly chosen cells per slide (two slides per culture) were analysed using a 400-fold magnification with a Zeiss fluorescence microscope (Zeiss Axioplan). A computerized image analysis system (Kinetic Imaging 4.0, Optilas, München, Germany) was employed to measure different Comet parameters. As a measure of DNA damage tail length (in µm), Tail Extent Moment, Olive Tail Moment (OTM) and % of DNA in tail were automatically calculated. To determine

DNA migration of exposed, sham-exposed or control cultures, 100 cells were scored microscopically for Comet formation on 2 slides for each experimental point. As a positive control hydrogen peroxide at a final concentration of 100 µmol/l for 1h was used. Experiments were repeated at least three times independently. The results reported are the mean values ± standard deviation (SD).

Positive control through Gamma-Irradiation

Irradiation was administered with 6 MeV X-rays on an linear accelerator to the HL-60 cells (0.75 x 10^6) in dishes at doses of 0.5, 1.0, 2.0 and 3.0 Gy (dose rate: 5.8 Gy/min). A control dish received no irradiation. Then, both irradiated and non-irradiated samples were returned to the incubator and cultured until analyses at each relevant point were performed.

Viability test

Viability of the cell samples was assessed using the trypan blue exclusion test. The percentages of viable cells were then determined by placing aliquots of the treated cells in a Neubauer chamber and scoring cells for either the absence (viable cells) or the presence (dead cells) of blue staining. Only cultures with a viability more than 90% were analysed.

2.3.4 *in vitro* cytotoxicity testing

In order to exclude in vitro cytotoxic effects different approaches were used to verify cell viability, including trypan blue staining, flow cytometry tests, by which cells with reduced viability are marked by nuclear propidium iodide and the MTT assay, a colorimetric assay, that is based on the ability of viable, i.e. metabolically active cells to cleave tetrazolium salts to form formazan dye.

Cell viability and cell cytotoxicity were assessed by using the MTT assay. MTT is a sensitive first indicator of mitochondrial damage induced by oxidative stressors (Wasserman and Twentyman 1988). To analyse HL-60 cell proliferation, the MTT assay (Cell Proliferation Kit I, Roche, Mannheim, Germany) was used according to the manufacturer's protocol, and the data reported as OD units. This assay is very sensitive for the measurement of cell proliferation based upon the reduction of the tetrazolium salt 3,[4,5-dimethylthiazol-2-yl]-2,5-diphenyltetrazolium bromide (MTT).

Briefly, around 2 x 10^3 cells per well were plated in 96-well microtiter plates with 100 µl of medium. 10 µl of a MTT (5 mg/ml) solution (Roche, Mannheim) was added. Incubation occurred for 4h at 37°C. 100 µl of solubilisation solution was added to each well. The plate was allowed to stand overnight in the incubator (37°C, humidified atmosphere). Absorbance was measured at 570 nm. Performing analysis on micronuclei induction, the ratio of BNC against mono-, bi-, tri- and tetranucleated cells is determined, giving a measure of cell division and cell cycle progression. Performing the flow cytometric analysis of micronuclei induction, an assessment of cell viability and also of DNA distribution and therefore of cell cycle alterations become feasible.

2.3.5 Preparation of nuclei suspensions from cells for flow cytometry analysis

The method was performed according to Nüsse and Kramer (1984), Nüsse and Marx (1997) and Wessel and Nüsse (1995). After exposure of cells and subsequent incubation for 24h (recovery time) the medium was removed and cells were washed twice with PBS and counted. Cells were then spun at 100 x g for 5 min at room temperature. Supernatants were removed carefully, the remaining cell pellet was re-suspended by gently shaking. FACS solution I (10 mM NaCl, 3 mM sodium citrate, 10 mg/l RNase A, 3 ml/l of 10% Igepal solution in water, 25 µg/l ethidium bromide freshly prepared before use) was added to the cell pellet and cells were suspended to a density of approximately 1 x 10^6 cells per ml. The suspension was stirred for 2 sec and was kept for 30-60 min at room temperature in the dark. After adding FACS solution II (70 mM citric acid, 250 mM sucrose, 40 mg/l of ethidium bromide) the suspension was stirred for 2 sec and subjected to FACS analysis.

2.3.6 Flow cytometric exclusion of apoptosis via Annexin V assay and TUNEL assay

Annexin V assay

After exposure to RF-EMF 10^7 cells were centrifuged, washed several times with PBS and the pellet was resuspended with Annexin V binding buffer (Becton Dickinson Biosciences, Heidelberg, Germany), 1 ml of this suspension was incubated for 20 min in the dark in the presence of 100 µl Annexin V binding buffer and 3 µl Annexin V FITC (Becton Dickinson Biosciences, Heidelberg, Germany). After washing with Annexin V binding buffer, cells were resuspended in 300 µl Annexin V binding buffer + 5 µl Propidium Iodide (PI) solution (50 µg/ml) and were analysed by flow cytometry using a FACSCalibur Analytic Flow Cytometer (Becton Dickinson Biosciences, Heidelberg, Germany).

TUNEL assay

After exposure to RF-EMF 10^7 cells were centrifuged, washed several times with PBS and then fixed for 1h by PBS/formaldehyde (4%). Then the cells were washed again, resuspended with PBS and permeabilised with 100 µl Triton X solution (0.01% Triton in 0.1% sodium citrate solution) for 2 minutes, followed by labelling with 50 µl TUNEL reaction mixture (Roche, Mannheim) for 1 h at 37°C. After this incubation the cells were washed and resuspended with 500 µl PBS. The cells then underwent flow cytometric analysis in order to determine the number of green stains (representing apoptotic DNA fragmentation). DNA content analysis was performed on a Becton Dickinson FACScan according to the manufacturer's protocol.

2.3.7 Reactive oxygen species (ROS) and antioxidant enzyme activity

Reactive oxygen species (ROS), including superoxide anion (O_2^-), hydrogen peroxide (H_2O_2), hydroxyl free radical ($OH^\cdot$) and singlet oxygen ($^1O_2$) have powerful oxidative potential. ROS are capable of attacking lipids, nuclear acids and proteins, resulting in certain degree of oxidative damage. The cell possesses an efficient antioxidant defence system, mainly composed of antioxidative enzymes such as superoxide dismutase, and glutathione peroxidase. These enzymes are able to scavenge excessive ROS to cellular metabolism, and thereby lead to a relative stabilisation of the ROS level under physiological conditions. To evaluate the ROS level differences in RF-exposed and sham-exposed HL-60 cells the Nitric Oxide Assay, the oxyDNA assay, the direct detection by flow cytometry using the fluorescent dye Dihydrorhodamine 123 and the Lipid Peroxidation Assay were used. For measuring the antioxidative enzyme capacity the activities of superoxide dismutase and glutathione peroxidase were evaluated. The tests mentioned above were chosen within a first screening approach in order to assess qualitatively gross changes in ROS levels and antioxidative enzyme activities. All analyses were performed at room temperature unless otherwise stated.

Nitric oxide (NOx)

Nitric oxide (NOx) was measured using the colorimetric Nitric Oxide Assay Kit from Calbiochem (Cat. No. 482650, Calbiochem-Novabiochem GmbH, Bad Soden, Germany). Briefly, nitrate in aqueous solutions (supernatant after centrifugation of 7 x 10^5 cells/ml) was reduced to nitrite by enzymatic conversion by nitrate reductase and was estimated spectrophotometrically at 540 nm using the Griess reaction. The absorbance obtained is compared against a standard curve of known concentrations of NOx (1-25 µmol/l) and the results were expressed as µmol/l NOx. Detection limit is <1 µmol/l for NOx (Miles et al. 1996).

oxy DNA

Oxidative DNA damage, with 8-oxoguanine as the major oxidative DNA product, was measured using the fluorogenic OxyDNA Assay Kit from Calbiochem (Cat. No. 500095, Calbiochem-Novabiochem GmbH, Bad Soden, Germany). The assay utilizes a direct fluorescent probe directly binding to the DNA adduct of 8-oxoguanine (de Zwart et al. 1999, Kasai 1997, Cooke 1996). Briefly, cells (1 x 10^6) were washed first in 1× PBS, then in wash solution, and then by the addition of 100 µl blocking solution with a 1-hour incubation at 37°C. After 2 washes in working solution, cells were incubated with 100 µl FITC conjugate for 1 hour in the dark at room temperature before they were washed twice in washing solution and once in PBS. The FITC labelled protein conjugate binds to the 8-oxoguanine moiety present in the 8-oxoguanosine of oxidized DNA. Finally, cells were resuspended in FACS buffer and were analysed by flow cytometry (FACScan, Becton Dickinson). The presence of oxidized DNA is indicated by a

green/yellow fluorescence. A partial augmentation (shoulder at the right side of the signal) of FL-1 fluorescence intensity indicates an increase in level of oxidative DNA damage, i.e. 8-oxoguanine. In the present study, assays for the screening of oxidative DNA damage were performed after exposure to RF-field (1800 MHz, continuous wave, SAR 1.3 W/kg, 24h) or sham-exposed cells. Oxidatively damaged DNA was quantified by determination of the area under the curve (AUC) of the shoulder at the right side of the signal fluorescence intensity in RF-field exposed cells.

Detection of ROS level with Dihydrorhodamine 123

7.5 x 10^5 cells were incubated with 5 µmol/l dihydrorhodamine123 (DHR123, Sigma, Germany), as a ROS capture (Lopez-Ongil et al. 1998), during sham- or RF-exposure for 24h. Additionally, positive controls were run, in which 100 µmol/l of hydrogen peroxide (H_2O_2) was added for 1h prior to the end of the experiment. Intracellularly, DHR123 is oxidized by ROS to form the fluorescent compound rhodamine123 (Rh123), which is pumped into mitochondria and remains there. After the experiment, cells were harvested, washed with PBS and immediately analysed for Rh123 fluorescence intensity by flow cytometry (FACScan, Becton Dickinson). The percentage of oxidative damage was defined as the percentage of gated HL-60 cells with Rh123 fluorescence. The results presented represent the means of three independent experiments.

Lipid Peroxidation Assay

Lipid Peroxidation was measured using the colorimetric Lipid Peroxidation Assay Kit from Calbiochem (Cat. No. 437634, Calbiochem-Novabiochem GmbH, Bad Soden, Germany). Malondialdehyde (MDA) and 4-hydroxy-2(E)-nonenal (4-HNE), products of lipid peroxidation, can be estimated spectro-photometrically at 586 nm after reaction with a chromogenic reagent at 45°C to obtain an index for lipid peroxidation (Melchiorri et al. 1995, Öllinger and Brunmark 1994, Sewerynek et al. 1995).

Briefly, 3 x 10^6 cells were used per assay. The cells were lysed by repetitive freezing/thawing in 1000 µl distilled water. The cellular membranes were not removed until after the incubation with reagent R1 and R2. The samples were centrifuged at 15.000 x g for 10 minutes to clarify the homogenate supernatant. Immediately prior to reading the absorbance at 586 nm, 200 µl of sample solution, 650 µl of diluted reagent R1 and 150 µl of diluted reagent R2 were mixed to a volume of 1000 µl. A least-square linear regression demonstrates that the standard curve (concentration range 0-20 µmol/l) is a linear function of the concentration of either MDA or 4-HNE. The absorbance values obtained were compared against a standard curve of known concentrations of MDA/4-HNE (1-20 µM). The results were reported as µmol (MDA + 4-HNE)/l. Detection limit is 0.1 µmol/l for (MDA + 4-HNE).

To screen the possible effect of RF-EMF on endogenous antioxidant enzyme activity, the activities of superoxide dismutase (SOD) and glutathione peroxidase (GPX) were determined in HL-60 cells that exposed to RF-EMF (1800 MHz, continuous wave at SAR 1.3 W/kg for 24h) or sham-exposed

Superoxide dismutase (SOD) activity

Superoxide dismutase (SOD) activity of cell homogenates was determined using the Superoxide Dismutase Assay Kit from Calbiochem (Cat. No. 574600, Calbiochem-Novabiochem GmbH, Bad Soden, Germany). Briefly, 4 x 10^6 cells were washed with PBS buffer, diluted in 250 µl of PBS buffer and extracted with 400 µl of a chloroform/ethanol mixture (62.5/35.5 v/v). 40 µl of the aqueous layer of this sample extract was mixed with 30 µl of diluted chromogenic reagent (R1) and 30 µl reagent R2 in 900 µl of an aqueous alkaline solution buffer. The SOD-mediated increase in the rate of auto-oxidation of this reaction mixture was utilised to yield a chromophore with maximum absorbance at 525 nm (Wang et al. 1991, Vilim and Wilhelm 1989). Results were expressed as SOD units. Detection limit for SOD activity is 0.2 U/ml.

Glutathione peroxidase (GPx) activity

Glutathione peroxidase (GPx) activity of cell homogenates was determined using a cellular glutathione peroxidase assay Kit from Calbiochem (Cat. No. 354104, Calbiochem-Novabiochem GmbH, Bad Soden, Germany). Briefly, to assay cellular glutathione peroxidase, 70 µl of cell homogenisate of 1 x 10^6 cells is added to a 1050 µl of a solution containing glutathione (GSH, 1 mmol/l), as a source of reducing equivalents, GSH reductase (0.4 U/ml) and NADPH. The reaction is initiated by the addition of 350 µl of the diluted organic peroxide t-butyl hydroperoxide and the absorbance at 340 nm was recorded over a period of 5 minutes. The rate of decrease in the absorbance (NADPH is converted to NADP) is directly proportional to the GPx activity in the cell homogenisate. Therefore, the difference in absorbance per min

was used to calculate the enzyme activity and results were expressed as GPx units/ mg protein. As a positive control cellular glutathione peroxidase at an activity of 288 mU/ml was assayed at 23°C.

2.3.8 Analysis of cellular growth behaviour

Cellular doubling time

Cellular growth behaviour of HL-60 cells following RF-exposure for 24h (1800 MHz, continuous wave, SAR 1.3 W/kg) with respect to growth velocity as compared to sham and incubator controls was assessed by determination of the cellular doubling time td:

$$\mathrm{td} = \frac{\log 2 \cdot dt}{\log N - \log No}$$

with dt = time of exposure with RF field or sham-exposure, No = number of cells at the beginning of the experiment and N = number of cells at the end of experiment.

Thymidine kinase (TK) assay

Thymidine kinase activities were determined by radioenzyme assay Prolifigen® TK-REA (AB Sangtec Medical, Bromma, Sweden) with ^{125}I-deoxyuridinemonophosphate as substrate. Briefly, assay buffer containing ^{125}I-labelled substrate was added to the HL-60 cell lysate (lysate diluted 1:100) and incubated for 4h. Lysis was performed with 5 x 10^4 cells and a NP40/Tween 20 containing lysis buffer. The reaction was stopped by addition of a separator tablet which binds the phosphorylated product. After washing, radioactivity was measured. The level of radioactivity is directly proportional to the enzyme activity in the original sample. The TK value was calculated from the standard curve and expressed as U/l.

2.3.9 Statistics

To compare the results of the different groups listed above, the Student´s t-test (two-sided test) was used.

2.3.10 Proteomics

Different optimisation strategies for enhancement of 2-dimensional resolution of highly complex cellular protein mixtures were performed during the project. First of all we started with the IPG-strip approach/Pharmacia. Alternatively we also tested the tube gel approach and found, that for our system this proofed to be the most suitable one with the best resolution. This is essential for the following identification steps. Therefore we here focus on the description of the tube gel technology. In general, the methodology for two-dimensional electrophoresis of protein mixtures described by Klose and Kobalz (1995), was performed. Alternatively, a protocol with slight modifications was applied, described below.

IEF-sample preparation

For separation of cellular proteins by 2-dimensional gel electrophoresis cells were lysed after thorough washing with PBS by repeated freezing and thawing. Proteins were solubilised in: 56 mg urea lyophilised with 16.8 µl 0.6 M DTE, 41 µl protein (corresponds to 250 µg of protein)/water, 5 µl Ampholyte 9-11, 8 µl 25% CHAPS, mixed for 30 minutes at room temperature, centrifuged 6 minutes at 14000 g, then the supernatant was taken off as sample.

IEF/2-D PAGE

High resolution 2-dimensional SDS-polyacrylamide gel electrophoresis (2-D PAGE, 23 x 30 cm gels, pI 2-9.5; 14 x 16 cm gels alternatively, pI 2-11) was performed as follows. For the isoelectric focussing of the small gels a pH-gradient extending from pH 2 to pH 11 was generated by means of carrier ampholytes. For the 14x16 cm 2D-gels six 13 cm long and 2.2 mm thick isoelectric focusing gels were prepared with 3.3 g urea, 780 µl acrylamide / N,N'-methylene-bis-acrylamide (30% T, 5.4% C), 480 µl 25% CHAPS, 1.92 ml water and 300 µl ampholyte mix. The ampholyte mix, which can be stored at -20°C, consisted of 340 µl servalytes 5-7, 340 µl ampholines, 113 µl servalytes 3-10, 113 µl servalytes 2-11 and 113 µl servalytes 3.5-10. The IEF-samples were loaded on the tube gel, overlaid with 10 µl sample overlay (12 M urea, 8% w/v CHAPS, 4% ampholyte 9-11, 0.16 M DTE) and with the upper chamber

buffer consisting of a sodium hydroxide solution (20 ml 1N NaOH in 980 ml water). The lower chamber buffer contained 0.6 ml 85% phosphoric acid in 900 ml water. Gels were run in a tube gel apparatus at room temperature. The samples are focused for 9000 Vh. After extrusion gels were equilibrated for 5 minutes in SDS equilibration buffer (10% v/v 0.5 M Tris HCl pH 6.8, 5% v/v 20 mM EDTA 2Na, 20% of a 10% SDS solution, before usage 1.54% w/v DTE was added) and then loaded onto the 14 x 16 cm second dimension vertical slab gel. This gel consisted of a 12.5% SDS separation gel (7.5 ml 2M Tris HCl pH 8.8, 0.4 ml 10% SDS, 1.9 ml 20 mM EDTA 2Na, 12.7 ml water, 15.1 ml of an acrylamide/bisacrylamide solution (30% T, 2.67% C), 12.7 ml water; polymerisation with 20 µl TEMED and 200 µl of a 10% ammonium persulfate solution) and a stacking gel (2 ml Tris HCl pH 6.8, 80 µl 10% SDS, 400 µl 20 mM EDTA 2 Na, 1.1 ml of an acrylamide/bisacrylamide solution (30% T, 2.67% C), polymerised with 8 µl TEMED and 80 µl of a 10% ammonium persulfate solution). The lower chamber buffer for the second dimension consisted of 400 ml Tris/glycine 10x stock solution, 40 ml 10% SDS, diluted to 4000 ml with water, the upper chamber buffer consists of 50 ml Tris/glycine 10x stock solution, 5 ml 10% SDS, diluted to 500 ml with water, 230 mg DTE and 50 µl 0.5% BPB. The isoelectric focussing gel was layered on top of the SDS stacking gel and overlaid with top chamber buffer. Each gel was run for approximately 4 h beginning with 20 mA, 30 mA within the stacking gel and finally 50 mA in the separation gel. After finishing electrophoresis the gels were fixed in 40% ethanol/10% glacial acetic acid overnight, then silver stained according to the method applied by Klose and Kobalz (1995) and then dried.

Two-dimensional polyacrylamide gels were first qualitatively analysed on a light box visually. Clear changes in the protein secretion pattern like newly expressed or disappearing proteins can be detected by this means. The human eye is capable of registering even very small variations like an increasing or decreasing secretion of a characteristic protein, whereas a quantitative analysis of changes protein secretion is not possible. Protein spots of the 2-D gels were displayed by standard staining procedures with silver for image analysis. The corresponding gels were digitised. The spots were detected and the master gel image was calibrated. Image analysis was performed with Proteom Weaver (Definiens, München, Germany). Known proteins serve as "landmark proteins". With the help of their isoelectric points and molecular weights an internal two-dimensional co-ordinate system can be generated. In this system an evaluation of the isoelectric point and molecular weight of any protein of interest together with the determination of its amount expressed in the sample is possible. Qualitative and quantitative analysis of single gels and a direct gel-to-gel comparison was performed by this method.

2.3.11 Gene expression profiling

In an approach to examine effects of RF-EMF on gene expression on the transcriptional level (transcriptome), changes of cellular RNA profiles were analysed by use of the array technology in collaboration with the Resource Center of the German Human Genome Project (Participant 12). Methodological details and detailed presentations of the results obtained together with Participant 12 are provided under 2.10.3 and 2.10.4.

2.4. Experiments with the human neuroblastoma cell line NB69 (Participant 5)

2.4.1 ELF-EMF exposure setup

50 Hz, sine wave magnetic fields (MF) at 10 µT, 100 µT or 2000 μT_{rms} were generated by a pair of coils in a Helmholtz configuration energised by a wave generator Newtronic Model 200MSTPC, (Madrid, Spain). The exposure setup used in these experiments was reproduced from that described by Blackman et al., (1993). Each exposure system consisted of two 1000-turn, 20-cm-diameter coils of enamelled wire, aligned coaxially 10 cm apart and oriented to produce vertically polarised magnetic fields. Cell culture dishes were placed in the uniform MF space within the coils for exposure or sham-exposure. Currents in the coils were adjusted and monitored using a multimeter (Hewlett Packard, model 974A, Loveland, CO) after the flux density was established with fluxgate magnetometers (Bartington, model MAG-3, GMW Assoc and Wandel and Goltermann S.A, EFA-3, Model BN 2245/90.20. Two pairs of coils were mounted

in the centre of magnetically shielded (co-netic alloy) boxes (Amuneal Corp., Philadelphia, PA) housed in incubators (Forma, Models 3121 and 3194) with a 5% CO, 37ºC. The magnetic shielding allowed for reduced environmental fields at the samples' locations. With DC MF = 0.02-0.08 µT and AC MF = 0.07 - 0.1 µT. Each incubator contained a coil system and shielding box, but only one set was energised for each experiment.

Two sets of coils, shielding rooms and incubators were used. In each experimental run, one set of coils was energised at random. The samples in the unenergised set were considered sham-exposed control. See also 2.1.1

2.4.2 RF-EMF exposure setup

See 2.1.2

2.4.3 Cell culture and EMF-Exposure

The human neuroblastoma cell line NB69 was obtained from Dr. M.A. Mena, (Hospital Ramón y Cajal, Madrid) and cultured in Dulbecco's Minimum Essential Medium (D-MEM) supplemented with 15% (ELF-EMF) or 10% (RF-EMF) heat inactivated foetal calf serum (FCS, Gibco), 2 mM L-Glutamine and 100 U/ml penicillin / 100 U/ml streptomycin. The cells were grown at 37ºC in a CO_2 incubator. In each experiment, cells were seeded at a density of 4.5 x 10^4 cells/ml in ∅ 60 mm plastic dishes. NB69 cells cultured in D-MEM were exposed and/or incubated in the presence or absence of retinoic acid (RA). In the experiments with RA, 40 dishes were supplemented with 0.0 µM (20 dishes) or 2.0 µM all trans RA (20 dishes) in absolute ethanol dissolved (1:1000) in culture medium. This vehicle was proven not to affect significantly cell growth when compared to cultures treated with the same volume of medium alone. In the RF-EMF experiment, cells were seeded at a density of 4.5 x 10^4 cells / ml in ∅ 35 mm dish (NUNC) in 12 dishes, supplemented with 0.0 ng/ml (6 dishes) or 20 ng/ml of bFGF (human recombinant, Boehringer Mannheim GmbH, 6 dishes). Immunocytochemical and *in situ* hybridisation studies were carried out 4 days post-plating.

Isolated embryonic neural stem cells

Striata from E15 Sprague-Dawley rat embryos were dissected and mechanically dissociated. Cell suspensions were grown in a defined medium (DF12), composed of Dulbecco's modified Eagle's medium and Ham's F-12 (1:1), 2 mM L-glutamine, 1 mM sodium piruvate (all from Gibco BRL, Life Technologies Inc, Grand Island, New York), 0.6% glucose,25 mg/ml insulin, 20 nM progesterone, 60 µM putrescine, and 30 nM sodium selenite (all from Sigma Chemical Co, St Louis, MO), 100 mg/ml human transferrin and 50 ng/ml human recombinant EGF (both from Boehringer Mannheim GmbH, Germany). After a minimum of five passages, cells were plated at a density of 500.000 cells/dish (Ø 35 mm) on 12 mm glass coverslips coated with 15 µg/ml poly-l-ornithine (immunocytochemistry) or 50 µg/ml poly-l-lysine (in situ hybridisation). The cultures were maintained in DF12 and EGF for 3 days and then switched to DF12 without EGF for longer culture periods. Immunocytochemical and in situ hybridisation studies were carried out at day 3 post-plating. For additional information see Reimers et al., (2001). Neural stem cells (NSCs) are self-renewable, multipotential cells capable of differentiating into the three major neural cell types. The mechanisms, involved in the regulation of NSC's differentiation are not fully understood.

Test for cellular response to retinol (ROL) or retinoic acid (RA)

Different concentrations of ROL and RA were selected within the physiological range in mammals: 0.1 µM to 5 µM. Cells were seeded and supplemented with ROL concentrations of 0.0, 0.1, 0.5, 1.0, 2.0, or 5.0 µM or with RA concentrations of 0.0, 0.5, 1.0, 2.0, or 5.0 µM. Seventy-two hours after plating, the medium was removed and replaced with fresh medium supplemented with the corresponding ROL or RA concentrations. Each of the retinoid concentrations was triple tested (a total of 15 petri dishes per experimental replicate), and a total of 3 experimental replicates were carried out. At the end of five days of incubation in the absence or presence of ROL or RA the cells were scrape-collected in 1 ml of culture medium. Aliquots of the cell suspensions received 1 ml of 0.4% Trypan Blue, and the number of total cells and of viable cells were calculated using a Neubauer chamber. Each sample was double counted.

ELF-EMF exposure conditions

In each experimental replicate 20 dishes with cells (10 with 0.0 µg/ml RA and 10 with 2.0 µg/ml RA) were incubated for three days inside pairs of unenergised Helmholtz coils placed in a shielded chamber, inside a 5% CO_2 incubator, at a 37ºC and 100% RH atmosphere. At the end of day 3 the media were renewed and 10 dishes (5 with 0.0 µg/ml RA and 5 with 2 µg/ml RA) were placed in one incubator; the remaining ten dishes (5 with 0.0 µg/ml RA and 5 with 2 µg/ml RA) were placed in an identical incubator. Both incubators were used, in a random sequence, alternatively for MF exposure and sham-exposure. The exposed group was treated intermittently, 3h on/3h off, to 50 Hz ELF-EMF at 10 or 100 µT magnetic flux densities (MFD) for 42h or 63 hours. At the end of this period the cells were checked for appropriate viability and proper inmunocytochemical characteristics before being processed for analysis of their responses to the physical and chemical treatments. Spectrophotometric analysis of total protein and DNA contents were done following the methods described in Mena et al., (1995). As we described below, cell counting by Trypan Blue exclusion, BrdU incorporation in DNA, PCNA labelling and flow cytometry were assayed in cells exposed to 10 or 100 µT as an estimation of the proliferative activity of NB69 cell line. The percent of apoptotic cells was estimated with TUNEL-labelling (TdT-mediated dUTP nick labelling) and the expression of the phosphorilated cyclic adenosine monophosphate response-element binding protein (p-CREB) was analysed using phosphorylation site-specific antibodies. Assays and analysis were performed blinded to treatment condition. The statistical test used was ANOVA followed by Student's T-test for unpaired data.

RF-EMF exposure condition

Neural stem cells (NSC) and NB69 cells grown on coverslips were exposed for 21 or 24 hours, respectively to 1800 GSM signals (Talk, Basic, CW and DTX signals), at 1-2 W/kg SAR), in 5 min On/10 min Off cycles. In the experiments with neural stem cells a total of 10 replicates were carried out. In each replicate a total of 12 dishes (with three coverslips per dish) were RF-EMF-exposed or sham-exposed, in groups of 6 samples. In the experiments with human neuroblastoma cells a total of 27 replicates were carried out. In each replicate a total of 12 dishes were exposed, in groups of 3 samples, to one of the following treatment combinations: untreated controls, bFGF alone, EMF alone, bFGF + EMF. The sham-exposure and the RF-EMF exposure were carried out inside shielded chambers (IT'IS Setup, Schuderer et al., 2001), in a 5% CO_2, 37ºC and 100% humidity atmosphere. At the end of the 21-h (NSC) or 24-h (NB69) period of RE-EMF exposure or sham-exposure the cell responses were checked for appropriate viability and proper inmunocytochemical characteristics before being processed for analysis of their responses to the physical and chemical treatments through Trypan Blue exclusion, immunocytochemical and in situ hybridisation studies.

Cell counting and cell viability

After treatment the cells were detached from culture dishes and resuspended in 1 ml of media. The cell number was determined in aliquots of 50 µl using a haemocytometer and each sample was double-counted by Trypan Blue exclusion. Doubling time (DT) of proliferating cells was calculated according to Falasca et al., (1999) using the formula DT = T2 - T1 / 3.32 log (X2 / X1), where T1 and T2 are the culture times in hours, and X1 and X2 are number of cells at the corresponding time. The ANOVA test followed by Student's T-test for unpaired data was used for statistical significance ($p < 0.05$).

2.4.4 Immunocytochemical characterisation of NB69 Cells

Cells were grown in Ø 60 mm dishes onto 12 mm-diameter round coverslips for immunocytochemical detection. After fixation with 4% (wt/vol) paraformaldehyde in 0.1 M phosphate buffer, the cells were incubated for 30 min in a blocking solution containing 2.5% (wt/vol) BSA in phosphate-buffered saline (PBS) to prevent non-specific antibody binding. The same solution was used to dilute the different antibodies. Cells were successively incubated with a mouse monoclonal antibody raised against the neuron-specific intermediate filament BIII-tubulin, and for the astrocyte-specific glial fibrillary acidic protein, GFAP), (1:1000, Promega; 1:300, Sigma, respectively). Nestin immunostaining was carried out by 1:5000 dilution of a rabbit antiserum, followed by an anti-rabbit IGL labelled with FITC (1:200; Jackson ImmunoResearch, West Grove, PA, USA).

2.4.5 Immunocytochemical characterisation of neural stem cells (NSC)

EGF-expanded neurospheres were seeded onto adherent substrate and treated with EGF during their first 3 days in culture, in order to enhance expansion of precursor cells. After this period the mitogen was withdrawn, and cells grew in a defined medium, which promoted cell differentiation to neurons, astrocytes and oligodendrocytes. Between 2h and 3 days, the cultures, mainly contained nestin-positive, undifferentiated precursors. At later stages, the total number of cells dropped, as a gradual loss of nestin content occurred, together with and an enhancement in the differentiation processes of neurons, oligodendrocytes and astrocytes.

2.4.6 Immunocytochemical staining for the Cell Nuclear Antigen (PCNA).

PCNA, the auxiliary component of DNA polimerase delta, is a proliferation-induced, 36 kD nuclear protein. The expression of PCNA in tissues has been found to be correlated with proliferative activity. In fact, it has been suggested (Kawasaki et al. 1995) that PCNA levels may reflect differences in the proliferative activity of neuroblastomas, as they evolve through different stages of the disease. However, PCNA is also necessary for nucleotide-excision repair of DNA. In the present work, we estimate PCNA positive cells in eight experiments with cells exposed to the MF at 10 µT on day 3 after plating. At the end of the 42-h exposure period, PCNA positive cells were determined by immunostaining, using PCNA-labelling and Hoechst for quantification of total number of cells. Cells were stained with 2 µg/ml Hoechst dye 33342 for 10 min at room temperature, studied and photographed with fluorescence microscope. In a total of 13 experiments the cells were exposed to the MF at 100 µT on day 3 after plating, and processed for PCNA labelling at the end of the 42 and 63-h exposure (day 5 and 6 postplating). The proportion of PCNA+ cells was quantified by counting 15 microscope fields per coverslip, in a total of 4 coverslips (two control and two exposed) per experimental replicate. All determinations were carried out following blind protocols.

2.4.7 5-bromo-2'-deoxyuridine (BrdU) labelling for identification of cells synthesising DNA.

Samples exposed to 100µT were labelled with BrdU at different times during the exposure period: Time 0 of exposure, (day 3 after plating); time 21h (day 4) or time 42h (day 5). The cells were always analysed 21 hours after the BrdU application, i.e. at 21, 42 or 63 hours of exposure. The results were compared to those in the respective controls (BrdU-treated, MF-unexposed). The analysis was performed through total cell number counting (Trypan Blue exclusion protocol) and by quantification of anti-BrdU antibody positive cells. The proportion of BrdU+ cells was quantified by counting 15 microscope fields per coverslip, in a total of 4 coverslips per experimental replicate. All determinations were carried out following blind protocols.

2.4.8 Flow cytometry assay

DNA content and cell cycle phase distribution were analysed by flow cytometry with propidium iodide DNA staining, in cells exposed to 100 µT for 42 or 63 hours (day 5 or 6 post-plating, N= 3 or 6 experiments, respectively, with two replicates per experimental condition). Cells were harvested, fixed with 70% ethanol and incubated with RNAse A (100 µg/ml) and the DNA intercalating dye propidium iodide (20 µg/l) in citrate buffer (3.4 mM). The cell cycle phase analysis was performed by flow cytometry using a Becton Dickinson FAC flow cytometer and Becton Dickinson CellQuest software. All determinations were carried out following blind protocols.

2.4.9 Apoptosis assay

In order to investigate the potential influence of 50 Hz MF on apoptosis the percent of apoptotic cells was estimated with TUNEL-labelling (TdT-mediated dUTP nick labelling) after 63 hours of exposure. Additional assays for apoptosis were carried out through flow cytometry in propidium iodide-stained neuroblastoma cells, exposed to the MF for 42 or 63 h (N= 7 experimental replicates).The distribution pattern of apoptotic nuclear DNA was determined using a Becton Dickinson FAC flow cytometer and Becton Dickinson CellQuest software. Three additional experiments were conducted and the cellular

response was analysed through TUNEL procedure. After fixation in 4% paraformaldehide, cells were washed with PBS, permeabilised with 0.1% Triton X-100 in 0.1% sodium citrate, washed again with PBS, and incubated for 60 min at 37ºC with biotin-conjugated dUTP in a TdT (terminal deonucleotidyl transferase, 25 U/ml) catalysed reaction (Roche Molecular Biochemicals) in a humidified atmosphere in the dark. The labelled nuclei (dUTP) were revealed with 3,3'-diaminobenzidine. The cells were counterstained with methyl green. *In situ* labelled nuclei were quantified by image analysis and photographed under light microscope. All determinations were carried out following blind protocols.

2.4.10 Immunocytochemical staining for the expression p-CREB

CREB is a nuclear transcription factor that regulates expression of genes controlling cell proliferation, differentiation, and survival. In fact, this protein is known to play an important role in neuronal survival and plasticity. Besides, different alterations of the CREB family of transcription factors have been observed in tumours. The cells were grown on coverslips. The MF-exposed samples (50 Hz; 100 µT, 30 or 60 minutes exposure) and their respective controls were labelled at the end of the exposure period for 30 min, 60 min, or 2 hours using phosphorylation site-specific antibodies. As positive controls, samples were treated with bFGF at a concentration known to activate p-CREB immunoreactivity in neuronal cells. The proportion of p-CREB cells was quantified by counting 15 microscope fields per coverslip, in a total of 4 coverslips per experimental replicate. All determinations were carried out following blind protocols. For analysis of Ser^{133}- phosphorilated CREB and total CREB, Western blotting was performed on 2 $x10^6$ cells per experimental point. Cell pellets were added at 4ºC with a lysis buffer containing 1% deoxycholate, 1 µg/ml aprotinin, 2 µg/ml leupectin, 1 mM phenylmethylsulfonyl fluoride, and 1mM sodium orthovanadate for 10 min. Cell lysates were sonicated and either immediately processed by Western or kept frozen until assayed. Protein concentration in the samples was estimated by the method of Lowry et al., (1951). Equivalent (50 µg) amounts of proteins per sample were subjected to electrophoresis on a 10% sodium dodecyl sulphate-acrilamide gel. The gel was then blotted onto a nitrocellulose membrane. Blotted membranes were blocked for 1h in a 4% suspension of dried skimmed milk in PBS and incubated overnight at 4ºC with a rabbit polyclonal anti-P-CREB serum; against the phosphorilated Ser133 form of CREB (1:1000 dilution). The membranes were washed and incubated for 1h at room temperature with peroxidase-conjugated anti-rabbit immunoglobulin G (dilution 1:1000). Specific reactions were revealed by the ECL Western blotting detection reagent (Amersan Biosciences).

2.4.11 Indirect immunocytochemistry

Rabbit polyclonal antibodies and mouse monoclonal antibodies against neural antigens and receptors for FGF were used as primary antibodies for indirect immunocytochemistry. Polyclonal anti-FGFR1, anti-FGFR2 and anti-FGFR3 were purchased to Santa Cruz Biotechnology Inc. Burlingame, CA. Anti-GFAP was obtained from Dakopatts a/s, Glostrup, Denmark. Monoclonal antiβ-tubulin isotype III and anti-GFAP were obtained from Developmental Studies Hybridoma Bank (University of Iowa), Sigma Chemical Co, and Boehringer Mannheim GmbH, respectively. Secondary antibodies raised in goat against rabbit, and in sheep against mouse immmunoglobulins, conjugated to alexafluor were purchased to Jackson Boehringer Mannheim GmbH. After appropriate culture time, cells grown on poly-l-ornithine coated coverslips were fixed with 4% paraformaldehyde for 10 min, rinsed 3 times in phosphate-buffered saline, then blocked with 10% foetal calf serum, and subsequently incubated in primary antibodies for 1 hour at room temperature (for growth factor receptors). Permeabilisation for intracellular antigens was achieved by incubation with ethanol acetic solution at –20ºC for 20 min. To assess non-specific binding for each antibody, adjacent cultures were incubated in buffer, without primary antibody. For dual labelling, primary antibodies generated by different species were added together. Secondary antibodies were administered for 45 min in the dark at room temperature. The coverslips with cells were mounted in a medium containing p-phenylenediamine and bisBenzimide (Hoechst 33342, Sigma Chemical Co). In selected experiments, FGFR1 was immunoperoxidase detected, using a biotin-linked (Vector Laboratories Inc, Burlingame, CA), instead of a fluorescence-linked secondary antibody, followed by incubation with an avidin-biotinylated horseradish peroxidase complex (Vectastain Elite ABC Kit, Vector Laboratories Inc). Finally, peroxidase was developed with 0.05% DAB, 0.005% hydrogen peroxide. The samples were counterstained with haematoxylin.

2.4.12 Hybridisation histochemistry

The hybridisation protocol has been adapted for all cell cultures from that reported by Simmons et al. (1989). The cells were fixed with 4% paraformaldehyde for 30 min at room temperature, dehydrated, air dried for 2 hours, and stored at –80ºC. Before hybridisation, the cultures were treated with proteinase K at a doses ranging from 0.1 to 1 µg/ml for 10 min at 37ºC, acetylated with acetic anhydride, dehydrated and air dried. Each coverslip was overlaid with 50 µl of hybridisation solution (50% formamide, 0.3M ClNa, 10mM Tris pH 8.0, 1mM EDTA, 0.5 mg/ml transfer RNA, 0.5 mg/ml total yeast RNA, 1x Denhardt's solution, 10% dextran sulphate, 10 mM DTT) containing $1x10^7$cpm/ml [^{35}S]-radio-labelled probe (FGFR1, FGFR2, FGFR3, FGFR4 cRNAs). In each experiment parallel cultures were hybridised with the complete probes and with the hydrolysis product of each type of probe. Alkaline hydrolysis was performed by incubating probes at 60ºC with bicarbonate buffer, pH 10.2, during appropriate periods of time, in order to obtain fragments of 250 bp. Hybridisation was carried out at 55ºC overnight, and thereafter coverslips were treated with 20 µg/ml ribonuclease A for 30 min at 37ºC. Coverslips were washed at increasing stringency with the final wash in 0.1x SSPE (10mM NaH_2PO_4, pH 7.4, 0.15M NaCl, 1mM EDTA), containing 1mM DTT, for 1 hour at 45ºC. After dehydration, cultures were air dried for 2 hours. In order to facilitate subsequent manipulation of coverslips, they were fixed to slides with DPX, so that 2 similar cultures, hybridised with the antisense and sense probes respectively, were attached to the same slide. Cultures were exposed to X-ray film for 5 days, and then dipped in Kodak NTB-2 liquid autoradiographic emulsion, and exposed for 4 weeks at 4ºC prior to development in Kodak D-19. Finally, the cultures were counterstained with haematoxylin and eosin and analysed.

2.4.13 Nucleic acid probes

[^{35}S]-UTP (ICN Pharmaceuticals Inc, Irvine, CA) labelled probes were synthesised in a run-off transcription reaction, using T3 or T7 and SP6 or T7 polymerases to generate antisense or sense RNAs, respectively.

2.4.14 Analysis of inmunocytochemical data

The results were expressed as mean ± SEM from 4 to 6 independent experiments (per treatment) done in duplicates (two coverslips). Where indicated, data are normalised in relation to their own controls, and represent the mean ± SEM of two coverslips from 4 independent experiments. In each coverslip, 30 predetermined visual fields (400X amplification) were counted under fluorescence microscopy through a program of Image Analysis. Statistical analyses were performed using Student's T test, and differences were considered significant when $p \leq 0.05$.

2.5 Experiments with human lymphocytes and thymocytes and embryonic stem cells of mice during cardiac differentiation (Participant 8)

2.5.1 ELF-EMF exposure setup

The ELF-EMF exposure setup used by Participant 8 is based on two unshielded 4-coil systems arranged in the same incubator; B-fields up to 1 mT (50 Hz) can be applied (see 2.1.1). It was composed by two systems, one used for the active exposure and one used as sham. Each system was composed by four circular coils; each coil being double-wrapped, in order to obtain a wound (active) or counter-wound (sham) configuration. The characteristics of the coils were the following: internal radius of the top and bottom coils 9.2 cm, numbers of turns 40 (20+20); internal radius of the two central coils 6.6 cm, numbers of turns 40 (20+20); distances between the coil centres 7.9 cm. The coil configuration was calculated in order to have a large zone of high uniformity (1%). The two systems were powered in series by an home-made DC amplifier connected to a function generator (Beckman FG3A). The ELF set up was kept inside a commercial CO_2 incubator (HeraCell) and the temperature was monitored by means of an high precise thermoresistor. At variance with the ELF set up used by Participant 4 the automated blind protocol was not implemented in the system by means of a suitable switcher and the experiments were

done in blind by the experimental protocol.

2.5.2 RF-EMF exposure setup

See 2.1.2

2.5.3 Cell proliferation by ^{3}H-TdR incorporation test

Peripheral blood mononuclear cells (PBMCs) from 20 young donors, were separated by centrifugation on Histopaque-1077 (Ficoll Histopaque, Sigma Chemical, St. Louis, MO, USA) discontinuous density gradient (Böyum 1968). One hundred µl of cell suspension containing 10^5 PBMC in complete medium (RPMI 1640 with 2 mM glutamine, 100 U/ml penicillin, 100 µg/ml streptomycin and 10% heat-inactivated AB serum from a pool of 10 human donors) was distributed in microplate wells (Costar, Cambridge, Ma, USA) and added with 0.1 ml of medium with or without mitogen. The following mitogens were used to promote lymphocyte proliferation: phytohemoagglutinin (PHA-P, Difco, Detroit, MI, USA) at the final concentrations of 0.1, 1, 5 and 10 µl/ml; anti-CD3 monoclonal antibody (mAb) (OKT3, an IgG2a mAb, from ATCC, Rockville, MD, USA) at the final concentration of 10 ng/ml. Each point was performed in quadruplicate. Cultures were incubated and sham-exposed or exposed to 50 Hz magnetic field (50 µT) for 2 up to 6 days (5% CO_2 in a humidified atmosphere). ^{3}H-methyl-thymidine (^{3}H-TdR, Amersham Int., UK, specific activity 5 Ci/mM) was added for the last 6 hours of culture (0.5 µCi/well). At the end of the incubation period, PBMC were harvested and washed on fibre filters by a multiple cell culture harvester (Skatron, Norway); ^{3}H-TdR incorporation was measured by liquid scintillation counting (*b*-counter, Beckman).

2.5.4 Cell proliferation by flow cytometry

PBMCs from young donors were marked by using the fluorescent cell tracer Carboxyfluorescein diacetate, succinimidyl ester (CFDAse, Serotec, UK). It couples irreversibly intracellular proteins by reaction with lysine side-chains and other available amine groups. Cells become fluorescent and after mitogenic stimulation (with 1 or 0.1 µl/mL PHA, phytohaemoagglutinin; in some experiments anti-CD3 10 ng/mL was also used), the dye is divided between the daughter cells. Each division results in generation of a population of cells that is marked by half of the cellular fluorescence intensity. PBMCs were cultured in petri dishes (35mm) at the concentration of $1x10^6$/mL of medium and exposed to RF. Two intermittent types of exposure were applied using Talk modulated RF signal (SAR 2 W/kg): (1) 10 min on/20 min off for 44 h; (2) 2h on/22h off for 72 hours. We performed experiments with cells from 6 donors using the former, from 11 donors using the latter. All cells were acquired and analysed after 72 h and 120 h of culture. At the end of time culture, cells were harvested and labelled by anti-CD4, anti-CD8 and anti-CD28 monoclonal antibodies (Serotec, UK), in order to discriminate helper and cytotoxic T cells with or without the co-stimulating molecule CD28, fundamental for the activation of lymphocytes.

2.5.5 Cell cycle analysis by flow cytometry

Cell cycle was analysed in PBMCs exposed either to ELF and RF-EMF. In ELF experiments, PBMCs from 9 young donors were stimulated by PHA (optimal dose, i.e. 1 µl/ml) or anti-CD3 (10 ng/mL) and exposed or sham-exposed for 24, 48, 72 and 96 hours. In RF experiments, PBMCs from 8 young donors were exposed to GSM basic signal (SAR=2W/Kg), PBMCs from 10 young and 8 elderly donors to TALK signal (SAR=2W/Kg) and PBMCs from 8 young subjects were exposed to DTX signal (SAR= 1.3 W/Kg).The exposure time was 10 minute on and 20 minute off for 44 hours.

Cell cycle analysis was performed by the method of 5-bromo-2'-deoxyuridine (BrdU) incorporation and propidium iodide (PI) staining. Briefly, at the end of the incubation period, cells were labelled with 20 µM BrdU for 30 min., centrifuged for 1 min., washed twice with 1 ml of PBS solution containing 0.5% Tween 20, and resuspended in 1 ml HCl 1N. After a 30 min. incubation at room temperature, cells were centrifuged at 300g for 1 min. washed once in 0.1 M $Na_2B_4O_7$, and added with 5 µl of anti-BrdU mAb (Becton Dickinson, San Josè, CA, USA). Cells were incubated for 60 min. at 4°C, washed twice and

resuspended in 200 µl of diluted secondary antibody (goat-anti-mouse IgG conjugated with fluorescein isothiocyanate, FITC). After a 30 min. incubation at 4°C, cells were washed twice and resuspended in 200 µl of PBS solution with 0.5% Tween 20 and 200 µl of PI working solution (50 mg/ml in 3.4 mM trisodium citrate, 9.65 mM NaCl plus 0.03% Nonidet P40). After 15 min. at 4°C in the dark, cells were acquired and analysed by flow cytometer.

2.5.6 Expression of membrane receptors on T lymphocytes by flow cytometry

Phenotypical analysis of T lymphocytes was performed in PBMCs exposed either to ELF and RF. In ELF experiments, HLA-DR and CD25 membrane expression were analysed on CD3+ T and CD4+ T helper lymphocytes respectively. The analysis was performed on cells from 9 young donors, before and after stimulation with PHA (1 µl/ml) or anti-CD3 mAb (10 ng/ml). Briefly, cells were stimulated and exposed from 24h to 72 h, collected, washed twice with cold PBS and stained with different mAbs directly conjugated with FITC or phycoerythrin (PE). The following mAbs from Becton Dickinson and from Serotec (Oxford, UK), were used: anti-CD3, recognising all T cells; anti-HLA-DR, recognising B cells and activated T cells; anti-CD4, reactive with helper/inducer T cell subset; anti-CD25, reactive with the p55 chain of IL-2 receptor. The expression of HLA-DR and CD25 molecules was studied on CD3+ and CD4+ lymphocytes at 24, 48, 72h after mitogen stimulation. In RF experiments, PBMCs from 8 young donors were exposed to GSM basic signal (SAR=2W/Kg), PBMCs from 10 young and 8 elderly donors were exposed to TALK signal (SAR=2 W/Kg) and PBMCs from 8 young subjects were exposed to DTX signal (SAR=1.3 W/Kg). CD25, CD95 and CD28 in CD4+ helper and CD8+ cytotoxic T lymphocytes, respectively, were analysed by flow cytometry technique. (In specific: CD95 is the receptor activating the pathway of programmed cell death). Lymphocytes before and after exposure to RF were phenotypically analysed. Cells, unstimulated or stimulated with anti-CD3 mAb (10 ng/ml), immediately after exposure or sham-exposure, were collected, washed twice with cold PBS and stained with three different mAbs (CD25, CD95, CD28, CD4 and CD8, Serotec, Oxford, UK) directly conjugated with FITC or phycoerythrin (PE), or tricolor fluorocromes. The analysis was performed on 10,000 lymphocytes for each sample and the three fluorescences were analysed using “paint-a-gate” software (Becton Dickinson).

We performed also from 5 up to 8 replications, using PBMCs from the same young donor. Cells were un-stimulated or anti-CD3-stimulated (10 ng/mL) and exposed or sham-exposed to TALK modulated RF (SAR 2 W/kg) for 44h (10 min on/20 min off). After exposure, cells were stained using the same protocol describe before. The following membrane molecules were analysed: CD25, CD95, CD28, CD45RO, HLA-DR on CD4+ and CD8+ T lymphocytes, respectively. Moreover, a more sophisticated analysis was performed on fluorescence distribution of CD4+ helper T lymphocytes from 10 young and 8 elderly donors

2.5.7 Spontaneous and induced apoptosis by flow cytometry

PBMCs from 8 young donors were exposed to GSM basic signal (SAR=2W/Kg), PBMCs from 10 young and 8 elderly donors to TALK signal (SAR=2W/Kg) and PBMCs from 8 young subjects were exposed to DTX signal (SAR=1.3 W/Kg). PBMCs were induced to undergo apoptosis by 2-deoxy-D-ribose (dRib) (Barbieri et al, 1994), which acts through an oxidative pathway (Monti et al. 2000) and the early stage of apoptosis was assessed by Annexin-V and propidium iodide kit (ANX-V , Bender, Vienna, Austria) using flow cytometry technique. Briefly, cells were collected, washed in PBS and resuspended in 200 µL of ANX-V binding buffer (10 mM Hepes/NaOH pH 7.4, 140 mM NaCl, 2.5 mM $CaCl_2$), stained with 5 µL of ANX-V and incubated for 10 minutes at room temperature. Then, cells were washed with binding buffer to remove the excess of ANX-V, resuspended in PBS, counterstained with 5 µg/ml PI and analysed by flow cytometry. ANX-V, the probe used for the detection of early stage apoptotic cells, is able to recognise phosphatidylserine (PS) when present on the outer leaflet of the plasma membrane. It is well known that PS is normally found only on the inner leaflet of the cell membrane double layer, but it is actively transported to the outer layer as an early event in apoptosis and becomes available for annexin binding (Green and Steinmetz 2002).

2.5.8 MMP modifications in induced and spontaneous apoptosis

PBMCs from 8 young donors were exposed to GSM basic signal (SAR=2W/Kg), PBMCs from 10 young

and 8 elderly donors to TALK signal (SAR=2W/Kg) and PBMCs from 8 young subjects were exposed to DTX signal (SAR=1.3 W/Kg). Changes in MMP have been evaluated by using the lipophilic cationic probe JC-1, which changes reversibly its colour from green to orange as MMP increases (over values of about 80-100 mV). This property is due to the reversible formation of JC-1 aggregates upon membrane polarisation that causes a shift in the emitted light from 530 nm (*i.e.*, emission of JC-1 monomeric form) to 590 nm (*i.e.*, emission of J-aggregates) when excited at 490 nm; the colour of the dye changes reversibly from green to orange/red as the mitochondrial membrane becomes more polarised. Both colours can be detected using the filters commonly mounted on flow cytometers, so that green emission can be analysed in one fluorescence channel, and orange/red emission in the other. Briefly, cells were stained with 2.5 μg/mL JC-1 and kept at room temperature for 10 minutes, washed twice with PBS, resuspended in a total volume of 400 μL PBS and analysed (Cossarizza et al. 1993b; Salvioli et al. 1997).

2.5.9 Cytokine production by ELISA

The production of interleukin-1 β (IL-1 β) and interleukin-6 (IL-6) in unstimulated and stimulated PBMCs from young donors was determined in the surnatant of cultures. Two types of stimuli were used: a) 10 ng/mL anti-CD3, b) 10 ng/mL TPA (12-O-tetradecanoylphorbol-13-acetate) plus 1 μ/mL PHA (phytohaemoagglutinin). PBMCs from 26 donors were stimulated with the former and 24 were stimulated with the latter. The second stimulus is stronger than the first, since it is directed on monocytes. PBMCs were exposed both to GSM talk (2 W/kg SAR) and DTX only (SAR 1.4 W/kg) RF for 44 hours (10 min on/20 min off). At the end of time culture, surnatants were harvested and frozen. After the collection of all the samples we analysed the presence of cytokines by ELISA (Enzyme linked Immuno-adsorbant assay), a well known immuno-enzimatic method, by which cytokine is revealed by a coloured end-product. By using an ELISA plate reader final data are produced as pg/mL units.

2.5.10 Hsp70 levels in induced and spontaneous apoptosis by flow cytometry

PBMCs, obtained from 7 healthy young donors, were treated by 2-deoxi-d-Ribosio (dRib, 10 mM) for 44 h and in the meantime cells were exposed to RF (GSM Talk signal, SAR 2W/kg; 10 min ON and 20 min OFF). Detection of intracellular Hsp70 was performed by flow cytometry techniques (Bachelet et al., 1998). At the end of culture, cells were collected, fixed and permeabilised by ethanol 95% and acetic acid 5% for 15-30 minutes, at -20°C. Then, cells were washed with PBS with 1% of BSA and labelled with Hsp70 primary antibody (Mouse IgG, 70 KDa for human target, Pharmingen, BD, San Josè, CA, USA) for 1h at 4°C in the dark. Then, cells were incubated with a secondary fluorescent antibody (GOT anti-mouse, Becton Dickinson), FITC conjugated (isothiocyanate of fluorescein) for 30 min at 4°C in the dark. At the end of the incubation cells were washed and analysed by flow cytometer (FCScalibur, BD). Fluorescence intensity was evaluated by CellQuest® programme.

2.5.11 Thymocyte development and apoptosis by HTOC and flow cytometry

Pieces of human thymus were obtained by cardio-surgery from S.Orsola-Malpighi Hospital (Bologna, Italy) from 6 human newborn. (5 days-8 months). Small fragments of tissue (2-3 mm^3) were cut and cultured above a sterilised filter on a small piece of gelfoam which was embedded of medium (20% of FCS, 1% of penicillin-streptomycin, 79% of DMEM). Each gelfoam was placed inside the Petri dishes containing the DMEM medium. This is a standard technique used to analyse in vitro thymocyte differentiation (Anderson and Jenkinson 2000). Human thymus organ cultures (HTOC) were incubated for 48 h, but the exposure (or sham-exposure) was performed only during the first 24h (DTX only at SAR 1.4 W/kg; 10 min on / 20 min off). At the end of culture (48 h), thymocytes were separated by gentle pressing through a fine stainless steel screen submerged in PBS. Single cell suspensions were obtained by passing the cells through a steel filter, and washing twice in PBS. Thymocytes were directly labelled with FITC or PE conjugated mAbs; such as, CD4, CD8, αβTCR (T cell receptor), γδTCR, CD71 (transferrin receptor on proliferating cells) and CD16 (receptor for IgG) in order to discriminate different phenotypical phases of differentiation. Moreover, apoptosis and viability were assessed by annex-V (see the methods described above) and PI staining, respectively. 10,000 cells from each sample were acquired by flow cytometer and analysed by paint-a gate-software.

2.5.12 T lymphocyte gene expression by microarray technology

Quiescent T lymphocytes were separated by MACS® (Magnetic Cell Sorting, Miltenyi Biotec, Germany). Three samples were obtained from control cultures, sham-exposure and exposure to DTX only RF for 44h (10 min on/20 min off). These samples were sent to Participant 12 for gene expression analysis by microarray technology. Data analysis were performed in Bologna by Participant 8.

2.5.13 Cell culture of embryonic stem cells and EMF-Exposure

GTR1 ES cells, a derivative of R1 ES mouse cells (Nagy 1993) bearing the puromycin-resistance gene driven by the cardiomyocyte-specific MHC promoter (GTR1 cells were kindly provided by Dr. William L Stanford (University of Toronto and Centre for Modelling Human Disease, Canada). ES cells were maintained in the undifferentiated state by culturing in DMEM containing 15% FBS, supplemented with a final concentration of 1000 U/ml ESGRO-LIF (LIF). To induce cardiac differentiation, cells were plated onto bacterial Petri dishes, containing DMEM lacking supplemental LIF. After 2 days of culture, the resulting embryoid bodies (EBs) were plated onto tissue culture dishes. When spontaneous contractile activity was noticed, puromycin (2 µg/ml) was added to eliminate non-cardiomyocytes. After 2 days, puromycin-selected myocytes were transferred to new tissue culture dishes. As indicated in the legend of each figure, EBs, collected at several stages after plating, as well as puromycin-selected cells, were processed for gene expression analyses. Following LIF removal and throughout puromycin selection, GTR1 cells were exposed to ELF-EMF (50 Hz, 0.8 mT_{rms}).

2.5.14 Analysis of mRNA expression

Expression of GATA-4, Nkx-2.5, prodynorphin, alpha-myosin heavy chain and myosin light chain-2V mRNA was assessed by RT-PCR as previously described (Ventura 2000), using GAPDH mRNA as a measure of equal loading and mRNA stability. GATA-4 mRNA levels were also quantitated by RNase protection assay, as described elsewhere (Ventura 1997, Ventura 2003a, Ventura 2003b). Briefly, fragments of the main exon of the mouse GATA-4 (292 bp) gene was inserted into pCRII-TOPO (Invitrogen, CA). Transcription of the plasmid linearised with *BamHI* generated a sense strand of GATA-4 mRNA, which was used to construct a standard mRNA curve. Transcription in the presence of [^{32}P]CTP (800 Ci/mmol) (Amersham International) of plasmids linearised with *Xba*I produced an antisense strand of GATA-4 mRNA (radio-labelled cRNA probe). Samples were then incubated with a combination of RNase A and T1 and exposed to proteinase K. The protected fragments were recovered after phenol chloroform extraction and electrophoretically separated in a polyacrylamide non-denaturing gel. Autoradiographic exposure was performed for 48h. The individual bands were counted for radioactivity by liquid scintillation spectrometry, and cpm values were translated to pg values on a correlated standard curve. Data were expressed as pg of mRNA/µg of total RNA.

2.5.15 Transcriptional analysis in isolated nuclei

Nuclear run-off was performed. 90 µl of nuclear suspension were added with 100 µl of 2 x reaction buffer (10 mmol/L Tris/HCl, pH 7.5, 5 mmol/L $MgCl_2$, 0.3 mol/L KCl, 5 mmol/L dithiothreitol, 1 mmol/L each of ATP, GTP, and CTP), and 5 µl of [α-^{32}P]UTP (3000 Ci/mmol), followed by incubation at room temperature for 15 min. DNA was digested by incubating the transcription mixture for 5 min at room temperature in the presence of 1 µl of 20,000 units/ml RNase-free DNase. Equal counts of ^{32}P-labeled nuclear RNA (about 5 x 10^6 cpm) were then subjected to a solution hybridisation RNase protection assay and were hybridised for 12h at 55°C in the presence of unlabelled antisense GATA-4 mRNA Samples were then incubated with a combination of RNase A and T1 and exposed to proteinase K. The protected fragments were recovered after phenol chloroform extraction and electrophoretically separated in a polyacrylamide non-denaturing gel. Autoradiographic exposure was for 48h. ^{32}P-labeled nuclear RNA was also hybridised with unlabeled antisense cyclophilin mRNA synthesised from a *Nco*I-linearised pBS vector containing a 270-base pair fragment of plB15, a cDNA clone encoding for rat cyclophilin (6). Cyclophilin mRNA was utilised as a constant mRNA for control.

2.6 Experiments with brain cells of different origin and human monocytes and endothelial cells (Participant 9)

2.6.1 Exposure setup and exposure conditions

The wire-patch cell (WPC) is the setup that was used for exposure to frame-scheme (FS) GSM-900 signals. This exposure system accommodates 8 Petri dishes to be built as a double Petri dish, i.e. a 3.5-cm diameter Petri dish (where cells are cultured) is positioned inside a 5-cm diameter dish (outer dish with distilled water inside). Two double Petri dishes are pilled-up and placed in the wire-patch antenna (Figure 3) so that a total of 8 dishes can be exposed at a time. Two successive WPC models were used. The second one shown in Figure 1, built by Participant 10, was fitted with electric field probes that allowed monitoring of the SAR in real time.

Cells were cultured in 3.2 ml of culture medium and the outer Petri dishes are filled with 5 ml of distilled water. Cultured cells in Petri dishes were placed in a standard CO_2 air-flow incubator inside a WPC for a minimum of 3 hours to allow for temperature stabilisation. Sham exposed samples were treated in the same way in a non-activated WPC placed in a second, identical incubator. Each WPC was fitted with a square annular ring made of absorbing foam (Figure 3) to block emission sideways towards the metallic walls of the incubators and allow for a good adaptation at 900 MHz. The foam is sealed with waterproof lining.

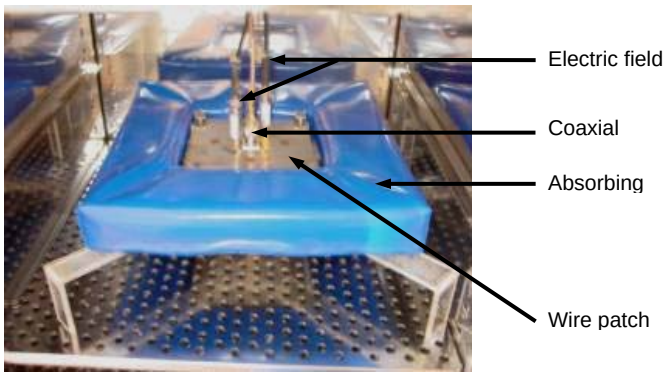

Figure 3. Image of a wire-patch antenna surrounded by the absorbing foam in a dedicated incubator

Dosimetry

The WPC's dosimetry (temperature measurement and modelling) was performed in collaboration with French experts (P. Lévêque, IRCOM, France and J. Wiart, France Télécom R&D). A good efficiency was found (around 0.6 W/kg per incident watt) and the uniformity for cell exposure was found to be very good (ca. 15%) (Figure 4). Experimental Specific Absorption Rate (SAR) evaluation was undertaken in order to validate the data obtained by numerical dosimetry (see Participant 10). Based on the measurement of temperature increase after the RFR generator was turned on, this technique gives also information on the thermal consequences at the level of the whole setup. Temperature was recorded in the inner part of a double Petri dish using optical fibres (Luxtron probes, that are immune to the microwaves), as well as in the incubator throughout the first hours of exposure (until temperature stabilisation was reached). Temperature measurements also showed that it took at least 2 hours for temperature to equilibrate, after the cell cultures were introduced, in the absence of microwaves. This needed to be taken in account in the exposure protocol. Experimental dosimetry showed that the mean SAR was 0.77 W/kg at the level of the cell monolayer, which is in good agreement (within 15%) with numerical data. The corresponding temperature rise was 0.2°C (i.e. temperature difference between the Petri dish inner part and the incubator).

Since heating is produced by absorption of the microwaves by the samples, care was taken to keep the temperature of the exposed and sham-exposed samples identical during the experimental trial. For that purpose, the “exposed “ incubator temperature was first set at a lower value than that of the “sham” side, depending on the SAR level chosen for a given experiment. For a SAR of 2 W/kg for instance, the temperature difference was 0.5°C for an input power of 3.4 W, in very good agreement with numerical FDTD modelling (Figure 4) Those data have been confirmed for quality control purposes by Participant 10.

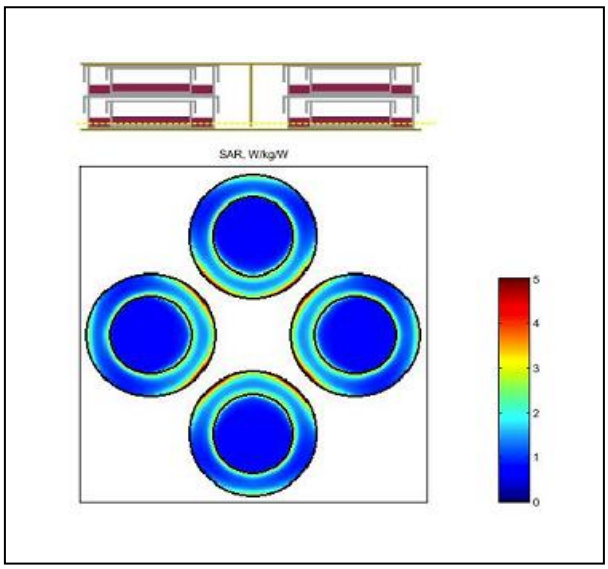

Figure 4. FDTD simulation of SAR in the Petri dishes (outer and inner parts) using an input power of 1 W. Upper panel shows the Petri dishes disposition in the wire-patch antenna.

2.6.2 Cell culture and RF-EMF exposure

For each exposure condition, at least three independent experiments were performed in a blind manner. For that purpose, all samples are coded prior to exposure, one researcher is in charge of exposure and codes are broken after completion of the analysis of all parameters investigated in the experiment by researchers unaware of the exposure conditions.

Culture of nerve cells

Rat primary neurons (granule cells) - a very critical cell type in the central nervous system-, rat primary astrocytes and rat C6 astrocytic cell line were used. Both primary cell types were prepared from newborn rat cerebella. Human nerve cell lines were also used to look at possible species specificity as well as at differences between transformed and normal cells. Human U87 astrocytic- and SH-SY5Y neuronal- cell lines were chosen as models.

i) Rat brain primary cultures: Primary cultures were prepared from postnatal day 4-9 (P4-P9) rat cerebella. Two types of cultures were prepared: neuronal-astroglial and glial (astrocytes) cultures.

Neuronal-astroglial cultures, with approximately 80% neurons and 20% glia in the cell population, were obtained from P4 rat cerebella. The cells were plated on polylysine-coated dishes at 10^6 cells/dish in Hanks Minimum Essential Medium supplemented with 10% horse serum. They were maintained in 3% CO_2 in air at 37°C for 4-6 days. Astrocyte cultures, where very few neurons survived, were obtained from P8 rat cerebella and plated at 10^6 cells/dish in Dulbelco Miminum Essential Medium (DMEM) supplemented with 10% fetal calf serum (FCS) and antibiotics (AB, 100 U/ml penicillin and 100 µg/ml streptomycin) and maintained in 9% CO_2 in air at 37°C for 13-15 days. For the experiments, all primary cells were plated in 35 mm diameter Petri dishes and used as it, without any further handling. The endpoint investigated in these cells was apoptosis. Rat primary neurons were sham-exposed or exposed to GSM-900 for one or 24 hours and apoptosis was evaluated following a time-kinetics (4, 8 and 24 hours

after exposure began) or immediately after exposure, respectively. Rat primary astrocytes were sham-exposed or exposed to GSM-900 for 1 hour and apoptosis was evaluated as described previously. Three to six independent experiments were performed for each exposure condition. Results are expressed as the percentage of apoptotic cells in GSM-900- exposed versus sham-exposed samples. The Student t test was used for statistical analyses.

ii) Human neuroblastoma cells: Human SH-SY5Y neuroblastoma cells (ECACC N° 94030304) were cultured in Ham's F12 medium supplemented with 15% FCS, 1% non-essential amino-acids and AB The endpoint investigated in these cells was apoptosis. Human SH-SY5Y neuronal cells – as rat primary neurons – were sham-exposed or exposed to GSM-900 for one or 24 hours and apoptosis was evaluated following a time-kinetics (4, 8 and 24h after exposure began) or immediately after exposure, respectively. Three to six independent experiments were performed for each exposure condition. Results are expressed as the percentage of apoptotic cells in GSM-900- exposed versus sham-exposed samples. The Student t test was used for statistical analyses.

iii) Human glioblastoma cells: Human U87 glioblastoma cells (ECACC N° 89081402) were grown in Eagle Minimum Essential Medium supplemented with 10% FCS, 1% non-essential amino-acids and AB. The endpoint investigated in these cells was apoptosis. Human U87 astrocytic cells -as rat primary astrocytes - were sham-exposed or exposed to GSM-900 for 1 hour and apoptosis was evaluated following a time-kinetics (4, 8 and 24h after exposure began). Three to six independent experiments were performed for each exposure condition. Results are expressed as the percentage of apoptotic cells in GSM-900- exposed versus sham-exposed samples. The Student t test was used for statistical analyses.

iv) Rat glioma cells : Rat C6 glioma cells were obtained from the European Collection of Cell Cultures (ECACC N° 85040101, UK) and maintained in DMEM-F12 medium (Biomedia, France) containing 10% fetal bovine serum (Gibco), 2 mM sodium pyruvate (Biomedia, France) and 1% antibiotics (100 U/ml penicillin and 100 µg/ml streptomycin, Biomedia, France) at 37°C in a standard culture incubator. The endpoint investigated in these cells was expression and activity of the inducible isoform of the Nitric Oxide Synthase (iNOS or NOS_2). C6 cells were sham-exposed or exposed to GSM-900 alone (0.2 W/kg or 2.0 W/kg, 48h) or in the presence of a cocktail of lipopolysacharide and cytokines CK (see below). Following RFR or sham-exposure the cells were harvested for western blot analysis and culture medium collected for the determination of nitrite accumulation, to test iNOS expression and activity, respectively. Randomised sham/sham exposures were included in the schedule of exposure, so that the engineer responsible for the analysis never was aware of any exposure condition. A total of four sham/sham exposures, six sham/exposed experiments at 0.2 W/kg and three sham/exposed experiments at 2 W/kg were conducted. The Student t test was used for statistical analyses.

Culture of immune cells

i) Human monocytes: Human U937 monocytic cells (ECACC N° 85011440) are grown as a cell suspension in RPMI 1640 medium complemented with 10% FCS plus AB. Two endpoints were investigated in these cells:

- Apoptosis in cells submitted either to a 48 hour-exposure to GSM-900 at a SAR of 0.7 W/kg or to a 1 hour-exposure at 0.7 W/kg and 2.0 W/kg followed by a treatment with camptothecin (CPT). Three to six independent experiments were performed for each exposure condition. Results were expressed as the ratio of apoptotic cells in GSM-900-exposed versus sham-exposed samples with or without CPT treatment. The Student t test was used for statistical analyses.
- Gene expression in cells submitted to a 1 hour-exposure to GSM-900 at a SAR of 2.0 W/kg.

ii) Human microglial cells: The human cloned microglial cells (CHME 5) were plated at a density of 10^6 cells/35mm diameter dishes in 2 ml of complete Dulbecco's MEM medium. Cultures were carried out for 3 days in water-saturated 5% CO_2 in air at 37°C before GSM exposure. The endpoint investigated in these cells was gene expression in cells after a 1 hour-exposure to GSM-900 at a SAR of 2.0 W/kg.

Culture of endothelial cells

Two EA.hy926 cell lines were tested: one was a generous gift from Participant 6, the other one from Dr. Cora-Jean S. Edgell who first developed the cell line and gave permission to use these cells in Bordeaux. The purpose for using both cell lines was to look at potential different behaviour of cells cultured in slightly different conditions that may have led to possible genotypic drift. Human EA.hy926 endothelial cells were cultured according to the provider's instructions.

i) EA.hy926 (a gift from Participant 6): Cells were grown in DMEM supplemented with 1% penicillin-streptomycin, 2% L-glutamine (200 mM), HAT-supplement and 10% FCS.

ii) EA.hy926 (a gift from Dr. Cora-Jean S. Edgell, North Carolina University at Chapel Hill, NC, USA): Cells were grown in DMEM supplemented with 1% penicillin- streptomycin, 2% L-glutamine (200 mM) and 10% FCS. For the RF-EMF experiments, cells were removed from culture flasks with trypsin, washed and seeded at a density of 0.26 x 10^6 cells/12 mm-diameter glass coverslips corresponding to 1.2 x 10^6 cells/55 mm-diameter dishes (as mentioned in Leszczynski et al. 2002). After an overnight culture, coverslips were transferred to 35-mm diameter Petri dishes and EA.hy926 cells were sham-exposed or exposed to RF-EMF for one hour at 2.0 W/kg. The endpoint to be studied in these cells is the expression of the heat-shock protein 27 (hsp27). EA.hy926 cells were sham-exposed or exposed to RFR for one hour at 2.0 W/kg.

2.6.3 Chemicals and other treatments

Positive controls used chemicals or other treatments. In order to look at possible interactions between RFR and chemicals, different protocols used RFR exposure combined to or prior chemical treatment.

Lipopolysaccharide plus cytokine treatment

Lipopolysaccharide plus cytokine treatment was used as a positive control for iNOS expression in C6 glial cells (Hewett et al., 1993; Nomura 1998). Two days before RFR exposure, C6 cells are plated in custom-made Petri dishes at a density of $5x10^4$ cells/dish. At the day of experiment, Petri dishes are filled with culture medium containing 4% FCS for cell deprivation. Half of the samples are treated with a cocktail of *e.coli* lipopolysacharide (LPS 10 µg/ml) and cytokines IFNγ (50 U/ml) plus TNFα (50 ng/ml) before Petri dishes are placed in the wire-patch antenna. Cells were then put in the exposure-dedicated incubators during 3 hours for temperature stabilisation before exposure to RFR started.

Camptothecin treatment

The apoptosis-inducer camptothecin (4 µg/ml, 4 hours) as a positive control in U937 monocytic cells. Camptothecin is a topoisomerase I inhibitor. As such, it inhibits the topoisomerase molecule from religating DNA strands after cleavage. This leaves a cell with DNA breaks, which if not repaired, become lethal (Holden 2001). When cells of the immune system are exposed the topoisomerase I inhibitor campthothecin, they rapidly undergo cell death via apoptosis, irrespective of what phase of the cell cycle a cell is in (Cotter 1992).

Heat shock

Positive controls for heat shock proteins (Hsp27 and Hsp70) induction were performed by exposing the different cell lines (U87, C6 and SH-SY5Y cell lines) to a heat shock at 43°C for 20 min.

2.6.4 Detection of apoptosis

The occurrence of apoptosis was assessed using two markers and flow cytometry.

Double staining with Annexin-V/FITC and propidium iodide

During apoptosis, phosphatidyl-serine is exposed on the outer leaflet of the plasma membrane that causes a loss of membrane asymmetry. Annexin V preferentially binds to phosphatidylserine (Van Engeland et al. 1998) and can be detected by flow cytometry using the APOPTEST^{TM}-FITC kit (Dako, France) according to manufacturer' instructions. Immediately after the complete treatment, cells were harvested so that all cells, including floating cells, were taken in account for the apoptotic test. Where needed, cells were scrapped (nerve cells) before being washed with PBS, and centrifuged at 200 g for 5 minutes. Cell pellet was resuspended and 10^6 cells were incubated for 15 minutes in 100 µl of cold labelling solution (1 µl of Annexin-V/FITC and 2.5µl of propidium iodide (PI) 250 µg/ml) in 96 µl of the kit's labelling buffer. Then 250 µl of labelling buffer were added and samples are analysed on a flow cytometer.

Double staining with $DiOC_6(3)$ and propidium iodide

Mitochondrial physiology is disrupted in cells undergoing apoptosis via intrinsic pathways. Mitochondrial membrane potential ($\Delta\Psi_m$) decrease has been largely described which can be measured using the

carbocyanine dye ($DiOC_6(3)$, Zamzami et al., 1995). Briefly, immediately after exposure, cells were washed and centrifuged as indicated above. Then 10^6 cells were incubated for 10-15 minutes in 500 µl of PBS containing 40 nM of $DiOC_6(3)$. Propidium iodide (2.5 µl of PI; 50 µg/ml) was added before analysis on a flow cytometer.

Data acquisition was performed using a FacScan® flow cytometer (Becton Dickinson) with the following parameters: 488 nm excitation, 515 nm bandpass filter for the Annexin V and $DiOC_6(3)$ dyes and filter > 560 nm for PI detection. Analysis was performed on 10000 events using the Cell-Quest® software. Analysis was performed blindly.

2.6.5 Western Blot analysis

Western Blotting was used for the detection of iNOS expression in C6 cells. C6 cells were lysed using RIPA buffer [0.5 mM Tris (pH 8.0), 0.5% Sodium Deoxycholate, 10% SDS,150 mM NaCl, 1% Triton X100 and protease inhibitors (16 mg/ml Benzamidin, 10 mg/ml Aprotinin, 10 mg/ml Pepstatin, 10 mg/ml Leupeptin, 10 mg/ml Phenanthroline and 1 mM Phenylmethylsulfonyl Fluoride)] using methods adapted from Schreiber et al. (1989).

Proteins were extracted from cell lysates and the concentration was determined by Bradford reaction (Biorad Protein Assay®). Protein samples (10-20µg) were electrophoretically separated through a 7.5% polyacrylamide SDS-page gel, electroblotted to polyvinylidene difluoride membranes and probed with mouse anti-iNOS (Transduction Laboratories N-39120, 1/5000°). In addition, we used ß-actin as an internal control for protein loading (all blots were de-hybridised and reprobed for ß-actin detection). Immunoreactive bands were visualised using ECL Western Blotting System® (Amersham-Pharmacia Biotech, RPN 2108) followed by exposure to autoradiography film (Biomax, Kodak). The NIH Image 1.54 software was used for blot quantitative analysis (based on OD measurements).

2.6.6 Griess reaction

iNOS activity in C6 cells was quantified as nitrites accumulation in culture media by the colorimetric assay based on the Griess reaction. 50µl of culture medium collected in triplicate from the samples were added to 60µl of Griess A solution (sulfanilamide 1% in 1.2N HCl) and 60µl of Griess B solution (Naphtylene Diamine Dichlorhydrate 0.3% in distilled water). The mixture was incubated 10 min at room temperature and red at 540 nm with a spectrophotometer. Fresh corresponding culture medium served as blank for NO_2^- content determination. Results were expressed as µg of nitrite per million cells.

2.6.7 Hsp immunolabelling and image analysis

Hsp70 expression was evaluated in human neuronal (SH-SY5Y) and rat (C6) or human (U87) astrocytic cell lines. Three days before the experiment, cells were plated on glass coverslips in 24-well plates at a density of 0.5×10^5 cells/well. The day before the experiment, coverslips were transferred to 35-mm diameter Petri dishes before being placed in the sham- and RFR-dedicated incubators.

U87, C6 and SH-SY5Y cell lines were sham-exposed or exposed to GSM-900 for 24 hours and the expression of Hsp70 was evaluated at the end of exposure. Hsp27 expression was evaluated in human EA.hy926 cells at the end of a-one hour sham- or RFR exposure at 2.0 W/kg. Following RFR or sham exposure, the cells were fixed in PBS-paraformaldehyde (4%) for immunocytochemistry. Anti-hsp70 and anti-hsp27 antibodies were obtained from Stressgen®. The first antibody was revealed using a FITC-labelled antibody. Coverslips were mounted on slides with Mowiol® before microscopy observation. For each exposure condition, three (hsp70) to five (hsp27) independent experiments have been performed in a blind manner. After immunocytochemistry labelling, fluorescence analysis was performed using the Aphelion® image software. Results are expressed as arbitrary units of fluorescence intensity.

2.6.8 RNA extraction and cDNA array hybridisation

Based on the data available within the REFLEX consortium on the effect of RF-EMF exposure on gene expression (see Participant 12), we chose two human cell lines involved in inflammatory processes (brain

human microglial and monocytes cells). Indeed, one of the gene families that were shown to be sensitive to exposure to electromagnetic fields is the gene family involved in inflammation. The human cloned microglial CHME-5 cells and the monocytic U937 cells were sham-exposed or exposed for one hour at 2 W/kg. Immediately after exposure, they were harvested for RNA extraction using Nucleospin® RNA purification kit (BD Biosciences Clontech, Palo Alto, USA). Total RNA purification was performed following user manual instructions. The amount of total RNA was measured by spectrophotometry. RNA samples were then frozen at –80°C before being sent to Participant 12 who performed cDNA array hybridisation.

2.7 Experiments with embryonic stem cells of mice (Participant 4)

2.7.1 Exposure setups

See 2.1.1 and 2.1.2.

2.7.2 Cell culture and EMF exposure

Pluripotent R1 ES cells (Nagy et al. 1993), wild type (wt) D3 (Doetschman et al. 1985) and p53-deficient ES cells (p53-/-; a gift of Dr. T. Jacks, Howard Hughes Medical Institute, Cambridge, MA, see Jacks 1994) derived from D3 cells were cultured as described (Wobus et al. 2002) except that p53-/- ES cells were maintained on neomycin-resistant SNL feeder cells (a gift of Dr. A. Bradley, Baylor College of Medicine, Houston, TX) in presence of 300 µg/ml G418. EC cells of line P19 (Edwards and McBurney 1983) were cultured without feeder cells (Wobus et al. 1994). For differentiation, P19, R1, and wt or p53-/- D3 cells were cultivated as EB in hanging drops in Dulbecco's modified minimal essential medium (DMEM, Gibco) supplemented with 20% FCS, L-glutamine, non-essential amino acids (NEAA) and β-mercapthoethanol (β-ME) as described (Wobus et al. 2002). Briefly, cells (n=400) in 20 µl of differentiation medium were incubated in hanging drops as embryo-like aggregates ("embryoid bodies", EBs) for 2 days and in suspension for 3 days. EBs were plated separately onto gelatin-coated 24-well microwell or tissue culture plates (∅ 6cm) at day 5 for morphological and reverse transcriptase polymerase chain reaction (RT-PCR) analyses, respectively. For the induction of P19 cell differentiation, EBs were cultivated in the presence of 1% DMSO (Sigma) during the first 2 days of EB development (Wobus 1994).

EBs derived from p53-/- and wt D3 ES cells were RF- or ELF-EMF- exposed in hanging drops for 6 or 48 hours (Figure 5). For 6h experiments, samples were collected immediately after exposure and used for RT-PCR analysis (Figure 5). After 48h exposure, EBs were further cultivated and samples were sequentially collected during differentiation for RT-PCR analyses. EBs derived from R1 cells were EMF (GSM-217)- or sham-exposed in hanging drops (SAR: 1.5 W/kg) for 2 days and in suspension (SAR: 2.0 W/kg) for 3 days. P19 cells (n=200,000) were seeded into 0.1% gelatin-coated tissue culture dishes, cultured in DMEM (see above) and after 2h pre-incubation at 37°C placed into the exposure setup for EMF and sham-exposition. As control, non-exposed cells were cultured in a separate humidified 5% CO2 incubator at 37°C. P19 cells were exposed to EMF at SAR value of 2.0 W/kg for 22 or 40h. After exposure, cells were immediately processed for flow cytometric analysis (P19), and in parallel, R1 and P19-derived EBs were prepared for differentiation and RT-PCR analysis

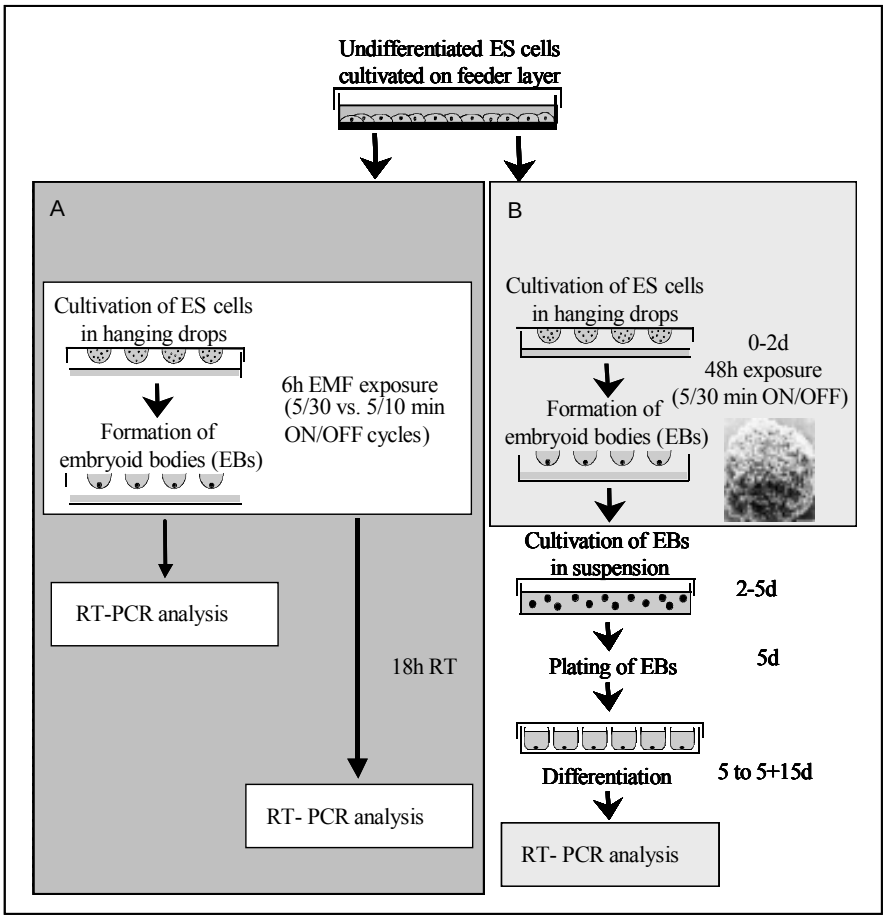

Figure 5. Experimental protocol for the exposure of undifferentiated and differentiating ES cells to EMF. Wild type (wt) and p53-deficient (p53-/-) D3 ES cells were grown on feeder layer. (A) ES cells were RF-EMF or PL-MF exposed for 6 h at the initial stage of hanging drop formation, when the differentiation processes are initiated. mRNA levels of genes encoding egr-1, p21, c-jun, c-myc, hsp70 and bcl-2 were analysed immediately after exposure (or after 18 h recovery time for PL-MF). (B) ES cells were exposed to EMF in hanging drops for 48 h and were monitored at different stages of the differentiation process.

For differentiation of neural phenotypes, R1 ESs were cultivated in 'hanging drops' (n = 200 cells/drop) for 2 days. EBs were transferred to bacteriological petri dishes (Greiner, Germany) and cultivated for two days in Iscove's modification of DMEM (IMDM, GIBCO) containing 20% FCS and supplements as described (Wobus et al., 2002), with the exception that ß-mercaptoethanol was replaced by 450 µM α-monothioglycerol (Sigma, Steinheim, Germany). EBs (n=20-30) were plated onto tissue culture dishes (∅ 6cm) at day 4 and cultivated in IMDM +20% FCS. The selection of neural precursor cells was carried out according to (Rolletschek 2001). After attachment of EBs, one day later, the medium was exchanged by DMEM/F12 medium supplemented with 5 µg/ml insulin, 30 nM sodium selenite (all from Sigma), 50 µg/ml transferrin and 5 µg/ml fibronectin (all from GIBCO) referred as "nestin-selection media". The culture medium was replenished every 2 days. RF-EMF or ELF-EMF exposure was performed for 48h between 4+4d and 4+6d. Nestin-positive neural precursor cells were selected after cultivation for 7 days (= 4+7d). At day 4+8, EBs were dissociated by 0.1% trypsin (GIBCO)/0.08% EDTA (Sigma) in PBS (1:1) for 1 min, collected by centrifugation, and replated onto poly-L-ornithine/laminin-coated tissue culture dishes into DMEM/F12 containing 20 nM progesteron, 100 µM putrescin, 1µg/ml laminin (all from Sigma), 25 µg/ml insulin, 50 µg/ml transferrin and 30 nM sodium selenite, referred to as "nestin-expansion media", for six days until day 4+13. The medium was changed every 2 days. 10 ng/ml basic fibroblast growth factor (bFGF) and 20 ng/ml epidermal growth factor (EGF; Strathmann Biotech, Hannover, Germany) were added daily. At day 4+14, the differentiation of neurons was induced by 'Neurobasal' medium plus 2% B27 (GIBCO), 10% FCS and maintained by the addition of survival

promoting factors such as interleukin-1ß (IL-1ß, 200 pg/ml daily; PeproTech, London, UK) and db-cAMP (700 µmol every four days; Sigma). Glial cell line-derived neurotrophic factor (GDNF, 2 ng/ml; R&D Systems) and transforming growth factor-ß3 (TGF-ß3, 2 ng/ml) were applied at day 4+18 and at day 4+21, respectively. Neurturin (NTN, 10 ng/ml; all from PeproTech) was applied at day 4+21. The application of survival promoting factors during terminal stages was combined with medium changes at three-day intervals. The total time of cultivation was 4+23d (Figure 6).

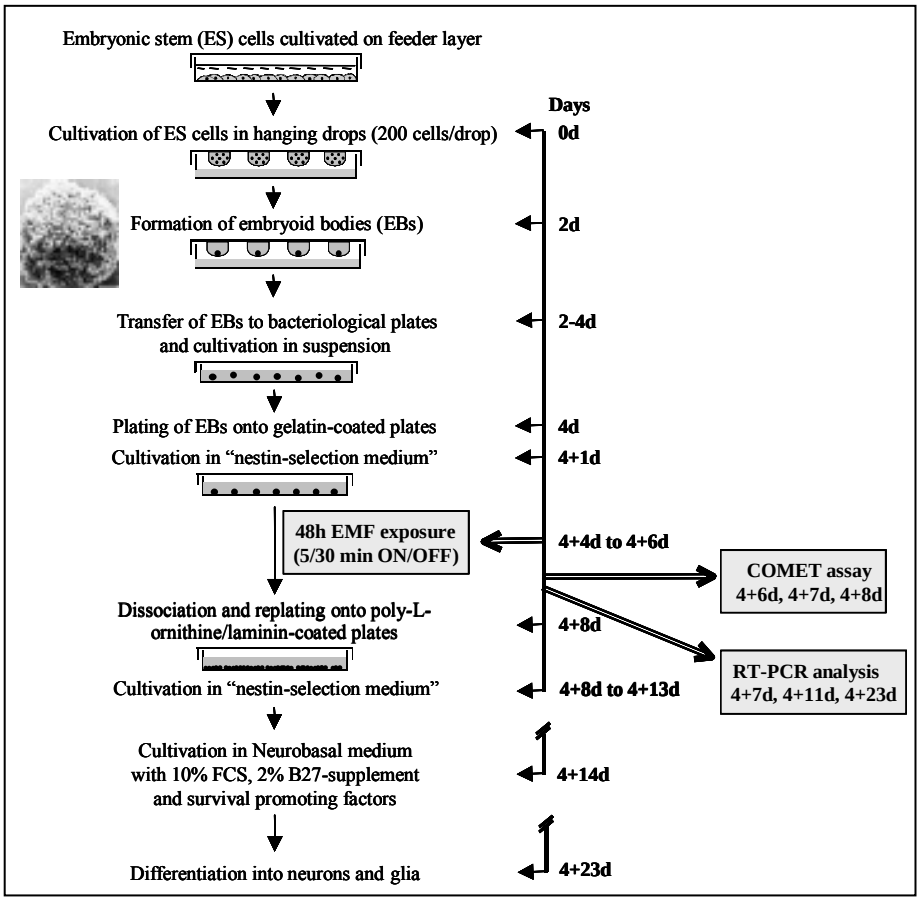

Figure 6. Experimental protocol for EMF exposure of R1 ES cells differentiating into the neural lineage. For differentiation of neural phenotypes, ES were cultivated in 'hanging drops' as EBs (embryoid bodies) for two days, then transferred to bacteriological petri dishes and cultivated two more days. EBs (n = 20-30) were plated onto tissue culture dishes (∅ 6cm) at day 4. After attachment of EBs, one day later, the medium was exchanged with medium supporting the development of neural precursor cells (replenished every 2 days). Nestin-positive neural precursor cells were selected after cultivation for 7 days (= 4+7d). Cell samples were analysed for primary DNA damage (24 and 48h after exposure) measured by the Comet assay, and mRNA levels of various regulatory, tissue-specific and neuronal genes at different stages of differentiation.

2.7.3 Detection of mRNA levels by semi-quantitative RT-PCR analysis

The expression of early response and growth regulatory genes as well as genes involved in neural and cardiac differentiation was analyzed in ES and EC cells after differentiation by semi-quantitative RT-PCR as described (Wobus et al. 2002). EBs or cells differentiating after the dissociation of EBs collected at days 4+4, 4+7, 4+11 and 4+23 were suspended in lysis buffer (4 M guanidinium thiocyanate, 25 mM sodium citrate, pH 7; 0.5% sarcosyl, 1% ß-mercaptoethanol). Total RNA was isolated by the single step extraction method according to (Chomczynski, 1987). RNA was reverse transcribed using Oligo $d(T)_{16}$ primers (Perkin-Elmer, Überlingen, Germany) for the genes encoding c-fos, c-jun, c-myc, early growth response-1 (egr-1), hsp70, p21, p53, bcl-2, bax, growth arrest and DNA-damage inducible –45

(GADD45), engrailed-1 (en-1), nurr-1, nestin, tyrosine hydroxylase (TH), GFAP (glial fibrillary acidic protein), α-myosin heavy chain (α-MHC) (primer sequences and the number of PCR cycles are available on request).

Reverse transcription was performed with MuLV reverse transcriptase (Perkin-Elmer) for 1h at 42°C, followed by denaturation for 5 min at 99°C and cooling to 4°C according to the protocol supplied by the manufacturer. For semi-quantitative determination of mRNA levels, PCR analyses were carried out with Ampli Taq DNA polymerase (Perkin-Elmer). For determination of relative mRNA levels, two separate PCR reactions, either using primers of the analyzed gene or primers specific for ß-tubulin were performed with 3 µl from each RT reaction.

One third of each PCR reaction was electrophoretically separated on 2% agarose gels containing 0.35 µg/ml ethidium bromide. Gels were illuminated with UV light and the ethidium bromide fluorescence signals were stored by the E.A.S.Y. system (Herolab, Wiesloch, Germany) and analysed by the TINA2.08e software (Raytest Isotopenmeßgeräte, Straubenhardt, Germany). Data of the target genes were plotted as percentage changes in relation to the expression of the housekeeping gene ß-tubulin. Gels of four independent experiments were analysed.

2.7.4 Detection of mRNA levels by quantitative RT-PCR (Q-RT-PCR)

Quantitative RT-PCR was performed with specific primers and TaqMan probes designed with Primer Express 2.0 (Applied Biosystems). All oligonucleotides were obtained by Metabion (Germany). The TaqMan probes for Q-RT-PCR were 5´-labelled with FAM (6-carboxyfluorescein) and with 3' prime quencher, TAMRA. The primer and TaqMan probe sequences are available on request. The mouse GAPDH gene was used as endogeneous reference. Reactions were carried out in 96-well plates using iCycler, Version 3.0.6070 (BioRad). The threshold cycle (Ct) , which is the cycle number, at which the amount of the amplified product of the analysed genes reached a fixed threshold, was determined subsequently. The relative quantitaion of bcl-2 and GADD45 mRNA levels was calculated using the comparative Ct method. In order to avoid amplification of contaminating DNA, all primers were designed with an intron sequence inside the amplicon, template-free controls were used as negative controls, the melting temperature of the TaqMan probe was adjusted to be at least 10° higher than the melting temperatures of the sense and anti-sense primers. After Real-time RT-PCR, gel electrophoresis was performed to confirm the correct size of the amplified product.

2.7.5 Single cell gel electrophoresis (Comet assay)

The lkaline version of the Comet assay was applied for detection of single-strand break and alkali-labile site induction, and neutral Comet assay for detection of double-strand breaks.In order to obtain single-cell suspensions, control, sham-exposed or exposed EB outgrowths were trypsinised by addition of 2 ml prewarmed at 37°C mixture of 0.1% Trypsin : 0.01% EDTA (1:1, v/v) per 6 cm tissue culture dish, incubated for 60 sec at room temperature, then the mixture was carefully aspirated as previously described (Wobus et al. 2002). The procedure was repeated. Thereafter, the cells were resuspended into cold Dulbecco's modified Eagle's medium (Gibco BRl, cat. No. 52100-039) with 15% FCS, the cell density was adjusted at ~$5x10^5$ cells/ml and the test-tubes were placed on ice.

For the Comet assay procedure, the protocol of the original technique described by Östling and Johanson (1984) was followed with minor modifications by (Singh et al. 1991, Morris et al. 1999, Speit et al. 2000, Ivancsits et al. 2002b). Briefly, 20 µl of cell suspension (~10 000 cells) was mixed with 200 µl prewarmed (37°C) 0.5% low melting point agarose in PBS. The cell suspension was rapidly pipetted onto slides with frosted ends precoated with 1.5% normal melting point agarose in PBS and evenly spread using a coverslip. The slides were incubated at 4°C for 15 min. to allow the microgel to solidify. Then the coverslips were removed by pulling them carefully aside. The slides were immersed in precooled (4°C) lysis solution (2.5 M NaCl, 100 mM Na_2EDTA, 10 mM Tris, 1% sodium sarcosinate, 10% DMSO, pH 10 for the alkaline Comet assay and pH 7.5 for the neutral COMET assay) and lysed for 60 min at 4°C in the dark. After lysis, the slides were removed from the lysis buffer, drained, placed into a horizontal electrophoresis tank and covered with the precooled (4°C) electrophoresis buffer (1 mM Na_2EDTA, 300 mN NaOH , pH 13 for the alkaline Comet assay and 100 mM Tris, 300 mM sodium acetate, 500 mM sodium chloride, pH 8.5 for the neutral Comet assay, respectively). After 20 min incubation for DNA

alkaline denaturation and expression of the various types of alkaline labile sites (alkaline Comet assay) and for washing away the lysis buffer and equilibration (neutral Comet assay), the electrophoresis was performed in the dark at 4°C for 10 min. The electrophoretic conditions (25 V, 300 mA, field strength 0.7 V/cm) were identical for both versions (alkaline and neutral) of the single cell gel electrophoresis assay. After removal from the electrophoresis tank, the slide surface was carefully covered 3x with a neutralization buffer (400 mM Tris, pH 7.5, 5 min. incubation), then the slides were rinsed briefly in distilled water and fixed in 100% ethanol for 5 min. The slides were air-dried at a slanted angle for at least 2 hours and stained with 50 µl ethidium bromide solution (20 µg/ml in bidistilled water). The analysis was done using the fluorescence microscope ECLIPSE E600 (Nikon, Germany), appropriate excitation and barrier filters (excitation 540-580 nM, barrier 600-660 nm) at 200 fold magnification and the imaging software Lucia (Version 4.71 for Windows). A total of 1000 nuclei were scored (500 per slide) for exposed, sham exposed and control cells and classified into 5 groups according to tail length and intensity using the classification proposed by Anderson et al. (1994): Group A corresponding to <5% DNA damage; B (5-20%); C (20-40%); D (40-95%) and E (>95%). All analyses were performed by the same investigator blind. Results were expressed as 'tail factors', calculated according to Ivancsits et al. (Ivancsits et al. 2002a; Ivancsits et al. 2002b) by the following formula: Tailfactor (%) $=AF_A+BF_B+CF_C+DF_D+EF_E/n$, where A is the number of nuclei classified to group A, F_A is the average DNA damage of group A, which is 2.5% in Anderson's classification; B is the number of nuclei classified to group B, F_B is the average DNA damage of group B (12.5%); C is the number of nuclei classified to group C, F_C is the average DNA damage of group C (30%); D is the number of nuclei classified to group D, F_D is the average DNA damage of group D (67.5%); E is the number of nuclei classified to group E, F_E is the average DNA damage of group E (97.5%); n – the number of scored nuclei (n= 1000).

The results on DNA damage in the alkaline and neutral Comet assay were obtained from 6 separate experiments. The statistical analysis was performed with the SigmaPlot for Windows Version 3.06 package (Jandel Corp.). All data are presented as mean values ± standard error of the mean (SEM). The differences between exposed, sham exposed and control cells were checked for statistical significance using the independent Student's *t* test.

2.7.6 Analysis of cardiac differentiation

Cardiac differentiation of EC or ES cells was used as a parameter of differentiation according to the embryonic stem cell test, EST (Spielmann et al. 1997), established for in vitro analysis of embryotoxic agents. Spontaneously beating cardiomyocytes were estimated at various stages after EB plating. The percentage of EB containing beating cardiomyocytes and mRNA levels of α-MHC were used for the estimation of the degree of cardiac differentiation.

2.7.7 Flow cytometric analysis of cell cycle phases

RF-EMF- and sham-exposed P19 cells were processed according to the two-step procedure of DNA staining (Sehlmeyer et al. 1996). Cells were analysed with a FACStar^{PLUS} flow cytometer (Becton Dickinson, Heidelberg, Germany). Data from 3 (22h) and 4 (40h) independent experiments with 3 to 6 parallels were subjected to statistical analysis performed with the 'ModFitLT' software (Verity Software House, Inc.).

2.8 Experiments with the human neuroblastoma cell line SY5Y (Participant 11)

2.8.1 ELF-EMF exposure setup

See 2.1.1

2.8.2 Cell culture and exposure conditions

The human neuroblastoma cell line was grown in RPMI, 10% foetal calf serum, 100 units/ml penicillin, 100 µg /ml streptomycin, and 2 mM L-glutamine at 37°C and 5% CO_2. Cells were plated one day prior to exposure at densities varying with the exposure protocol: $2.6x10^6$ cells per 100 mm dish for 16 hours exposure protocol; 2 x 10^6 cells per 100 mm dish for 48 hours exposure protocol followed by recovery of the cells immediately after the end of the exposure; and 10^6 cells per 100 mm dish when cells were exposed to the electromagnetic field for 48 hours and harvested 48 hours after the end of the exposure. This was to ensure the collection of the same amount of cells at the end of the different exposure protocols.

Human neuroblastoma cells (SY5Y) were exposed to ELF-EMF (50 Hz, powerline) in a "blind trial" system that allows direct comparison to control unexposed cells. Different exposure protocols, varying in the density of ELF-EMF and in the time of exposure, were applied: a) 2 mT magnetic flux density, intermittent exposure of 5 min on/5 min off, duration 16h; b) 1 mT magnetic flux density, intermittent exposure 5 min on/5 min off, duration 16h; c) 2 mT magnetic flux density, continuous exposure, duration 16h; d) 1 mT flux density, continuous exposure, duration 16hs; e) 1 mT magnetic flux density, continuous exposure, duration 48h. Harvesting of the cells was performed immediately after the end of exposure, unless indicated otherwise.

2.8.3 RNA preparation and Northern blot analysis

Total RNA from exposed and sham exposed SY5Y cells was extracted using RNA Fast II (Molecular Systems, San Diego, CA, USA) according to manufacturer's instructions and size fractionated on 1% agarose gel containing 2.2 M formaldehyde as described in Sambrook et al. (1989). RNA was subsequently transferred and cross-linked to a nylon membrane (Biodyne A, Pall Europe Ltd., UK). After two hours of pre-hybridisation at 65°C in 0.125 M Na_2HPO_4, 1 mM EDTA, 0.25 M NaCl, 7% SDS, 10% polyethylene glycole and 1% BSA, RNA was hybridised with 10^6 cpm/ml of ^{32}P labelled cDNA probe corresponding to the cytoplasmic domain of the human α3 (nucleotides +975/+1404; Fornasari et al. 1997) and α5 (nucleotides +1005/+1263, Chini et al. 1992) nAChR subunits and to the full length coding region of the human α7 nAChR subunit (Groot Kormelink and Luyten 1997). Following hybridisation, membrane was washed at a final stringency depending on the probe used: α3, 0.1x SSC/0.1% SDS at 50 °C; α5, 0.2x SSC/0.1% SDS at 55 °C; α7, 0.1x SSC/0.1 % SDS at 65°C.

The human Phox2a probe corresponds to the 5'UTR region (nucleotides +26/+219) obtained by digestion of the construct SacI-NcoI (Flora, 2001) with Eag I and NcoI. The human Phox2b probe corresponds to the 5'UTR specifying region (nucleotides -299/-90 with respect to the ATG; GenBank accession number NM_003924) and was obtained by RT-PCR. The primers used were: upper primer 5'-GTG CCA GCC CAA TAG ACG GAT G-3'; lower primer 5'-CTC AAC GCC TGC CTC CAA ACT G-3'. The human DβH probe (nucleotides +728/+1337; GenBank accession number NM_000787) was obtained by RT-PCR using the following primers: upper primer 5'-GCT TCT CTC GGC ACC ACA TTA TC-3'; lower primer 5'-TGA GGG CTG TAG TGA TTG TCC TG-3'. The final stringency washings were Phox2a, 0.2x SSC/0.1% SDS at 55°C; Phox2b, 0.2x SSC/0.1% SDS at 50°C; DβH, 0.1x SSC/0.1% SDS at 55°C, respectively.

After stripping the probe, blots were re-hybridised to a human 18S cDNA probe (nucleotides 715-794; Ambion, Austin, TX, U.S.A.) to check the quality of the RNAs and normalise the amount of RNA loaded.

2.8.4 Radioligand assay with ^{125}I-α Bungarotoxin and ^{3}H-Epibatidine

After the end of the exposure, the cells were detached with buffer A (50 mM Tris-HCl pH 7, 150 mM NaCl, 5 mM KCl, 1 mM $MgCl_2$, 2.5 mM $CaCl_2$, 2mM PMSF (buffer A) and centrifuged at 10000g for 60 min. The pellets were washed and then homogenised using an Ultra Turrax homogeniser in an excess of buffer A containing 10 µg/ml of a mixture of the protease inhibitors leupeptin, bestatin, pepstatin A and aprotinin in order to block possible proteolysis during the incubation time of the assays.

^{125}I-αBungarotoxin (αBgtx) was from Amershan, England, and had a specific activity of 200 Ci/mmol; ^{3}H-Epibatidine (Epi; NEN, Boston, USA) had a specific activity of 56 Ci/mmol.

In preliminary experiments we determined the affinity of ^{125}I-αBgtx by performing saturation binding experiments on the cell homogenate. The ^{125}I-αBgtx concentrations ranged from 0.1 to 20 nM, and aspecific binding was determined, after overnight incubation at room temperature, using 1 μM unlabeled αBgtx. The affinity of ^{3}H-Epi was determined by performing saturation binding experiments on the cell homogenate using ^{3}H-Epi concentrations between 0.005 and 10 nM, diluted in buffer A, and incubated overnight at 4°C.

After having determined the affinity of nicotinic ligands, the determination of the number of nicotinic receptors was performed using ^{3}H-Epi binding and ^{125}I-αBgtx-binding to membrane homogenates using saturating concentrations of nicotinic ligands (2 nM ^{3}H-Epi or 10 nM ^{125}I-αBgtx) and subtracted for the aspecific binding performed in parallel using 2 nM ^{3}H-Epi or 10 nM ^{125}I-αBgtx and 100 nM cold Epi or 1 μM cold αBgtx. For total and aspecific ^{3}H-Epi binding membranes were always preincubated with 2 mM cold αBgtx.^{125}I-αBgtx binding was performed overnight at room temperature and the ^{3}H-Epi binding overnight at 4°C. At the end of the incubation, the samples were filtered on GF/C filters and radioactivity counted in a α- or β- counter, respectively. The number of receptor present was expressed as fmol of ^{3}H-Epi or ^{125}I-αBgtx bound/mg of protein. Protein measurement was done using the BCA protein assay (Pierce) with bovine serum albumin as the standard.

2.8.5 Protein preparation and Western blot analysis

Total protein extract was prepared from sham and exposed cells by the freezing and thaw method. Briefly, cells were detached by scraping in PBS 1x and collected by centrifugation at 1000 rpm for 15 min at 4°C. The pellet was resuspended in PBS 1x containing protease and phosphatase inhibitors (purchased by SIGMA) and 20 mM Phenyl-Methyl-Sulphonyl-Fluoride (PMSF). Cells were lysed by four repeated passages between liquid nitrogen to freeze and 37°C to thaw. NaCl at a final concentration of 400 mM was subsequently added, to allow extraction of nuclear protein. Samples were incubated 10 min on ice and extract clarified by centrifugation at 14000 rpm for 30 min at 4°C in a table-top centrifuge (Eppendorf). Twenty micrograms of total extract were then separated by SDS-PAGE and transferred to nitrocellulose membrane (Schleicher & Schuell). The membranes were pre-incubated with blocking buffer (5% non-fat dry milk, 20 mM Tris-HCl pH 7.5, 150 mM NaCl, 0.1% Tween 20) for one hour, after which the primary antibodies were added at appropriate dilutions and incubated for two hours; the secondary antibodies conjugated with horseradish peroxidase were then added and incubated for one hour. The bands were revealed using Super Signal West Dura (Pierce). Standard molecular weights (New England Biolabs) were loaded in parallel.

2.9 Experiments with *Xenopus laevis* oocytes, granulosa cells of rats, HeLa cells, Chinese Hamster Ovary (CHO) cells and human fibroblasts (Participant 7)

2.9.1 ELF-EMF-exposure setup

See 2.1.1

2.9.2 ELF-EMF exposure, expression in Xenopus oocytes and RNA preparation of rCx46

The cDNA for rCx46 were subcloned in the SP64T vector for RNA transcription. SP64T contains 250 bp of the non-coding sequence from *Xenopus laevis* b-globin including a poly-A tract that increases translational efficiency. RNA was prepared by using a synthesis kit containing SP6 RNA polymerase and CAP analogue purchased from Ambion (Austin, USA). The Xenopus expressions construct was linearised with XbaI for RNA transcription. The transcript concentration was estimated spectrophotometrically and analysed on agarose gels. The oocytes were isolated from *Xenopus laevis* ovaries and stage V-VI oocytes were collected and defolliculated by collagenase treatment (5 mg/ml, 355 U/mg, 1.5 h; Worthington, Type 2) in Ca^{2+}-free ND96 solution (96 mM NaCl, 2 mM KCl, 1 mM $MgCl_2$, Na-HEPES at pH 7.4 and adjusted with sorbitol to 240 mosmol/l). An injection apparatus

(Nanoliter Injector, World Precision Instruments) was used to inject 23 nl of 25 ng/µl of Cx46 cRNA and 23 nl of DNA antisense to the endogenous XenCx38 oligo 5¢-gCT gTG AAA CAT ggC Agg Atg (500 ng/µl) (Tib Molbiol) to eliminate endogenous hemi-channel currents. Oocytes were incubated in ND96 supplemented with antibiotics (100 U/ml penicillin/streptomycin) at 17°C. During the expression period of 14h, 17h and 20h the oocytes were exposed to ELF-EMF of 50 Hz powerline or sham exposed. Field strength of 2.3 mT was either continuously or intermittently (5 min on/10 min off) applied. In a further series of experiments 1.0 mT was applied with the intermittent application protocol. For the cell-to-cell coupling assay of paired oocytes, each cell of a pair of oocytes were injected with 23 nl of DNA antisense to the endogenous XenCx38 in order to suppress endogenous coupling in addition 23 nl of rCx46 cRNA (25 ng/µl)were injected. The expressing oocytes were incubated for 16h in ND96 medium, followed by manual removal of the vitelline layers. Two oocytes were paired at their vegetal poles and incubated with ND96 at 17°C for further 8h in the ELF-EMF setup (Participant 10). During this incubation the oocytes pairs were exposed to ELF-EMF (50 Hz, powerline, 1.0 mT, intermittently (5 min on/10 min off)).

2.9.3 Electrophysiological recordings of single and paired oocytes

The two electrode voltage clamp technique was applied to measure the expressed and conducting rCx46 gap-junctional hemi-channels in single *Xenopus laevis* oocytes using a voltage-clamp amplifier Turbo TEC-10 CD (npi electronic, Tamm, Germany). Voltage protocols were applied by a Pentium 100 MHz Computer linked to an ITC-16 interface (Instrutech. Corp., NY). The following pulse protocol was used throughout the experiments: From a constant holding potential of -90 mV or -80 mV variable test potentials were applied for 15 s in the range from -110 mV to +70 mV in steps of 10 mV after repolarisation of the oocyte at a holding potential of -90 mV or -80 mV. The latter was constantly applied for at least 70s. The current signals were filtered at 1 kHz and were sampled at 0.5 or 0.25 kHz. Data acquisition and analysis were performed by using Pulse/PulseFit (HEKA, Germany), Igor Pro (Wave Metrics, USA), Origin (Microsoft), PatchMaschine (V. Avdonin, University of Iowa, USA). n denotes the numbers of individual oocytes. The data are given as mean ± s.e.m. For electrophysiological recordings on paired oocytes the setup was extended by a second amplifier and a further pair of micromanipulators /electrodes. For the pulse protocol of paired oocytes a holding potential of -40 mV, close to the resting potential, was used for both oocytes. The depolarising test pulses were applied for 5s (10s) in the range from -120 mV to +120 mV and the corresponding holding potential was held for 15s (30s). For the electrophysiological recordings the micropipettes were filled with 3 M KCl resulting in input resistances of 1-1.5 M. During the current recordings the oocytes were continuously superfused with the corresponding solution at a rate of 0.5 ml/min and all recordings were performed at room temperature (20-22°C). The standard bath was a nominal Ca^{2+}- free ND96 solution at pH 7.4. The different Ca^{2+} concentrations of ND96 were obtained by addition of suitable concentrations of $CaCl_2$ to the standard solution. For experiments on single oocytes Ca^{2+}-concentrations of 0.0, 0.25 and 0.5 mM and on paired oocytes 1.8 mM and 5 mM were used.

2.9.4 Voltage-jump current-relaxation and membrane conductance of hemi-channels

The steady-state current amplitudes were leak-subtracted and denoted as Iss. The Iss values are presented as function of driving voltage (V-Vrev). The leak current at the applied test potential V was determined by extrapolation of the corresponding current values in the range of -100 mV to -70 mV, at this voltage the voltage dependent hemi-channels are closed.. The reversal potential (Vrev) of the rCx46-mediated current was calculated by a 4-point interpolation polynom of third order. The corresponding membrane conductance G(V) was calculated from the steady-state current amplitude divided by the driving voltage (V-Vrev) and plotted as function of test potential V. In the absence of a significant time- and voltage-dependent current inactivation the corresponding G(V) values in the range of -110 mV < V < +40 mV could be fitted by a simple Boltzmann distribution according to: $G(V)=(A/(1+\exp(-(V-V1/2)zF/RT))+B)$. R, T, F have their usual meanings. V1/2 denotes the half-activation voltage at which 50% of the maximal membrane conductance is observed. z gives the number of membrane bound equivalent gating charges. The parameter A denotes the maximal membrane conductance Gmax of expressed and conducting rCx46-connexons hemi-channels and B the corresponding leak conductance of the oocyte. B is assumed to be voltage independent. For different experiments G(V) was normalised to the corresponding values

obtained at A=1 and B=0, respectively. A similar subtraction of the leak-current was considered in the experiments on paired oocytes.

2.9.5 Cell cultures

Granulosa cell line GFSHR-17 (rat) (Keren-Tal et al. 1993), HeLa cells (human), Chinese Hamster Ovary (CHO) cells and fibroblasts (human, Participant 3) were cultivated in Dulbecco´s modified Eagle´s medium F-12 Ham (DMEM-F12, Sigma Corp., USA) added with 10% fetal calfserum (FCS, Sigma Corp., USA) and 50 U/ml Penicillin, 50 µg/ml Streptomycin (Gibco BRL, G) (300 mosmol, pH 7.4). Both cell lines were incubated under an atmosphere containing 5% CO_2 at 37°C. The culture dishes (35 mm in diameter) for the measurement of the intercellular free calcium ([Ca^{2+}]i) contained six coverslips of 10 mm diameter. Under these conditions the cultured cells were ELF-EMF exposed (50 Hz sinusoidal, 4h - 24h, 1.0 mT, 5 min on/10 min off) or sham exposed. The culture dishes (50 mm in diameter) for the measurement of volume regulation and the Comet assay analysis for contained a coverslip of 25 x 50 mm diameter. Under these conditions the cultured cells were ELF-EMF exposed or sham exposed.

2.9.6 Measurement of [Ca2+]I

Measurement of [Ca^{2+}]i was performed according to Grynkiewicz et al. (1985). For measurement of [Ca^{2+}]i the cells were loaded with fura 2-AM (5 µM and 1% DMSO) for 60 min under ELF-EMF exposure. Fura 2-AM was added to the bath during an off phase of ELF-EMF exposure, respectively. After the indicated time of exposure Fura 2-Amloaded loaded cells grown on a coverslip were transferred to an exposure-free superfusion chamber mounted on an inverted Axiovert (Zeiss, Germany) microscope. The cells were superfused with a bath solution containing (in mM): 145 NaCl, 5 KCl, 2 $CaCl_2$, 1.5 $MgCl_2$, 5 glucose, 10 Hepes, (pH 7.4, adjusted with NaOH; 300 mosm) at 2 ml/min for 3 min to wash-off extracellular fura 2-AM and DMSO at room temperature. The cells were excited at 340 nm and 380 nm using a monochromator polychrome II (T.I.L.L. Photonics GmbH, Planegg; Germany) by a 75 W XBO xenon lamp and the corresponding fluorescence was registered with a digital CCD camera (C4742-95, Hamamatsu Photonics K.K.; Japan). The ratio of excitation at 340 nm to 380 nm was calculated and calibrated to determine [Ca^{2+}]i using the program Aquacosmos (Hamamatsu Photonics K.K.; Japan). Measurement of [Ca^{2+}]i was started about 10 min after completion of ELF-EMF exposure and recorded for 4-8 cells simultaneously. In a further series of experiments two additional stressors were applied after the period of ELF-EMF exposure, respectively. Either 200 µM H_2O_2 was added to the bath or 30 mM NaCl was replaced by KCl. The cells were superfused with the corresponding solution (2 ml/min) for 10 min. Thereafter the solution was replaced by the bath and the recording of [Ca^{2+}]i started.

2.9.7 Comet assay

The granulosa cell line of rat (GFSHR-17), HeLa cells (human) and Chinese Hamster Ovary (CHO) were cultivated as described above. The cells were ELF- and sham- exposed at various frequencies using the exposure parameters 5 min on/10 min off, 1.0 mT applied during 12 to 20 hours. After exposure the Comet assay was performed as described by Ivancsits et al. (2003a, b). The viability of the cells was determined by trypan blue and only slides containing cells with a viability of more than 90% were analysed. For each experiment 3000 nuclei are scored (1000 per slide) for exposed and sham exposed cells and classified into 5 categories according to material and methods of Ivancsits et al. (2002b). The results for DNA damage in the Comet assay are obtained from at least 2 independent exposure experiments. Analysis of exposed and sham-exposed cells was performed in a double-blind approach.

2.9.8 Measurement of cell volume regulation

For measurement of the cell volume the cells were trypsinised (0.25% Trypsin, pH 7.4), collected and centrifuged for 5 min at 500 xg after ELF exposure (18h expression time, 1.0 mT, 50 Hz, 5 min on/10 min off). The pellet was resuspended in 10 ml PBS (in mM: 140 NaCl, 2.7 KCl, 8 Na_2HPO_4, 1.5 KH_2PO_4, 300 mosmol, pH 7.4). For the volume measurements, 1-2 µl of the cell suspension were placed on a cover slip in an exposure-free superfusion chamber mounted on an inverted Axiovert (Zeiss, Germany) microscope. After 5 min, the cells adhered and 2-3 ml of PBS-solution (300 mosmol) were added to the

dish. The cells were superfused with the PBS-solution (300 mosmol) and the cell volume was recorded at time intervals of 30s about 40 minutes. The cell sizes were registered with a digital CCD camera (C4742-95, Hamamatsu Photonics K.K.; Japan). After 30 sec the 300 mosmol PBS-solution was replaced by a 250 mosmol PBS-solution (or 350 mosm solution). This hypotonic (or hypertonic) solution was exchanged after 20 min by PBS-control (300 mosmol), again. The diameter of the cells of spherical shape (breath, height) were measured and the corresponding rotationellipsoid volume determined. The time dependent volume V(t) was subtracted by the basis volume V0, normalised to the maximal volume and the mean calculated.

2.10 Experiments with the human endothelial cell lines EA.hy926 and EA.hy926v1 (Participant 6)

2.10.1 RF-EMF 900 MHz GSM signal exposure system dosimetry

Cells were irradiated with a simulated mobile phone microwave radiation in specially constructed exposure system, which is based on the use of high Q waveguide resonator operating in TE_{10} mode. The irradiation chamber has been placed vertically inside a cell culture incubator with two 55 mm-diameter glass Petri dishes placed so that the E-field vector was parallel to the plane of the culture medium. Temperature controlled water was circulated through a thin (9 mm) rectangular glass-fiber-molded waterbed underneath the Petri dishes. In all experiments reported here, cells were exposed for 1 hour to 900 MHz GSM signal at an average SAR of 2.4 W/kg. SAR values ranged from 1.8 W/kg to 2.5 W/kg depending on the area of the dish, what was caused by the non-uniform distribution of the RF-EMF radiation field. The average SAR level of 2.4 W/kg was selected because it is slightly above of the safety limit for the mobile phone microwave radiation emission as defined by ICNIRP (International Commission on Non-Ionizing Radiation Protection). RF-EMF signal was generated with EDSG-1240 signal generator and modulated with pulse duration 0.577 ms and repetition rate of 4.615 ms to match the GSM signal modulation scheme. Signal was amplified with RF Power Labs R720F amplifier and fed to the exposure waveguide via monopole type feed post. The SAR distribution in the cell culture and the E-field above the cell culture were determined using computer simulations (FDTD method). The simulations were done with commercial XFDTD code (Remcom, USA) with simulation grid size of 3x3x3 mm^3 in the main grid and 1x1x1 mm^3 in sub grid, consisting of the culture dishes and part of the waterbed. The maximum SAR was obtained in the centre of Petri dish, decreasing to about 6 dB at the edges of dish. Simulation results were verified with measurements. Electric field in the air above cell cultures was measured with a calibrated miniature Narda 8021B E-field probe. The measured E-field values differed less than 15% from the corresponding simulated E-fields. The SAR distribution was measured with small, calibrated temperature probes (Luxtron and Vitek) directly from the culture medium. The measurements were done at room temperature outside the incubator with increased culture medium height, in order to reduce the measurement uncertainty at air-medium boundary. The temperature was measured (Vitek probe, BSD Medical, USA) for 10 sec. in order to limit the effect of heat convection and conduction (Moros and Pickard, 1999). The Luxtron probe has lower temperature resolution (0.1°C) compared to Vitek probe (0.001°C) and thus the temperature had to be measured for 1 min. to achieve sufficient temperature rise (1°C). Due to these short measurement times the power fed to the chamber was increased up to 25 W and the resulting SAR value was afterwards scaled down to 1 W of input power. The measured SAR values at the centre of the culture medium (3-mm depth) were 2.5 W/kg (Luxtron, USA) and 5.0 W/kg (Vitek, USA). These values can be compared to the simulated value of 2 W/kg and 3.6 W/kg, respectively, with simulation parameters changed to correspond with the measurement situation. The measured values can be considered as the upper and lower limits of SAR due to measurement uncertainties described above and thus they validate the simulations. Waveguide resonator's water-cooling system was tested with long-term temperature measurements by using Luxtron probe. The temperature was recorded twice a minute over normal 1-hour exposure period at 2 W/kg. The temperature remained at 37±0.3°C during the whole measurement time. Therefore, the reported biological effects are of non-thermal nature. Additionally, human endothelial cells were also exposed to GSM 1800 MHz radiation in talk and cw mode. See also 2.1.

2.10.2 Cell cultures and exposure

EA.hy926 and EA.hy926v1 cells (gift from Dr. Cora-Jean S. Edgell, North Carolina University at Chapel Hill, NC, USA) (Edgell et al. 1983) were grown Dulbecco's MEM, supplemented with antibiotics, 10% fetal bovine serum, L-glutamine and HAT-supplement. For experiments, cells were removed from culture flasks with trypsin, washed and seeded at density of 1.2 x 10^6 cells per 55 mm-diameter glass Petri dish (900 MHz GSM exposure) or seeded at density of 0.4 x 10^6 cells per 35 mm-diameter plastic Petri dish (1800 MHz GSM signal exposure). After overnight culture semi-confluent monolayers of EA.hy926 cells were exposed to sham or RF-EMF radiation. Cell cultures for sham and irradiation were prepared in the same kind of glass dishes, derived from the same batch of cells, were seeded at the same cell density and were grown for the same period of time before experiment. The only difference between irradiated and sham samples was that the irradiated dishes resided for 1-hour in incubation chamber with RF-EMF radiation turned-on whereas sham dishes resided in the irradiation chamber for the same period of time but with irradiation turned off.

2.10.3 ^{32}P-othophosphate metabolic labelling

To determine changes in protein phosphorylation ^{32}P-orthophosphate was present in cell culture during the 1-hour sham or RF-EMF exposure. In experiments where the time-course of hsp27 phosphorylation was determined, ^{32}P-orthophosphate was present in cell cultures during the whole post-exposure incubation period. During the phosphorylation cells were incubated in culture medium consisting of phosphate-free DMEM that was supplemented with dialysed FBS and with ^{32}P- orthophosphate (NEN, Cat no. NEX-053s). Briefly, confluent monolayers of endothelial cells were washed twice with the pre-warmed (37°C) labelling medium that did not contain ^{32}P-orthophosphate, in order to wash away residual phosphates from the cell cultures. Thereafter, pre-warmed ^{32}P-orthophosphate-containing medium (5 mCi) was added to the cells and dishes were irradiated immediately for one hour. Following irradiation petri dishes were placed on ice, labelling medium was aspirated, cells were rinsed with cold PBS supplemented with protease/phosphatase inhibitors (1 mM PMSF; 0,4 mM orthovanadate) and cells were scraped and collected with ice cold PBS. From this point onwards orthovanadate was present in all solutions used to extract phosphoproteins. In experiments where the time-course of hsp27 phosphorylation was determined, ^{32}P-orthophosphate was present in cell cultures during the whole post-exposure incubation period (up to 5 hours).

2.10.4 2D-electrophoresis - for protein phosporylation studies

Cells were harvested, washed once with ice cold PBS containing 1mM PMSF and lysed on ice for 10 minutes in buffer consisting of 9.5 M Urea, 2% CHAPS, 0.8% Pharmalyte pH 3-10 and 1% DTT. Lysates were cleared of debris by centrifugation 42000 xg at +15°C for 1 hour. The pellet containing insoluble debris was discarded and supernatant was collected and its protein concentration was measured with the Bradford method. Proteins in the lysates were separated using standard 2D-electrophoresis method - isoelectrofocusing (IEF) in the first dimension and SDS-PAGE in the second dimension.

1st-dimension isoelectric focusing

The 125 ug protein was applied to the groove of the re-swelling tray that contained 11 cm-long IPG strip with pH range of 3-10 (APBiotech, Sweden). The IPG strips were incubated overnight with the protein lysate solution. The proteins in IPG strips were separated by isoelectrofocusing (IEF) using the programmable power supply with the following protocol:

- 300 V, 1 W, 1 mA for 6 minutes at 20°C
- 3500 V, 1 W, 1 mA for 6 minutes at 20°C
- 3500 V, 1 W, 1 mA for 24 hours at 20°C

After completion of the IEF-separation the strips were equilibrated for 10 minutes on a rocking platform in solution-I consisting of urea (6 M), glycerol (30% w/v), SDS (2% w/v), DTT (100 mg/10 ml) in 50 mM Tris-HCl buffer pH 8.8 with a trace of bromphenol blue (migration marker). Thereafter, the strips were placed in a solution-II that contained iodocetamide (480 mg /10 ml) instead of DTT and equilibrated on a rocking platform for another 10 minutes at room temperature.

2nd-dimension SDS-PAGE

Equilibrated IPG strips were attached on the top of 8% SDS-PAGE gel with melted agarose to ensure firm contact. Gels were run with 40 mA/gel for ca. 2.5 hours at 4°C.

After completion of the electrophoretic separation gels were silver stained using Morrissey's modification of the Merril's method and images for computerised analysis were acquired into PC using the Bio-Rad GS-710 densitometer.

2.10.5 ^{32}P-autoradiography

2D-gels, containing metabolically ^{32}P-labelled phosphoproteins, were dried in gel dryer and used for autoradiography. Images generated on X-ray films were acquired into PC for computerised analysis using the Bio-Rad GS-710 densitometer.

2.10.6 2D-electrophoresis - protein expression screening

Immediately after the end of the exposure to 900 MHz GSM mobile phone radiation-like signal at the average specific absorption rate (SAR) of 2.4 W/kg cells were placed on ice, washed with ice-cold PBS and lysed with buffer consisting of: 7 M urea, 2 M thiourea, 4% chaps, 2% IPG buffer pH 3-10 NL, and 1% dithioreitol (DTT), 1 mM sodium orthovanadate and 1 mM PMSF. Protein concentration in lysates was measured using Bradford-method and 175 µg of total protein was used for 2-DE.

IEF was performed using IPGphor apparatus and non-linear pH 3-10 18 cm long IEF strips (Amersham Biosciences, Sweden). The samples were loaded using in-gel rehydration in a buffer containing 9 M urea, 2% chaps, 0.2% DTT, 0.5% IPG buffer pH 3-10 NL for 12 hours. IEF was run at 20°C using step-and-hold and gradient methods as follows: 30 V - 2 hrs, 100 V - 0.5 hrs, 300 V - 0.5 hrs, 600 V - 0.5 hrs, 1500 V - 0.5 hrs, 8000 V gradient 4 hrs, 8000 V - until the 65000 volt-hours were achieved.

For SDS-PAGE the IEF strips were equilibrated for 15 min with 6 M urea, 30% glycerol, 50 mM Tris-HCl pH 8.8, 2% SDS, and 10 mg/ml DTT for 15 min and then for another 15 min in the same buffer 25 mg/ml iodoacetamide replacing DTT. SDS-PAGE was run in 8% gel using Protean IIxi Multicell apparatus (Bio-Rad, UK) and a constant current of 40 mA/gel at 10°C.

After electrophoresis gels were fixed with 30% ethanol and 0.5% acetic acid overnight, washed with 20% ethanol and ddH_2O, sensitised with sodium thiosulfate (0.2 g/l), incubated in silver nitrate solution (2 g/l) and developed in a solution of potassium anhydride (30 g/l), 37% formaldehyde (0.7 ml/l) and sodium thiosulfate (0.01 g/l). The development was stopped with Tris (50 g/l) and acetic acid (0.05%) solution. Silver stained gels were stored in ddH_2O at 4°C. The gels were scanned using GS-710 densitometer (Bio-Rad, UK).

The MALDI-MS analysis service was purchased from the Protein Chemistry Laboratory of the Institute of Biotechnology at the Helsinki University, Finland. The spots were reduced with DTT and alkylated with iodoacetamide before overnight digestion with trypsin (Sequencing Grade modified Trypsin, promega, USA). The peptide mixture was concentrated and desalted using Millipore ZipTip^{TM} µ-C18 pipette tips. The peptide mass fingerprints were measured with Bruker Biflex^{TM} MALDI-ToF mass spectrometer in a positive ion reflector mode using α-cyano-4-hydroxycinnamic acid as a matrix. The MALDI spectra were internally calibrated with the standard peptides, angiotensin II and adrenocorticotropin-18-39. The database searches were performed using ProFound (http://prowl.rockefeller.edu/cgi-bin/ProFound) and Mascot (http://www.matrixscience.com) searches.

2.10.7 Western blotting

Immediately after the completion of 2D-electrophoretic separation of protein lysates, gels were placed into the transfer buffer (25 mM Tris, 192 mM glycine, 20% methanol and 0.1% SDS) and blotted onto PVDF membrane (Bio-Rad) using Novablot semi-dry blotting apparatus (APBiotech, Sweden). The transfer of proteins on the membrane was performed with current of 0.8 mA/cm^2 for 45 minutes at room temperature. Following transfer, the membranes were blocked overnight at 4°C in Tris-buffered-saline (TBS, pH7.4) containing 5% of non-fat milk proteins. The expression of Hsp27, MAP p38 kinase and protein phosphatase-1α was detected in western blot membranes by ECL method using specific polyclonal antibodies, peroxidase-conjugated second antibody and West Pico ECL kit (Pierce, USA).

2.10.8 Immunoprecipitation

Immunoprecipitation experiments were performed using cells that were metabolically labelled with ^{35}S-methionine (APBiotech, Sweden) as follows. Briefly, confluent EA.hy926 monolayers were washed twice with the pre-warmed (37°C) labelling medium (phosphate-free) to remove phosphates. After completion of washing, the pre-warmed ^{35}S-methionine-containing (2 mCi) labelling medium was added to culture dishes and cells were allowed to incorporate ^{35}S-methionine overnight. Then, ^{35}S-methionine-containing cultures were irradiated for 1 hour. After the end of irradiation dishes were placed on ice, cells scraped in 1 mM PMSF containing PBS and used in immunoprecipitation. In experiments where the time-course of protein expression changes was determined the ^{35}S-methionine was present in the cell cultures during the whole post-exposure incubation period (up to 8 hours). Harvested cells were lysed in ice-cold RIPA buffer. Lysates were centrifuged 10000 xg at 4°C for 10 minutes to remove debris and lysates' protein concentration was measured with the Lowry-Ciocalteau method. Samples containing 230 µg of proteins were placed in eppendorf tubes and pre-cleared with 2.3 µg of non-immune goat IgG (Santa-Cruz, USA; sc-2028) and 20 µl of recombinant-Protein-G-conjugated Sepharose-4B (Zymed, USA, Cat. no. 10-1242) at 4°C on a shaker for 30 minutes. After pre-clearing the Sepharose-beads were removed by centrifugation (1000 xg; 4°C; 10 min) and selected proteins (hsp27, MAP p38 kinase, protein phosphatase-1α) were immunoprecipitated with 2 µg of specific antibody and 20 µl of recombinant-Protein-G-Sepharose-4B-conjugate (overnight at 4°C on a shaker). Thereafter, beads were collected by centrifugation, washed 4 times with RIPA buffer, dispersed in the electrophoresis sample buffer, boiled on water-bath for 3 minutes and proteins released from the beads were resolved using 8% SDS-PAGE gel (40 mA/gel). Gels were stained with coomassie blue, dried between cellophane sheets and exposed with X-ray film for different periods of time to detect the ^{35}S-methionine labelled immunoprecipitated proteins.

2.10.9 cDNA Expression Arrays

Total RNA isolation

For the isolation of total RNA from RF- or sham-exposed cells we used NucleoSpin RNA II kit (Clontech, USA). Briefly, confluent cell cultures we directly lysed on glass culture dishes. RNA, from the cleared cell lysates, was directly immobilised in Spin columns provided by the manufacturer. After DNAse treatment the total RNA was eluted from the columns and analysed for the possible remaining DNA contamination by PCR using b-actin primers against genomic DNA. RNA from several independent experiments were pooled and stored at -80°C for further use.

Probe synthesis and analysis of gene expression

For the synthesis of cDNA probes and differential analysis of gene expression we used Atlas Pure Total RNA Labelling System (Clontech) and Atlas cDNA Expression Arrays (Clontech), respectively. In this system mRNA was enriched from the total RNA by binding it to Streptavidin-biotin-oligo- (dT) coated magnetic beads. After enrichment of the mRNA they were reverse transcribed to radioactive cDNA probes directly when still bound to magnetic particles. Purified probes were hybridised with Atlas filters containing complementary cDNA spots and analysed by autoradiography. AtlasImage 2.0 software was used for the differential gene expression analysis of autoradiograms.

2.10.10 Cell cycle analysis

Cell cycle distribution among the EA.hy926 cells was detected by staining the DNA with propidium iodide followed by flow cytometry analysis. Briefly, cells were collected by centrifugation, washed once with phosphate-buffered saline (PBS) and fixed in 90% methanol on ice for 10 min. After fixation, the cells were washed twice with PBS and suspended in RNAse solution in PBS (100 units/ml) and incubated at 37°C for 30 minutes. At this point the propidium iodide solution (10 mg/ml in PBS) was added to the cells in RNAse solution, and the incubation was continued on ice overnight. Upon termination of incubation, cells were washed once with PBS and analysed by FACScan (Becton Dickinson, USA).

2.10.11 Caspase-3 activity

Caspase-3 activity was detected in non-fixed cells using CaspaTaq Caspase-3 Activity Kit (Intergen, USA). The active caspase-3 molecules are labelled in cells with a green fluorescent probe (FAM-DEVD-FMK) which only binds to the active caspase-3. Dead cells were excluded from the analysis by staining with propidium iodide that, when used with non-fixed cells, labels only cells with permeable membrane (necrotic or late apoptotic cells). The cell cultures were either sham- or RF-EMF-exposed with or without staurosporin (positive control of caspase-3 activation). Activity of caspase-3 was analysed either immediately after the exposure or 4h to 24h after exposure. Fluorescent content of the cells was analysed by flow cytometry with Lysys II software (Becton-Dickinson, USA).

2.10.12 Immunhistochemistry

A standard indirect immunofluorescence method was used for immunohistochemistry. Cells were washed twice with PBS and fixed in cold 3.7% paraformaldehyde in fixing buffer (0.1 M Pipes, 1 mM EGTA, 4% polyethyl glycol 8000, 0.1 M NaOH pH 6.9) overnight at 4°C. After fixing cells were rinsed twice with PBS, permeabilised with 0.5% Triton X-100 in fixing buffer 10 min, rinsed with PBS and permeabilised with 0.1% sodiumborohydride in PBS. After permeabilisation cells were rinsed with PBS and blocked with 5% BSA in PBS for 30 min. The primary antibody (Hsp27 StressGen, Canada) was incubated for an hour as well as the TRITC-labelled secondary antibody (DAKO, Denmark). After antibody incubations cells were rinsed with PBS and stained with Alexa Fluor 488 phalloidin for 30 min. Specimens were observed using a Leitz fluorescense microscope and computerized image acquisition system (Metafer, Germany)

2.10.13 Image analysis

Images of 2D-gels and X-ray films were analysed with the PDQuest 6.1.0/6.2.0 software (Bio-Rad, UK) or Phoretix 1D Advanced 5.0 (Nonlinear Dynamics, USA).

2.10.14 cICAT method

Protein Labelling and Purification

1 mg each of sample (talk and cw exposed) was labelled separately using the acid cleavable isotope-coded affinity tag (cICAT) reagent (Applied Biosystems, USA) following the vendors protocols as has been described (Burlingame). Briefly, the protein samples were separately reduced at cysteine residues using Tris (2-carboxyethyl) phosphine (TCEP, Pierce, USA), and the free sulfhydryl groups labelled using either the normal ($C^{13}(0)$) cICAT reagent, or the isotopically heavy ($C^{13}(9)$) cICAT reagent containing nine C^{13} atoms. The samples were then combined, enzymatically digested using trypsin (Promega, USA) and the resulting peptides were fractionated using strong-cation exchange (SCX) HPLC. The SCX HPLC was carried out on an Integral HPLC system (Applied Biosystems, USA) using a 2.1 mm x 250 mm polysulfoethyl A SCX HPLC column (PolyLC). The A buffer was 5 mM KH_2PO_4/25% acetonitrile pH 3.0 and the B buffer was 5 mM KH_2PO_4/25% acetonitrile pH 3.0 containing 300 mM KCl. The peptides were eluted and collected in one minute fractions using a gradient profile of 0-25% B over 30 minutes, followed by 25-100% B over 20 minutes, followed by washing of the column for 10 minutes at 100% B. Collected peptide fractions were affinity purified using avidin chromatography columns. The purified, labelled cysteine-containing peptides were then subjected to an acid incubation to cleave the biotin affinity tag from the peptides (Burlingame). The cleaved samples were then separated using offline microcapillary reverse-phase liquid chromatography (μLC) with collection in one minute fractions onto a MALDI sample target using a 180 μm x 15 cm reverse phased column home-packed with 5 μm, 300 Å C18 material (Magic, Michrom Inc., USA) and an Ultimate capillary LC system coupled to a Probot sample spotter (Dionex, USA). The MALDI matrix α-cyanohydroxycinnamic acid (CHCA, Agilent, USA) was automatically added to the eluent at each spot on the sample plate.

Automated mass spectrometric analysis

After μLC fractionation to the MALDI sample plate, the samples were analysed using an abundance-ratio dependent methodology on a oMALDI qQTOF mass spectrometer (oMALDI Qstar, MDS-Sciex/Applied

Biosystems). First, a single-stage mass spectrum of each sample spot on the plate is acquired for 30 seconds at each spot. The relative intensity ratios, as well as singlet peaks for all of the detected, cICAT labelled peptides are then automatically calculated using an automated software algorithm. Those peptides showing $C^{13}(0):C^{13}(9)$ relative intensity ratios of >1.7 or <0.6 were outputted to an inclusion list for identification by tandem mass spectrometry (MS/MS). All those peaks identified as singlets (i.e. no matching $C^{13}(0)$ or $C^{13}(9)$ peak) were also selected for MS/MS analysis. The peptide masses contained in the inclusion list at each sample spot were then analysed by MS/MS analysis, using one minute data acquisition time for each peptide.

Sequence database searching and quantitative analysis

The acquired MS/MS data were searched against the human protein sequence database maintained at the National (USA) Cancer Institute using the search program Sequest. For all MS/MS data, the search was run with no enzyme constraint, or amino-acid composition constraint (i.e. only those sequences containing cysteine), and a mass tolerance of 0.1 Da was used for the precursor peptide mass. A differential mass addition to cysteine of 227.13 was indicated in the search parameters for the $C^{13}(0)$ reagent, and 236.16 for the $C^{13}(9)$ reagent. Only matches to peptide sequences containing cysteine were kept after the database search. The results were further statistically scored using a recently described statistical algorithm for validation of sequence database search results. Only those peptides having a confidence score of 0.85 or greater using this tool were considered to be accurate matches. The quantitative $C^{13}(0)/C^{13}(9)$ values determined by the automated software described above were matched to each identified peptide, and these ratios were each checked for accuracy by manual inspection of the raw mass spectral data.

2.11 Effects of ELF-EMF and RF-EMF on gene expression in human cells analysed with the cDNA array (Participant 12)

2.11.1 ELF-EMF and RF-EMF exposure setups

See 2.1

2.11.2 Cell cultures and RNA isolation

See reports of the REFLEX Participants who provided samples for this investigation.

2.11.3 RZPD cDNA arrays

The whole-genome Human Unigene RZPD-2 cDNA array contains about 75,000 cDNA clones (I.M.A.G.E. clone collection), the Mouse Unigene RZPD-1 array about 25,000 clones, each selected from UniGene clusters (group of Bernhard Korn (RZPD), see also: http://www.ncbi.nlm.nih.gov/ entrez/query.fcgi?db=unigene). The cDNA products were PCR amplified by M13 forward and reverse standard primers and spotted in duplicates on 22 x 22 cm nylon membranes (mouse: 1 part, human: 3 parts) in a 5 x 5 pattern (group of Uwe Radelof (RZPD), see also Boer et al. (2001) Genome Res. 11, 1861-1870). Each 5 x 5 field contained 11 genes spotted in duplicates as well as the E.coli kanamycin gene (1 spot) and an Arabidopsis gene (2 spots) as “empty” spots for background subtraction during data analysis. For quality control, M13 forward and reverse primers were end labelled with ^{33}P gamma ATP and hybridised to each membrane to control of all filters of the same robot run were spotted even and complete. After quality control, the membranes were stripped and used for complex hybridisation after about 6 weeks. Only filters from the same robot run containing comparable concentrations of PCR products representing single genes or ESTs were used for hybridisation with the different samples to be compared. One individual hybridisation experiment was done on the same filter batch with all 4 samples. Repetitions, however, were performed with different filter batches to exclude biases caused by using filters from only one robot run.

2.11.4 Hybridisation of global cDNA arrays and image analysis

RNA was isolated from exposed and as a control sham-exposed cells from different cell lines (Table 1). RNAs coming from individual experiments were checked separately for degradation (28S/18S rRNA ratio 1.5-2.0) and concentration (at least 1 µg/µl in H2O) with the Bioanalyzer (Agilent). Afterwards, RNAs from 2 individual exposures were pooled for each hybridisation sample in same concentrations. Hybridisation was performed according to Boer et al. (2001) with minor modifications: 10 µg of total RNA per sample was reversely transcribed using (dT)18 primer and 33P alpha-dCTP without amplification (Superscript II reverse transcriptase, Invitrogen) and purified. The labelled cDNA was hybridised with the arrays. The hybridisation solution contained 6 x SSC/5 x Denhardt's, as well as Cot-1 DNA (Invitrogen Co., Germany) and (dA)40 oligonucleotide for blocking. After exposition of the hybridised membranes, the PhosphorImager screens were scanned (Fuji FLA-3000, 100 µm resolution, Fuji BAS-reader software). The primary image analysis (estimation of nVol grey level values for each individual spot) was done by the help of the ArrayVision software package (Interfocus), which had been adjusted to the 5x5 array before. The background was corrected locally in each 5x5 field by subtracting the empty spot signal (average signal of 3 spots, see above). Normalisation was done via the average signal intensity (without empty spots) on the whole membrane. Two independent hybridisations were performed for each experiment (4 data points per gene because of spotting of each gene in duplicates).

2.11.5 Pre-processing (data cleaning) and Modified SAM method (and Selective SAM method)

Original expression profiling data ("control" data *ctrl*, related to gene expression without the applied EMF, and "exposed" *exp*, related to gene expression after EMF exposure) were normalised and the background was removed as mentioned above. For each experiment (Table 1) at least two hybridisations were performed. In a first pre-processing, signals were removed giving a zero or an infinite ratio (*ratio = exp/ctrl*), that could lead to a reduction of the available measurements for some genes.

Table 1. Gene expression profilings on human and mouse global cDNA arrays

Cell line	Exposition	Exposure experiments/ profiling	Array	Participant
ES-1 human primary fibroblasts	ELF/EMF: 50 Hz, 1 mT 5 min ON, 10 min OFF, 24 h	4	Human Unigene RZPD-2	3
ES-1 human primary fibroblasts	ELF/EMF: 50 Hz, 1 mT 5 min ON, 10 min OFF,15 h	4	Human Unigene RZPD-2	3
SY5Y human neuroblastoma	ELF/EMF: 2 mT 5 min ON, 5 min OFF, 16 h	4	Human Unigene RZPD-2	11
ES mouse embryonic stem cells	ELF/EMF: 50 Hz powerline 2.3 mT	3	Mouse Unigene RZPD-1	4
NB69 human neuroblastoma	RF/EMF: 1800 MHz (GSM Basic) SAR 2 W/kg 5 min ON, 10 min Off, 24h	2	Human Unigene RZPD-2	5
EA.hy926 human endothelial	RF/EMF: 900 MHz, GSM SAR 1.8-2.5 W/kg, 1h	2	Human Unigene RZPD-2	6
EA.hy926 human endothelial	RF/EMF: 1800 MHz, GSM SAR 1.8-2.5 W/kg, 1h	2	Human Unigene RZPD-2	6
EA.hy926 human endothelial	RF/EMF: 1800 MHz, GSM SAR 1.8-2.5 W/kg, 1h	2	Human Unigene RZPD-2	6
T-lymphocytes human, quiescent from peripheral blood	RF/EMF: 1800 MHz DTX only SAR 1.4 W/kg 10 min ON, 20 min OFF, 44 h (RNA prepared in Heidelberg)	2	Human Unigene RZPD-2	8
U937 human lymphoblastoma	RF/EMF GSM-900 MHz 2 W/kg, 1 h	5	Human Unigene RZPD-2	9
CHME5 (µglie) human microglial	RF/EMF GSM-900 MHz 2 W/kg, 1 h	5	Human Unigene RZPD-2	9
HL-60 human hematopoietic	RF/EMF: 1800 MHz DTX SAR 1.0 W/kg 5 min ON, 5 min OFF, 24 h	3	Human Unigene RZPD-2	2
HL-60 human hematopoietic	RF/EMF: 1800 MHz DTX SAR 1.3 W/kg continuous waves, 24 h	3	Human Unigene RZPD-2	2
HL-60 human hematopoietic	RF/EMF: 1800 MHz DTX SAR 1.3 W/kg continuous waves, 24 h	3	Human Unigene RZPD-2	2

2.11.6 Biostatistics (Dr. Daniel Remondini, Participant 8)

The statistical analysis to find those genes that significantly changed their expression level between the ctrl and the exp state was done as follows: In order to increase the statistical significance of the test, we considered only those genes with $NG = 4$ "good" measurements (both for ctrl's and exp's). The genes of each experiment were kept separated in 3 different groups, related to each part (nylon membrane) they belonged to ("Part 1", "Part 2", "Part 3"). Normalisations and analysis were performed on each part separately, in order to avoid possible biases due to different behaviour of the arrays during hybridisation or scanning. Data were processed in order to evaluate and reduce possible artefacts due to the array reading procedure:

- as a first step, data were rescaled by means of a cubic root function in order to gather the data in a smaller interval: $ctrl' = \sqrt[3]{ctrl}$, $\exp' = \sqrt[3]{\exp}$;
- the averages of all 8 measurements for each gene were taken as a "reference" set. A scatter plot was made of each measurement (ctrl or exp) versus the reference set, and the resulting plot was fitted linearly. On the basis of the fit parameters a rescaling was performed on data if they were not on a Y=X curve.

The "interesting" genes were found by calculating a normalised difference *diff(i)* between exp and ctrl values for each gene *i*:

$$diff(i) = \frac{E[\exp(i)] - E[ctrl(i)]}{\sqrt{\frac{\sigma_{ctrl}^{2}}{NG-1} + \frac{\sigma_{\exp}^{2}}{NG-1}} + s_0},$$

where "E[]" denotes "expected value of ", and s_0 is a correction term that removes possible divergences in the denominator, calculated as the median of the σ_i distribution for each gene (ctrl and exp distributions were merged). For a first selection, genes were considered outliers if they exceeded the threshold of 3σ calculated from the resulting distribution of *diff(i)*.

To increase the robustness of our selection, following the bootstrapping procedure as shown in [PNAS 2001, Vol. 98 no. 9, pg. 5116-5121], new datasets were generated as permutations of the original ones, and the same analysis was performed over these datasets, ranking the differences $diff_p(i)$ (*p* referring to the p-th permutation) from larger to smaller. A plot of *diff(i)* vs. E[$diff_p(i)$] was generated for each group of genes, and the interesting genes were chosen as those that significantly deviated from the y=x line: the distance of *diff(i)* from the y=x line, defined as *dist(i)*, was to be larger than a threshold value Δ=1.2.

Finally, the outlier genes selected for each part in each experiment were chosen from the intersection between the initial outliers ($|\mathrm{diff(i)}| \geq 3\sigma$) and those from the bootstrapping procedure ($|dist(i)| \geq \Delta$). In this way the outlier selection results more selective than just applying the technique as shown in [PNAS 2001, Vol. 98 no. 9, pg. 5116-5121].

2.11.7 Data mining

The ratio of the spot-to-spot comparison was taken for further analysis, without values smaller than 0.001 or bigger than 1,000, respectively, which were eliminated before. Since each PCR fragment was spotted twice on each membrane, and each hybridisation experiment was performed twice, four ratios went into an own database tool (Martin Holst, access database program, Microsoft) to make an analysis in a non-statistical manner: All eight values coming from two hybridisations had to show the same tendency to be taken over in the final list showing clones appearing up- or down-regulated in both experiments. The clones of this list were connected to the gene ontology data via a Stanford database (http://genome-www5.stanford.edu/cgi-bin/SMD/source//sourceBatchSearch) according to IMAGE IDs. With the help of these data and a text query tool (Microsoft Excel, Matthias Schick) regulated genes belonging to certain gene families of interest could be extracted manually. The same procedure was applied on genes extracted by bio-statistical analysis.

3.0 RESULTS

The studies in REFLEX cover a wide range of frequencies within the spectrum of electromagnetic fields (EMF). Based on the assumption that possible biological effects may be generated by EMF in a different way dependent on their frequencies the results of the REFLEX project are reported separately for extremely low frequency electromagnetic fields (ELF-EMF) and radio frequency electromagnetic fields (RF-EMF).

3.1 Results in ELF-EMF research

3.1.1 Genotoxic effects

3.1.1.1 Human fibroblasts, lymphocytes, monocytes, melanocytes and muscle cells and granulosa cells of rats (Participant 3)

Intermittent ELF-EMF exposure, but not continuous ELF-EMF exposure induced DNA strand breaks in human fibroblasts.

In the first set of experiments fibroblasts were continuously exposed to ELF-EMF at 1000 µT for 24h. In these experiments significant differences in DNA-breaks between exposed and sham-exposed cells were observed neither with the alkaline nor with the neutral Comet assay. As Nordenson et al. (1994) reported positive genotoxic effects applying intermittent field exposure, our next experiments concentrated on exposures at different intermittence conditions. Intermittence of 5 min on/5 min off and 15 min on/15 min off revealed an increase of DNA-breaks in both, the alkaline and the neutral Comet assay, compared to sham-exposed cells, whereas at 5 min on field/25 min off field did not enhance the frequency of DNA-breaks (Tables 2, 3).

Table 2. Mean values of alkaline Comet tailfactors at different exposure conditions (n = 2), cell strain IH-9

Alkaline Comet Assay - different exposure conditions				
	exposed		sham	
	Comet tailfactor %	±SD#	Comet tailfactor %	±SD#
Continuous exposure (24h)	4.29	0.02	4.27	0,03
15'/15' on/off	6.47*	0.14	4.23	0.05
5'/5' on/off	6.98*	0,04	4.41	0.16
5'/10' on/off	7.47*	0.13	4.48	0.05
5'/15' on/off	6.68*	0.17	4.42	0.03
5'/20' on/off	5.90*	0.12	4.38	0.12
5'/25' on/off	4.27	0.04	4.23	0.03
1'/10' on/off	5.89*	0.19	4.21	0.14
3'/10' on/off	6.60*	0.06	4.19	0.22
10'/10' on/off	6.91*	0.07	4.24	0.07
15'/10' on/off	6.56*	0.15	4.11	0.08
25'/10' on/off	5.37*	0.05	4.21	0.04

SD indicates standard deviation
* indicates significant differences ($p < 0.05$) exposed vs. sham

Table 3. Mean values of neutral Comet tailfactors at different exposure conditions (n = 2), cell strain IH-9

Neutral Comet Assay - different exposure conditions				
	exposed		sham	
	Comet tailfactor %	±SD#	Comet tailfactor %	±SD#
Continuous exposure (24h)	4.20	0.03	4.17	0.05
15'/15' on/off	5.72*	0.01	4.25	0.04
5'/5' on/off	6.09*	0.02	4.31	0.08
5'/10' on/off	6.21*	0.01	4.35	0.07
5'/15' on/off	5.66*	0.06	4.23	0-13
5'/20' on/off	4.52	0.16	4.50	0.21
5'/25' on/off	4.25	0.05	4.34	0.07
1'/10' on/off	4.16	0.15	4.16	0.13
3'/10' on/off	5.94*	0.05	4.20	0.06
10'/10' on/off	6.19*	0.11	4.11	0.11
15'/10' on/off	6.02*	0.03	4.21	0.10
25'/10' on/off	5.44	0.01	4.15	0.01

#SD indicates standard deviation
* indicates significant differences ($p < 0.05$) exposed vs. sham

Based on these findings, we tried to find out the optimal exposure conditions for maximal effects on DNA strand break levels. We started with a fixed field-on time of 5 min and varied field-off times from 5 to 25 min. These experiments indicated that DNA strand break levels (SSB and DSB) culminated at an off-time of 10 min and reached control levels at extended off-times (Figure 7). Significant differences ($p< 0.01$) between exposed and sham-exposed cells were found at 5 min on/5 min off, 5 min on/10 min off, 5 min on/15 min off and 5 min on/20 min off intermittence for alkaline Comet assay and at 5 min on/5 min off, 5 min on/10 min off and 5 min on /15 min off intermittence for neutral Comet assay, but not at 5 min on/ 25 min off for both assays.

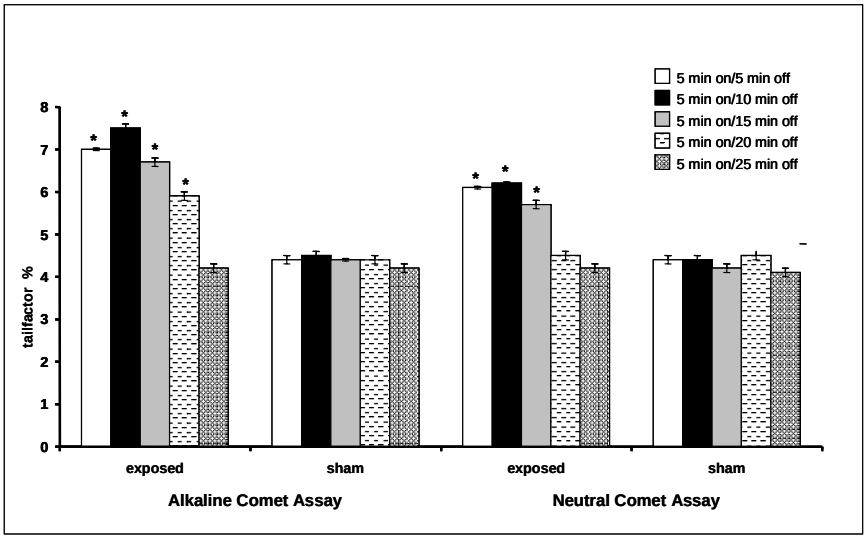

Figure 7. Alkaline and neutral Comet Assay tailfactors of ELF exposed fibroblasts (cell line IH-9, 50 Hz sinus, 24h,1000 µT, intermittent) - variation of off-time. * $p<0.01$ exposed versus sham-exposed

Subsequently, a fixed off-time of 10 min was chosen and on-times have been varied from 1 to 25 min. Again, the highest level of DNA strand breaks was obtained at an intermittence of 5 min on/10 min off (Figure 8). Comet tailfactors of exposed and sham-exposed cells differed significantly at each on-time in

alkaline Comet assay and at 3 to 15 min on in the neutral Comet assay. Solely the alkaline Comet tailfactors of 5 min on/10 min off, 5 min on/25 min off and 25 min on/10 min off-EMF exposed cells differed significantly to the other applied intermittence conditions. Since an intermittence of 5 min on/10 min off was able to induce the highest levels of DNA strand breaks in both alkaline and neutral Comet assay, further experiments were performed at 5 min on/10 min off.

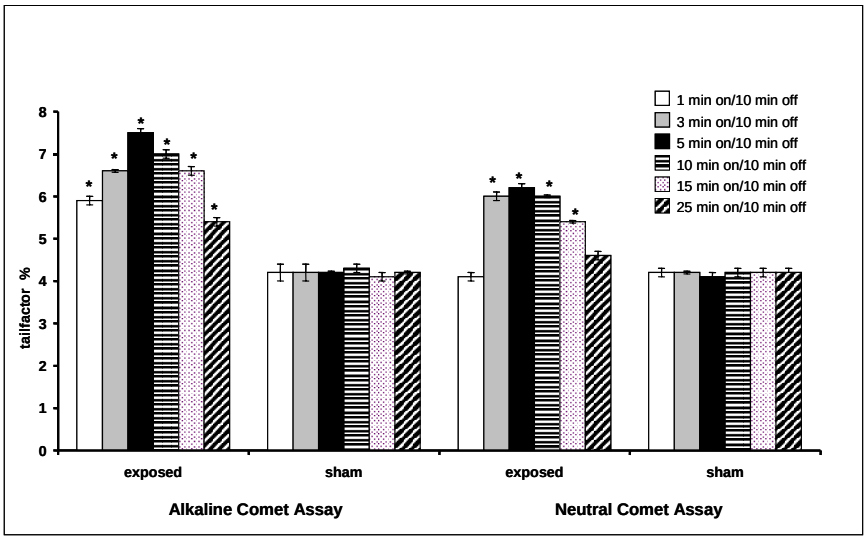

Figure 8. Alkaline and neutral Comet assay tailfactors of ELF exposed fibroblasts (cell line IH-9, 50 Hz sinus, 24 h, 1000 µT, intermittent) - variation of on-time. * $p < 0.01$ exposed versus sham-exposed

ELF-EMF 50 Hz sinus generated a higher rate of DNA strand breaks in human fibroblasts than ELF-EMF powerline.

By comparing 50 Hz sinus to the 50 Hz powerline signal it was found out that at 50 Hz powerline Comet assay tailfactors were significantly lower than at 50 Hz sinusoidal (Figure 9). All further experiments in the ELF-EMF range were, therefore, carried out with 50 Hz sinus.

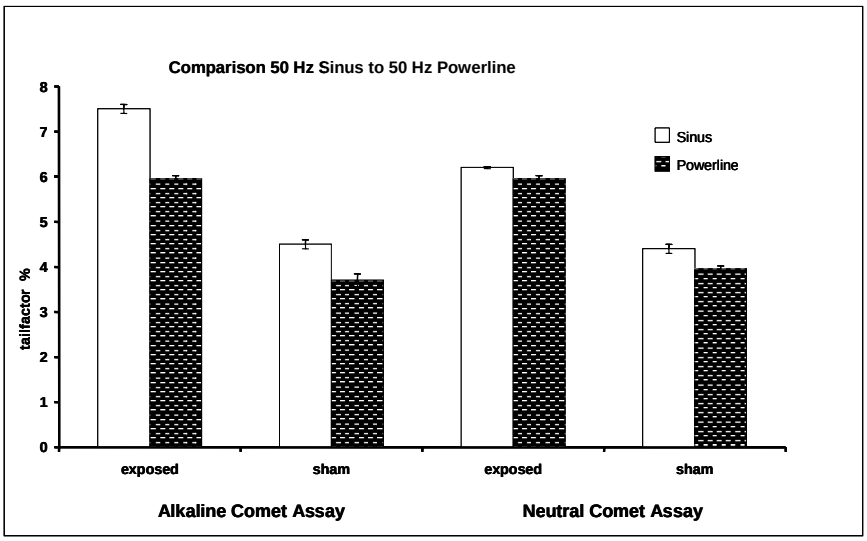

Figure 9. Alkaline and neutral Comet Assay tailfactors of ELF exposed fibroblasts (cell line IH-9, 24 h, 1000 µT, intermittent)

Genotoxic effects were frequency dependent.

In order to investigate the frequency dependence of genotoxic effects of ELF-EMF (1 mT, 5 min on/ 10 min off) cultured human fibroblasts were exposed to different frequencies (3-550 Hz). Exposure time was set to 15 hours. Genotoxic effects were evaluated using the alkaline Comet assay. Figure 10 presents the tailfactors in exposed and sham exposed cells. Significant increases in DNA damage could be found at 3 Hz, 16 2/3 Hz, 30 Hz, 50 Hz, 300 Hz, and 550 Hz. Effects on strand break levels varied with the applied frequencies and could be ranked as follows: 50 Hz > 162/3 Hz > 3 Hz > 300 Hz > 550 Hz > 30 Hz. Quite obviously, the extent of induced DNA damage did not correlate with the applied frequency.

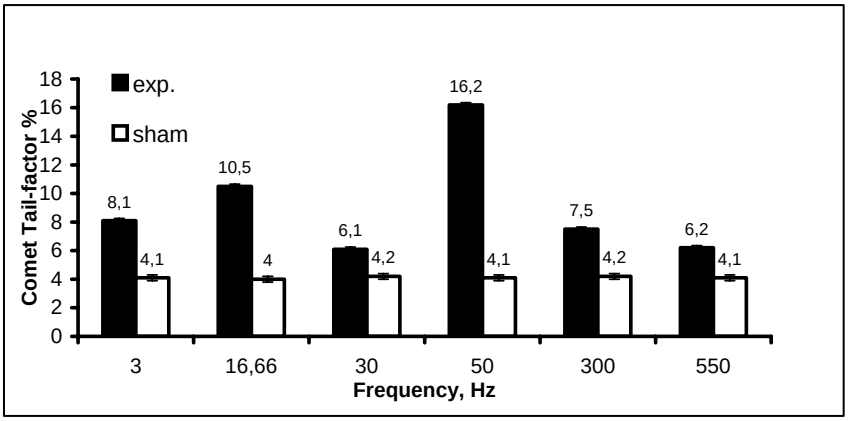

Figure 10. Alkaline Comet Assay tailfactors of ELF-EMF exposed and sham exposed fibroblasts (cell line ES-1, 15 hrs, 1000 µT, intermittent) after variation of exposure frequency (3-550 Hz).

Increase in DNA strand breaks in human fibroblasts after ELF-EMF exposure was dependent on exposure time.

Alkaline and neutral Comet tailfactors increased with exposure time (1-24 hours, 1000 µT, intermittent (5 min on/10 min off)), being largest at 15 hours (Figure 11). Comet assay levels declined thereafter, but did not return to basal levels.

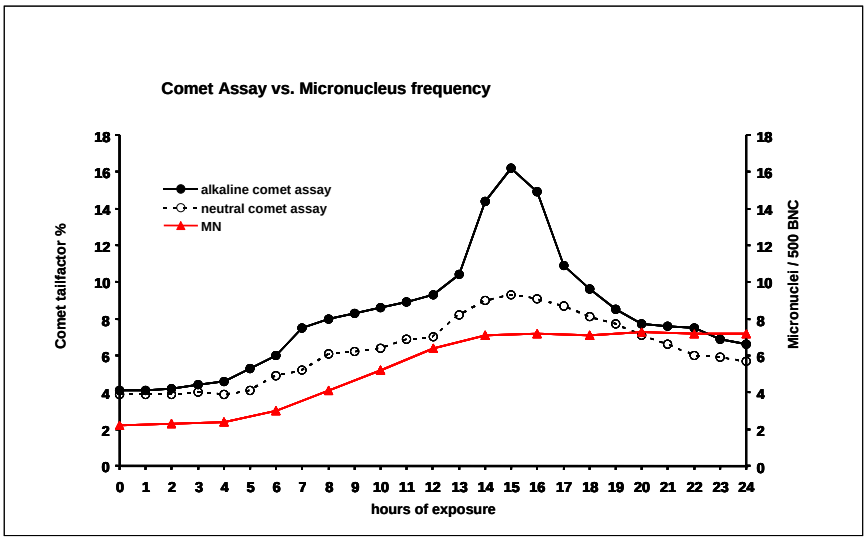

Figure 11. Influence of exposure time on formation of DNA single and double strand breaks and micronuclei in human fibroblasts (cell strain ES-1, 1 mT, 5 min on/10 min off cycles).

Increase in DNA strand breaks in human fibroblasts after ELF-EMF exposure was dependent on the age of the donors.

Fibroblasts from six healthy donors (ES1, male, 6 years old; AN2, female, 14 years old; IH9, female, 28 years old; KE1, male, 43 years old; HN3, female, 56 years old; WW3, male, 81 years old) revealed differences in response to ELF-EMF exposure (Table 4). Cells from older individuals exhibited a higher rate of single and double strand breaks and their break levels started to decline later than in cells from younger donors (Figures 12, 13).

Table 4. Alkaline and neutral Comet assay tailfactors of donors with different age (ES-1: 6, AN2: 14, IH9: 28, KE1: 43, HN3: 56, WW3: 81 years of age) - variation of exposure duration (basal-, maximum-, and end-levels)

			Alkaline Comet Assay		Neutral Comet Assay	
	cell strain	hours exposure duration	Comet tailfactor %	±SD#	Comet tailfactor %	±SD#
basal levels	ES1	0	4.112	0.018	3.901	0.006
	AN2	0	4.077	0.064	3.900	0.035
	IH9	0	4.223	0.047	4.161	0.148
	KE1	0	6.227	0.044	5.224	0.013
	HN3	0	6.802	0.018	6.313	0.064
	WW3	0	7.101	0.064	6.816	0.023
maximum levels	ES1	15	16.155	0.184	9.305	0.057
	AN2	15-16	16.501	0.004	9.394	0.134
	IH9	16	16.707	0.040	9.716	0.054
	KE1	18	17.300	0.064	10.462	0.277
	HN3	18-19	18.311	0.078	11.364	0.122
	WW3	19	18.517	0.069	12.822	0.076
and levels	ES1	24	6.611	0.017	5.742	0.023
	AN2	24	7.210	0.062	5.824	0.030
	IH9	24	7.511	0.017	6.127	0.054
	KE1	24	8.242	0.038	6.738	0.023
	HN3	24	8.718	0.008	6.761	0.006
	WW3	24	9.229	0.037	8.010	0.063

#SD ....standard deviation

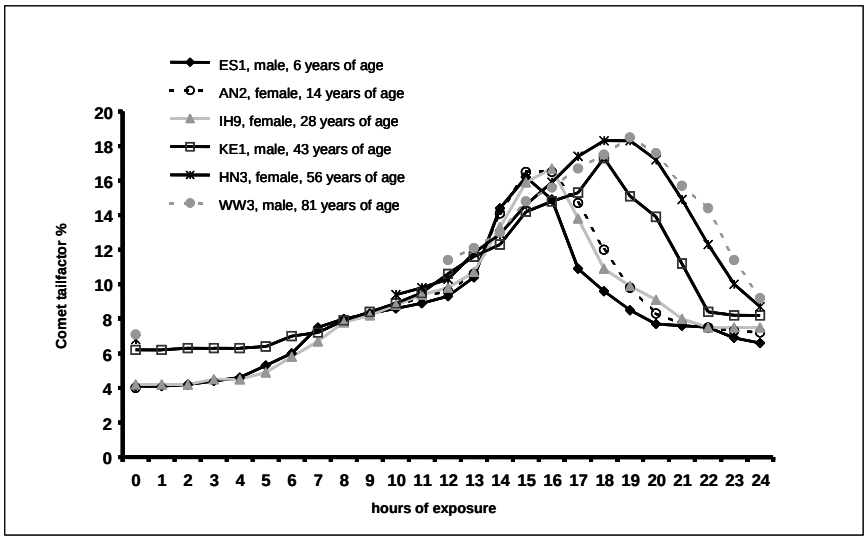

Figure 12. Alkaline Comet tailfactors of human diploid fibroblasts of donors with different years of age exposed to ELF-EMF (1 mT, intermittent 5 min on/10 min off) for 1-24 hours

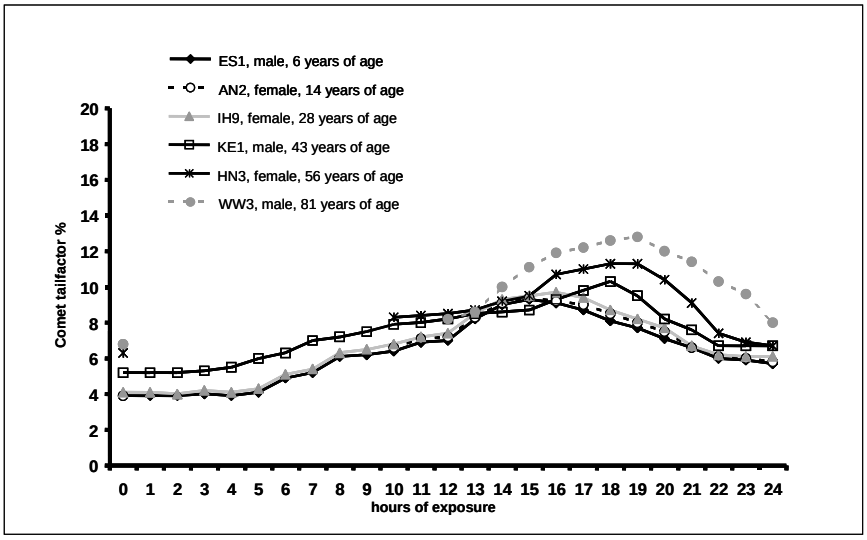

Figure 13. Neutral Comet tailfactors of human diploid fibroblasts of donors with different years of age exposed to ELF-EMF (1 mT, intermittent 5 min on/10 min off) for 1-24 hours

Increase in DNA strand breaks in human fibroblasts after ELF-EMF exposure was accompanied by a rise in micronuclei frequencies.

In addition, variation of exposure time from 2 to 24 hours revealed a time dependent increase in micronucleus frequencies. As shown in Figure 11, this increase became significant ($p<0.05$) at 10 hours of ELF-EMF exposure. Thereafter, micronucleus frequencies reached a constant level, which was about 3-fold as compared to the basal levels (Figure 14).

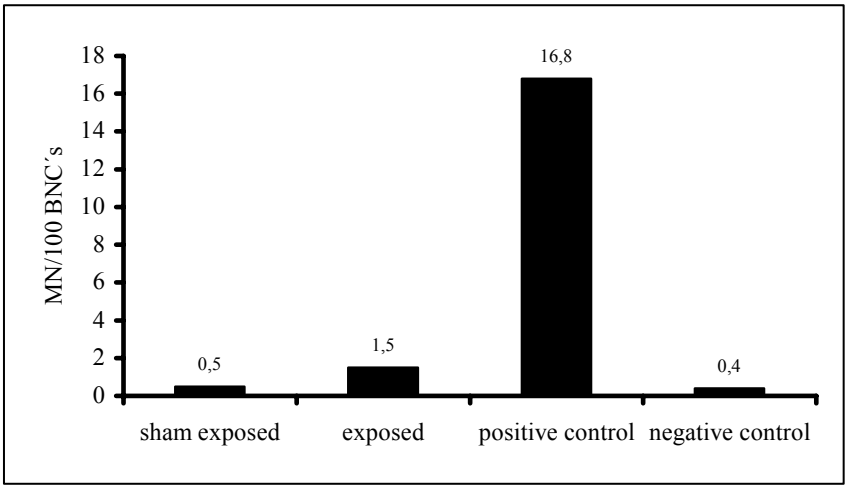

Figure 14. Micronucleus frequencies of ELF-EMF exposed (50 Hz, 1 mT, 15 h, 5 min on/10 min off) cultured human fibroblasts and controls (Vienna). Bleomycin 10µg/ml was used as a positive control.

ELF-EMF exposure did not diminish the number of fibroblasts in culture.

No differences in cell count between exposed and sham exposed cells at any exposure duration could be detected. Therefore, an elimination of cells by apoptosis and cell death during ELF-EMF exposure can probably be ruled out.

ELF-EMF exposure induced DNA strand breaks in human fibroblasts in a dose dependent way.

When magnetic flux density increased from 20 to 1,000 µT, a dose dependent rise in Comet assay tailfactors could be observed. At an exposure time of 24 hours a magnetic flux density as low as 70 µT produced significantly elevated ($p < 0.01$) alkaline and neutral Comet assay levels as compared to sham-exposed controls (Figure 13). At 15 hours of exposure genotoxic effects already occurred at 35 µT (Table 5, Figure 12). Using regression analysis, a significant correlation between Comet tailfactors and applied magnetic field (alkaline Comet assay: $r = 0.843$, $p = 0.004$; neutral Comet assay: $r = 0.908$, $p = 0.0007$), as well as between alkaline and neutral Comet assay could be found ($r = 0.974$, $p = 0.00001$).

Table 5. Mean values of alkaline and neutral Comet tailfactors at intermittent ELF exposure (5/10 on/off, 1000 µT, 24 h) (n = 2) dose response, cell line ES-1

	Alkaline Comet Assay				Neutral Comet Assay			
	exposed		sham		exposed		sham	
µT magnetic flux density	tailfactor %	±SD#	tailfactor %	±SD#	tailfactor %	±SD#	tailfactor %	±SD#
20	4.16	0.02	4.21	0.13	3.63	0.01	3.60	0.08
50	4.16	0.06	4.20	0.12	3.70	0.16	3.72	0.03
70	4.87*	0.03	4.28	0.02	3.99*	0.01	3.71	0.01
100	5.25*	0.06	4.28	0.05	4.32*	0.00	3.73	0.04
250	5.31*	0.02	4.25	0.07	4.24*	0.06	3.60	0.02
500	5.52*	0.01	4.22	0.01	4.48*	0.02	3.79	0.05
750	6.17*	0.08	4.26	0.11	5.08*	0.08	3.67	0.10
1000	6.50*	0.18	4.27	0.10	5.71*	0.01	3.79	0.16
2000	6.62	0.01	4.13	0.04	5.79*	0.05	3.70	0.01

SD indicates standard deviation
• indicates significant differences ($p < 0.05$) exposed vs. sham

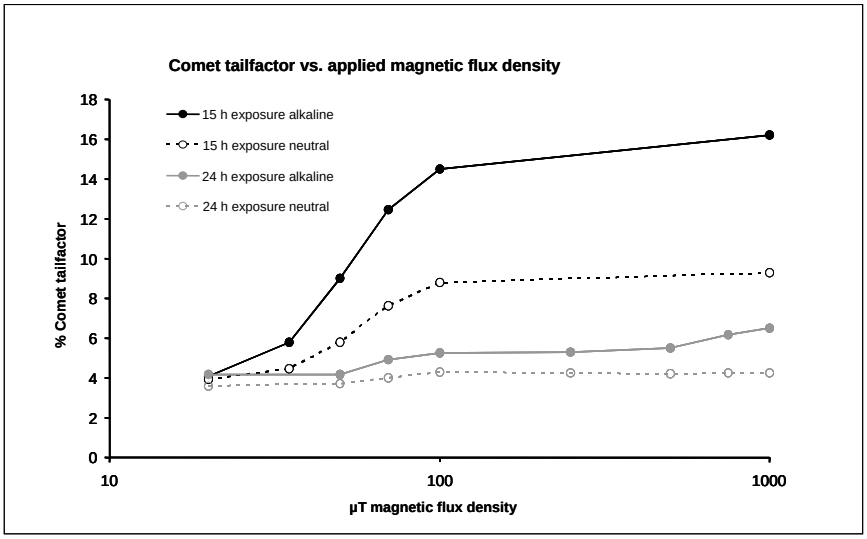

Figure 15. Dose dependent formation of DNA single and double strand breaks determined with Comet assay under alkaline and neutral conditions with cell strain ES-1 (exposure time 15 and 24 hours, 5 min on/10 min off cycles)

DNA strand breaks in human fibroblasts after ELF-EMF exposure were rapidly repaired.

After having demonstrated a time dependent relationship between alkaline and neutral Comet assay tailfactors and ELF-EMF exposure, the next aim was to find an explanation for the declining of the Comet assay levels after reaching the peak value. When exposure was terminated after 12 or 15 hours the Comet tailfactors returned to basal levels after a repair time of 7 to 9 hours (Figures 15, 16), comprising in a fast repair rate of DNA single strand breaks (< 1 hour) and a slow repair rate of DNA double strand breaks (> 7 hours). The marked Comet peak value between 12-17 hours disappeared when the Comet assay was performed at pH 12.1 instead of pH >13, thereby eliminating the cleavage of alkali labile sites in the DNA (Figure 18). The decline of Comet tailfactors after 15-20 hours of exposure could be prevented, when the cells were exposed in the presence of 10 µg/ml cycloheximide, an inhibitor of protein synthesis (Figure 18.

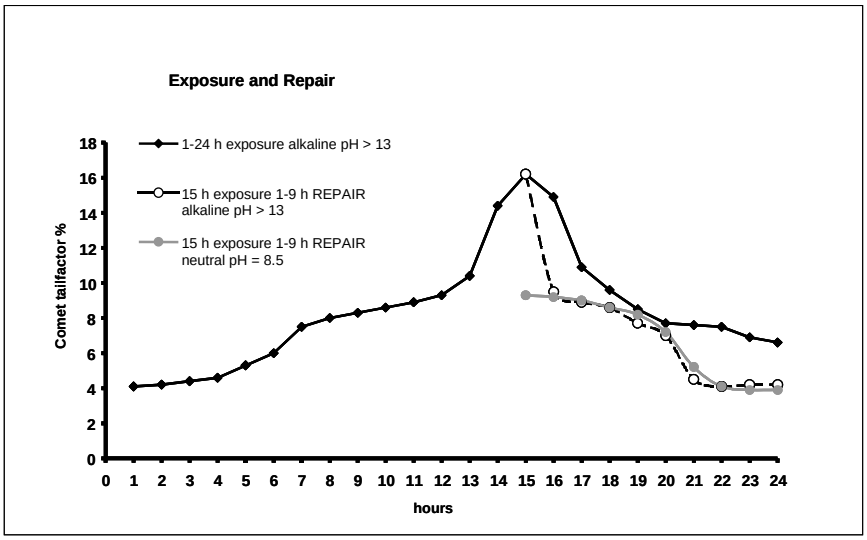

Figure 16. Repair kinetics of DNA single and double strand breaks in human fibroblasts (cell strain ES-1) after termination of ELF-EMF exposure (cell strain ES-1, 1 mT, 5 min on/10 min off cycles) using alkaline and neutral Comet assay - repair after 15 h ELF-EMF exposure

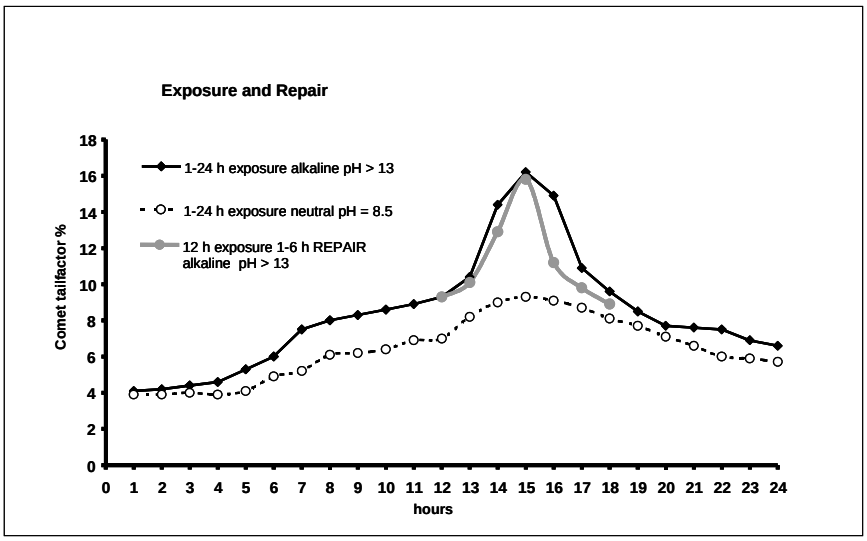

Figure 17. Repair kinetics of DNA single and double strand breaks in human fibroblasts (cell strain ES-1) after termination of ELF-EMF exposure (cell strain ES-1, 1 mT, 5 min on/10 min off cycles) using alkaline and neutral Comet assay - repair after 12 hours ELF-EMF exposure

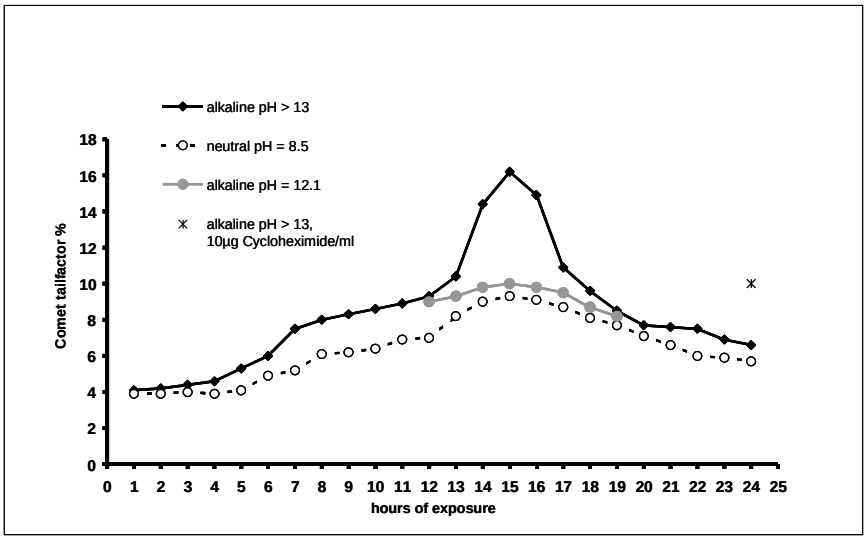

Figure 18. Comet assay of exposed human fibroblasts was performed at different pH (1 mT, intermittent 5 min on/10 min off)

DNA repair deficient cells react differently to ELF-EMF exposure.

Diploid human fibroblasts from patients with the genetically determined DNA repair defects Cockayne Syndrome, Ataxia Teleangiectatica, and Bloom Syndrome were obtained from Coriell Cell Repository (Camden, New Jersey, USA). The cells were cultured under standardized conditions and exposed (24 hours, 1 mT, 5 min on/10 min off) or sham exposed, and alkaline Comet assay was performed as described. As a result the Cockayne and Bloom Syndrome fibroblasts exhibited a similar pattern of genotoxicity as normal control fibroblasts, whereas the cells from a patient with Ataxia Teleangiectatica showed an almost threefold increased ELF-EMF induced Comet tailfactor as compare to normal cells (Figure 19).

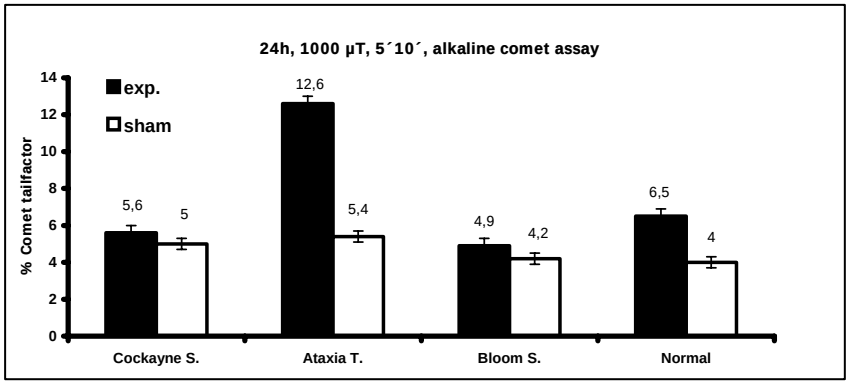

Figure 19. Alkaline Comet assay tailfactors of ELF-EMF exposed human fibroblasts from patients with various genetically determined DNA repair defects and normal controls.

Generation of DNA strand breaks through ELF/EMF was cell type specific.

ELF-EMF exposure (50 Hz sinusoidal, 1 mT, 5 min on/10 min off, 1-24 hours) of different human cell types (melanocytes, skeletal muscle cells, fibroblasts, monocytes, stimulated and quiescent lymphocytes) and of SV40 transformed rat granulosa cells revealed differences in induced DNA damage. Rat granulosa cells exhibited the highest DNA strand break levels and seemed to be most sensitive to intermittent ELF-

EMF exposure (Figures 20, 21). Human melanocytes also reacted, but not as strong as fibroblasts or rat granulosa cells. In contrast, stimulated or non-stimulated lymphocytes, monocytes and skeletal muscle cells did not respond at all.

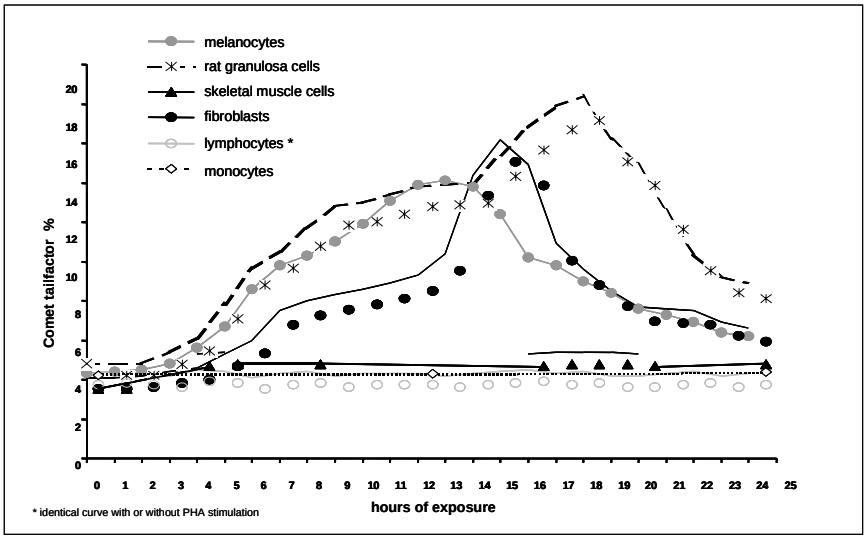

Figure 20. Alkaline Comet tailfactors of different human cell types (fibroblasts, melanocytes, monocytes, lymphocytes, skeletal muscle cells) and SV 40 transformed rat granulosa cells exposed to ELF-EMF (50 Hz sinusoidal, 1 mT, intermittent 5 min on/10 min off) for 1 to 24 hours.

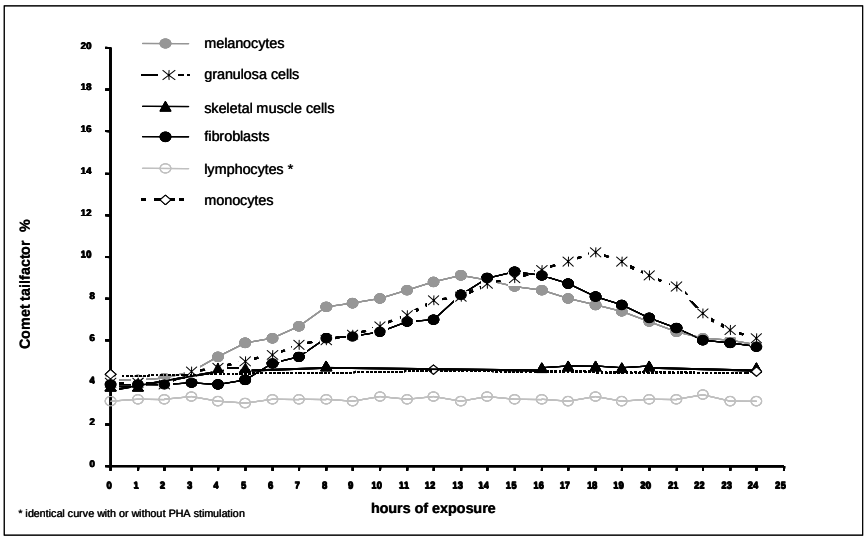

Figure 21. Neutral Comet tailfactors of different human cell types (fibroblasts, melanocytes, monocytes, lymphocytes, skeletal muscle cells) and SV 40 transformed rat granulosa cells exposed to ELF-EMF (50 Hz sinusoidal, 1 mT, intermittent 5 min on/10 min off) for 1 to 24 hours.

Generation of DNA strand breaks in human fibroblasts through ELF-EMF and their repair were modified by UVC or heat stress.

To test a possible impact of ELF-EMF exposure on DNA repair, cells were subjected to combined exposures to ELF + UVC or ELF-EMF + heat stress. In the first set of experiments fibroblasts were pre-exposed to UVC (10 min., 1.2 kJ/m^2). Subsequently, ELF-EMF exposure (50 Hz, sinus, 1000 µT) was varied from 1-24 hours. Results of the alkaline Comet assay showed that DNA damage caused by UVC could be removed within 7 hours of ELF-EMF exposure (Figure 22). UV/ELF-EMF exposed cells

resulted in 50 % higher Comet assay levels than UV/sham exposed cells after 1 hour of ELF-EMF exposure. In UV/ELF-exposed cells DNA-damage was repaired very slowly, but the maximum at 15 hours ELF-EMF-exposure could not be detected any more. The results were similar with the neutral Comet assay, but DNA damage (DNA double strand breaks) was repaired within a shorter time (Figure 23)

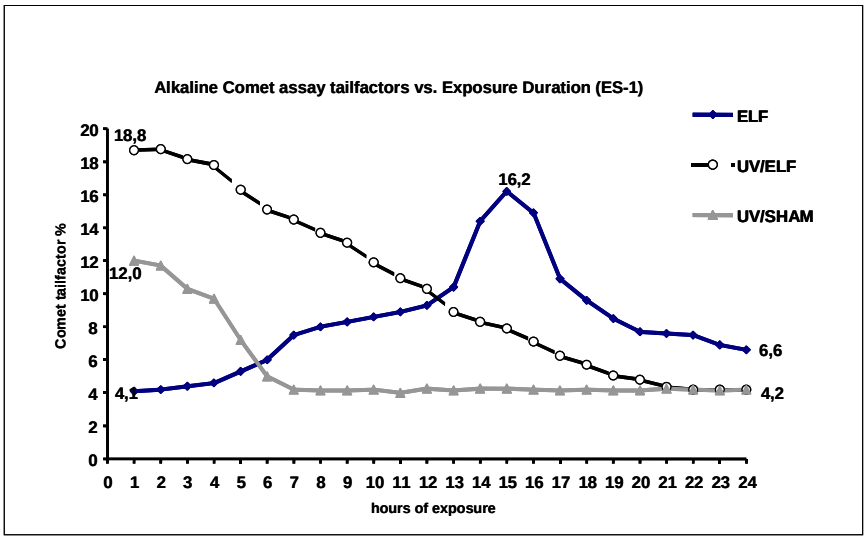

Figure 22. Repair kinetics of DNA single and double strand breaks in human fibroblasts (cell strain ES-1) after exposure with UV-C, ELF-EMF or UV C + ELF-EMF (cell strain ES-1, 1 mT, 5 min on/10 min off cycles) using alkaline Comet assay

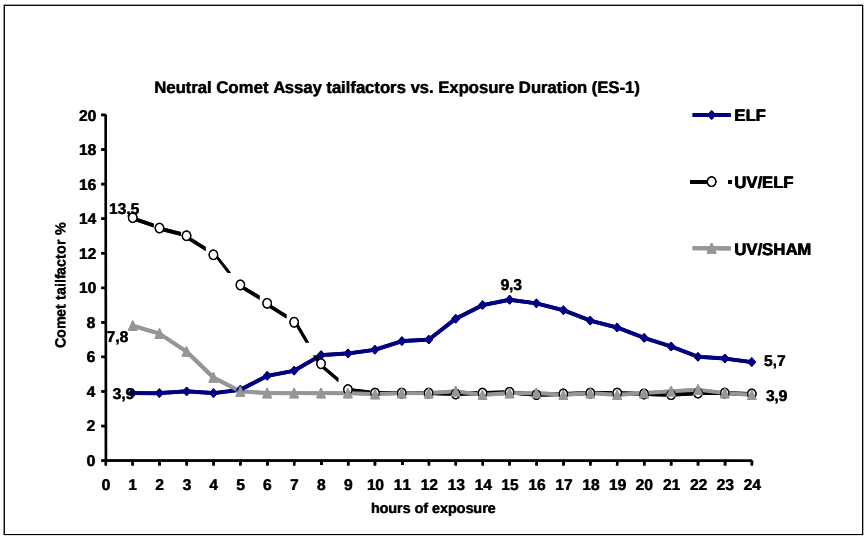

Figure 23. Repair kinetics of DNA single and double strand breaks in human fibroblasts (cell strain ES-1) after exposure with UV-C, ELF-EMF or UV C + ELF-EMF (cell strain ES-1, 1 mT, 5 min on/10 min off cycles) using neutral Comet assay

Based on the results with human fibroblasts, which suggest an induction of DNA repair upon intermittent ELF-EMF exposure, we concluded that pre-exposure to ELF-EMF would have a protective effect and diminish effects of additional exposures from other genotoxic factors. To check this assumption, fibroblasts were pre-exposed to ELF-EMF (50 Hz sinusoidal, 5 min on/10 min off, 1 mT) for 20 hours to ensure maximum induction of DNA repair. Subsequently, cells were either exposed to UVC (254 nm, 4.5

kJ/m², 30 min) or to mild heat stress (38.5°C, 4 h). Recovery of DNA damage was evaluated using alkaline and neutral Comet assay. UVC-exposure produced 50 % higher DNA strand break levels than ELF-EMFs alone and DNA damage was completely repaired after 3 hours (Figure 24). DNA damage induced by mild thermal stress was even higher and persisted longer than 6 hours after exposure termination. Pre-exposure to ELF-EMF intensified and elongated UVC or temperature induced DNA damage. After 24 hours of recovery time ELF-EMF pre-exposed cells still exhibited higher DNA strand break levels and just about 50% of the initially induced DNA damage had been repaired after this time. The results were similar with the neutral Comet assay, indicating induction and repair of DNA double strand breaks (Figure 25).

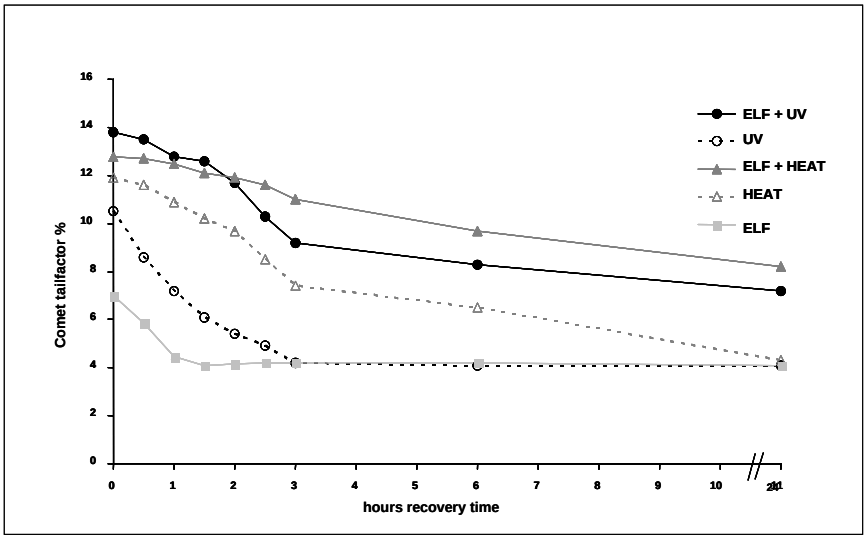

Figure 24. DNA damage and repair of cultured human fibroblasts pre-exposed to ELF-EMF (50 Hz sinusoidal, 5 min field-on/10 min field-off, 1 mT, 20 hours) and additionally exposed to UVC (254 nm, 30 min, 4.5 kJ/m²) or mild thermal stress (38.5°C, 4 hours) evaluated using alkaline Comet assay.

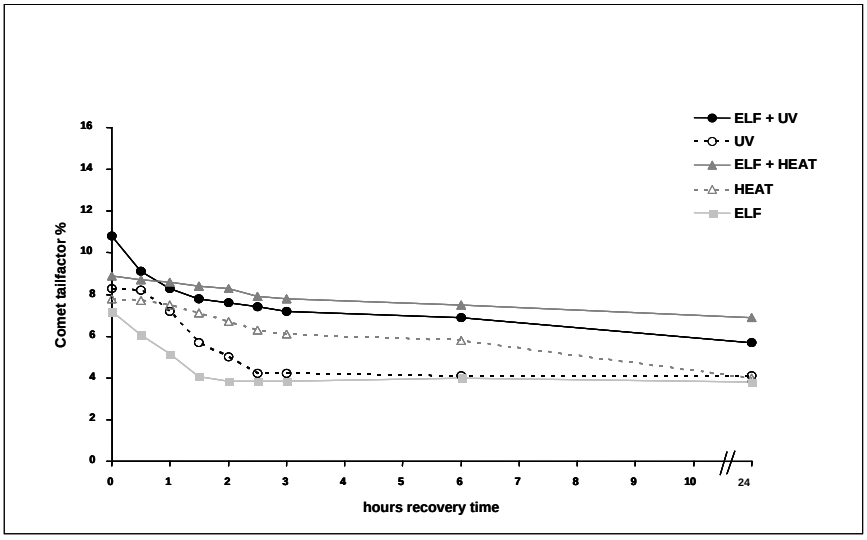

Figure 25. DNA damage and repair of cultured human fibroblasts pre-exposed to ELF-EMF (50 Hz sinusoidal, 5 min field-on/10 min field-off, 1 mT, 20 hours) and additionally exposed to UVC (254 nm, 30 min, 4.5 kJ/m²) or mild thermal stress (38.5°C, 4 hours) evaluated using neutral Comet assay.

ELF-EMF generated chromosomal aberrations in human fibroblasts.

Chromosomal aberrations were evaluated at exposure conditions producing maximum effects in the Comet assay and in the micronucleus test (15 h, 1 mT, 5min on/10 min off). Five different types of aberrations were separately scored (gaps, breaks, rings, dicentric chromosomes, acentric fragments). Significant increases ($p < 0.05$) between exposed and sham exposed cells could be demonstrated for all types of aberrations (Table 6). Gaps were 4-fold increased, breaks 2-fold, and dicentric chromosomes and acentric fragments 10-fold. Translocations were evaluated using the fluorescence in situ hybridisation (FISH) technique. 1,000 metaphases were scored for each specifically labeled chromosome (1-22, X and Y) after ELF-EMF exposure (50 Hz, 24h, 5 min on/10 min off, 1 mT). No stable translocation in any of the 24,000 metaphases of ELF-EMF exposed cells could be detected (data not shown).

Table 6. Percentage of chromosomal aberrations induced by ELF-EMF exposure (50 Hz, 5´field-on/10´field-off, 1 mT, 15 h) in cultured human fibroblasts.

Types of aberrations	ELF-exposed (% ± SD)	sham-exposed (% ± SD)	p-value*
chromosome gaps	24.3 ± 1 %	5.5 ± 0.7 %	< 0.001
chromosome breaks	2.2 ± 0.3 %	1.3 ± 0.3 %	0.0015
ring chromosomes	0.1 ± 0.07 %	---	0.0133
dicentric chromosomes	0.4 ± 0.1 %	0.06 ± 0.05 %	< 0.001
acentric chromosomes	0.3 ± 0.07 %	0.02 ± 0.04 %	< 0.001

[a] A number of 1,000 metaphases were scored in each of five independent experiments. Results are expressed as percentage chromosomal aberrations per cell.
[b] Significant differences ($p < 0.05$) as compared to sham-exposed controls using Student's t-test for independent samples

ELF-EMF did not alter the mitochondrial membrane potential in human fibroblasts.

The experimental settings in the present tests were based on conditions, which resulted in the highest inducible frequencies of these DNA strand breaks in human fibroblasts. Evaluating changes in the mitochondrial membrane potential after ELF exposure (50 Hz, 15 hours, 1 mT, 5 min on/10 min off) using JC-1, revealed no significant differences between exposed and sham-exposed fibroblasts.

3.1.1.2 Granulosa cells of rats, Chinese hamster ovary cells (CHO) and HeLa cells (Participant 7)

ELF-EMF exposure caused a significant increase of DNA strand breaks in cultured rat granulosa cells, CHO cells and HeLa cells.

The effect of ELF-EMF was analysed on the genomic level by use of the Comet assay. Especially the dependence on exposure time and frequency was analysed. Figure 26 shows that exposure to ELF-EMF at 16 2/3 Hz (5 min on/10 min off, 1.0 mT) caused a significant increase in single and double DNA strand breaks in cultured granulosa cells. The same result was obtained with CHO and HeLa cells (not shown). The data presented in Figure 26 indicate that the genotoxic effect at 16 2/3 Hz is time dependent with a maximum after about 18 hours of exposure, which resembles the results obtained at 50 Hz by Participant 3 (Ivancsits et al., 2003).

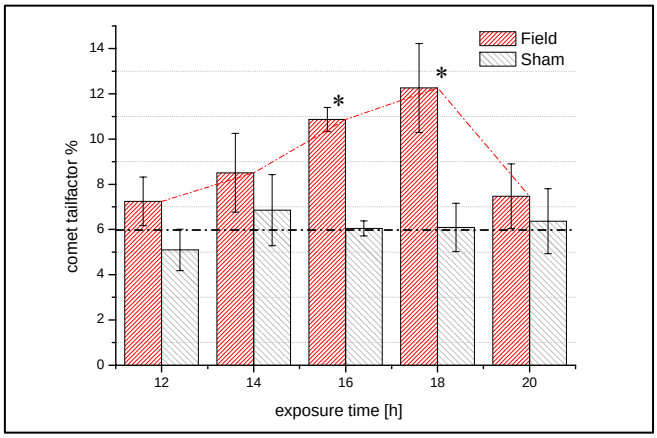

Figure 26. DNA damage of rat granulosa cells after exposure for 12 to 20 hours to ELF-EMF (16 2/3 Hz, 5 min on/10 min off, 1 mT) evaluated using alkaline Comet assay. For values of n see Material and Methods. (* p< 0.05)

To investigate the frequency dependence of the genotoxic effect of ELF-EMF (5 min on/10 min off) exposure of rat granulosa cells a constant exposure time of 18h was selected. Figures 27 and 28 present the tailfactors of exposed and sham exposed granulosa cells using the alkaline and neutral Comet assay. At the applied frequencies within the range of 8 Hz to 1000 Hz a significant frequency dependence was not observed for the rate of double DNA strand breaks as derived from the neutral Comet assay (Figure 28). The corresponding results of the alkaline Comet assay are presented in Figure 27. At 8 Hz, 16 2/3 Hz and 50 Hz an intensity of 1 mT could be applied (Figure 27a). A significant increase of DNA strand breaks was found at 16 2/3 Hz. Surprisingly, especially at 50 Hz the s.e.m. data of sham and ELF-EMF exposed cells differ significantly. The large error could be caused by a variable time dependent location of the maximum and/or the influence of the specific cell passage. Further experiments are under analysis to confirm the data presented in Figure 27a. At 1000 Hz the recorded DNA damage is significantly lower than observed at 16 2/3 Hz (Figure 27b). But it has to be noted that the maximal applied flux density was limited to 0.6 mT due to the used exposure system (Participant 10). Furthermore, DNA damage was measured at 20 µT, which approximately corresponds to the maximal acceptable magnetic flux density as recommended by the 26. BlmSchV[1]. Again a significant increase of DNA strand breaks was observed (Figure 27b).

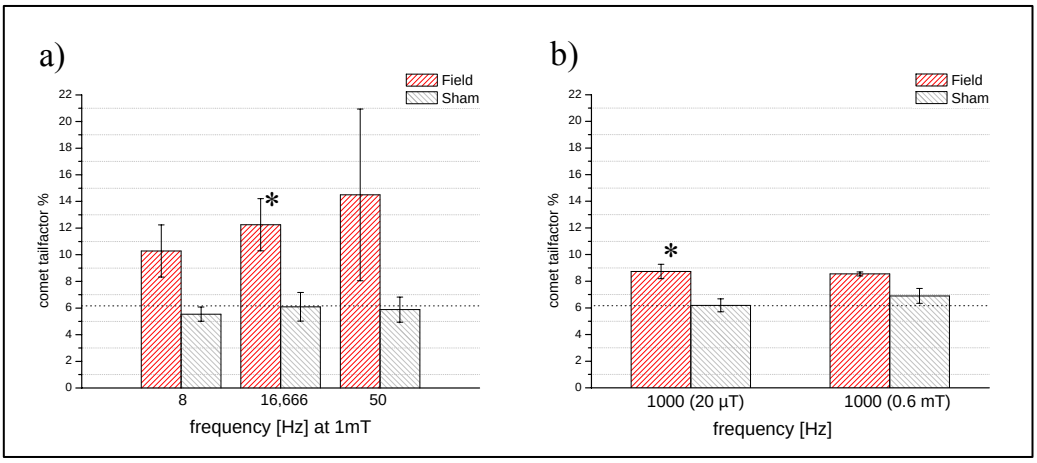

Figure 27. DNA damage of rat granulosa cells as function of frequency of ELF-EMF (5 min on/10 min off) after an exposure for 18 hours as derived by the alkaline Comet assay. **a)** In the frequency range of 8 to 50 Hz the flux density was set to 1 mT. **b)** At 1000 Hz the flux density was adjusted to 20 µT and 0.6 mT (for further explanation, see text). For values of n see Material and Methods. (* p< 0.05)

[1] 26. Verordnung zur Durchführung des Bundes-Immissionschutzgesetzes (Verordnung über elektromagnetische Felder – 26. BlmSchV)

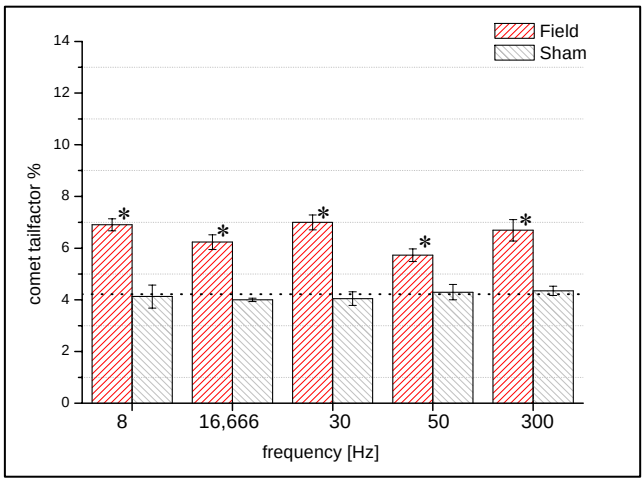

Figure 28. Double DNA strand breaks of rat granulosa cells as function of frequency of ELF-EMF (5 min on/10 min, 1 mT) after an exposure time of 18 hours as derived by the neutral Comet assay. For values of n see Material and Methods. (* $p < 0.05$)

3.1.1.3 Embryonic stem cells (ES) of mice (Participant 4)

Lack of effects on single and double strand break induction 0, 18, 24 and 48 hours after completion of a 6 or 48 hours ELF-EMF exposure.

The effects of ELF-EMF on the integrity of DNA strands in differentiating ES cell from EB outgrowths were studied. Two schemes were applied: (1) For ELF-EMF exposure (50 Hz Powerline, 2.0 mT, 5 min on/30 min off, 6 hours) the percentage of primary DNA damage was measured immediately after ELF-EMF exposure at the stage of neural differentiation (4+4d - 4+6d) and 18 hours after exposure using the alkaline and neutral Comet assay. (2). In the second set of experiments, the same ELF-EMF exposure conditions were applied for 48 hours instead of 6 hours, and the alkaline Comet assay was done immediately after exposure, while the neutral Comet assay was done 24 or 48 hours post exposure. No significant differences were observed in the induction of single or double DNA strand breaks between sham-exposed or ELF-EMF exposed neural progenitors.

3.1.1.4 Summary (Participant 1)

Our data indicate a genotoxic action of ELF-EMF in various cell systems. This conclusion is based on the following findings:

- Intermittent exposure to 50 Hz ELF-EMFs generated DNA single and double strand breaks in various cell systems such as human fibroblasts, melanocytes, granulosa cells of rats, Chinese hamster ovary cells (CHO) and HeLa cells, but not in human lymphocytes, monocytes, myelocytes and neural progenitors from mouse embryonic stem cells (see 3.1.1.1, 3.1.1.2 and 3.1.1.3).
- DNA damage generated by ELF-EMF in human fibroblasts was dependent on time and dose of exposure, on the age of the donors the cells derived from, and on the genetic background of the cells. A flux density of 35 µT was high enough to significantly increase the number of DNA strand breaks (see 3.1.1.1)
- The increase in DNA strand breaks in human fibroblasts due to ELF-EMF exposure was accompanied by an enhanced formation of micronuclei which was also dependent on the exposure time (see 3.1.1.1).
- The DNA repair system in human fibroblasts which was strongly activated by ELF-EMF during exposure did not work error-free as shown by a significant increase of different types of chromosomal aberrations (see 3.1.1.1).
- Genotoxic effects were frequency dependent. Significant increases in DNA strand breaks were found, when an ELF-EMF of 3 Hz, 16 2/3 Hz, 30 Hz, 50 Hz, 300 Hz, 550 Hz and 1000 Hz was applied. The

effect was strongest with 50 Hz ELF-EMF and second strongest with 16 2/3 Hz (see 3.1.1.1 and 3.1.1.2).

3.1.2 Cell proliferation and differentiation

3.1.2.1 Human neuroblastoma cell line NB69 (Participant 5)

ELF-EMF promoted the growth rate of NB69 neuroblastoma cells.

Immunocytochemical staining using antibodies against phenotype-specific antigens revealed that NB69 cells contain the neuroblast-specific protein ßIII-tubulin. However, these cells do not contain the neuroepithelial marker nestin, which is present in immature progenitors and in some neuroblastoma cells, nor the astrocyte-specific antigen GFAP. The cells remained in an undifferentiated state throughout the experimental period. Only the treatment with retinoic acid induced neurite extension accompanied by cell growth reduction.

Two series of experiments were carried out to analyse the cell growth response of NB69 cells to ELF-EMF. In the first series, the ELF-EMF administrated alone (42 hours) provoked a modest, though significant increase in the number of cells at day 5 postplating (5 dpp), both at 10-µT (12% over controls, **$p<0.01$) and 100-µT MFD (17 % increase over controls, ***$p<0.001$) as shown in Figure 29A). Retinol (ROL) alone or in combination with ELF-EMF did not change significantly the cell growth (data not shown). The ELF-EMF exposure also provoked modest increases in the total DNA levels, the effect being statistically significant at 10 µT (8 % over controls, $p<0.05$, Figure 29B). However no significant changes were observed in the protein or protein/DNA contents in the ELF-EMF exposed samples. Taken as a whole, these results indicate that exposure to 50 Hz ELF-EMF at 10 or 100 µT promote cell growth in the NB69 human neuroblastoma cell line.

In the second series of experiments, the 42-hours exposure to ELF-EMF at a flux density of 100 µT significantly increased cell growth (11 % over controls, ***$p<0.001$, Figure 30A). This result confirms the growth-promoting response obtained in the first experimental series. However, such an effect was not observed, when the ELF-EMF exposure was maintained for a longer period of time, i.e. 90 hours (Figure 30B). The treatment with retinoic acid (RA) alone significantly reduced the cell number, both at 42 and 90 hours, when compared to untreated controls. Also, RA-treated cells did show the growth-promoting effects of a 100 µT ELF-EMF, these samples demonstrating reduced growth rates when compared to unexposed controls: 35% reduction at the end of 42 hours-treatment ($p<0.0001$) and 57% reduction at the end of 90 hours-treatment ($p<0.0001$).

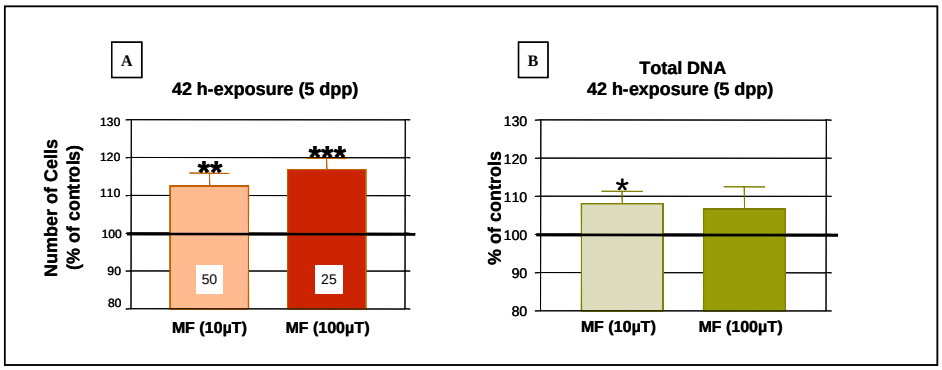

Figure 29. First series of experiments. A-Cell growth estimated by cell counting (Trypan blue exclusion) and B-Total DNA estimated by spectrophotometry.

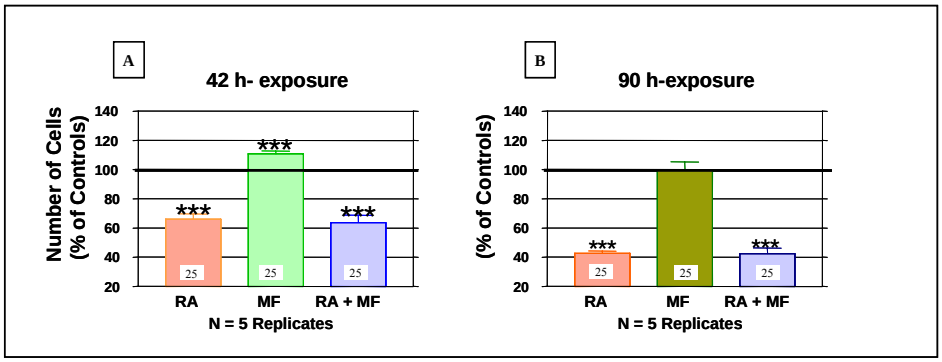

Figure 30. Second series of experiments: A-Number of cells at day 5 postplating (after 42 hours-exposure) and B-Number of cells at day 7 postplating (after 90 hours-exposure).

No experiment could be performed at a flux density of 2.0 mT following the 3 hours on/3 hours off exposure protocol, since the ohmic heat in the coils due to the electric current could not be compensated by the incubator resulting in an unstable ambient temperature. When the samples were exposed to 2 mT ELF-EMF in a 5min on/30 min off cycle, no effect was observed on the cell growth. Similarly, the cells did not respond to a 5 min on/30 min off cyclic exposure to a 100 µT ELF-EMF. It is possible that the NB69 cell line requires a longer exposure cycle to show significant changes in the cell growth.

A growth-promoting effect of ELF-EMF in NB69 neuroblastoma cells was not observed after an extended exposure period.

As described above, the growth promoting effect of a 100-µT EMF was not observed when the exposure was maintained for a longer period of time, i.e. 90 hours (Figure 30B). In NB69 cultures kept in control conditions, the number of cells peaks at day 6 and then decays (Figure 31). In the present experiments, long-term cultures (7 days postplating) reached a confluence stage close to saturation. This physiological condition could be the cause of the lack of response to ELF-EMF after long-term exposures between 3 and 7 days postplating.

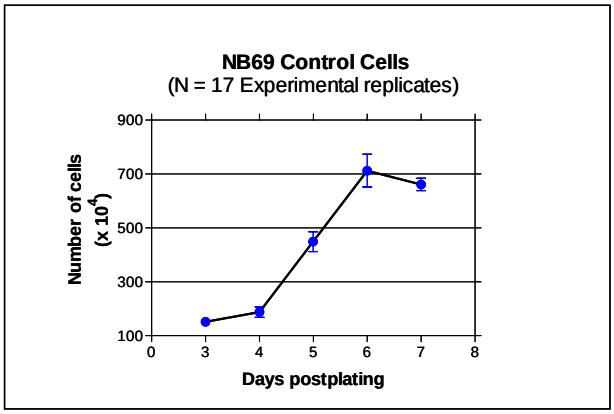

Figure 31. Growth pattern of NB69 cells: On day 7 the number of cells is reduced when compared to that at day 6. Long-term cultures (7 days postplating), reached a confluence stage close to saturation.

ELF-EMF did not counteract the retinoic acid-induced inhibition of cell proliferation in NB69 neuroblastoma cells.

To better characterise the potential ELF-EMF effects on the proliferation/differentiation rate, NB69 cells were treated with a chemical agent that inhibits proliferation and induces differentiation. All trans retinoic

acid (RA) promotes differentiation in NB69 cells, inducing outgrowth of long neurite-like processes and driving of the cell morphology along a neural pathway. As shown in Figure 30AB, the cell growth decreases after treatment with RA (2 µM) for 5 or 7 days. This response to RA remained unchanged after exposure to the ELF-EMF during 42 or 90 hours.

ELF-MF enhanced the cellular proliferation rate NB69 neuroblastoma cells as revealed through analysis of cell proliferation markers (PCNA).

Studies of expression of cell proliferation markers (PCNA) reinforce the described effects of ELF-EMF on cell growth: To determine whether the above growth-promoting effect detected by Trypan Blue exclusion involves changes in cell proliferation, we searched for changes in the proliferating cell nuclear antigen (PCNA). PCNA immunolabelling shows that exposure to 10 µT ELF-EMF significantly increases the proportion of PCNA-positive cells (24% increase; Figure 32). This effect was associated with an increase in the number of cells (15% increase), showing a significant linear correlation between both of the parameters, PCNA positive cells and total number of cells, at the end of 42 hours exposure ($p<0.01$). These results confirm and reinforce the previous observations that a 42 hours exposure to ELF-EMF at a flux density of 10 µT can modulate cell growth in NB69 cells. The mean value of PCNA positive cells in controls is 32 % ± 1,3).

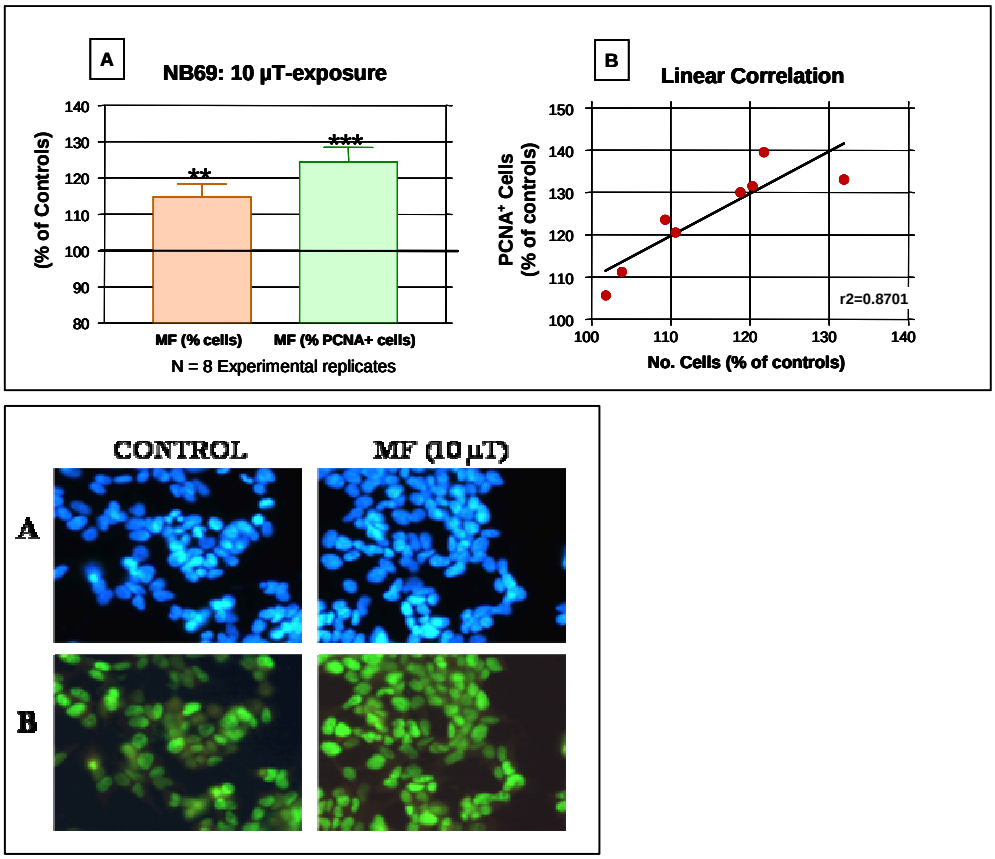

Figure 32. A) Growth response of NB69 to 10 µT after a 42 hours exposure as revealed by Trypan (brown) and PCNA content (green). Student T' test: **$p<0.01$; ***$p<0.001$. B) Linear correlation between these two parameters. Photomicrographs of NB69 cells. A: Hoechst-marked nuclei. B: PCNA labelling. The ELF-EMF exposure induced an increase in the number of cells expressing PCNA.

Neuroblastoma cell cultures contain two different phenotypes. One type is characterised by flattened, "sail-like" morphology and shows a strong adherence to the culture flask. These cells are called S-cells. The second phenotype corresponds to much smaller, triangular cells that adhere to the culture flask loosely. These cells, called N cells have a neuroblastic phenotype, are clonigenic and tumorigenic and

grow rapidly in the culture flask. We have observed that the relative proportion of both phenotypes evolves along the successive subcultures, which seems to significantly influence the response of the culture, as a whole, to the field exposure. In fact, young passages, having a high proportion of N cells, are particularly sensitive to ELF-EMF, whereas older passages, very rich in S-cells and with virtually no N cells, are not responsive to ELF-EMF exposure. Consequently, we conducted experiments with young passages, where the cells were exposed to a 100-µT ELF-EMF during 63 hours (day 6 post-plating). A significant increase in the number of cells was observed in the exposed samples (9.7% over controls $p<0.0001$, Figure 33A). The mean cell number in controls was 621.689 ± 62.314 ($x10^4$). The increase in the number of cells was found to be associated with significant increases in the proportion of PCNA-positive cells. Figure 33B shows the percent of PCNA positive cells at days 5 and 6 post-plating (dpp). Only at 6 dpp significant changes in the number of PCNA positive cells were observed (31.7% over controls, $p<0.01$, N = 3 experimental replicates). Those changes do not represent an ELF-EMF-induced increase in PCNA labelling, since the percent of PCNA positive cells in the control cultures spontaneously decreased between days 5 and 6 post-plating (Student T'test *, $p<0.05$). Such a decrease did not occur in the exposed cultures. The present results indicate that the regulation of the kinetics of the cell cycle could be altered by ELF-EMF at 100 µT. Provided that in the proliferating cell the PCNA levels are maximal at late G1 and S phases, it is possible that such phases of the cell cycle are implicated in the above described responses.

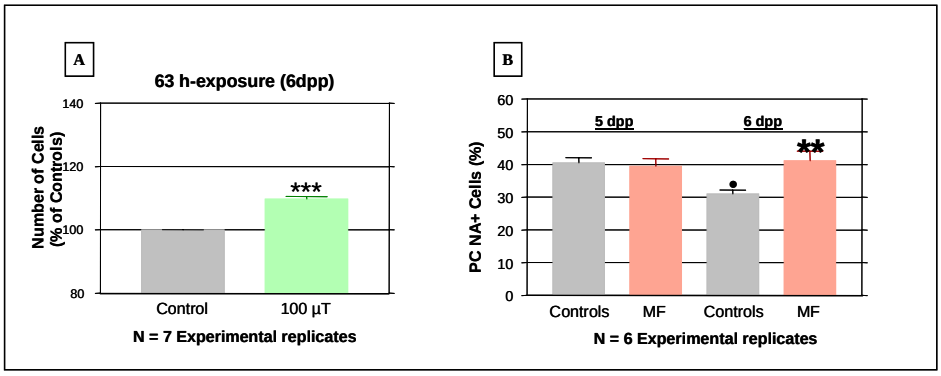

Figure 33. A) Percent of cells at the end of 63-hours exposure and/or incubation (6 day post-plating). B) Percent of PCNA positive cells at 5-6 days post-plating (dpp). In controls the percent of PCNA positive cells significantly decreases between the days 5 and 6 post-plating (Student T'test ●, $p<0.05$), whereas in exposed cells at 100 µT this decrease did not occur).

ELF-EMF increased the DNA synthesis in NB69 neuroblastoma cells.

We also tested the BrdU incorporation into DNA. As shown in Figure 31, at the end of a 42-hours exposure (5 pp) to the 100 µT ELF-EMF a significant increase of BrdU- positive cells was observed in the treated cultures (41 % over controls, Student's T test $p<0.01$). Such an effect was followed (63-hours exposure, 6 pp) by a subsequent increase in the number of cells (9.7% over controls, $p<0.001$, Figure 34). This response was accompanied by a significant reduction in the percent of spontaneously apoptotic cells (58.5 % of that in controls, $p<0.05$).

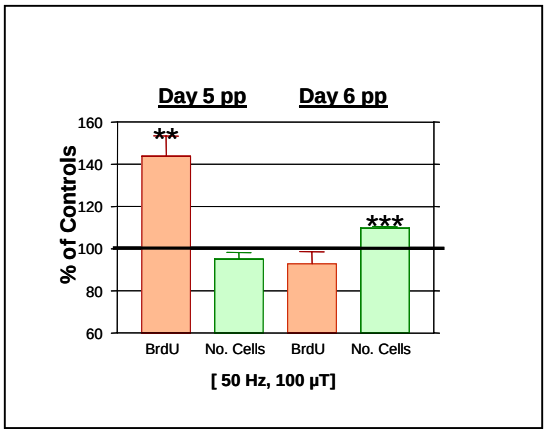

Figure 34. Cell growth in a total of 18 experiments: ELF-EMF effects at 5 days post-plating (42 hours exposure) or at 6 days post-plating (63 hours exposure): Red, percent of BrdU-positive cells; Green, Number of Cells analysed by Trypan blue exclusion. Student T'test: **p< 0.01; ***p< 0.001.

ELF-EMF affected the cell cycle in NB69 neuroblastoma cells.

The experiments performed to test the DNA content and the cell cycle distribution by flow cytometry showed that at the end of day 5 post-plating (Figure 35A), the 42-hours exposure to 100 µT ELF-EMF induces increases in the number of cells in G2-M phase of the cell cycle (28% over controls; N= 3 experimental replicates). The exposure also provoked a modest reduction of cells in G0-G1. However, no significant changes were observed in the number of cells in S-phase and in the number of total cells (Trypan Blue exclusion, Figure 352A). The flow-cytometry assay at the end of day 6 post-plating did not reveal EMF-induced changes in the cell cycle (G0-G1; S and G2-M), even thought a significant increase in the number of alive cells was observed (16.7% over controls, p<0.05; N= 5 experimental replicates, Figure 35B). These results confirm and reinforce our previous observations using other techniques, that 100 µT 50-Hz ELF-EMF can promote cell growth in the NB69 cell line from a human neuroblastoma.

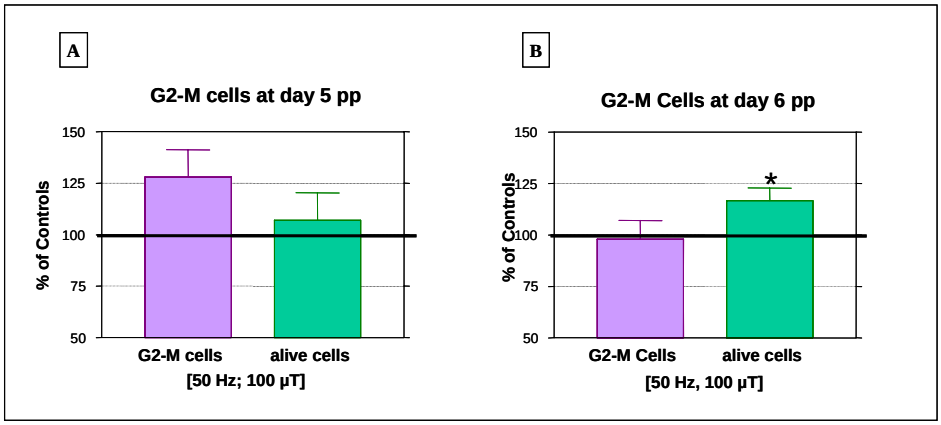

Figure 35. A) A 42 hours-exposure to a 100-µT field provokes an increase in the percent of G2-M cells at day five postplating (5 pp). B) This increase was not observed one day later, after 63 hours- exposure, however, a significant increase in the number of alive cells occurred.

ELF-EMF diminished the spontaneous apoptosis in NB69 neuroblastoma cells.

In order to investigate the potential influence of 50 Hz ELF-EMF on apoptosis the percent of apoptotic cells was estimated with TUNEL-labelling after 63 hours of exposure. Also, the number of cells was

quantified by Trypan Blue exclusion. The results (Figure 36A) indicate that ELF-EMF of 50 Hz at a flux density of 100 µT (3 hours on/3 hours off) induces a significant reduction in the spontaneous apoptosis of the NB69 cell line. This response was associated with an increase in the number of cells (9.7% over controls, p<0.001, Figure 36B as we previously observed in experiments described above. Apoptosis was also determined through flow cytometry analysis; the results confirming a reduction at the end of 63 hours-exposure (data not shown).

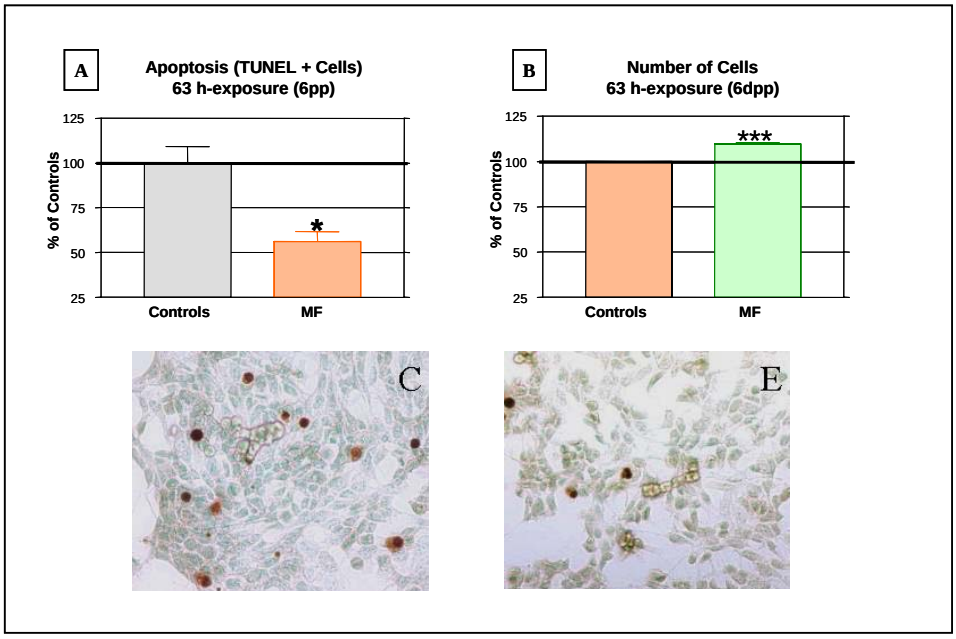

Figure 36. A) ELF-EMF (50 Hz, 100 µT) induce a significant reduction in the spontaneous apoptosis of the NB69 cell line. B) This described response is associated with an increase in the number of cells. (* p< 0.05, ***p<0.001, Student T´ test, three independent experimental replicates).Photomicrographs showing TUNEL-positive cells in controls (C) and exposed (E) samples.

ELF-EMF altered the activation of the phosphorylated cyclic adenosine monophosphate response-element binding protein (p-CREB).

The results of a total of 8 experiments show that both, the labelling/cell in NB69 cells and the proportion of phospho-CREB positive cells increase after 60 min of exposure (35.4% over controls, p<0.01, Figure 37 and photomicrograph). The percent of p-CREB positive cells in controls after 60 min of exposure was 32%. However, no differences were observed between ELF-EMF-exposed and controls samples after 30 or 120 min of exposure. These preliminary results suggest that the activation of p-CREB is involved in the previously described effects of 50 Hz 100 µT ELF-EMF on cell growth/apoptosis. In additional experiments the analysis of Western confirms that the ELF-MF induced a short-time dependent activation of the transcriptional factor CREB, with a peak at 60 min followed by a recovering of the basal levels at 120 minutes of exposure (data not shown).

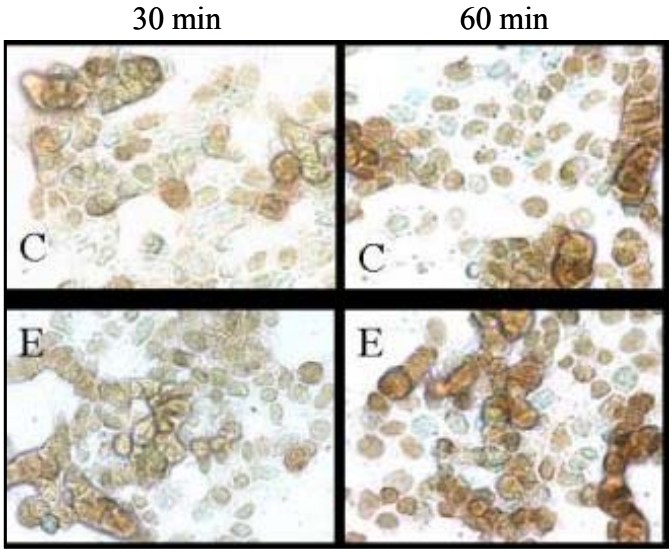

Figure 37. Immunocytochemistry for phospho-CREB. Changes in p-CREB positive cells showed a time-dependent response in the presence of the 100µT ELF-EMF. Photomicrograph showing the p-CREB labelling in brown and the counterstaining in green(methylgreen).

3.1.2.2 Embryonic stem cells of mice during cardiac differentiation (Participant 8)

ELF-EMF accelerated the cardiac differentiation of embryonic stem cells through enhanced expression of cardiac genes.

See 3.1.4.3

3.1.2.3 Human lymphocytes (Participant 8)

ELF-EMF exposure did not have any influence on proliferation, cell cycle and functionality of human lymphocytes.

The experiments with ELF-EMF (50 Hz) were performed at 50 µT magnetic field intensity on cells from 20 donors. Cell proliferation, cell cycle together with membrane activation markers were studied on lymphocytes from young donors. Data obtained by all the experiments performed indicated that no significant differences exist on cell proliferation or DNA synthesis at any time during the continuous exposure up to 6 days, as well as on cell cycle during the continuous exposure up to 96 hours. Cell activation phase was studied on CD3+HLA-DR+ T lymphocytes and CD4+CD25+ T helper lymphocyte subpopulation, but also in this case no differences were found between cells exposed and not exposed.

3.1.2.4 Embryonic stem cells of mice (Participant 4)

ELF-EMF did not have any influence on the growth and neuronal differentiation of embryonic stem cells of mice.

See 3.1.4.1

3.1.2.5 Summary (Participant 1)

Our data show some influence of ELF-EMF on proliferation and differentiation of some, but not all cell systems investigated. This conclusion is based on the following findings:

- ELF-EMF at a flux density of 0.1 mT significantly increased the proliferation of neuroblastoma cells (NB69 cell line) after exposure for 42- and 63-hrs (see 3.1.2.1).
- ELF-EMF at a flux density of 0.8 mT accelerated the cardiac differentiation of embryonic stem cells through enhanced expression of cardiac genes (see 3.1.2.2 and 3.1.4.3)

- ELF-EMF at a flux density of 2 mT did not have any influence on the growth and neuronal differentiation of embryonic stem cells of mice (see 3.1.2.4 and 3.1.4.1)
- ELF-EMF at a flux density of 0.8 mT did not have any influence on proliferation, cell cycle and activation of lymphocytes, either (see 3.1.2.3).

3.1.3 Apoptosis

3.1.3.1 Embryonic stem cells of mice (Participant 4)

ELF-EMF at a flux density of 2 mT up-regulated the transcript levels of the anti-apoptotic gene bcl2 and the growth arrest and DNA damage inducible gene GADD45 and down-regulated bax in ES cell-derived neural progenitor cells. This may indirectly influence the apoptotic process in neural progenitor cells.

See 3.1.4.1

3.1.3.2 Neuroblastoma cell line NB69 (Participant 5)

ELF-EMF at a flux density of 100 µT inhibited the spontaneous apoptosis in NB69 neuroblastoma cells.

See 3.1.2.1

3.1.3.3 Human fibroblasts (Participant 3)

No differences in cell count between ELF-EMF exposed and sham exposed human fibroblasts at any exposure duration could be detected. Therefore a possible elimination of cells by apoptosis and cell death can probably be ruled out.

See 3.1.1.1

3.1.3.4 Summary (Participant 1)

Our data indicate that ELF-EMF may have some indirect effect on apoptosis in certain, but not all cell systems investigated. This conclusion is based on the following findings:

- ELF-EMF at a flux density of 2 mT up-regulated in neural progenitor cells the transcript levels of the GADD45 gene and down-regulated the transcript levels of the bax gene by which the apoptotic process may be modulated (see 3.1.3.1 and 3.1.4.1).
- ELF-EMF at a flux density of 0.1 mT inhibited the spontaneous apoptosis in neuroblastoma cells in a way which is at present not well understood (see 3.1.3.2 and 3.1.2.1).
- ELF-EMF at a flux density of 1 mT did neither measurably affect the apoptotic process nor could a cytotoxic effect be detected in human fibroblasts in the course of a 24h exposure (see 3.1.1.1 and 3.1.3.3).

3.1.4 Gene and protein expression

3.1.4.1 Embryonic stem cells of mice (Participant 4)

ELF-MF exposure resulted in up-regulation of egr-1, c-jun and p21 transcript levels in p53-deficient, but not in wild type ES cells.

To analyse the effects of ELF-EMF, undifferentiated wild type (wt) and p53-deficient ES cells were exposed at different intermittence schemes and flux densities of 0.1, 1,0 and 2.3 mT for 6 and 48 hours, respectively (Table. 7). The exposition of ES cells to 5 min on followed by 30 min off cycles applied at

the high flux density of 2.3 mT resulted in a statistically significant up-regulation of egr-1, p21 and c-jun mRNA levels in p53-deficient ES cells (Figure 38A and C), whereas wild type cells showed no variations in transcript levels compared to sham exposure and control cells (Figure 38A). In contrast, low flux densities of 0.1 and 1 mT ELF-EMF applied at 5 min on/30 min off intermittence cycles induced no significant effects on transcript levels indicating that a high flux density of ELF-EMF signals is necessary to affect mRNA levels of regulatory genes (Table 7).

Table 7. Conditions of the exposure of p53-proficient and deficient pluripotent embryonic stem cells embryonic stem cells to ELF-EMF and summary of the effects on transcript levels of regulatory genes.

Intermittent exposure (5min on/30 min off)			
6 hours ELF-EMF exposure ; wt, p53$^{-/-}$		48 hours ELF-EMF exposure; wt, p53$^{-/-}$	
0.1 mT	no ELF-EMF effect (n=3)	0.1 mT	no ELF-EMF effect (n=3)
1.0 mT	no ELF-EMF effect (n=3)	1.0 mT	no ELF-EMF effect (n=3)
2.3 mT	up-regulation of egr-1, p21 and c-jun in p53$^{-/-}$ cells (without recovery time, RT); no ELF-EMF effect after 18 h RT (n=6)	2.3 mT	no ELF-EMF effect (n=3)

Intermittent exposure (5min on/10 min off)			
6 hours ELF-EMF exposure; wt, p53$^{-/-}$; without RT		6 hours ELF-EMF exposure; wt, p53$^{-/-}$; 18h RT	
2.3 mT	no ELF-EMF effect (n=6)	2.3 mT	no ELF-EMF effect (n=6)

Continuous exposure			
6 hours ELF-EMF exposure; wt, p53$^{-/-}$		48 hours ELF-EMF exposure; wt, p53$^{-/-}$	
0.1 mT	no ELF-EMF effect (n=3)	0.1 mT	no ELF-EMF effect (n=3)
1.0 mT	no ELF-EMF effect (n=3)	1.0 mT	no ELF-EMF effect (n=3)

ELF-MF exposure of p53-deficient cells induced only short-term and transient effects on gene expression levels.

To elucidate, whether ELF-EMF induce short- or long-term responses, p53-deficient and wt ES cells were exposed to intermittent 5 min on/30 min off ELF-EMF signals for 6 hours. In parallel, the cells were analysed after a recovery time of 18 hours. No statistically significant effects could be seen after 18 hours recovery in control, sham- and field-exposed variants suggesting that ELF-EMF induced only an immediate transient response in p53-deficient cells (Figure 38B).These observations correlated with the results of the 48 hours ELF-EMF exposure to p53-deficient ES cells at early differentiation stage, where no ELF-EMF effects on transcript levels were found (data not shown, see Table 7).

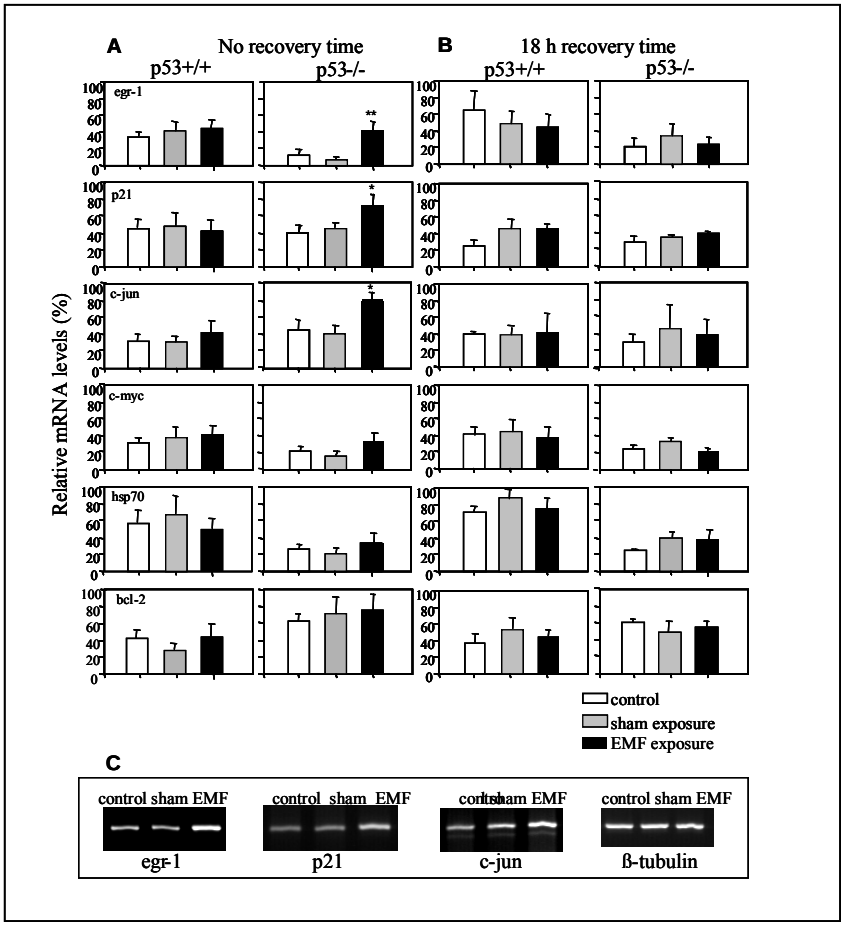

Figure 38. Relative mRNA levels of genes encoding egr-1, p21, c-jun, c-myc, hsp70 and bcl-2 in p53-deficient ($p53^{-/-}$) EC cell-derived embyoid bodies (EB) compared to wild-type (wt, $p53^{+/+}$) D3 cells immediately after 6h ELF-EMF (2.3 mT, intermittency 5 min on / 30 min off cycles) exposure (A) and after 18h recovery time (B) analysed by semi-quantitative RT-PCR. ELF-EMF exposure resulted in a significant, but transient up-regulation of egr-1, c-jun and p21mRNA levels in undifferentiated p53-deficient (C), but not wt ES cells. Statistical significance was tested by Studentt's t-test for significance levels of 1% and 5% (**p<0.01; *p<0.05)

ELF-MF effects on transcript levels of regulatory genes in p53-deficient cells were dependent on intermittence cycles (on/ off cycle duration).

In addition, we analysed in wt and p53-deficient ES cells the influence of ELF-EMF signals applied at another intermittence scheme of 5 min on/10 min off for 6 hours with a flux density of 2.3 mT. We found that 5 min on/10 min off ELF-EMF signals with or without recovery time had no effects on the transcript levels of the investigated regulatory genes in both, wt and p53-deficient cells. Further, continuous ELF-EMF signals at flux densities of 0.1 and 1 mT were applied to wt and p53-deficient ES cells. We found no influence of continuous ELF-EMF on the mRNA levels of the regulatory genes included in the study (data not shown). Experiments with the highest flux density (2.3 mT) could not be performed with the continuous exposure protocol, because the generated ohmic heat of the coils could not be compensated by the incubator and would have resulted in an unstable ambient temperature.

ELF-EMF exposure up-regulated the transcript levels of bcl-2, the growth arrest and DNA damage inducible gene (GADD45) and down-regulates bax in ES cell-derived neural progenitor cells.

Elf-EMF (50 Hz-Power line, 2 mT, 5 min.on/30min. off, Table 8) was applied for 6 or 48 hours on neural progenitors (Table 8). Semi-quantitative RT-PCR analysis revealed no effect of ELF-EMF on transcript levels of genes involved in neuronal differentiation (nurr1, en-1) and on markers of differentiating

(nestin) or differentiated neuronal (TH) or astrocytic (GFAP) cells. In addition, we studied the effect of ELF-EMF on transcript levels of genes involved in the regulation of cell homeostasis (hsp70), cell cycle (p21) and anti-apoptosis (bcl-2). RT-PCR analysis revealed that, whereas transcript levels of p21 and hsp70 remain similar in sham and ELF-EMF exposed variants, a significant up-regulation of the growth arrest inducible gene GADD45 was observed at stage 4d+11d. (Figure 39). The quantitative RT-PCR (Q-RT-PCR) with specific primers and TaqMan probes showed that bcl-2 was first down-regulated at stage 4+7d ($p<0.05$), then up-regulated in the intermediate stage 4+11d ($p<0.01$) and at the terminal stage 4+23d ($p<0.05$). GADD45 was significantly up-regulated at stage 4+11d, then down-regulated at the terminal stage 4+23d (Figure 40). These studies were further substantiated by immunofluorescence analyses of neuronal markers. However, by immunofluorescence analysis, no changes in intracellular distribution and number of cells expressing neuronal markers (ßIII-tubulin, TH, GFAP) were observed (data not shown).

Table 8. Conditions of the exposure of neuronal progenitor cells to ELF-EMF and summary of the effects on transcript abundance, neural differentiation induction and DNA break induction.

Intermittent exposure (5min on/30 min off)			
48 hours, ELF-EMF (Power line, 50Hz)		6 hours, ELF-EMF (Power line, 50Hz)	
2.0 mT	up-regulation followed by down-regulation of GADD45 up-regulation of bcl-2 down-regulation of bax no effect on neural differentiation no effect on DNA break induction (n=6)	2.0 mT	no effect on DNA break induction (n=3)

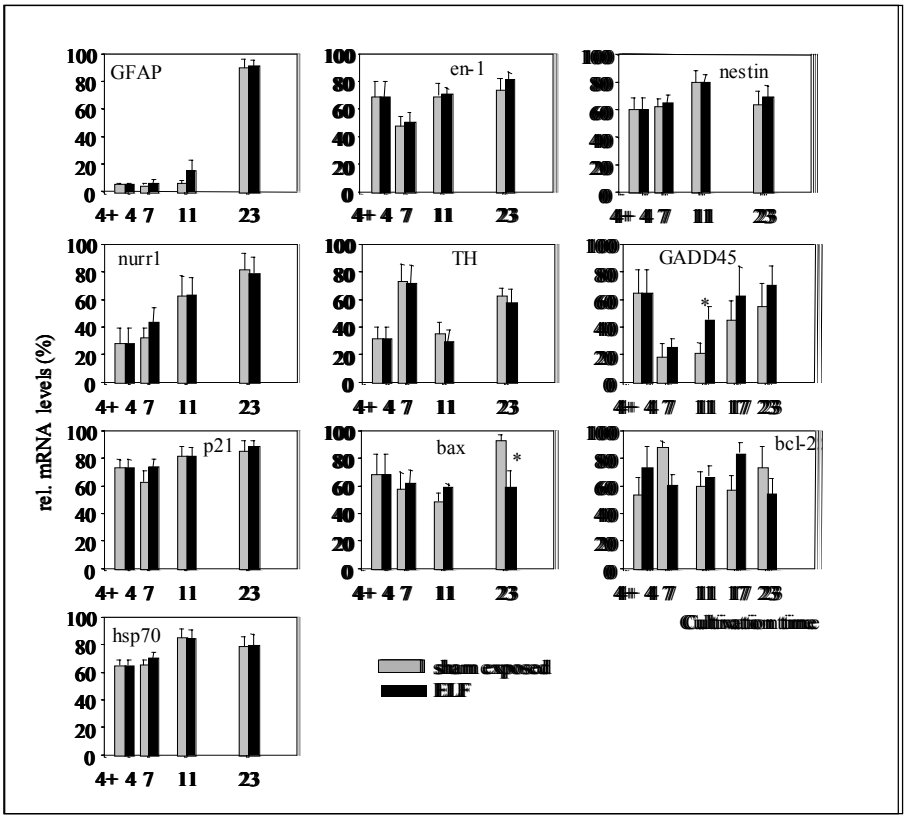

Figure 39. Relative mRNA levels of genes encoding the regulatory genes bcl-2, bax, p21, hsp70 and the genes involved in neuronal differentiation en-1, nurr1, TH, GFAP and nestin in ES-derived neural progenitors after 48 hours ELF (50Hz Powerline) EMF exposure (2.0 mT, intermittence 5 min ON/30 min OFF), at stage 4+4d - 4+6d. EMF exposure resulted in a significant transcript up-regulation of GADD45 and down-regulation of bax. Error bars represent standard deviations. Statistical significance was tested by the Student's t-test for a significance level of 5% (*, p£ 0.05).

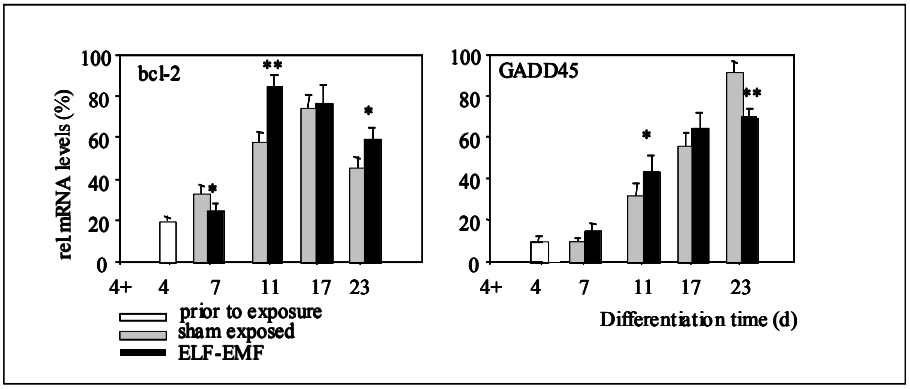

Figure 40.: Quantitative RT-PCR for estimation of relative mRNA levels of genes encoding the regulatory genes bcl-2 and GADD45 in ES-derived neural progenitors after 48 hours ELF (50Hz Powerline) EMF exposure (2.0 mT, intermittence 5 min on/30 min off), at stage 4+4d - 4+6d. EMF exposure resulted in a significant transcript down-regulation followed by up-regulation of bcl-2, which correlated with up-regulation followed by down-regulation of GADD45. Error bars represent standard deviations. Statistical significance was tested by the Student's t-test for a significance level of 5% and 1% (*, p< 0.05 ;**, p< 0.01).

3.1.4.2 Human neuroblastoma cell line SY5Y (Participant 11)

In order to obtain cellular models to study ELF-EMF, we have characterised some neuroblastoma cell lines for their ability to express nAchRs and evaluate whether ELF-EMF can interfere with the expression of alpha3, alpha5 and alpha7 nAchR subunits, as well as with that of Phox2a, Phox2b and dopamine-beta-hydroxylase (DβH).

Three human neuroblastoma cell lines (SH-SY5Y, SK-N-BE and IMR32) have been analysed, by means of northern blot analysis, for the expression of neuronal acetylcholine receptor subunits. Due to the high degree of homology between different subunits, the experiments have been carried out with probes derived from the cytoplasmic portion, the least conserved region of nAchR subunits, in order to avoid cross-contamination. The results showed that these cells express the ganglionic type of nAchRs (alpha3, alpha5 and alpha7), but not alpha 4, mainly expressed in the CNS (data not shown and Fornasari 1997; Flora 2000). Furthermore only human neuroblastoma cell lines SY5Y and IMR-32 appeared to express either Phox2a, Phox2b or DβH (Flora, 2001 and data not shown), although with differences in the level of expression. As the SY5Y lineage shows higher expression of the three genes, we decided to use this as a model in all the experiments.

ELF-EMF did not affect the expression of nicotinic acetylcholine receptors (nAchRs) which represent the neuronal nicotinic system in human neuroblastoma cells.

At the beginning of our experiment we decided to use field strengths which are larger than the maximum real-world exposure and eventually scale-down, in the case of measurable effect, establishing the minimum threshold level to which ELF-EMF do not represent a risk to human health. Neuroblastoma cell line SY5Y was then exposed to ELF-EMF (50 Hz, powerline signal) continuously for 16 hours at flux densities of 2 mT and 1 mT and the expression level of humaṇ alpha 3,alpha 5 and alpha 7 nAchRs subunits analysed by means of Northern blotting. Figure 41 (panel A) shows the results obtained by three independent exposures at 2 mT (lanes 1, 4 and 5) together with that of sham-exposed cells (lanes 2, 3 and 6). The densitometric quantification of the mRNA level, however, has shown no effect on the expression level of nAchR subunits as compared to that of the sham-exposed cells set as 100%, when cells were exposed either at 2 mT or 1 mT (Figure 41), panel B and C respectively). We then decided to explore whether an intermittent exposure might be influent on the expression of the nAchR subunits tested. Exposing the cells to intermittent magnetic field (5 min on/5 min off), 2 mT and 1 mT flux density, for 16 hours did not affect the expression of the alpha3, alpha5 and alpha7 nAchR subunit genes (Figure 42, panel A and B respectively).

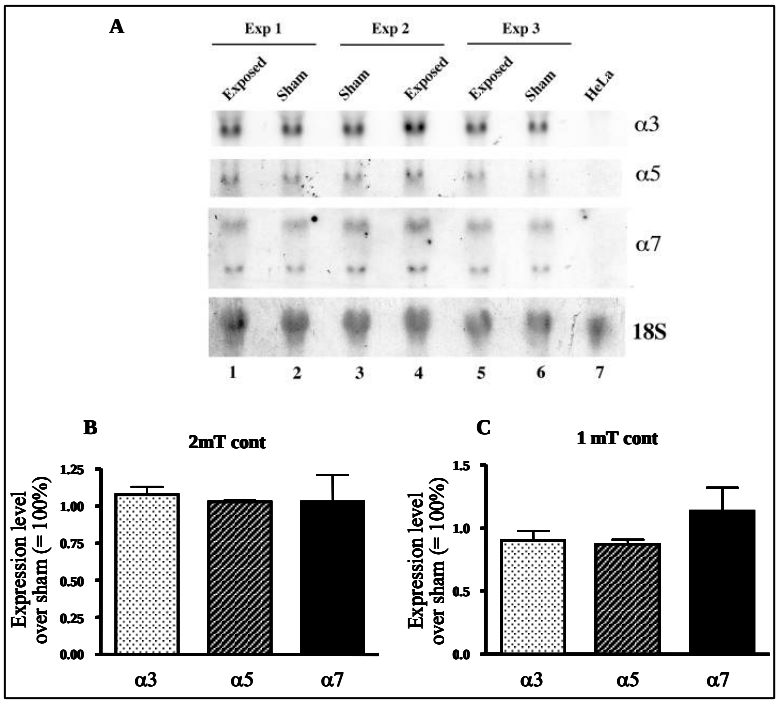

Figure 41. nAchR subunits expression upon exposure to 16 hours continuous ELF-EMF. 20 µg of total RNA extracted from SY5Y cells exposed to 2mT and 1 mT continuous 50 Hz magnetic field, for 16 hours, was hybridised to cDNA probes corresponding to the human alpha3, alpha5 and alpha7 nAchR subunits. The expression level was normalised to that of 18S RNA. A, Northern blot analysis of total RNA extracted upon exposure to 2mT ELF-EMF. Here reported are the results of three independent experiments (Exp1, lanes 1-2; Exp 2, lanes 3-4; Exp 3, lanes 5-6). Lane 7, HeLa total RNA has been used as a negative control. B and C, Densitometric quantification of the expression level of nAchR subunits upon exposure to 2 mT and 1 mT continuous ELF-EMF, respectively. The data are the mean of three independent experiments ± S.E., expressed as a percentage of the sham-exposed sample set equal to 100%.

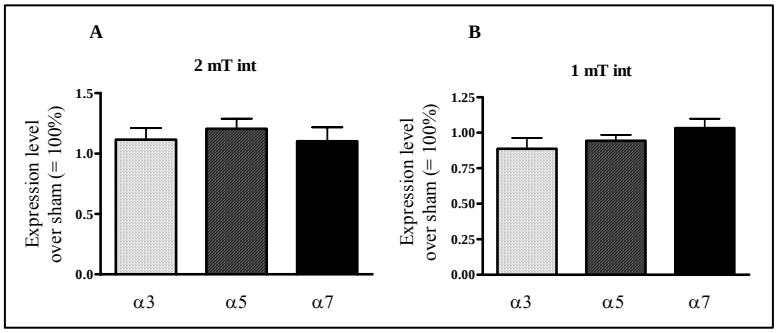

Figure. 42. nAchR subunits expression upon exposure to 16 hours intermittent ELF-EMF. 20 µg of total RNA extracted from SY5Y cells exposed to 2mT and 1 mT continuous 50 Hz magnetic field, for 16 hours, was hybridised to cDNA probes corresponding to the human alpha3, alpha5 and alpha7 nAchR subunits. The expression level was normalised to that of 18S RNA. The data are the mean of three independent experiments ± S.E., expressed as a percentage of the sham-exposed sample set equal to 100%. A, Densitometric quantification of the expression level of nAchR subunits upon exposure to 2 mT intermittent ELF-EMF. B, Densitometric quantification of the expression level of nAchR subunits upon exposure to 1 mT intermittent ELF-EMF.

As we were not able to measure any effect at the mRNA level, we wondered whether the exposure to ELF-EMF might have an effect at the level of receptor proteins. To this purpose we carried out radioligand assays on cells exposed to either continuous or intermittent 50 Hz ELF-EMF, flux densities of 1 mT and 2 mT for 16 hours, to assess the amount of protein functionally assembled in the receptors. The

binding was performed in the presence of radiolabelled ligands, ^{3}H-Epibatidine to quantitate alpha3-containing receptor and ^{125}I-alpha-bungarotoxin to quantitate alpha7-containing receptor. However, as shown in Figure 43, no change in the amount of either alpha3- or alpha7-containing receptor was detected under the same conditions used in Northern blot analysis of Figures 41 and 42, as compared to that of the sham-exposed cells set as 100%.

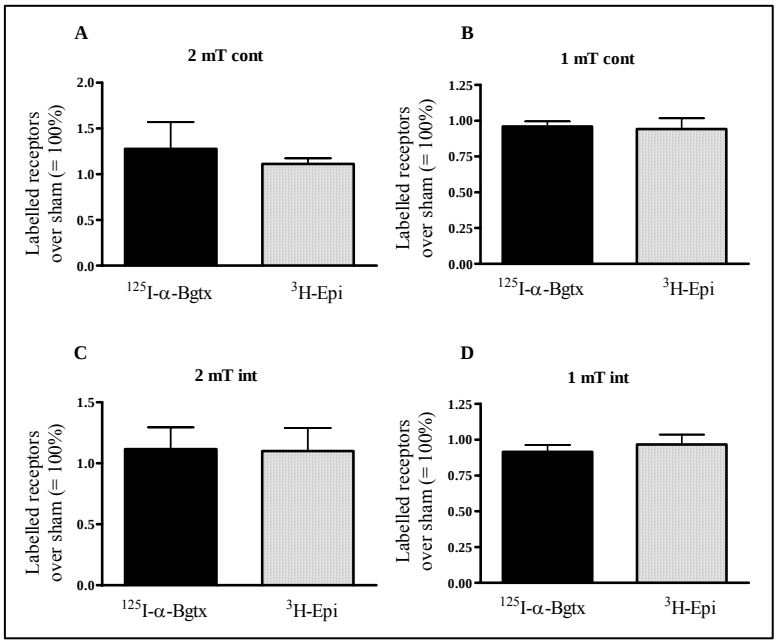

Figure 43. Quantitative analysis of the alpha3- and alpha7-containing receptors upon continuous and intermittent ELF-EMF exposure for 16 hours

The amount of labelled receptors were obtained from the binding of saturating concentration of ^{3}H-Epibatidine (grey bars) and ^{125}I-alpha-bungarotoxin (black bars) to the cell homogenates, performed in quadruplicate. The values are the mean of three independent experiments ± and S.E. are expressed as percentage of labelled receptors in the exposed samples with respect to the sham-exposed cells set as 100%. A and B, continuous exposure to 1 mT and 2 mT ELF-EMF, respectively. C and D, intermittent (5 min on/5 min off) exposure to 1 mT and 2 mT ELF-EMF.

The experiments carried out until now have showed that the ELF-EMF does not influence the expression of nAchRs upon exposure of the cells to magnetic field with flux densities of either 1 mT or 2 mT for a relatively short period of time (16 hours). We then investigated whether the duration time of the exposure of SY5Y cells to ELF-EMF might affect the expression of the genes encoding the nAchR subunits, and especially, whether longer exposure to ELF-EMF might affect the expression of some of the genes. To answer this question two different exposure protocols have been used: a) 50 Hz powerline signal, flux density 1 mT, continuous exposure, duration 48 hours. The RNA or proteins were extracted immediately after the end of exposure (immediate recovery); b) 50 Hz powerline signal, flux density 1 mT, continuous exposure, duration 48 hours. The RNA or proteins were extracted 48 hours after the end of exposure (delayed recovery).

As shown in Figure 44, panel A, the expression of nAchR subunits, as measured at mRNA level, was again not affected by a prolonged exposure to the ELF-EMF followed by an immediate recovery of the cells (protocol a). Furthermore, no effect was detected at the level of receptor proteins (Figure 44, panel B). We then wondered whether the effect could be a delayed one, that is mediated by the activation of a cascade of second messengers that results in a change of gene expression. To test this hypothesis, cells were collected for RNA and protein analysis 48 hours after the end of the exposure (protocol b). The

results shown in Figure 44 seemed to rule out an indirect effect as neither the level of mRNA (Figure 45, panel A) nor of the receptor proteins (Figure 45, panel B) changed under these experimental conditions.

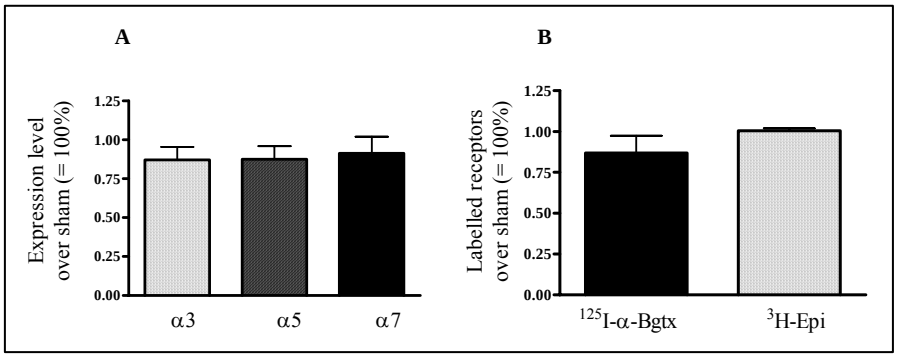

Figure 44. nAchR subunits expression and quantitative analysis of the alpha3- and alpha7 containing receptors upon continuous exposure to 1 mT ELF-EMF for 48 hours: Immediate recovery

Cells were exposed to 1 mT ELF-EMF for 48 hours and recovered immediately after the end of the exposure. A, Densitometric quantification of the expression level of nAchR subunits after Northern blot analysis. The data are the mean of five independent experiments ± S.E., expressed as a percentage of the sham-exposed sample set as 100%. B, quantification of the alpha3- (grey bars) and alpha7-containing (black bars) receptors. The values are the mean of three independent experiments ± and S.E. are expressed as percentage of labelled receptors in the exposed samples with respect to the sham-exposed cells set as 100%.

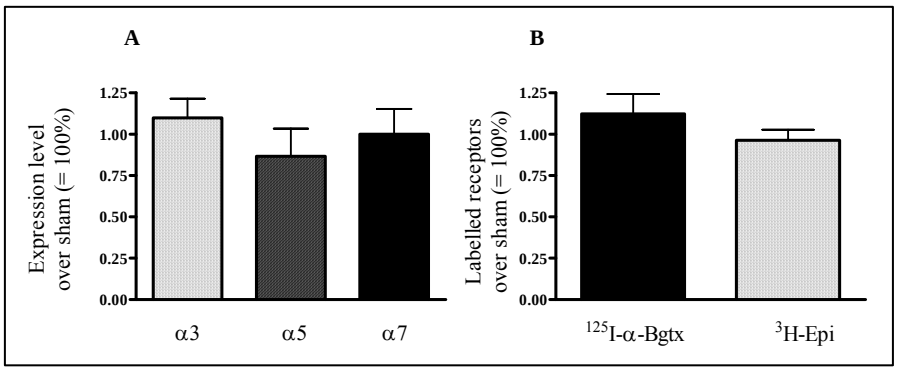

Figure 45. nAchR subunits expression and quantitative analysis of the alpha3- and alpha7 containing receptors upon continuous exposure to 1 mT ELF-EMF for 48 hours: Delayed recovery

Cells were exposed to 1 mT ELF-EMF for 48 hours and recovered 48 hours after the end of the exposure. A, Densitometric quantification of the expression level of nAchR subunits after Northern blot analysis. The data are the mean of five independent experiments ± S.E., expressed as a percentage of the sham-exposed sample set as 100%. B, quantification of the alpha3- (grey bars) and alpha7-containing (black bars) receptors. The values are the mean of three independent experiments ± and S.E. are expressed as percentage of labelled receptors in the exposed samples with respect to the sham-exposed cells set as 100%.

ELF-EMF did not affect the expression of markers of the cathecolaminergic system in neuroblastoma cells.

In collaboration with Participant 1 we decided to investigate the influence of ELF-EMF on neurotransmitter release. In particular, the activity of the dopamine-beta-hydroxylase (DβH) which is a key enzyme in the synthesis of noradrenaline has been studied. Furthermore, we investigated possible modifications on the expression of two related homeo-domain transcription factors, Phox2a and Phox2b, that are relevant for the specification of the autonomic nervous system. Moreover, in noradrenergic cells, they are directly involved in the determination of the neurotransmitter phenotype by regulating the expression of DβH. As protocols, we applied the same exposure conditions used for the analysis of the human nAchR subunits. As shown in Figure 46, panels A and B, continuous exposure of SY5Y neuroblastoma cells to 1 mT and 2 mT 50 Hz ELF-EMF did not affect the expression level of either Phox2a, Phox2b and DβH genes, as compared to that of the sham-exposed cells set to 100%. Again we asked whether an intermittent exposure might have an effect on gene expression of these proteins. We then measured the mRNA level upon intermittent exposure (5 min on/5 min off) to 1 mT ELF-EMF, but no change was observed (Figure 47). Previous experiments have shown that an exposure of SY5Y cells for 48 hours at 1 mT flux density reduced the amount of mRNA of Phox2a, but not of Phox2b and DβH. We then exposed the cells under these conditions up to nine times independently.

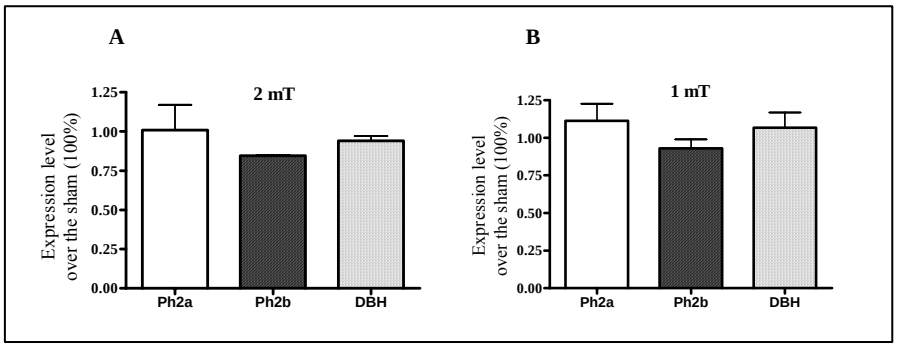

Figure 46. Noradrenergic phenotype specifying genes expression upon continuous exposure to ELF-EMF for 16 hours

20 µg of total RNA extracted from SY5Y cells continuously exposed to 1mT and 2 mT 50 Hz ELF-EMF for 16 hours was hybridised to cDNA probes corresponding to the human Phox2a, Phox2b and DβH genes. The expression level was normalised to that of 18S RNA. A Densitometric quantification of the expression level of the three genes upon continuous exposure to 2 mT ELF-EMF. B, Densitometric quantification of the expression level of the three genes upon continuous exposure to 1 mT ELF-EMF. The data are the mean of five independent experiments ± S.E., expressed as a percentage of the sham-exposed sample set as 100%.

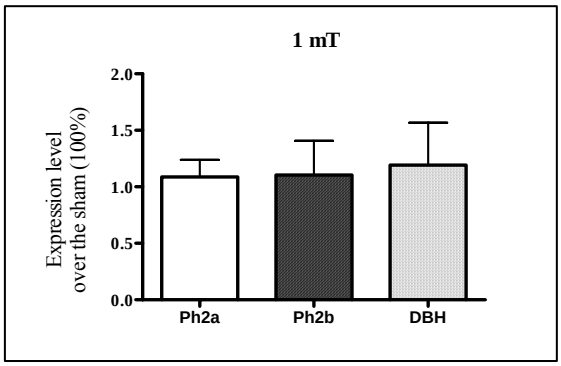

Figure 47. Noradrenergic phenotype specifying genes expression upon intermittent exposure (5 min on/5 min off) to ELF-EMF for 16 hours.

Densitometric quantification of the expression level of the three genes upon intermittent exposure to 1 mT ELF-EMF, after Northern blot analysis. The data are the mean of five independent experiments ± S.E., expressed as a percentage of the sham-exposed sample set as 100%.

Statistical analysis has ruled out that, upon this exposure protocol, the expression of the noradrenergic specifying genes was affected, as shown in Figure 48, either harvesting the cells immediately after the end of the exposure (Figure 48, panel A) or 48 hours later (Figure 48, panel B). As no change was seen at the level of mRNA we asked whether the exposure to ELF-EMF might affect the expression of Phox2a and Phox2b at protein level. To this purpose we decided to measure, by western blot analysis, the protein level upon continuous exposure to 50 Hz ELF-EMF, flux density 1 mT, for 16 and 48 hours (Figure 49). Cells were harvested immediately after the end of the exposure (Figure 49, lanes 10-13 and lanes 6-9, respectively). Also protein extract from cells harvested 48 hours after the end of the continuous 48 hours exposure was tested (Figure 49, lanes 2-5). Densitometric analysis of the signal obtained for Phox2a (Figure 49, panel A) and Phox2b (Figure 49, panel B), normalised to that of the beta-tubulin, revealed that exposure of SY5Y cells to relatively short or longer period of time did not affect the expression of Phox2a and 2b, at protein level, as compared to that of the sham-exposed cells (Figure 49, panel C).

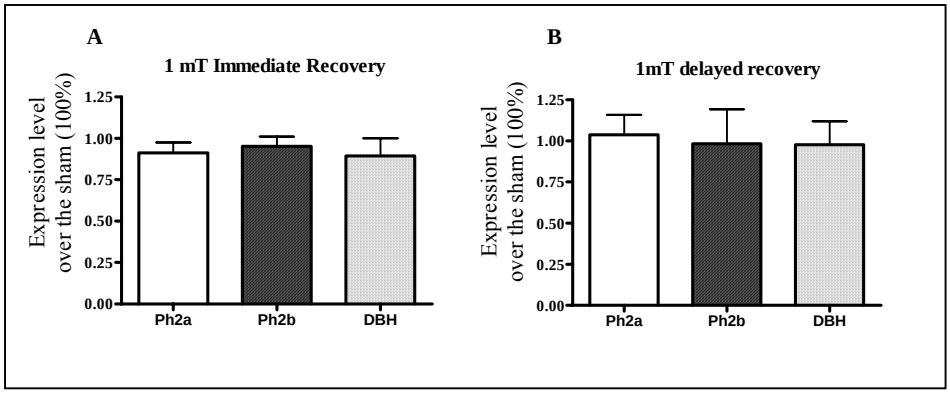

Figure 48. Noradrenergic phenotype specifying genes expression upon continuous exposure to ELF-EMF for 48 hours

SY5Y cells were continuously exposed to 1 mT 50 Hz ELF-EMF for 48 hours and collected either immediately (panel A) or 48 hours (panel B) after the end of the exposure. After northern blot analysis, the expression level of Phox2a, Phox2b and DβH genes was quantified by densitometric scanning of the autoradiogram. The data are the mean of six independent experiments ± S.E. (Phox2b and DβH) and nine independent experiments (Phox2a), expressed as a percentage of the sham-exposed sample set equal to 100%.

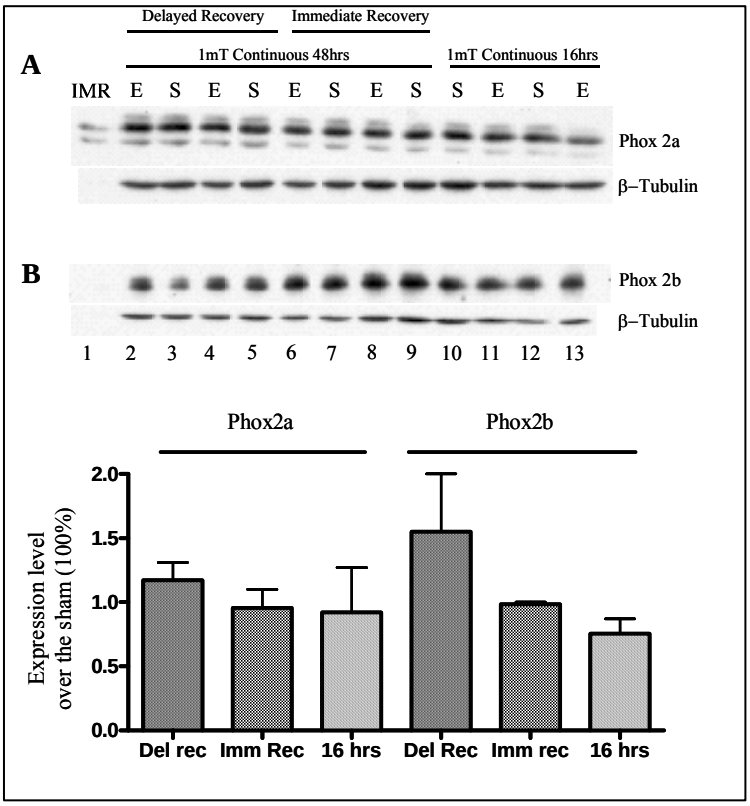

Figure 49. Western blot analysis of Phox2a and Phox2b expression upon continuous exposure to 1 mT ELF-EMF.20 µg of total protein extract were size-fractionated by SDS-PAGE and transferred to nitrocellulose membrane. The expression of Phox2a and Phox2b was detected by incubation with anti-Phox2a (panel A) and anti-Phox2b antibodies (panel B). Lanes 2-9, samples from continuous exposure to 1 mT ELF-EMF for 48 hours recovered 48 hours (lanes 2-5) or immediately (lanes 6-9) after the end of the exposure. Lanes 10-13, samples from 1 mT continuous exposure for 16 hours. Lane 1, IMR 32 neuroblastoma cells nuclear extract used as a control. E= exposed, S= sham-exposed. The expression of Phox2a and Phox2b was normalised to that of β-tubulin. C, quantification of the expression level of Phox2a and Phox2b. The data are the mean of two independent exposures ± S.E. and are expressed as percentage of the sham-exposed samples set as 100%. Del Rec = recovery 48 hours after the end of the exposure; Imm rec = recovery immediately after the end of the exposure; 16 hours = samples were exposed for 16 hours to 1 mT continuous ELF-EMF.

3.1.4.3 Embryonic stem cells of mice during cardiac differentiation (Participant 8)

In higher vertebrates, heart formation is a complex phenomenon that starts at early stages of embryogenesis, prior to the end of gastrulation, with commitment of anterior lateral plat mesoderm cells to cardiogenic lineage. Studies in different organ systems have shown that tissue-specific transcription factors which control the expression of differentiation markers are also regulators of cellular differentiation. Basic helix-loop-helix proteins such as the myogenic factor are key regulators of skeletal muscle differentiation, while the erythroid cell-specific zinc finger protein GATA-1 is crucial for erythroid cell differentiation. It is now becoming evident that inactivation of the mouse homologue of the Drosophila melanogaster homeobox gene tinman, the homeobox gene Nkx2.5 or Csx affects heart morphogenesis (Biben 1997, Lints 1993). Moreover, the GATA-4 protein, a member of the GATA family of transcription factors, has been found to be restricted to the hearts and to characterise very early stages of heart formation during embryonic development (Grepin 1995).

ELF-EMF affected the expression of cardiogenic genes in murine embryonic stem cells (GTR1).

In the first step of our study we looked at the effects of ELF-EMF (0.8 mT, 50 Hz sinusoidal) on the expression of cardiogenic genes in mouse embryonic carcinoma (EC) cells (P19 cells). Despite the encouraging results obtained in our pilot experiments, in a subsequent set of ten separate experiments P19

cells exposed to ELF-EMF desultorily underwent a gene program of cardiogenesis and revealed structural and functional cardiomyocyte features. Only in 2 experiments, exposure to ELF-EMF primed the expression of both GATA-4 and Nkx-2.5 genes, and led to the appearance of alpha-myosin heavy chain (MHC) and myosin light chain-2V (MLC), two cardiospecific transcripts. A representative RT-PCR analysis of cardiogenic and cardiac specific gene expression from ELF-EMF responsive cells is shown in Figure 50).

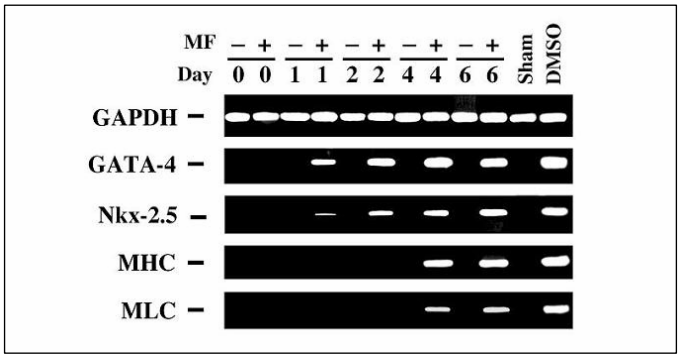

Figure 50. RT-PCR analysis of cardiogenic and cardiospecific transcripts in P19 cells exposed to ELF-EMF (continuous exposure, 4 days). MHC, alpha-myosin heavy chain. ML*C,* myosin light chain-2V.

We reasoned that the lack of data reproducibility of these results could be due to the consistent dilution of the myocardial phenotype within multiple non-myocardial cells encompassed by the P19 model of cell differentiation. To circumvent this problem, we decided to change the biological model, by using a line of pluripotent embryonic stem (ES) cells engineered for a gene trapping selection of a virtually pure population of ES-derived cardiomyocytes. RT-PCR analysis of targeted transcripts in unexposed cells indicated that, differently from undifferentiated LIF-supplemented cells, EBs expressed both GATA-4 and Nkx-2.5 mRNA (Figure 51). The expression of these cardiogenic genes resulted to be further enhanced in puromycin selected, ES-derived cardiomyocytes (Figure 52). Figures 51 and 52 show that ELF-EMF exposure remarkably increased GATA-4 and Nkx-2.5 gene expression in both EBs and cardiomyocytes, as compared to unexposed GTR1 cells. Interestingly, in both groups of cells ELF-EMF also increased the expression of the prodynorphin gene, an endorphin gene that has been recently shown to play a major role in orchestrating ES cell cardiogenesis (Ventura 2003(a), 2003(b), 2000). These responses were further inferred by the quantitative analysis of mRNA levels as shown in RNase protection experiments (Figure 53). Interestingly, nuclear run-off analyses of GATA-4 gene transcription indicated that the ELF-EMF action occurred at the transcriptional level (Figure 54). The activation of a program of cardiogenic gene transcription was also associated with the appearance of the cardiac specific transcripts alpha-myosin heavy chain and myosin light chain-2V (Figure 55).

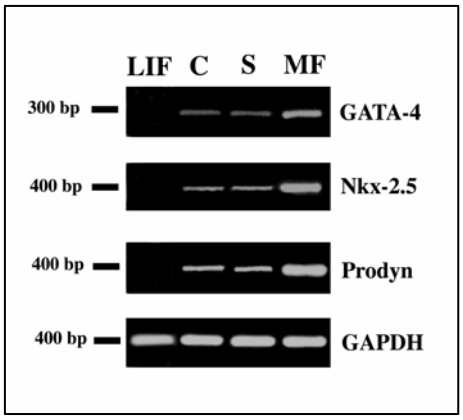

Figure 51. ELF-EMF was applied from the time of LIF removal and EBs were collected after 3 additional days. C: control EBs; S: sham. (Ethidium bromide-stained agarose gels, representative of 4 separate experiments).

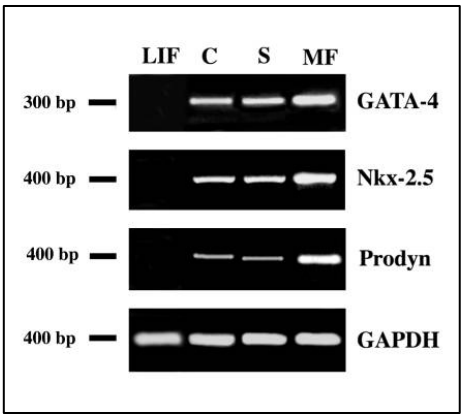

Figure 52. Effect of ELF-EMF (MF) on Cardiogenic gene expression in puromycin-selected cells. ELF-EMF was applied from the time of LIF removal throughout puromycin selection. Four days after puromycin addition (10 days from LIF withdrawal), ES-derived cardiomyocytes were processed gene expression analyses. C: control puromycin-selected cardiomyocytes; S: sham. (Ethidium bromide-stained agarose gels, representative of 4 separate experiments).

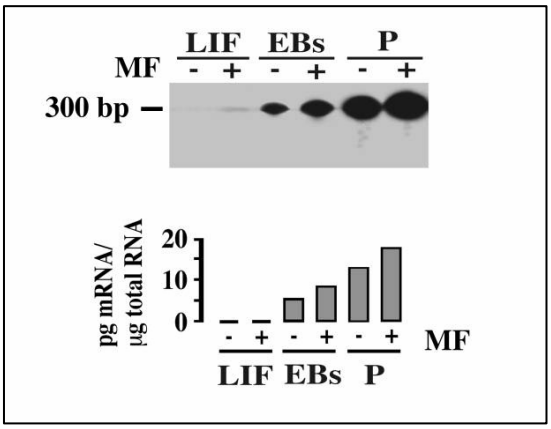

Figure 53. RNase protection analysis of GATA-4 mRNA expression in GTR1 ES cells cultured in the absence or presence of ELF-EMF.LIF, undifferentiated GTR1 cells. EBs, embryoid bodies collected 5 days after LIF removal. *P*, puromycin-selected cardiomyocytes: puromycin was added at day 8 following LIF removal. Each group of cells was cultured in the absence (-) or presence (+) of ELF-EMF. Autoradiograms are representative of 3 separate experiments.

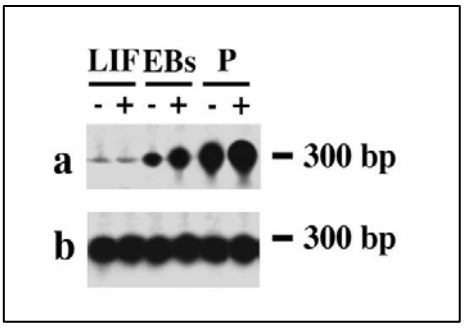

Figure 54. Nuclear run-off analysis of GATA-4 gene transcription in isolated ES cell nuclei. Nuclei were isolated from undifferentiated GTR1 cells (LIF), from EBs collected 5 days after LIF removal (EBs) or from puromycin-selected cardiomyocytes (P): puromycin was added at day 8 following LIF removal. Each group of cells was exposed in the absence (-) or presence (+) of ELF-EMF (MF). Puromycin was added at day 8 following LIF removal. Row a, GATA-4 gene transcription. Row b, cyclophilin gene transcription (cyclophilin was assessed as a constant gene for control). Autoradiograms are representative of 3 separate experiments.

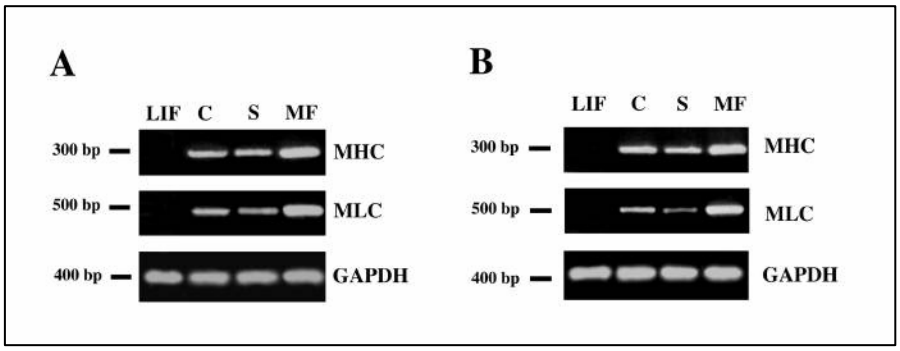

Figure 55: Effect of MF on the expression of cardiac specific genes.A: ELF-EMF (MF) was applied from the time of LIF removal and EBs were collected after additional 3 days. B: MF was applied from the time of LIF removal throughout puromycin selection. Four days after puromycin addition (10 days from LIF withdrawal), ES-derived cardiomyocytes were processed gene expression analyses. C: control cells; S: sham. (Ethidium bromide-stained agarose gels, representative of 4 separate experiments).

Exposure of GTR1 ES cells to ELF-EMF after LIF removal and throughout 4 days of puromycin selection for an overall period of 10 days from LIF withdrawal was able to increase the yield of ES-derived cardiomyocytes: the number of beating colonies reached 170.44 ± 28.0 % of the control value, estimated in cardiomyocytes selected from untreated cells (mean ± SEM of 4 separate experiments).

We finally investigated whether the transcriptional responses evoked by ELF-EMF may encompass genes that are essential for the specification of non-myocardial lineages. Noteworthy, the expression of MyoD, a gene involved in skeletal myogenesis was not affected in both EBs and puromycin selected cells (Figure 56), while the expression of neurogenin1, a neuronal specification gene, was slightly enhanced only in EBs (Figure 56).

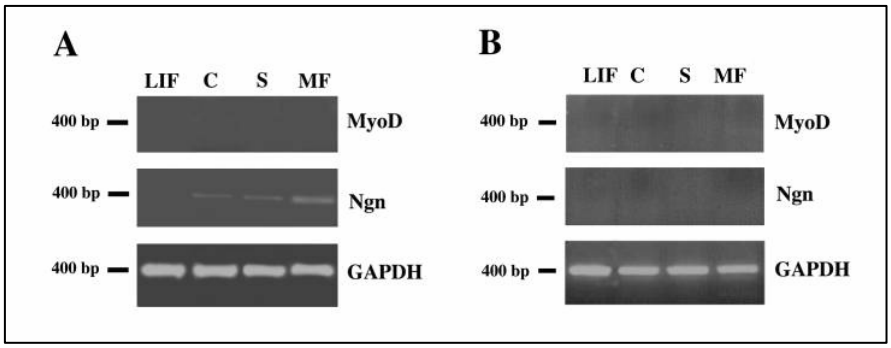

Figure 56. Effect of ELF-EMF (MF) on the expression of genes promoting non-myocardial lineages. A: MF was applied from the time of LIF removal and EBs were collected after additional 3 days. B: MF was applied from the time of LIF removal throughout puromycin selection. Four days after puromycin addition (10 days from LIF withdrawal), ES-derived cardiomyocytes were processed gene expression analyses. C: control cells; S: sham. MyoD and neurogenin1 (Ngn) are skeletal muscle and neuronal specification genes, respectively. (Ethidium bromide-stained agarose gels, representative of 4 separate experiments).

3.1.4.4 Membrane currents of oocytes of *Xenopus laevis* expressing rCx46 (Participant 7)

ELF-EMF did not significantly affect the leak-current of oocytes of Xenopus laevis expressing hemi-channels of rCx46.

During expression of hemi-channels, composed of the connexin rCx46, the oocytes were exposed to ELF-EMF (50 Hz). As suitable parameter for functional integrity of an oocyte the leak-current was selected which was electrophysiologically measured at voltage-clamp. A representative experiment of a sham exposed oocyte is shown in Figure 57. Figure 57a) shows membrane currents recorded at depolarising test potentials starting from a holding potential of –90 mV. The figure indicates that the rCx46-mediated current becomes activated by depolarising test potentials above about –10 mV. Figure 57b) shows the corresponding leak subtracted steady-state current values (I_{ss}) as function of driving voltage ($V-V_{rev}$) where V_{rev} denotes the corresponding reversal potential. The corresponding steady-state current values were derived at the end of the applied test pulse.

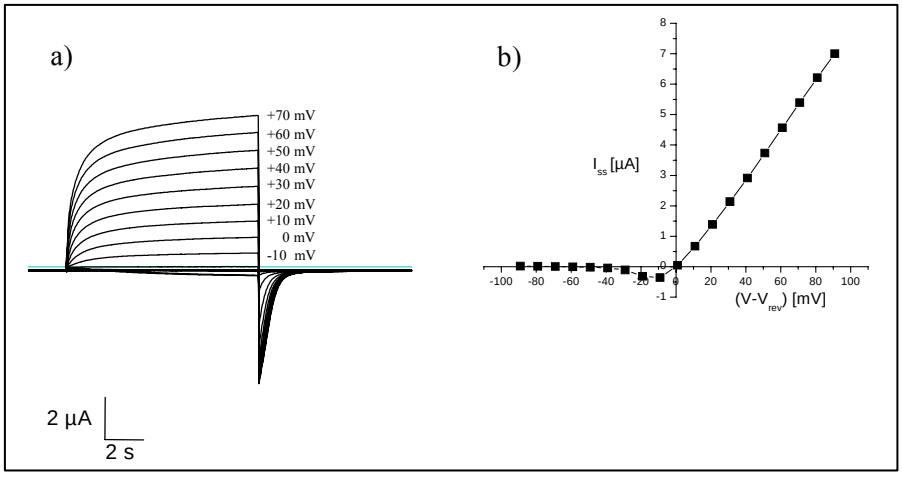

Figure 57. Voltage-dependent current activation of sham exposed *Xenopus* oocytes expressing rCx46 after an expression time of 16 hours.**a)** Representative voltage-jump current-relaxations at given test potentials. The common holding potential was set to -90 mV. The dotted line denotes the zero current level. **b)** Leak subtracted steady-state current amplitudes (I_{ss}, , ■) derived from the data in a) as function of driving voltage ($V-V_{rev}$)

The leak-current was derived at test potentials in the range of -70 mV to -100 mV using a constant holding potential of -90 mV. A comparison of leak-currents for exposed and sham exposed oocytes is given in Figure 58. Figure 58a shows the leak-current for oocytes which were continuously exposed for 16 hours at 2.3 mT and Figure 55b) the corresponding leak-current after an intermittent exposure (5 min on/10 min off) at 1.0 mT for 16h. A significant influence of ELF-EMF exposure on the leak current could not be observed for the different exposure conditions.

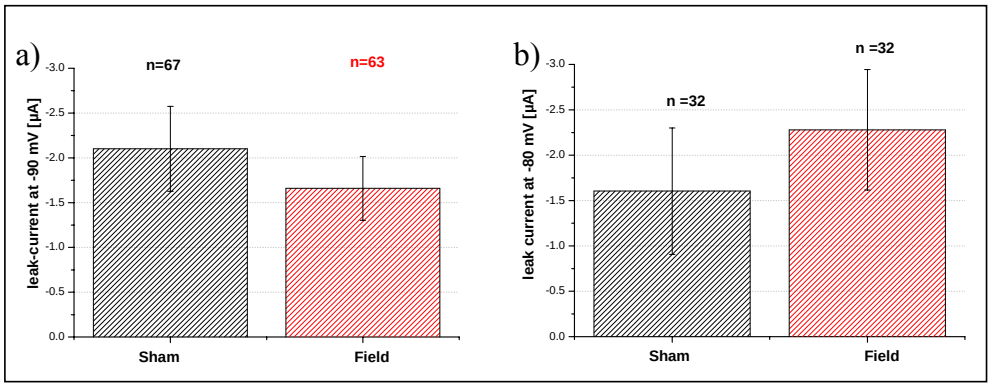

Figure 58. Leak-currents of single oocytes after expression of rCx46- hemi-channels at different holding potential.**a**) Leak current amplitudes at holding potential –90 mV of sham and ELF-EMF (2.3 mT, 16 hours) continuously exposed oocytes. **b**) Leak-currents at holding potential –80 mV of sham and ELF-EMF (1.0 mT, 16 hours, 5 min on/10 min off) exposed oocytes. Data are given as mean ± s.e.m. n denotes the number of different oocytes.

No significant influence of ELF-EMF on the number of expressed and conducting hemi-channels composed of rCx46 in oocytes.

The expression level of hemi-channels composed of rCx46 was estimated from the number of conducting hemi-channels which corresponds to the mean steady-state current amplitude (I_{ss}) and/or the maximal membrane conductance G_{max} at depolarising test potentials. Expression of endogenous hemi-channels was suppressed by injection of the corresponding anti-sense. Figures 59a, 60a and 61a show the relationship I_{ss} vs ($V-V_{rev}$) for different oocytes for the selected exposure condition. For clearer presentation G(V) was normalised to a maximal value of G(V) which is obtained at V = +50 mV (Figures 59b, 60 and 61b). A significant influence of ELF-EMF exposure on the number of expressed and conducting hemi-channels of rCx46 could not be read from the analysed data. This finding is also reflected in the frequency distribution of G_{max} for sham and exposed oocytes (Figure 59c).

No significant influence of ELF-EMF on the voltage-dependent gating properties of rCx46 expressing oocytes

A possible effect of ELF-EMF exposure on the voltage dependent gating properties of conducting hemi-channels of rCx46 was analysed. I_{ss} vs ($V-V_{rev}$) was measured and the corresponding relation G(V) vs ($V-V_{rev}$) derived. The latter relationship could be fitted by a simple Boltzmann equation. The fit yields as essential parameter the number of apparent equivalent voltage gating charges z. z was determined for the different exposure conditions. As can be read from Figure 59a) a significant effect of ELF-EMF exposure on the voltage-dependent gating which is reflected in the apparent number of equivalent charges z (Figure 59b) was not observed.

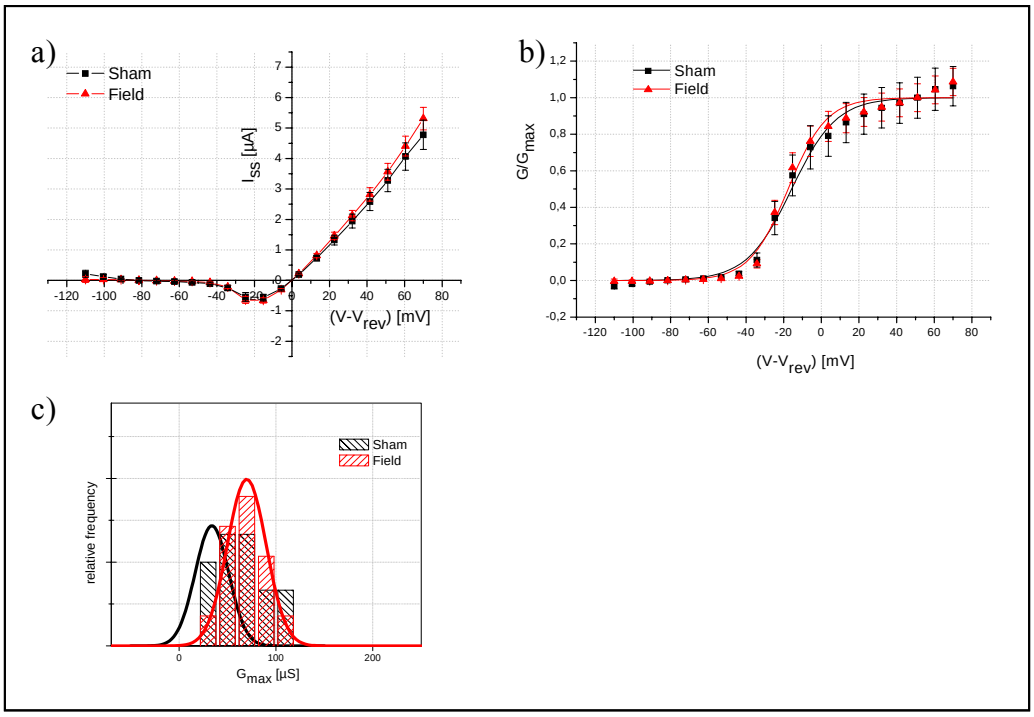

Figure 59. Voltage dependence of macroscopic rCx46-mediated membrane current and corresponding conductance after continuous ELF-EMF exposure for 16 hours at 2.3 mT. **a)** Mean ± s.e.m. of leak subtracted steady-state current amplitudes (I_{ss}) as function of (V-V_{rev}) in the absence and presence of ELF-EMF exposure (sham ■, n = 14; field ▲, n=15). **b**) Mean ± s.e.m. of corresponding normalised membrane conductance G/G_{max} = G(V)/G(V=+50 mV) as function of (V-V_{rev}) in the absence (■, n = 14) and presence of ELF (▲, n = 15). The solid lines show fits of the data by a simple Boltzmann function (for details see Materials and Methods). The derived parameters are z(sham) = 2.11 ± 0.17; z(field) = 2.45 ± 0.23; $V_{1/2}$(sham) = (-15.76 ± 1.06) mV; $V_{1/2}$(field) = (-17.66 ± 1.07) mV. **c**) Distribution of relative frequency of G_{max} = G(V=+50 mV) in the absence (n = 14) and presence (n = 15) of ELF-EMF. Solid lines present the Gauss distribution with the parameters: $G_{max, mean}$(sham)=64.2µS, corresponding standard deviation (sd) sd(sham) = 7.8 µS and $G_{max, mean}$(field) = 69.8 µS, sd(field) = 20.0 µS

To investigate an influence of field intensity on the results presented above, the experiments were repeated at 1.0 mT and the EMF-ELF was intermittently applied (5 min on/10 min off) for 16 hours. The corresponding results are given in Figure 60. Again, a significant effect of ELF-EMF on the number of expressed hemi-channels of rCx46 (Figure 59a) as well as their voltage dependent gating properties was not observed (Figure 60b).

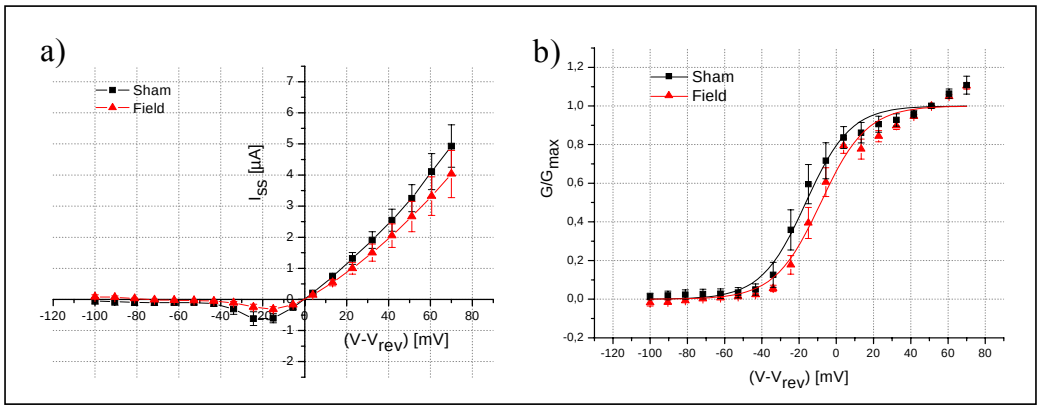

Figure 60. Voltage dependence of rCx46-mediated membrane currents and corresponding membrane conductance after intermittent ELF-EMF exposure (5 min on/10 min off) for 16 hours at 1.0 mT. **a)** Mean ± s.e.m. of leak subtracted steady-state current amplitudes (I_{ss}) as function of (V-V_{rev}) in the absence and presence of ELF-EMF exposure (sham ■, n = 5; field ▲, n = 5). **b)** Mean ± s.e.m. of normalised membrane conductance G/G_{max} = G(V)/G(V = +50 mV) as function of driving voltage (V-V_{rev}) in the absence (■, n = 5) and presence of ELF-EMF (▲, n = 5). The solid lines present fits of the data by a simple Boltzmann function, respectively (for details see Materials and Methods). The derived parameters are z(sham) = 2.08 ± 0.19; z(field) = 2.02 ± 0.20; $V_{1/2}$(sham) = (-16.39 ± 1.29) mV; $V_{1/2}$(field) = (-8.32 ± 1.38) mV

In a further series of experiments ELF-EMF at an intensity of 2.3 mT was intermittently (5 min on/10 min off) applied for 16 hours. The corresponding results are given in Figure 61. A significant effect of ELF-EMF exposure on the number of expressed hemi-channels of rCx46 (Figure 61a) was not observed. The data indicate a decrease of z after ELF-EMF exposure which appears not be significant (see legend of Figure 61b).

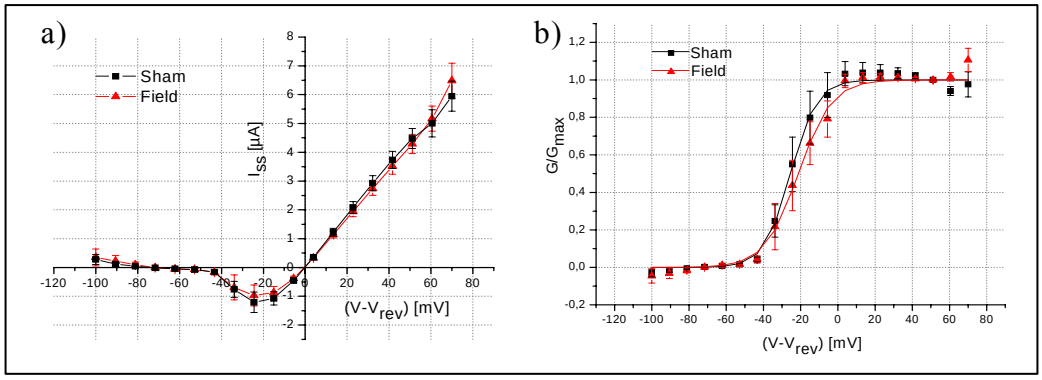

Figure 61. Voltage dependence of macroscopic rCx46-currents (I_{ss}) and corresponding membrane conductance (G) after intermittent exposure (5 min on/10 min off) for 16 hours at 2.3 mT. **a)** Mean ± s.e.m. of leak subtracted steady-state current amplitudes (I_{SS}) as function of (V-V_{rev}) in the absence and presence of ELF-exposure (sham ■, n = 4; field ▲, n = 5). **b)** Mean ± s.e.m. of normalised membrane conductance G/G_{max} = G(V)/G(V = +50 mV) as function of (V-V_{rev}) in the absence (■, n = 4) and presence of ELF-EMF(▲, n = 5). The solid lines show fits of the data by a simple Boltzmann function (see Material and Methods). The derived parameters are z(sham) = 3.54 ± 0.26; z(field) = 2.77 ± 0.24; $V_{1/2}$(sham) = (-25.51 ± 0.59) mV; $V_{1/2}$(field) = (-21.31 ± 0.88) mV

For a more detailed analysis of the voltage dependent gating properties the kinetics of rCx46- mediated current activation was considered. The time dependent current activation could be described by a sum of two exponential functions: $I(t) = a_0 + a_1*\exp(1-\exp(-t/\tau_1)) + a_2*\exp(1-\exp(-t/\tau_2))$. The corresponding time constants of activation τ_1 and τ_2 were obtained from corresponding fits to the experimental data and the

results are presented in Figures 62a-c. The figure indicates that ELF-EMF exposure does not influence the voltage dependent time constants of channel activation significantly.

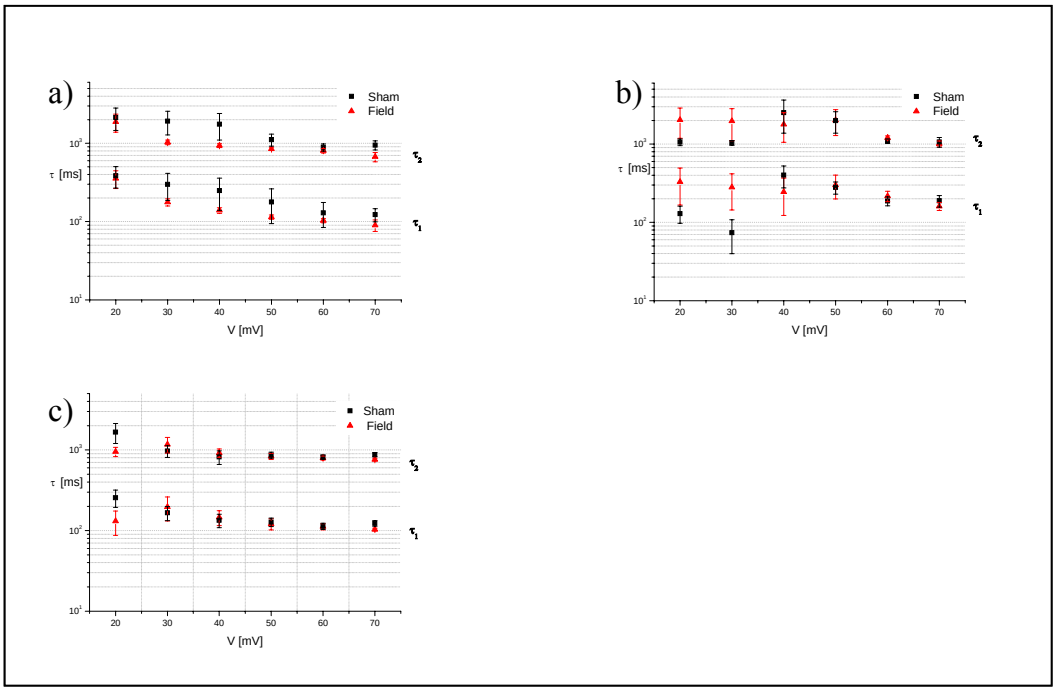

Figure 62. Time constants of voltage-dependent current activation. Time constants of current activation were plotted as function of voltage. Each point represents mean ± s.e.m of five different oocytes. The time constants of activation were obtained by fitting the time course of current activation by a sum of two exponential functions (see text). **a**), **b)** and **c)** present the time constants τ_1 and τ_2 at different exposure conditions: **a)** 2.3 mT, 16 hours continuous, **b)** 2.3 mT, 16 hours intermittent (5 min on/10 min off) and **c)** 1.0 mT, 16 hours intermittent (5 min on/10 min off).

No significant influence of ELF-EMF on the reversal potential of rCx46-mediated membrane current in oocytes.

Finally, the reversal potential V_{rev} of the rCx46-mediated membrane current was considered at different exposure conditions (Figure 63). The reversal potential is mainly determined by the expressed and conducting hemi-channels composed of rCx46, but also includes the contribution of all electrogenic transport systems. A field induced shift of the reversal potential would indicate a change of the intrinsic voltage sensor of the channel of by variation of the intracellular ion composition. No significant effect on the reversal potential of rCx46-mediated membrane current could be observed.

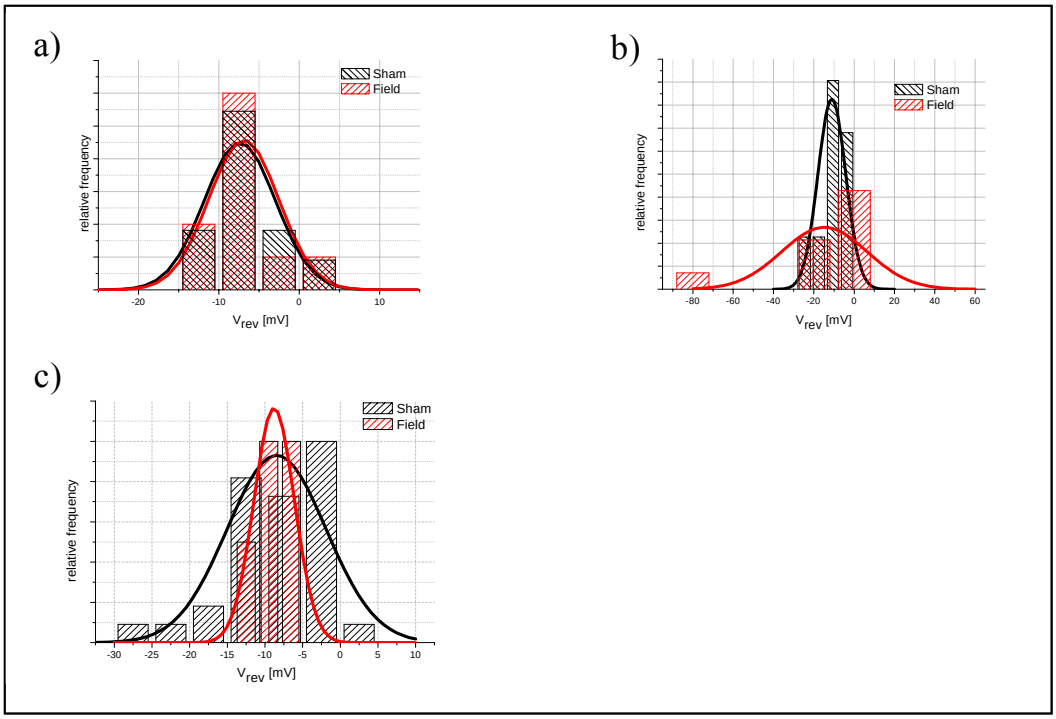

Figure 63. Relative frequency of reversal potential (V_{rev}) of conducting hemi-channels composed of rCx46 for different exposure conditions during an expression period of 16 h. The data were derived from the corresponding experiments given in Fig. 59. **a)** 1.0 mT, intermittent exposure: n = 11 for sham exposed and n = 10 for ELF-EMF exposed oocytes; **b)** 2.3 mT, permanent exposure: n = 18 for sham exposed and n = 20 for ELF-EMF exposed oocytes; **c)** 2.3 mT intermittent exposure: n =5 for sham exposed and n = 4 for ELF-EMF exposed oocytes. Solid lines present the corresponding Gauss distributions using the parameters mean of relative frequency ($V_{rev,\ mean}$) and standard deviation (sd): **a)** $V_{rev,\ mean}$(sham) = -6.9 mV, sd(sham) = 4.4 mV, $V_{rev,\ mean}$ (field) = -7.4 mV, sd(field) = 4.4 mV; **b)** $V_{rev,\ mean}$(sham) = -11.1 mV, sd(sham) = 6.9 mV, $V_{rev,\ mean}$(field) = -14.8 mV, sd(field) = 2.1 mV; **c)** $V_{rev,\ mean}$(sham) = -8.8 mV, sd(sham) = 2.1 mV, $V_{rev,\ mean}$(field) = -8.5 mV, sd(field) = 0.7 mV

A slight but not significant influence of ELF-EMF on the gating properties of hemi-channels expressed in Xenopus oocytes dependent on the external calcium concentration was observed.

The expression level of rCx46 in single were characterised by detailed biophysical analysis of corresponding voltage-jump current relaxation experiments. In parallel the gating by external Ca^{2+} concentration was characterised. A significant influence on the rCx46 mediated membrane conductance, the corresponding half-activation voltage ($V_{1/2}$) and the number of apparent equivalent gating charges (z) of the rCx46-hemi-channels in exposed and sham-exposed *Xenopus laevis* oocytes could not be observed for intermittently applied ELF-EMF at 50 Hz powerline signal (1.0 mT, 5 min on/10 min off) after an exposure time of 14 hours, 17 hours and 20 hours, respectively. Since it is known that external calcium significantly modulates the voltage dependent gating behaviour of expressed hemi-channels composed of rCx46, the experiments were repeated at various external calcium concentrations. The results indicate an influence by ELF-EMF exposure, but the differences are not significant (Figure 64). The membrane conductance and the gating parameters of exposed oocytes expressing rCx46 are smaller than those of sham exposed cells after an exposure time of 14 hours and 20 hours, respectively.

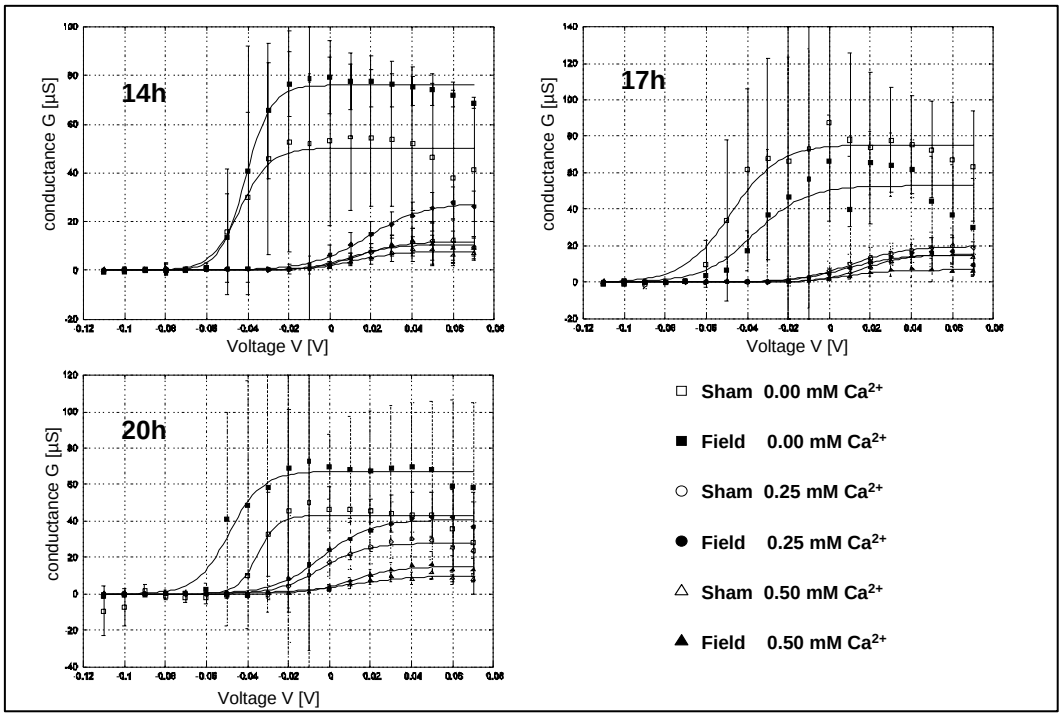

Figure 64. Conductance of hemi-channels composed of rCx46 expressed in oocytes after intermittent exposure (5 min on/10 min off) for 14 hours, 17 hours and 20 hours at 1.0 mT in the presence of 0.0 mM (n = 2-6), 0.25 mM (n = 2-4) and 0.5 mM (n = 2-5) Ca^{2+} in the bath. Closed symbols denote results of exposed oocytes and open symbols those of sham exposed oocytes.

ELF-EMF did not significantly affect the results of electrophysiological recordings of paired Xenopus oocytes.

The voltage-clamp experiments were repeated using paired oocytes. Paired oocytes expressing rCx46 form cell-to-cell channels (gap junctions) by head-to-head association of two hemi-channels which results in an increase of transjunctional conductance (G) between paired oocytes. Paired oocytes were intermittently ELF-EMF exposed (5 min on/10 min off) for 8 hours at 50 Hz powerline signal of 1.0 mT. The half-activation voltage ($V_{1/2}$) and the number of apparent equivalent gating charges (z) derived from the voltage-gating of junctional conductance of paired oocytes expressing rCx46 showed no significant change by ELF-EMF exposure (Figure 65). But the conductance of exposed paired oocytes is smaller than the conductance of sham exposed cell pairs. This finding is not significant on the basis of the 3 paired oocytes analysed so far.

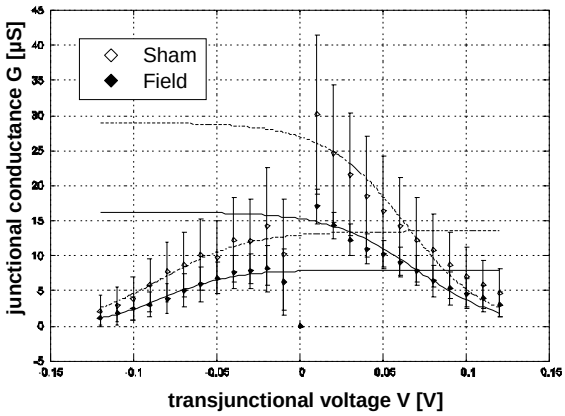

polarity of trans-junctional voltage	$G_{\pm 70}$ [µS]	$V_{1/2}$ [mV]	z
		Sham	
negative	13.53	-82.94	0.96
positive	28.97	69.32	-1.03
		Field	
negative	08.00	-82.54	1.19
positive	16.27	68.94	-0.99

Figure 65. Mean junctional conductance (G) of paired oocytes expressing cell-to-cell channels composed of rCx46 as function of transjunctional voltage. The table summarizes the maximal conductance $G_{\pm 70}$ = G(V=±70 mV) and the voltage-dependent gating parameters: the half-activation voltage ($V_{1/2}$) and number of apparent equivalent gating charges (z) of cell-to-cell channels after intermittent exposure (5 min on / 10 min off) for 8 hours at 1.0 mT, 50 Hz powerline (closed symbol: exposed cell pairs (n = 3); open symbol: sham exposed cell pairs (n = 3)). The parameter values were obtained by fitting the experimental data of G vs. V by a simple Boltzmann-distribution.

No significant influence of ELF-EMF on gap junctional coupling of rat granulosa cells was observed.

Gap junctional coupling by cell-to-cell channels of pairs of cultured granulosa cells was recorded after continuous exposure to ELF-EMF of 2.3 mT for 30 min. Figure 66a shows the maximal gap junctional conductance in the absence and presence of ELF-EMF exposure. The data were obtained as function of days in culture after passage, respectively. The corresponding mean gap junctional conductance of sham- and field-exposed cell all pairs is given in Figure 66b. No significant influence of ELF-EMF exposure on gap junctional coupling of rat granulosa cells was found.

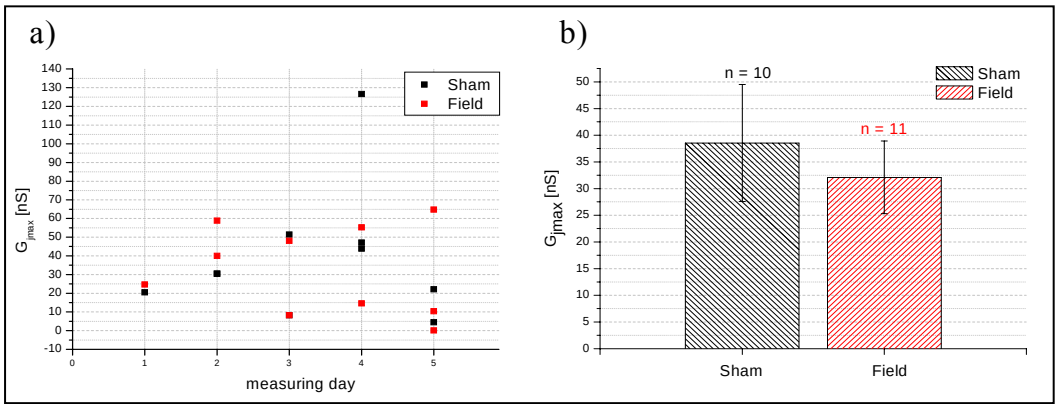

Figure 66. Gap junctional coupling of rat granulosa cell pairs as function of culture time in the presence and absence of ELF-EMF. **a.)** Maximal gap junctional conductance G_{jmax} of cultured pairs of granulosa cells in the absence (■, n = 10) and presence of ELF (■, n = 11) as function of time in culture. ELF-EMF was continuously applied with 2.3 mT for 30 min at room temperature, respectively. Measurements were performed by application of the double whole-cell patch clamp technique. **b**.) Mean ± s.e.m. of gap junctional conductance measured at 1 to 5 days (see a)), in the absence (n = 10) and presence of ELF-EMF (n = 11). n denotes the number of different cell-pairs.

An effect of ELF-EMF on cytoplasmic free calcium of cultured human fibroblasts and granulosa cells of rats was not observed.

After exposure of fibroblasts for 5, 6, 7, 9, 10 and 11 hours to ELF-EMF $[Ca^{2+}]_i$ was recorded. Measurement of $[Ca^{2+}]_i$ was started 10 min after end of exposure and recorded up to 40 min under exposure –free incubation conditions. In Figure 67 $[Ca^{2+}]_i$ was followed after exposure for 11 h (Figure 67a) and 15h (Figure 67b). During the presented recording time no significant change of $[Ca^{2+}]_i$ was observed. The described experiments were repeated for a cultured granulosa cell line (not shown). The observed variability in the time course of $[Ca^{2+}]_i$ of some sham- and field exposed cells seems not to be significant. As in the case of fibroblasts a long-lasting influence of ELF-EMF on the time course and amplitude of $[Ca^{2+}]_i$ was not observed for cultured rat granulosa cells. For clearer presentation the results of $[Ca^{2+}]_i$ recorded for fibroblasts and rat granulosa cells are summarised in Table 9.

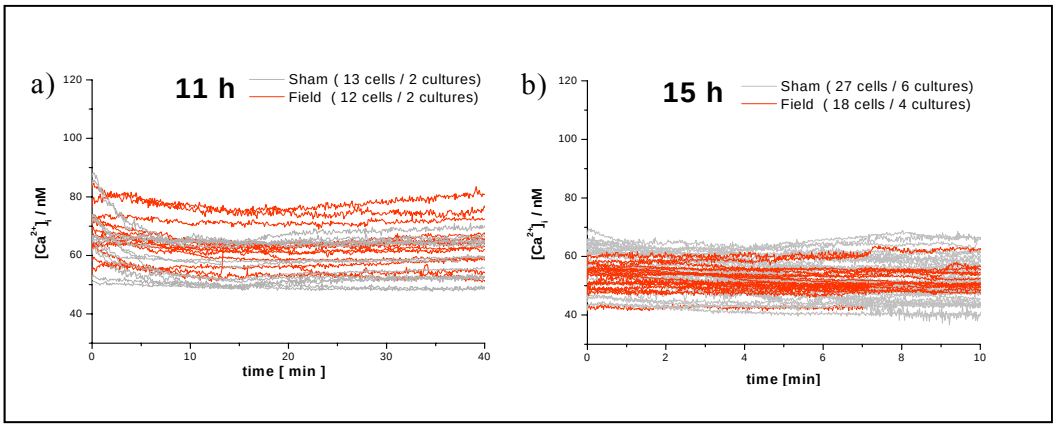

Figure 67. Time course of $[Ca^{2+}]_i$ in fibroblasts after ELF-EMF exposure at 50 Hz sinusoidal, 1.0 mT, intermittent (5 min on/10 min off) for **a)** 11 hours and **b)** 15 hours exposure time (grey curves denote sham- and red curves field-exposure)

Table 9. Summary of $[Ca^{2+}]_i$ data obtained on cultured fibroblasts and rat granulosa cells after ELF-EMF (5 min on/10 min off, sinusoidal 50 Hz, 1.0 mT) exposure

cell system	exposure time	7 h	9 h	11 h	15 h	17 h
Fibroblasts	sham	35 cells / 6 cultures	27 cells / 5 cultures	13 cells / 2 cultures	27 cells / 6 cultures	56 cells / 7 cultures
	field	37 cells / 6 cultures	15 cells / 3 cultures	12 cells / 2 cultures	18 cells / 4 cultures	14 cells / 3 cultures
		no ELF-EMF effect	**no ELF-EMF effect**	**no ELF-EMF effect**	**no ELF-EMF effect**	**no ELF-EMF effect**
Granulosa	**exposure time**	**4 h**	**5 h**	**6.5 h**	**7.75 h**	
	sham	11 cells / 1 culture	54 cells / 5 cultures	60 cells / 5 cultures	51 cells / 3 cultures	
	field	19 cells / 2 cultures	57 Cells / 5 cultures	47 cells / 3 cultures	7 cells / culture	
		no ELF-EMF effect	**no ELF-EMF effect**	**no ELF-EMF effect**	**no ELF-EMF effect**	
ELF-EMF stimulation: 50 Hz, sinusoidal, 1 mT (5 min on / 10 min off)						

In a further series of experiments the cells were exposed to an additional stressor added to the bath after the end of ELF-EMF exposure. Figure 65 shows the time course of $[Ca^{2+}]_i$ of fibroblasts during an additional exposure to 200 µM H_2O_2 in the bath. No significant effect on $[Ca^{2+}]_i$ could be found during a consecutive treatment by H_2O_2. Application of another stress condition like cell- depolarisation by high external KCl (30 mM) also did not affect the time course and amplitude of $[Ca^{2+}]_i$ for ELF-EMF exposed cells (data not shown).

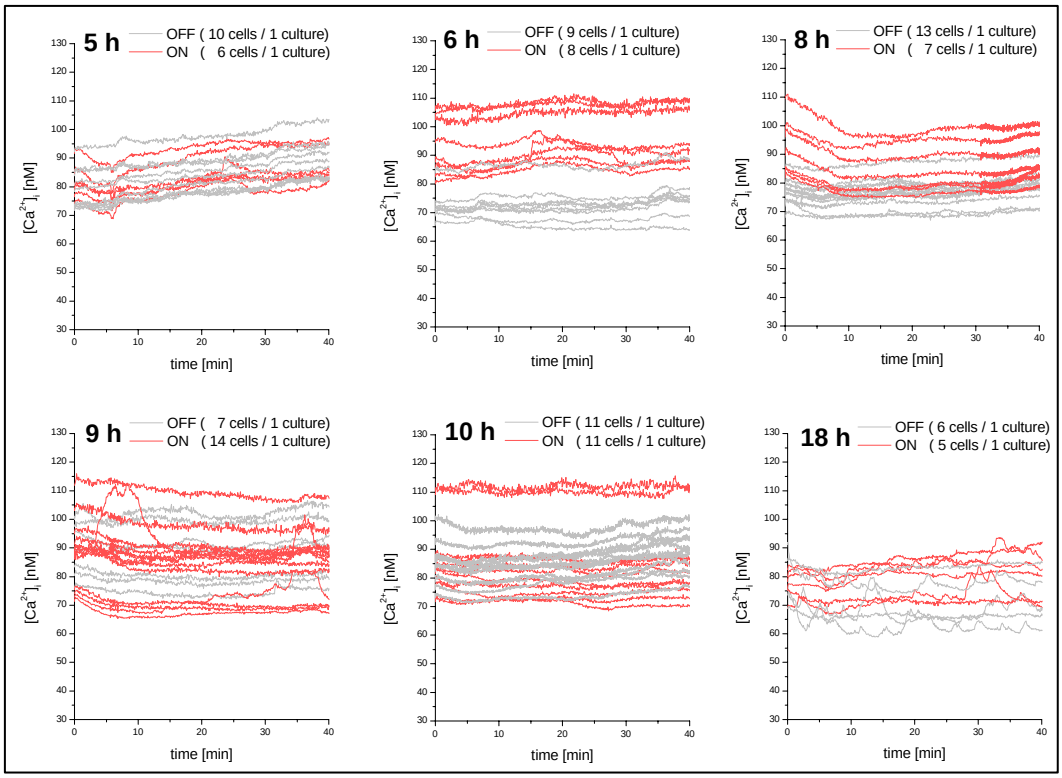

Figure 68. Time course of $[Ca^{2+}]_i$ in fibroblasts after end of ELF-EMF (5 min on/10 min off, 50 Hz sinusoidal, 1.0 mT) exposure for 5 , 6, 8, 9, 10 and 18 hours which was followed by an addition of 200 µM H_2O_2 to the bath for further 10 min (grey curves denote sham- and red curves field-exposure). For further details see text.

A summary of $[Ca^{2+}]_i$ measurements on fibroblasts and rat granulosa cells after application of ELF-EMF followed by addition of H_2O_2 to the bath is given in Table 10. $[Ca^{2+}]_i$ was recorded in the presence of 200 µM H_2O_2.

Table 10. Summary of $[Ca^{2+}]_i$ data obtained on cultured fibroblasts and rat granulosa cells after ELF-EMF (5 min on/10 min off, sinusoidal 50 Hz, 1.0 mT) exposure followed by addition of H_2O_2 to the bath.

cell system	stimulation	exposure time	5 h	6 h	8 h	9 h	10 h	18 h
Fibroblasts	ELF-EMF and 200 µM H_2O_2	sham	10 cells / 1 culture	9 cells / 1 culture	13 cells / 1 culture	7 cells / 1 culture	11 cells / 1 culture	6 cells / 1 culture
		field	6 cells / 1 culture	8 cells / 1 culture	7 cells / 1 culture	14 cells / 1 culture	11 cells / 1 culture	5 cells / 1 culture
			no ELF -EMF effect	no ELF -EMF effect	no ELF -EMF effect	no ELF -EMF effect	no ELF -EMF effect	no ELF -EMF effect
	ELF-EMF and 30 mM KCl	**exposure time**	**6.5 h**	**7.5 h**	**8.5 h**	**9.5 h**		
		sham	7 cells / 1 culture	7 cells / 1 culture	6 cells / 1 culture	7 cells / 1 culture		
		field	5 cells / 1 culture	5 cells / 1 culture	10 cells / 1 culture	8 cells / 1 culture		
			no ELF -EMF effect	no ELF -EMF effect	no ELF -EMF effect	no ELF -EMF effect		
Granulosa	ELF-EMF and 200 µM H_2O_2	**exposure time**	**5 h**	**6 h**	**7 h**	**8 h**	**18 h**	
		sham	14 cells / 1 culture	14 cells / 1 culture	20 cells/ 2 cultures	14 cells / 1 culture	14 cells / 1 culture	
		field	5 cells / 1 culture	5 cells / 1 culture	10 cells / 1 culture	8 cells / 1 culture	14 cells / 1 culture	
			no ELF -EMF effect	no ELF -EMF effect	no ELF -EMF effect	no ELF -EMF effect	no ELF -EMF effect	
ELF-EMF stimulation: 5o Hz, sinusoidal, 1 mT, 5 min on / 10 min off								

The volume regulatory response of granulosa cells appeared not to be influenced by ELF-EMF.

The volume regulatory response of cultured granulosa cells was studied after application of a hypotonic shock followed by a hypertonic shock. For clearer presentation for each experiment the volume change (v(t)–v(t=0)) of 10 cells was analysed as function of time and normalised to the maximal value v_{max}, respectively. As exposure period again 18 h were selected, since after this exposure period rat granulosa cells show the maximal response on the genomic level. The volume regulatory behaviour of rat granulosa cells appears not to be influenced by ELF-EMF. In addition, there was no significant difference between exposed and sham exposed cells for hypotonic (Figure 69) as well as hypertonic conditions (not shown). The volume analysis was started 15 min after end of ELF-EMF exposure.

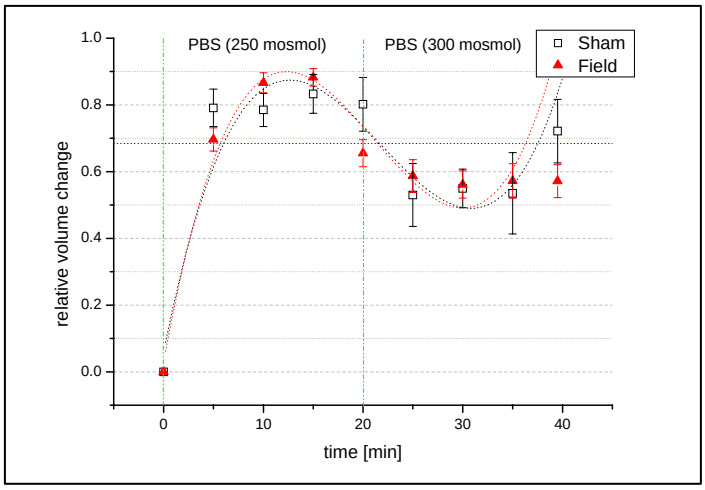

Figure 69. Relative volume change of granulosa cells (GFSHR-17) after addition of a hypotonic solution at t = 0. Prior to this treatment the cells were sham exposed (n = 7) or ELF-EMF exposed (n = 24) for 18 hours at 50 Hz, 1.0 mT, (5 min on/10 min off)). The mean ± s.e.m. is given, respectively.

3.1.4.5 Whole-genome analysis of various cell lines exposed to ELF-EMF (Participant 12)

Altogether, 58 whole-genome analyses of 10 different cell lines (sham-exposed cells and control cells) were performed (Table 1). After primary data analysis, we only worked on genes which were reproducibly regulated in several experiments (see materials and methods) and which belonged to certain gene families (Table 11). We defined gene families which are potentially relevant for the cellular answer on EMF exposure: signal transduction, ion/electron transport, metabolism of energy/proteins, cell proliferation/apoptosis, immune answer/inflammation and extracellular matrix/ cytoskeleton. Each gene family was sub-divided in subgroups again, e.g. GTP proteins in the signal transduction family (Tables 11, 12). In a first step, we did not go into single genes, but simply counted genes up- or down-regulated in the different gene families. The total number of regulated genes in a certain gene family is not very meaningful, because the sizes of the gene families are of course very different. Therefore, the total numbers of genes on the human array belonging to a gene family are shown in the first column of Tables 11 and 12. Although a single gene might appear in different categories (e.g. all small G proteins are GTP binding proteins), the Tables give a good overview on what might happen in the cells after EMF exposure on the molecular level.

In human fibroblasts (Participant 3), a number of G proteins and calcium associated proteins involved in signal transduction seem to be strongly regulated. Genes involved in adhesion of cells and cytoskeletal genes appear strongly regulated in several hybridizations, although the variances in numbers between the experiments are high (Table 11).

The fibroblast experiments (Participant 3) were also assessed by bio-statistics (Participant 8: Dr. Remondini, Table 12): Mitochondrial and ribosomal genes appeared strongly regulated, also Ca-related genes, cell cycle, apoptosis, extracellular matrix, and the cytoskeleton. The overall number of significantly regulated genes is higher in the ELF-EMF treated fibroblasts than e.g. in endothelial cells

exposed to RF-EMF (Participant 6). This was expected, since the number of regulated genes in fibroblasts after ELF-EMF exposure is pretty uniform in the non-statistically evaluated gene numbers (compare Table 12 with Table 11). From the experiments with SY5Y human neuroblastoma cells (Participant 11) and mouse embroyonic stem cells (Participant 4) it was not possible to extract bio-statistically significant data.

In detail, the following genes were extracted by bio-statistics so far:

Actin associated proteins (belong to cytoskeleton):
- Caldesmon (tropomysin binding, actin binding. Activation of ERK MAP kinases lead to phosphorylation of caldesmon. Regulatory protein of the contractile apparatus): down-regulated (fibroblasts, participant 3).
- Gamma-actin: down-regulated (fibroblasts, Participant 3).
- "coactosin-like": down-regulated (fibroblasts, Participant 3).
- "actin-binding": down-regulated (fibroblasts, Participant 3).
- "procollagen-proline 2": down-regulated (fibroblasts, Participant 3).
- "actin modulating activity": up-regulated (fibroblasts, Participant 3).
- "actin-binding, calcium ion binding": down-regulated (fibroblasts, Participant 3).
- CD2-associated protein, actin binding: down-regulated (fibroblasts, Participant 3).
- Tropomodulin 3: actin binding down-regulated (fibroblasts, Participant 3).

Calcium (Ca2+)-associated proteins:
- protein phosphatase 4: down-regulated (fibroblasts, Participant 3).
- Thrombospondin (cell adhesion): down-regulated (fibroblasts, Participant 3).
- "EGF-containing fibulin-like…" (cell adhesion): down-regulated (fibroblasts, Participant 3).
- matrix metalloproteinase 2 MMP 2 (extracellular matrix, collagen metabolism): down-regulated
- follistatin (extracellular matrix, heparin binding): down-regulated (fibroblasts, Participant 3).
- SPARC (extracellular matrix, collagen binding): down-regulated (fibroblasts, Participant 3).
- ("myosin light polypeptide": up-regulated (fibroblasts, Participant 3).
- ("hypothetical protein": up-regulated (fibroblasts, Participant 3).

Extracellular matrix (ECM):
- thrombospondin (see Ca): down-regulated (fibroblasts, Participant 3).
- "EGF-containing…." (see Ca): down-regulated (fibroblasts, Participant 3).
- MMP2 (see Ca): down-regulated (fibroblasts, Participant 3).
- Connective tissue growth factor CTGF (cell adhesion, obviously not influenced by Ca): up-regulated (fibroblasts, Participant 3).
- Collagen XV (obviously not influenced by Ca): up-regulated (fibroblasts, Participant 3).
- Lysyl oxidase (also processed by bone morphogenetic protein 1 BMP1, obviously not influenced by Ca): up-regulated (fibroblasts, Participant 3).

Cytoskeleton (see also actin and calcium-associated proteins):
- "hypothetical protein": down-regulated (fibroblasts, Participant 3).
- "protein phosphatase 4, caldesmon): down-regulated (fibroblasts, Participant 3).
- "SH3 protein interacting with Nck": down-regulated (fibroblasts, Participant 3).
- "in kinesin complex": down-regulated (fibroblasts, Participant 3).

Ion transport:
- "potassium channel activity": down-regulated (fibroblasts, Participant 3).
- SLC12A5 KCl (potassium chloride) transporter: down-regulated (fibroblasts, Participant 3).
- SLC26A3 sulfate porter: down-regulated (fibroblasts, Participant 3).
- "ferric ion binding": down-regulated (fibroblasts, Participant 3).
- (ATP synthase, H+ transport): down-regulated (fibroblasts, Participant 3).
- ("H+ transporter): down-regulated (fibroblasts, Participant 3).
- "iron ion transport": down-regulated (fibroblasts, Participant 3).

Ribosomal proteins:
- 7 ribosomal proteins down-regulated, 3 ribosomal proteins up-regulated, 1 ribosomal protein up-regulated in profile nr.1, down-regulated in profile nr.2 (fibroblasts, Participant 3).

Table 11. Numbers of genes regulated within different gene families

Gene Family	total number of clones in Human Unigene RZPD-2	partner 3 fibroblasts Exp1 ELF up-regulated genes	partner 3 fibroblasts Exp2 ELF up-regulated genes	partner 3 fibroblasts Exp1 ELF down-regulated genes	partner 3 fibroblasts Exp2 ELF down-regulated genes	Gene "Superfamily"
Signal	2528	251	232	296	190	signal transduction
GTP	560	66	73	66	52	signal transduction
Small G	235	31	32	28	27	signal transduction
Jak	23	0	0	5	3	signal transduction
Rab	80	0	9	11	13	signal transduction
Ras	66	10	7	10	5	signal transduction
wnt	5	0	0	0	0	signal transduction
phosphatase	334	39	36	35	26	signal transduction
protein kinase	304	28	29	35	24	signal transduction
phospholipase	72	9	8	10	7	signal transduction
calcium	715	67	72	80	50	signal transduction
calmodulin	131	6	13	17	11	signal transduction
channel	348	31	25	36	22	ion/electron transport
voltage-gated	164	16	13	16	6	ion/electron transport
electron transport	423	52	52	57	37	ion/electron transport
ion transport	501	49	48	45	29	ion/electron transport
metaboli	1241	122	128	135	96	metabolism of energy/proteins
ATP	1234	113	112	157	82	metabolism of energy/proteins
mitochon	574	84	82	70	65	metabolism of energy/proteins
ribosom	254	47	48	32	39	metabolism of energy/proteins
translation	168	30	28	20	13	metabolism of energy/proteins
transcript	1991	201	190	228	136	metabolism of energy/proteins
cell cycle	478	46	52	54	43	cell proliferation/apoptosis/differentiation
apoptos	373	31	37	37	23	cell proliferation/apoptosis/differentiation
differentiat	177	14	21	22	11	cell proliferation/apoptosis/differentiation
immun	390	31	37	38	32	immune answer/inflammation/stress answer
inflamma	184	10	20	24	11	immune answer/inflammation/stress answer
stress	118	12	11	14	13	immune answer/inflammation/stress answer
peroxidase	32	6	5	4	6	immune answer/inflammation/stress answer
heat shock	188	4	7	5	3	immune answer/inflammation/stress answer
DNA repair	154	14	19	19	10	immune answer/inflammation/stress answer
early	8	2	2	0	2	immune answer/inflammation/stress answer
adhesion	573	46	49	53	43	extracellular matrix/cytoskeleton/adhesion
extracellular matrix	226	19	34	31	16	extracellular matrix/cytoskeleton/adhesion
cytosk	529	45	50	47	42	extracellular matrix/cytoskeleton/adhesion
junction	129	11	10	13	10	extracellular matrix/cytoskeleton/adhesion
actin	494	32	32	38	32	extracellular matrix/cytoskeleton/adhesion

Table 12. Numbers regulated genes in different expression profiling experiments (bio-statistical analysis by Dr. Remondini/Participant 8)

Gene Family	total number of clones in Human Unigene RZPD-2	partner 3 fibroblasts ELF up-regulated genes	partner 3 fibroblasts ELF down-regulated genes	Gene "Superfamily"
Signal	2528	0	12	signal transduction
GTP	560	0	2	signal transduction
Small G	235	0	1	signal transduction
Rab	80	0	1	signal transduction
Ras	66	0	1	signal transduction
phosphatase	334	1	2	signal transduction
protein kinase	304	0	1	signal transduction
calcium	715	2	6	signal transduction
calmodulin	131	0	1	signal transduction
channel	348	0	2	ion/electron transport
voltage-gated	164	0	1	ion/electron transport
ion transport	501	0	7	ion/electron transport
electron transport	423	0	3	ion/electron transport
metaboli	1241	0	4	metabolism of energy/proteins
ATP	1234	2	7	metabolism of energy/proteins
mitochon	574	0	5	metabolism of energy/proteins
ribosom	254	3	7	metabolism of energy/proteins
translation	168	3	0	metabolism of energy/proteins
transcript	1991	2	9	metabolism of energy/proteins
cell cycle	478	1	4	cell proliferation/apoptosis/differentiation
apoptos	373	0	4	cell proliferation/apoptosis/differentiation
differentiat	177	0	2	cell proliferation/apoptosis/differentiation
immun	390	0	2	immune answer/inflammation/stress answer
DNA repair	154	0	0	immune answer/inflammation/stress answer
inflamma	184	0	1	immune answer/inflammation/stress answer
adhesion	573	2	3	extracellular matrix/cytoskeleton/adhesion
extracellular matrix	226	2	5	extracellular matrix/cytoskeleton/adhesion
cytosk	529	1	6	extracellular matrix/cytoskeleton/adhesion
actin	494	1	4	extracellular matrix/cytoskeleton/adhesion
junction	129	0	0	extracellular matrix/cytoskeleton/adhesion

3.1.4.6 Summary (Participant 1)

Our data indicate that ELF-EMF may affect the gene and protein expression in various cell systems. This conclusion is based on the following findings:

- ELF-EMF at a flux density of about 2 mT up-regulated the expression of early genes, such as p21, c-jun and erg-1, in p53-deficient mouse embryonic stem cells, but not in healthy wild-type cells suggesting that the genetic background affects the responsiveness of the cells (see 3.1.4.1).
- ELF-EMF at a flux density of 2 mT up-regulated in neural progenitor cells the transcript levels of the GADD45 gene and down-regulated the transcript levels of the bax gene by which the apoptotic process may be modulated (see 3.1.3.1 and 3.1.4.1).
- ELF-EMF at a flux density of 0.8 mT up-regulated the expression of cardiac specific genes in cardiomyocytes derived from embryonic stem cells thus promoting cardiogenesis (see 3.1.4.3).
- ELF-EMF did not affect the expression of neuronal genes in neuroblastoma cells (SY5Y) such as nAchRs, DβH, Phox2a and Phox2b, either at mRNA or protein level (see 3.1.4.2).
- ELF-EMF did not affect either the expression level of conducting hemi-channels composed of rCx46, nor their gating properties by voltage, pH, Ca^{2+} in *Xenopus laevis* oocytes (see 3.1.4.4).
- ELF-EMF appeared to regulate the expression of a series of genes and proteins in human fibroblasts such as mitochondral and ribosomal genes as well as Ca-, cell cycle-, apoptosis-, extracellular matrix-, and cytoskeleton-related genes, although it must be considered that the variances observed between the various experiments was high (see 3.1.4.5).

3.2 Results in RF-EMF research

3.2.1 Genotoxic effects

3.2.1.1 Human HL-60 cell line (Participant 2)

Genotoxic effects of EMF may occur directly either by damage to chromosomes and/or by damage to DNA repair mechanisms. Indirect genotoxic effects may arise by various processes such as generation of oxygen radicals or impairment of radical-scavenging mechanisms. Direct and indirect genotoxic effects of defined RF-EMF were investigated in the human cell line HL-60.

A. Direct genotoxicity

RF-EMF increased the micronucleus frequency and the number in DNA strand breaks in HL-60 cells dependent on the energy of radiation as determined by the cytokinesis-block in vitro micronucleus assay and the Comet assay.

The effect of RF-EMF on the formation of micronuclei (MN) and DNA strand breaks was examined by use of the cytokinesis-block in vitro micronucleus assay and the alkaline Comet assay. To validate the MN assay and to prove the susceptibility of HL-60 cells to physical noxes, cells were exposed to ionising-irradiation. As shown in Figure 70, a dose-dependent induction of micronuclei in HL-60 cells was found for doses of exposure increasing from 0.5 to 3.0 Gy. Cell division was effected by ionising-irradiation at doses ≥1.0 Gy as shown in Figure 71, inferred from the ratio of BNC against mono-, bi-, tri- and tetranuclear cells (in %).

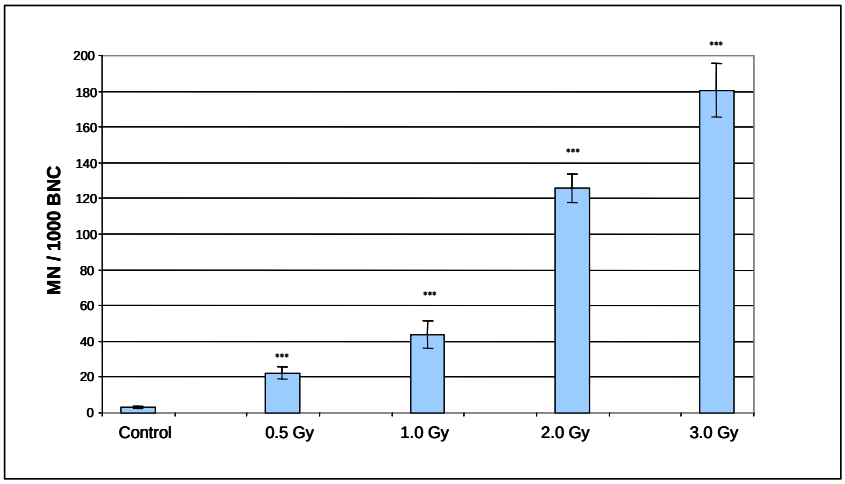

Figure 70. Effect of ionising-irradiation (6 MeV) on micronuclei formation in binucleated HL-60 cells. Each data point is based on at least three independent experiments. Each bar represents the mean ± SD of results obtained in three independent experiments. *** P<0.001 (Student's t-test, two-sided). All in all (mono-, bi-, tri-, and tetranucleated) 15000 cells were analysed.

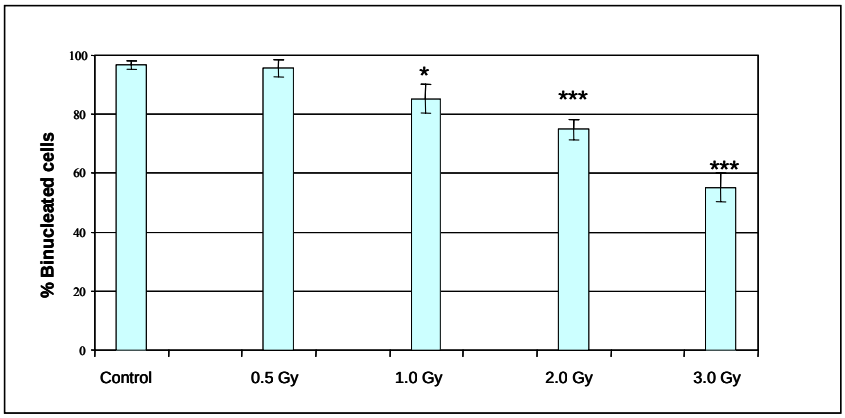

Figure 71. Effect of ionising-irradiation on HL-60 cell division. The number of binucleated cells relative to the number of mono-, bi-, tri-, and tetranuclear cells following ionising-irradiation (6 MeV) of HL-60 cells. Each bar represents the mean ± SD in % of results obtained in three independent experiments; *p<0.05, ***p<0.001 (Student's t-test, two-sided).

In a series of experiments SAR levels ranging from 0.2 W/kg to 3.0 W/kg were examined in order to clarify whether the effects of RF-EMF exposure (1800 MHz, continuous wave, 24 h) on MN frequencies in HL-60 cells are energy dependent (Figure 72). Whereas at SAR of 0.2 W/kg, 1.0 and 3.0 W/kg MN frequencies were not changed in RF-EMF-exposed cells as compared to sham controls and incubator controls, MN frequencies were significantly increased at SAR of 1.3 W/kg and above. The maximum increase was noted at a SAR of 1.3 and 1.6 W/kg. This effect was approximately 66 % of the effect observed after 0.5 Gy ionising-irradiation (6 MeV, exposure time: 5.2 s). At a SAR of 3.0 W/kg the MN frequency was similar to that found in sham-exposed cells. While MN frequencies of incubator controls were around 3.5, the MN frequency determined after RF-exposure at a SAR of 1.3 W/kg was 13.3 (approximately 3.8 fold higher). The MN frequency determined in cells after exposure to ionising-irradiation (0.5 Gy, exposure time: 5.2s), used as a positive control, was 22.3 ± 3.5 (n=3; 6.3 fold increase compared to control).

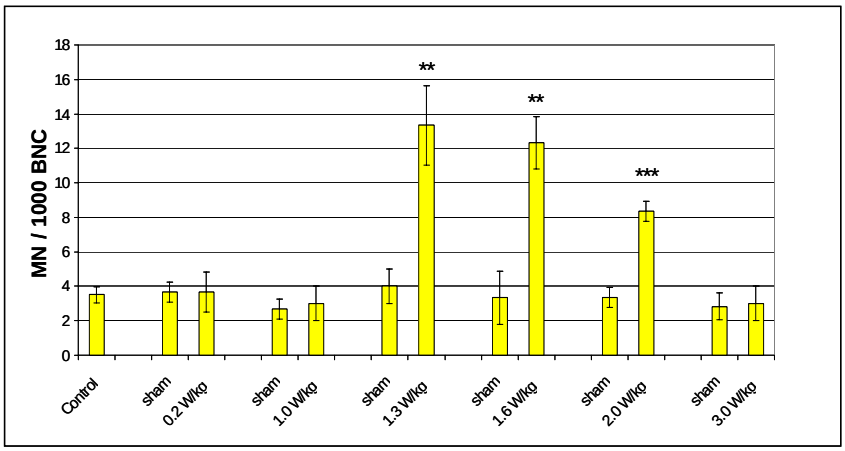

Figure 72. Micronucleus frequencies in binucleated HL-60 cells after exposure to RF-field (1800 MHz, continuous wave) for 24h ranging from SAR 0.2 to 3.0 W/kg, compared to control and sham-exposure. Each bar represents the mean ± SD of results obtained in three independent experiments (except of control: n = 11). Each data point is based on at least three independent experiments except of the control with 11 independent experiments and on a total number of 11000 (control), 18000 (sham-exposed) and 18000 (RF-exposed) bi-nucleated HL-60 cells. All in all (mono-, bi-, tri-, and tetra-nucleated) 47000 cells were analysed. The micronuclei frequency of BNC after exposure to ionising-irradiation (0.5 Gy, exposure time: 5.2s), which was used as a positive control, were on average 22.3 ± 3.5 (n=3). ** P<0.01; *** P<0.001 (Student's t-test, two-sided).

In order to compare micronuclei induction in cells exposed to RF-fields at different ranges of SAR, the average micronuclei frequencies (MN/1000 BNC) were calculated for the following groups: experiments performed at all SAR tested (range 0.2 W/kg to 3.0 W/kg, number of independent experiments n=18), experiments performed at SAR ranging from 1.0 W/kg to 2.0 W/kg (number of independent experiments n=12), and experiments at SAR of 0.2 W/kg and 1.0 W/kg (number of independent experiments n=6). While the calculated average of MN/1000 BNC in HL-60 cells at a SAR of 0.2 W/kg to 1.0 W/kg was not significantly different from that observed in sham-exposed controls, both groups ranging from 0.2 W/kg to 3.0 W/kg ($p<0.01$) or from 1.0 W/kg to 2.0 W/kg ($p<0.001$) exhibited a significant increase in micronuclei induction after RF-exposure as compared to sham-exposed controls (Figure 74A).

Previous experiments had clearly shown that RF-EMF exposure results in an increase of DNA strand breaks in HL-60 cells. In order to achieve a better understanding of whether these effects are energy dependent, additional experiments were performed applying RF-exposure (1800 MHz, continuous wave, 24h) at SAR of 0.2 W/kg to 3.0 W/kg. As shown in Figure 73 the effect of RF-EMF on DNA strand breaks at these exposure conditions exhibited a similar energy dependency as the effect of RF-EMF on micronucleus formation (Figure 72). RF-EMF exposure at a SAR of 1.0 W/kg and below had no effect on Comet formation in HL-60 cells (expressed as Olive Tail Moment OTM) as compared to control and sham-exposed cells. On the other hand RF-EMF at SAR of 1.3 W/kg and above caused a significant increase in DNA strand breaks. The maximum of this effect was observed at SAR 1.3 W/kg (OTM = 2.20 ± 0.16) and 1.6 W/kg (2.24 ± 0.10). At a SAR of 3.0 W/kg Comet formation in RF-EMF exposed cells (OTM 1.23 ± 0.12) was similar to that observed in sham-exposed cells (OTM 1.18 ± 0.03). While the Olive Tail Moment was around 1.0 in sham-exposed and incubator controls, the OTM determined after exposure at a SAR of 1.3 W/kg was approximately 2.2 fold higher (Figure 73). The OTM determined in cells after exposure to hydrogen peroxide (100 µmol/l, 1h), used as a positive control, was 8.3 ± 1.3 (n=3; 8 fold increase compared to control).

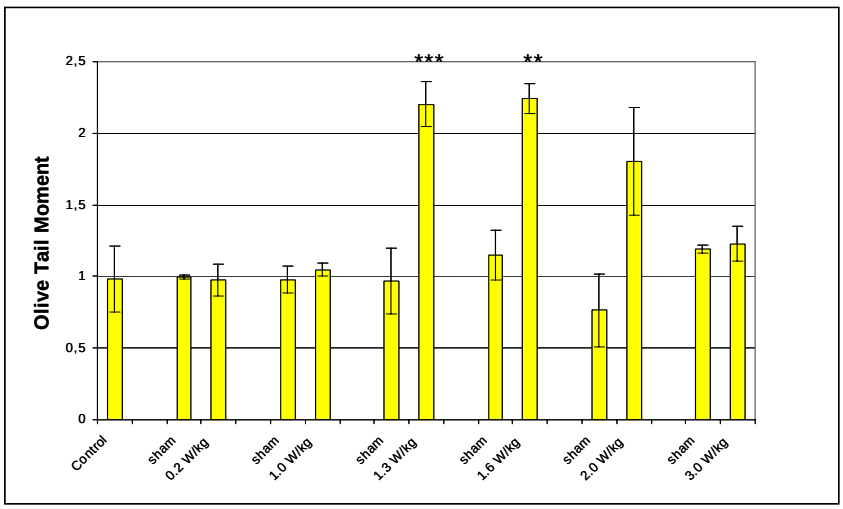

Figure 73. Comet formation in HL-60 cells after exposure to RF-field (1800 MHz, continuous wave) for 24h ranging from SAR 0.2 to 3.0 W/kg, expressed as Olive Tail Moment, compared to control and sham exposure. Each bar represents the mean ± SD of results obtained in at least three (except SAR 1.3 W/kg: n=4) independent experiments. The OTMs of the Comets after exposure to hydrogen peroxide (100 µmol/l, 1 h), which was used as a positive control, were on average 8.3 ± 1.3 (n=3). ** $P<0.01$; *** $P<0.001$ (Student's t-test, two-sided).

In order to compare Comet formation in cells exposed at different SAR ranges the average values of the Olive Tail Moments were calculated for the following groups: experiments performed at all SAR tested (range 0.2 W/kg to 3.0 W/kg, number of independent experiments n=18), experiments performed at SAR ranging from 1.0 W/kg to 2.0 W/kg (number of independent experiments n=12), and experiments at SAR of 0.2 W/kg and 1.0 W/kg (number of independent experiments n=6). While the calculated average of OTMs in HL-60 cells at SAR of 0.2 W/kg and 1.0 W/kg was not significantly different from that observed in sham-exposed controls, both groups ranging from 0.2 W/kg to 3.0 W/kg ($p<0.01$) or from 1.0

W/kg to 2.0 W/kg (p<0.001) exhibited a significant increase in Comet formation after RF-exposure as compared to sham-exposed controls (Figure 74B).

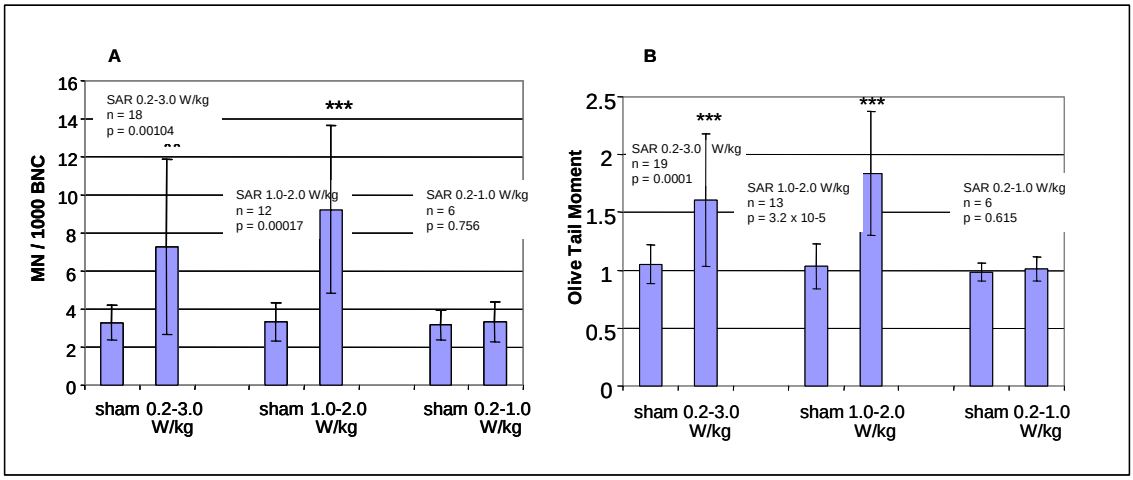

Figure 74. MN induction and Comet formation in HL-60 cells after RF-field exposure (1800 MHz, continuous wave, 24 h) over all SAR groups tested versus total sham, expressed as MN per 1000 BNC (A) and as Olive Tail Moment (B). Each bar represents the mean ± SD of results obtained in indicated number of experiments. ** P<0.01; *** P<0.001 (Student's t-test, two-sided).

RF-EMF increased the micronucleus frequency and the number of DNA strand breaks in HL-60 cells dependent on the exposure time as determined by the cytokinesis-block in vitro micronucleus assay and the Comet assay.

Using the cytokinesis-block MN assay it was also investigated, whether the duration of exposure of HL-60 cells to RF-fields has an influence on MN induction (Figure 75). Short exposure periods (6 h) caused no or less pronounced effects compared to longer exposure periods of 24 and 72h. The level of the effect on MN frequency noted after RF-EMF exposure for 72h (MN/1000 BNC: 20.22 ± 2.08) was comparable to that observed after 0.5 Gy ionising-irradiation (6 MeV, exposure time: 5.2 s) (MN/1000 BNC: 22.33 ± 2.48).

Furthermore, it was investigated, whether the duration of exposure of HL-60 cells to RF-EMF has an influence on Comet formation (Figure 76). Short exposure periods (2 and 6h) caused less pronounced effects compared to the longer exposure period of 24h. After 72h of exposure Comet formation was similar to that observed after short exposure times (2 and 6h).

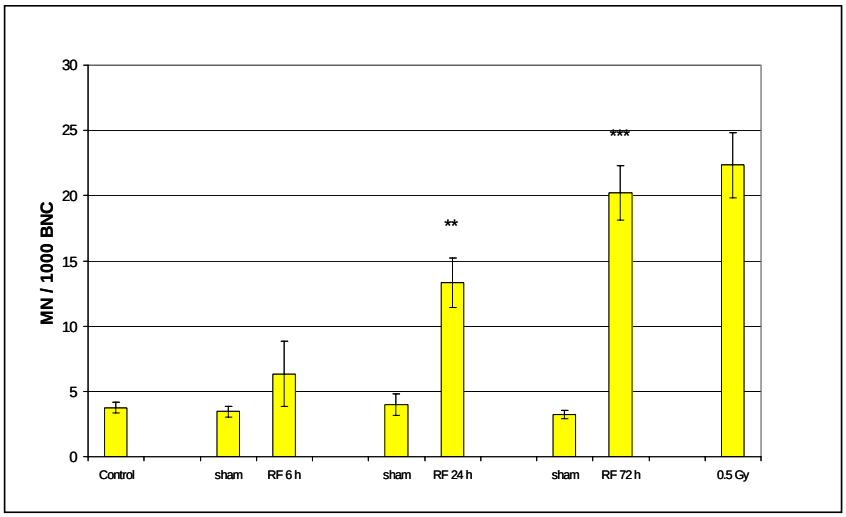

Figure 75. Micronucleus frequencies in binucleated HL-60 cells after exposure to RF-fields (1800 MHz, continuous wave, SAR = 1.3 W/kg) for 6, 24 and 72h, compared to control and sham-exposure. Positive control: 0.5 Gy ionising-irradiation (6 MeV). Each bar represents the mean ± SD of results obtained in three independent experiments (except control: n = 4). Data points are based on a total cell number of 4000 (control), 9000 (sham-exposed), 9000 (RF-exposed) and 3000 (0.5 Gy-exposed, exposure time: 5.2s) binucleated HL-60 cells. All in all (mono-, bi-, tri-, and tetranucleated) 25000 cells were analysed. ** P<0.01; *** P<0.001 (Student's t-test, two-sided).

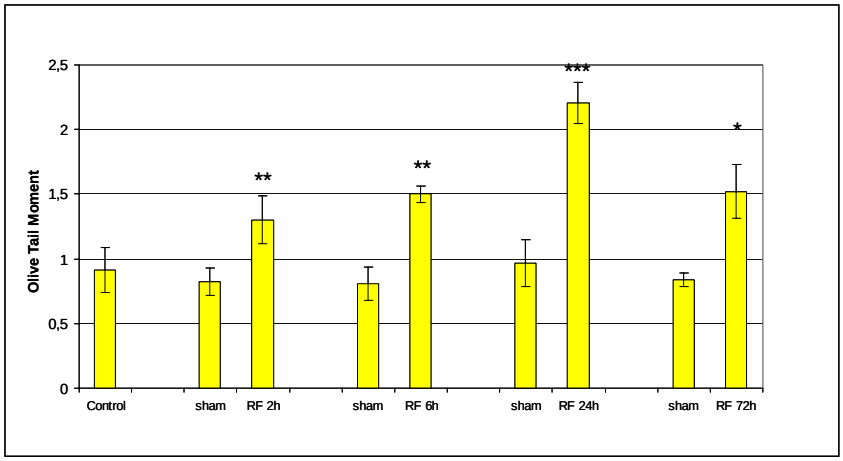

Figure 76. Comet formation in HL-60 cells after exposure to RF-fields (1800 MHz, continuous wave, SAR 1.3 W/kg) for 2, 6, 24 and 72h, expressed as Olive Tail Moment, compared to control and sham-exposure. Each bar represents the mean ± SD of results obtained in at least three (except RF-field exposure, 24h with n=4) independent experiments. * P<0.05; ** P<0.01; *** P<0.001 (Student's t-test, two-sided).

The effects of RF-EMF on genomic integrity of HL-60 cells were exposure-signal-dependent as determined by the cytokinesis-block in vitro micronucleus assay and the Comet assay.

In a further series of experiments it was studied, whether different RF-signals (1800 MHz, SAR 1.3 W/kg: continuous wave, C.W., 5 min on/10 min off; GSM-217Hz, GSM-Talk) for 24h are capable to cause MN induction in HL-60 cells (Figure 77) The number of independent experiments was extended to at least three independent experiments for each of the different types of RF-signals at that SAR with the most pronounced effect (SAR 1.3 W/kg). Using the cytokinesis-block MN assay the different RF-signals had similar effects on MN induction as observed following continuous wave exposure. While the MN frequency of continuous wave-exposed cells was 13.33 ± 1.89, the MN frequencies determined after different other RF-exposure signals were 16.11 ± 3.10 (C.W., 5 min on/10 min off), 13.22 ± 2.88 (GSM-

217Hz) and 17.66 ± 1.70 (GSM-Talk). The MN frequency determined in cells after exposure to ionizing-irradiation (0.5 Gy, 6 MeV, exposure time. 5.2 s), used as a positive control, was 22.3 ± 3.5 (n=3; 6.3 fold increase compared to control).

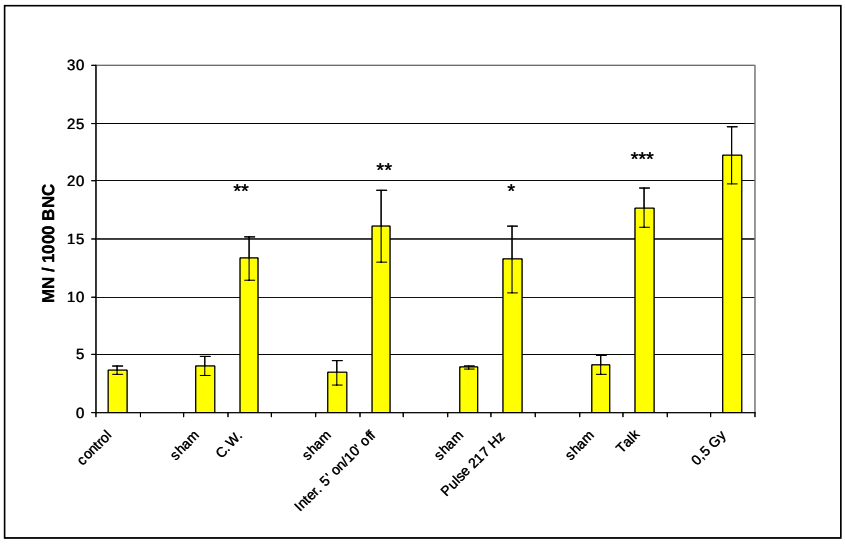

Figure 77. Micronucleus frequencies in binucleated HL-60 cells after exposure to RF-field (1800 MHz, SAR 1.3 W/kg, 24h) compared to control and sham-exposure for different signal modulations. Positive control: 0.5 Gy ionising-irradiation (6 MeV, exposure time: 5.2s). Bars represent means ± SD of three independent experiments (except control = 5). * P<0.01; ** P<0.01; *** P<0.001 (Student's t-test, two-sided). Each data point is based on at least three independent experiments except the control with five and the positive control with three independent experiments and on a total of 5000 (control), 12000 (sham-exposed), 12000 (RF-exposed) and 4000 (0.5 Gy-exposed) binucleated HL-60 cells. All in all (mono-, bi-, tri-, and tetranucleated) 32000 cells were analysed.

Calculation of the average numbers of micronuclei per 1000 BNC determined after exposure (SAR of 1.3 W/kg, 24h) to all RF-signals tested (continuous wave, C.W., 5 min on/10 min off; GSM-217Hz, GSM-Talk) showed an increase in micronuclei induction as compared to sham-exposure at a significant level (number of independent experiments n=12, P<0.001) (Figure 79A).

Using the Comet assay the different RF-signals had similar effects on Comet formation as observed after continuous wave exposure (Figure 78). While the OTM of continuous wave-exposed cells was 2.20 ± 0.16, the OTMs determined after different other RF-exposure signals were 2.11 ± 0.05 (C.W., 5 min on/10 min off), 1.77 ± 0.01 (GSM-217Hz) and 2.26 ± 0.24 (GSM-Talk).

Calculation of the average value of Olive Tail Moments determined after exposure to all RF-signals tested (continuous wave, C.W., 5 min on/10 min off; GSM-217Hz, GSM-Talk) showed a significant increase in Comet formation compared to sham-exposed controls (n=14, P<0.001 (Figure 79B).

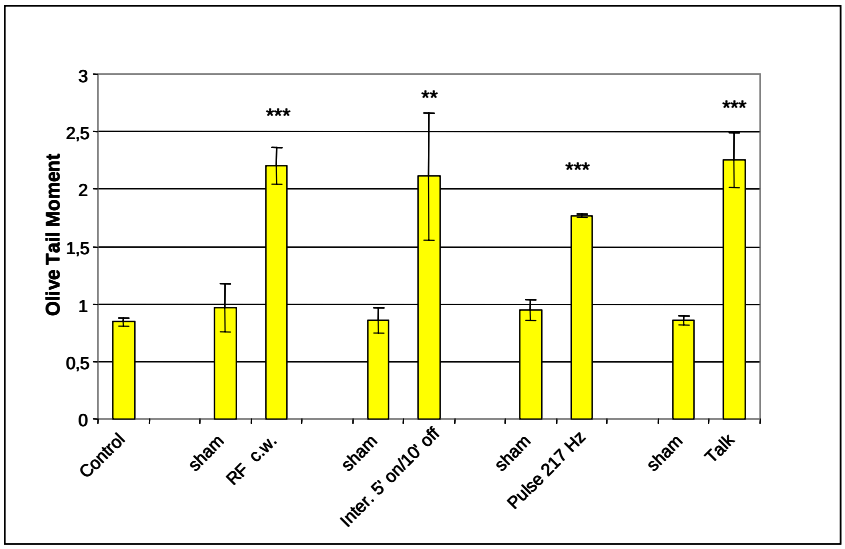

Figure 78. Comet formation in HL-60 cells after exposure to RF-fields (1800 MHz, SAR 1.3 W/kg) for different signal modulations, expressed as Olive Tail Moment, compared to control and sham exposure. Each bar represents the mean ± SD of results obtained in at least three (except continuous wave and C.W., 5 min on/10 min off: n=4) independent experiments. ** P<0.01; *** P<0.001 (Student's t-test, two-sided).

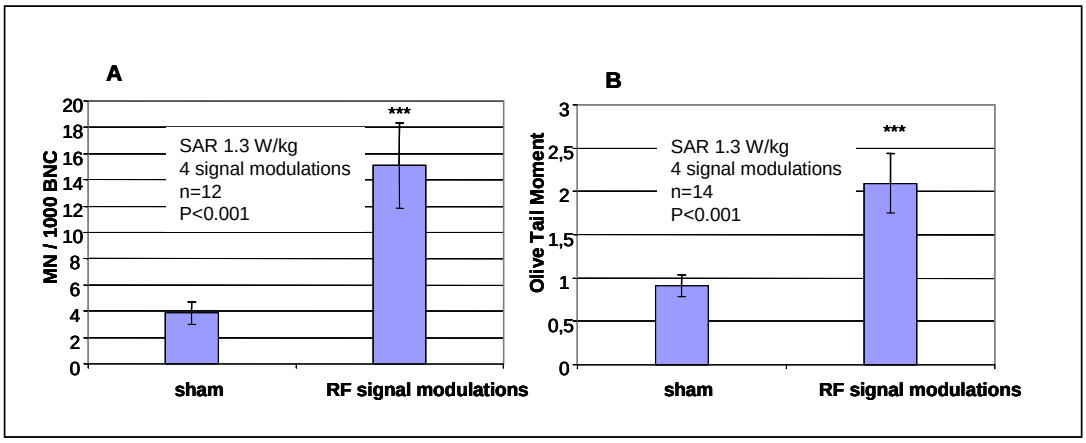

Figure 79. MN induction and Comet formation in HL-60 cells over all RF-field signal modulations at 1800 MHz, 24h, versus total sham, expressed as MN per 1000 BNC (A) and as Olive Tail Moment (B). Each bar represents the mean ± SD of results obtained in indicated number of experiments. *** P<0.001 (Student's t-test, two-sided).

As shown by flow cytometric analysis RF-EMF increased the micronuclei frequency, but did not affect cell cycle.

The results of the flow cytometric analysis of MN induction in HL-60 cells following RF-EMF exposure at the SAR level of 1.3 W/kg tested above using the continuous wave signal, according to the method of Nüsse et al. 1984, 1997, parallel the results obtained using the cytokinesis-block MN assay. Figure 80 shows a representative flow cytometric analysis of MN induction for sham-exposed (A) and RF-exposed (B) HL-60 cells after exposure to RF (1800 MHz, continuous wave, SAR 1.3 W/kg) for 24h. The DNA distribution of micronuclei (marker M1) and nuclei (marker M2) is obtained by projection of the particles defined by their side scatter intensities as micronuclei and nuclei. The percentage of MN is higher in the RF-exposed sample than in the sham-exposed sample (4.1% MN versus 2.7% MN).

The quantitative results of MN content analysis in four independent experiments are presented in Table 13. In all HL-60 cell experiments the MN content of the RF-exposed samples is higher than in sham-exposed samples. Normalisation of MN content in sham-exposed cells to 100% revealed a significant induction of MN after exposure to RF-field by 138.2 ± 18.4% ($P<0.01$; Student's t-test, two-sided). This result parallels those obtained using the microscopic analysis of MN frequencies.

Moreover, by means of flow cytometry the DNA-content of G1/G0, S and G2/M phase can be quantified by determining the fraction of each sub-population. The DNA-content distribution (ethidium bromide fluorescence) showed no differences between RF-field exposed and sham-exposed cells, indicating no influence of RF-EMF on cell cycle (Figure 80). Furthermore, cell cycle analysis demonstrated no accumulation of cells arrested in S and G2/M phase following exposure to RF fields. Additionally, for 24h RF-field exposure (1800 MHz, continuous wave, SAR 1.3 W/kg) no increase of the cell population in he sub G1 peak, which can be considered a marker of apoptotic cell death, was observed by flow cytometry.

Table 14 shows the data of DNA content distribution as percentage of gated cells for G1/G0, G2/M and S phase for RF-field exposed cells (continuous wave, SAR 1.3 W/kg, 24h), as compared to incubator control, sham-exposure and positive control hydrogen peroxide (100 µmol/l for 1 hour). The distribution of G1/G0, G2/M and S phase in the incubator control was 51.9 ± 4.2%, 18.3% ± 3.7 and 19.4 ± 1.7%; that of the positive control hydrogen peroxide: 28.4 ± 12.1%, 9.1 ± 5.2% and 9,0 ± 3.6%. Overall, the percentage of gated cells for the positive control was clearly lower than in all other conditions due to the fact, that here out of the gate analysed a high content of cellular debris was detected. This serves as a measure of cytotoxicity exerted by hydrogen peroxide. Sham-exposed and RF-exposed cells showed a similar DNA distribution as in the incubator control. No significant differences in DNA distribution of RF-exposed cells compared to sham-exposed cells were observed.

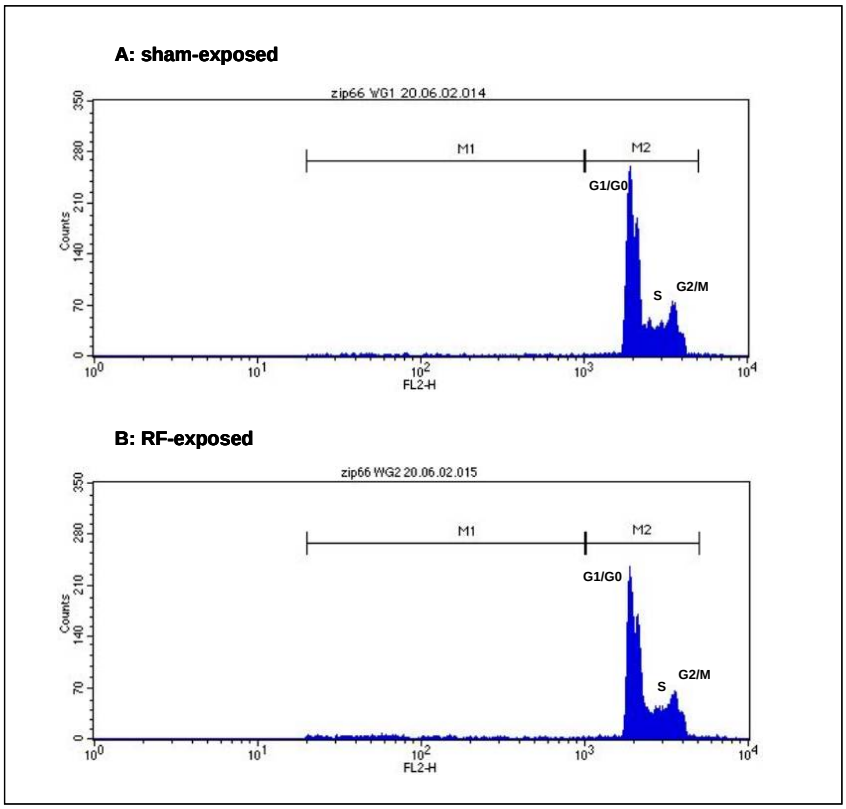

Figure 80. Flow cytometric analysis of micronuclei induction and determination of the proportions of cells in G1/G0, S and G2/M phases of the cell cycle after exposure of HL-60 cells to sham (A) or RF field (B, 1800 MHz, continuous wave, SAR 1.3 W/kg) for 24h.

The diagrams show representative ethidium bromide fluorescence histograms of micronucleated cells/nuclei suspension after treatment with FACS solution I and II. The method was performed according to Nüsse and Kramer (1984), Nüsse and Marx (1997) and Wessel and Nüsse (1995). G1/G0, S and G2/M peaks are indicated. For measurement of MN the G1/G0 peak was adjusted to approximately 2000 relative fluorescence units (FL2-H). The sort window for counting the MN comprised the relative DNA fluorescence units from 20 to 1000 (M1). For quantitative determination of MN the ratio of events in M1 (micronuclei) was compared to the events in M2 (nuclei) and expressed as % MN. For this representative experiment out of four the results for sham-exposure is 2.7% MN (A) and for RF-exposure is 4.1 % MN (B).

Table 13. Quantitative flow cytometric analysis of micronuclei frequencies after RF-field exposure (1800 MHz, continuous wave, SAR 1.3 W/kg, 24 h), compared to sham-exposure.

No. of experiment	Content of MN [%]		
	Sham-exposed	RF-field exposed	Content of MN in RF-exposed cells rel. to sham-exposed cells (100%)
1	2.69	4.08	151.67
2	5.49	6.37	116.03
3	4.24	6.57	154.95
4	1.85	2.41	130.70
mean	3.57 ± 1.62	4.86 ± 1.98	138.23 ± 18.41 **

Data of column 4 are values of RF-exposed cells in percentage relative to the corresponding sham-exposed value.
** Significant difference between the content of MN of RF-exposed cells to sham-exposed cells at P<0.01 (Student's t-test, two-sided).

Table 14. DNA distribution and cell cycle analysis of HL-60 cells after exposure to RF-field (1800 MHz, continuous wave, SAR 1.3 W/kg) for 24 h, compared to control, sham-exposure and positive control hydrogen peroxide (100 µmol/l for 1 h). Data represent DNA content distribution as percentage of gated cells in G1/G0, G2/M and S phase.

Group	n	G1/G0 [%]	S [%]	G2/M [%]
control	3	51.90 ± 4.17	18.25 ± 3.65	19.37± 1.71
sham	4	54.98 ± 6.69	19.45 ± 3.50	18.43 ± 4.07
RF-field	4	52.94 ± 6.19	19.01 ± 3.54	20.06 ± 2.73
positive control H_2O_2 (100 µmol/l for 1h)	3	28.37 ± 12.11	9.11 ± 5.17	8.96 ± 3.59

RF-EMF did not affect apoptosis as demonstrated by the Annexin V and TUNEL assay.

As the findings of structural alterations on the genomic level correlated with an external cellular stimulus do per se not prove a genotoxic effect, it has to be ruled out, that such changes are due to induction of apoptosis. Apoptotic cells typically undergo a series of structural changes: blebbing of the plasma membrane, condensation of the cytoplasm and intact organelles, and nuclear fragmentation. The most common biochemical property of apoptosis is the endonucleolytic cleavage of chromatin, initially to large fragments of 50-300 kilobase pairs and subsequently to monomers and multimers of 180-200 base pairs.

By establishing two flow cytometry methods for detection of apoptosis, Annexin V assay and TUNEL assay, a differentiation approach was included in the experimental strategy. By means of these two tests the detection of apoptotic changes at different stages in the apoptotic process became feasible. As a positive control for apoptosis induction by camptothecin, a topoisomerase I inhibitor, was used in the flow cytometry assays.

After initiation of apoptosis most cell types translocate phosphatidylserine (PS) from the inner plasma membrane leaflet to the cell surface. Once on the cell surface, PS can easily be detected by staining with a FITC conjugate of Annexin V, a protein that has strong natural affinity for phosphatidylserine. As

externalisation of phosphatidylserine occurs before nuclear changes, associated with apoptosis, take place, the Annexin V test detects apoptotic cells significantly earlier than do DNA-based assays.

Figure 81 shows a representative flow cytometric analysis of Annexin V staining following RF- (1800 MHz, 1.3 W/kg, continuous wave, 24h) and sham-exposure of HL-60 cells. As a positive control the apoptosis inducer camptothecin, a topoisomerase I inhibitor, was used to prove inducibility of apoptosis in the HL-60 cell system. The histograms show apoptosis associated Annexin V-FITC-signals (FL-1) versus DNA content propidium iodide (PI) signals. In order to prove that the gating of the corresponding cell populations for scoring the content of apoptotic cells did not select sub-populations, the histograms for “gated” and “not gated” cells are presented.

The TUNEL method (Terminal Deoxynucleotidyl Transferase Biotin-dUTP Nick End Labeling) identifies apoptotic cells *in situ* by using terminal deoxynucleotidyl transferase (TdT) to transfer FITC-dUTP to the free 3´-OH of cleaved DNA. These labelled cleavage sites can then be detected by flow cytometry.

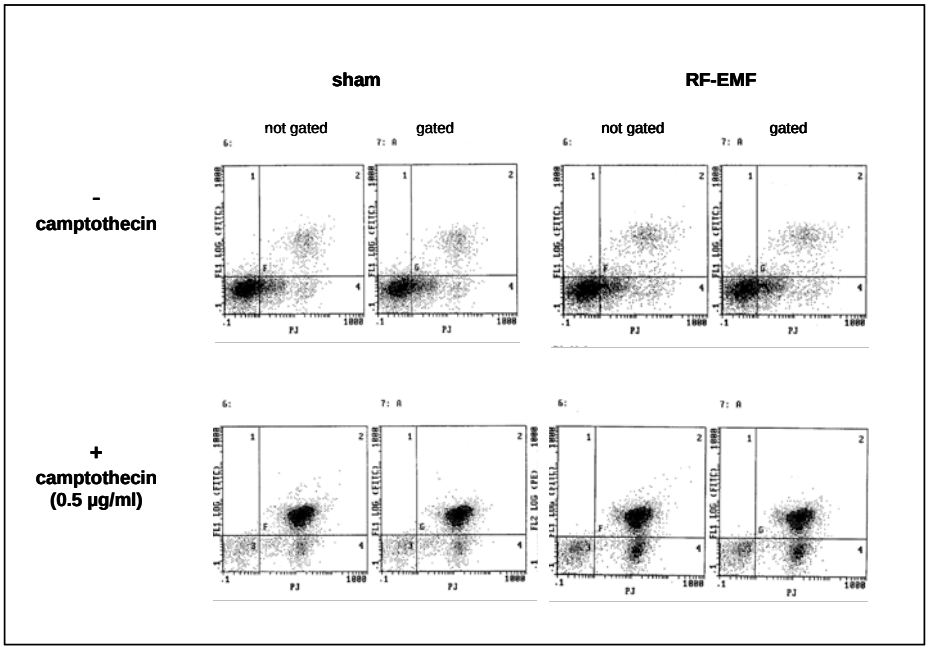

Figure 81. Flow cytometric analysis of RF- (1800 MHz, continuous wave, 1.3 W/kg, 24h) and sham-exposed HL-60 cells after staining with Annexin V-FITC (FL-1) and propidium iodide (PI, DNA content). The apoptosis inducer camptothecin is included as a positive control.

The histograms show apoptosis associated Annexin V-FITC (FL-1) versus DNA content propidium iodide (PI) signals. In order to prove that the gating of the corresponding cell populations for scoring the content of apoptotic cells did not select certain sub-populations, the histograms for “gated” and “not gated” cells are presented.

Figure 82 shows a representative flow cytometric analysis of TUNEL staining following RF-exposure (1800 MHz, , continuous wave, SAR 1.3 W/kg, 24h) and sham exposure of HL-60 cells. As a positive control the apoptosis inducer camptothecin, a topoisomerase I inhibitor, was used to prove inducibility of apoptosis in the HL-60 cell system. The histograms show apoptosis associated TUNEL-FITC-signals (FL-1) versus DNA content propidium iodide (PI) signals. In order to prove that within the quantification procedure no differences in cell population analysed occurs, histograms for “gated” and “not gated” cells are presented (Figure 82).

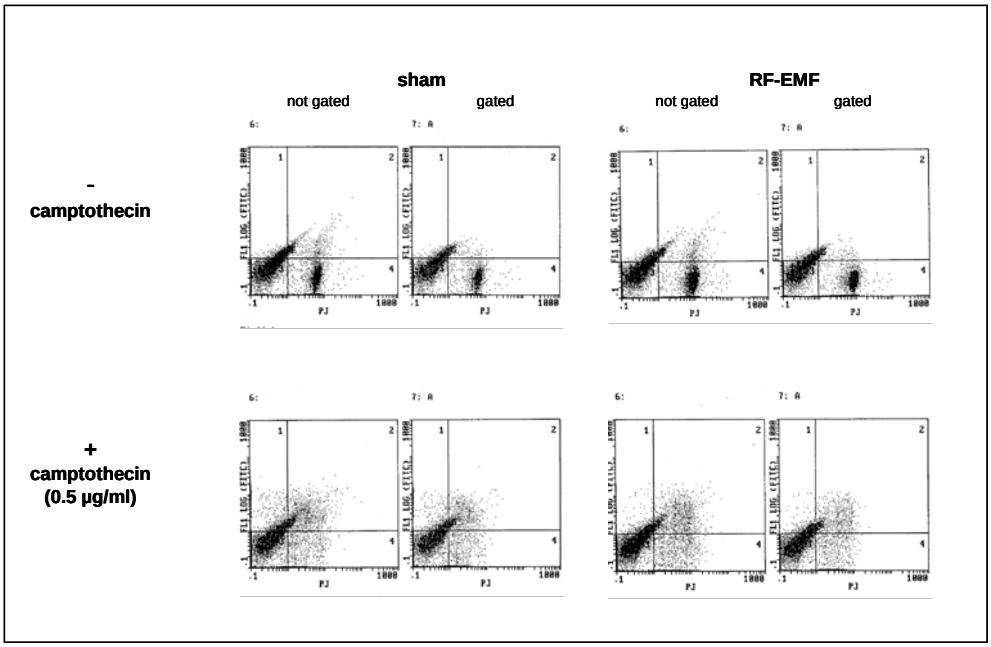

Figure 82. Flow cytometric analysis of RF- (1800 MHz, continuous wave, 1.3 W/kg, 24h) and sham-exposed HL-60 cells after labelling with TUNEL reaction mixture (Roche, Mannheim) for 1 hour at 37°C. The cells then underwent flow cytometric analysis in order to determine the number of green stains (representing apoptotic DNA fragmentation). DNA content analysis was performed on a Becton Dickinson FACScan by using the manufacturer's protocol. The apoptosis inducer camptothecin is included as a positive control.

The histograms show apoptosis associated TUNEL-FITC-signals (FL-1) versus DNA content propidium iodide (PI) signals. In order to prove that the gating of the corresponding cell populations for scoring the content of apoptotic cells did not select certain sub-populations, the histograms for “gated” and “not gated” cells are presented.

Neither by the Annexin V assay nor by the TUNEL assay, apoptosis induced by RF-electromagnetic fields (1800 MHz, continuous wave, SAR 1.3 W/kg, 24h) could be detected in HL-60 cells. Moreover, HL-60 cells exposed to RF-field at SAR 1.3 W/kg and continuous wave signal for 24h show no induction of the cell population in the sub G1 peak, which can be considered a marker of cell death by apoptosis (Figure 80).

RF-EMF did not exert a cytotoxic effect on HL-60 cells.

The trypan blue vitality test did not reveal any cytotoxic effects on the HL-60 cells from any RF-field applied. The vitality of the exposed cells was on the same order of magnitude (≈ 90%) as the cells of the sham-exposed and the incubator control. To exclude minor effects of RF-fields on viability of HL-60 cells, cell viability was examined spectrophotometrically by the MTT assay (Figure 83). Supplementary, also by this method no cytotoxic effect was detectable: absorbance A_{570nm} (RF-exposed HL-60 cells) = 0.91 ± 0.13 ; A_{570nm} (sham-exposed HL-60 cells) = 0.98 ± 0.15.

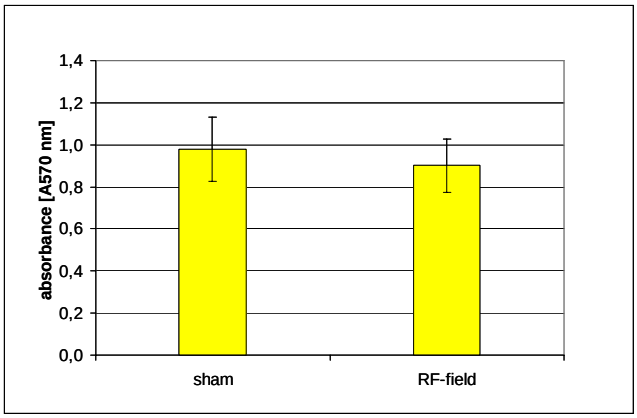

Figure 83. Viability of HL-60 cells after exposure to RF-field (1800 MHz, continuous wave, SAR 1.3 W/kg, 24h) compared to sham exposure. Cell viability was evaluated by the MTT assay and reported as absorbance at 570 nm. Bars represent means ± SD of 12 independent experiments.

In addition, the ratio of binucleated cells (BNC) against mono-, bi-, tri- and tetranucleated cells (% BNC) was determined as a measure of cell division and cell cycle progression. No effect of RF-EMF exposure on % BNC for different energies (Figure 84) or for different signal modulations (Figure 85) was found in comparison to sham-exposed or ionising-irradiated (0.5 Gy, 6 MeV, exposure time: 5.2s) HL-60 cells.

Additionally, no significant differences in DNA distribution of RF-exposed cells compared to sham-exposed cells were observed with respect to increased incidence of cellular debris as a measure of cytotoxicity (Table 14).

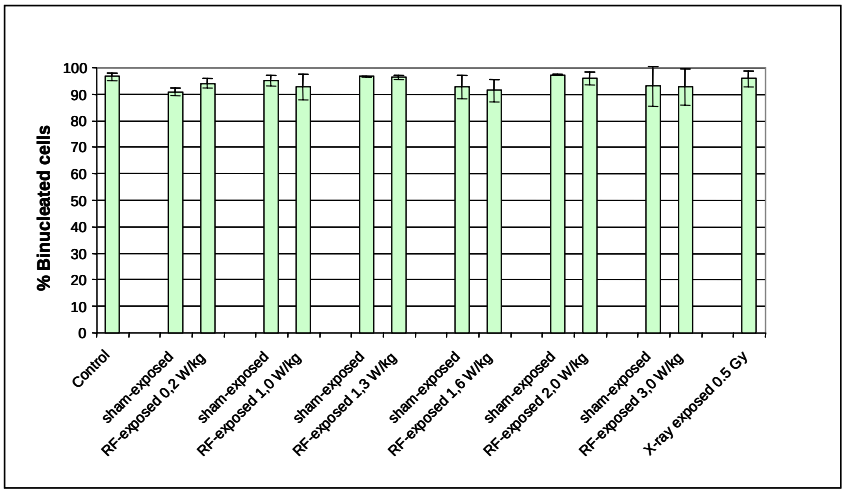

Figure 84. Effect of RF-field exposure on cell division. Shown is the number of binucleated HL-60 cells relative to the number of mono-, bi-, tri-, and tetra-nuclear cells (% BNC) following RF-field exposure (1800 MHz, continuous wave, different SAR levels, 24h). Positive control: 0.5 Gy ionising-irradiation (6 MeV, exposure time: 5.2s). Each bar represents the mean ± SD of results obtained in three independent experiments.

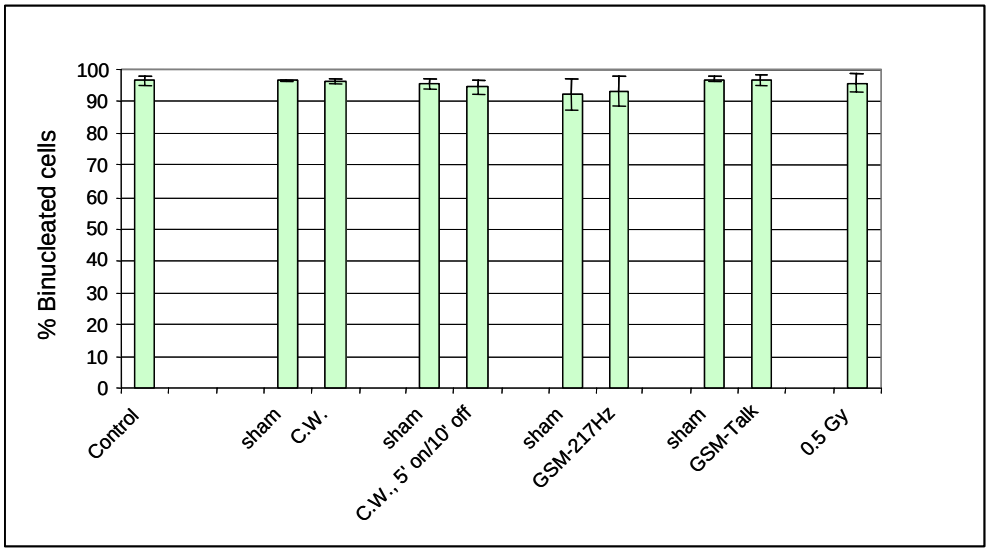

Figure 85. Effect of RF-field exposure on cell division. Shown is the number of binucleated HL-60 cells relative to the number of mono-, bi-, tri-, and tetranuclear cells (% BNC) following RF-field exposure (1800 MHz, SAR 1.3 W/kg, different signal modulations, 24h). Positive control: 0.5 Gy ionising-irradiation (6 MeV, exposure time: 5.2s). Each bar represents the mean ± SD of results obtained in three independent experiments.

Concludingly no in vitro cytotoxic effects of RF-EMF could be detected in RF-EMF-exposed and sham-exposed cells for the exposure conditions tested using either microscopic evaluation (trypan blue exclusion, % BNC), colorimetric MTT assay or flow cytometric analysis (nuclear ethidium bromide staining).

B. Indirect genotoxicity (by reactive oxygen species)

RF-EMF induced formation of reactive oxygen species as shown by flow cytometric detection of oxyDNA and rhodamine fluorescence.

It was the aim of these series of experiments to examine whether RF-EMF (1800 MHz at SAR 1.3 W/kg, 24h exposure) is capable to induce indirect genotoxic effects by affecting the generation and elimination of reactive oxygen species (ROS). For monitoring these ROS-formation and elimination steps, different assays, measuring nitric oxide, oxyDNA, oxidative DNA-damage via Dihydrorhodamine 123 (DHR123), lipid peroxidation, glutathione peroxidase activity, superoxide dismutase activity, have been established and were applied following RF-field exposure of HL-60 cells at that exposure condition with the most significant effect on DNA integrity (1800 MHz, continuous wave, 1.3 W/kg, 24h).

Nitric oxide (NOx)

Nitric oxide (NOx), was measured using the colorimetric Nitric Oxide Assay Kit, Calbiochem, Bad Soden, Germany. The data in Table 15 show the NOx production from HL-60 cells after exposure to RF-field (1800 MHz, continuous wave, SAR 1.3 W/kg, 24h), compared to control and sham-exposed cells. For an amount of 0.25 x 10^5 cells, in neither treatment group the detection limit of 1 µmol NOx/l was exceeded. The results presented are the means of three independent experiments. Concludingly, with this assay no in vitro effect of RF-field exposure on NOx formation was detected for the exposure conditions tested.

Table 15. NO_x formation in HL-60 cells after exposure to RF-field (1800 MHz, continuous wave, SAR 1.3 W/kg, 24h), compared to control and sham-exposure.

Group	NOx [µmol/l]
control	< 1
sham	< 1
RF-field	< 1

0.75×10^6 viable HL-60 cells/3 ml cell culture medium were cultivated for 24h at 37°C. After centrifugation, aliquots of culture media corresponding to 0.25×10^5 cells were collected and analysed for nitric oxide (NOx) by the colorimetric Nitric Oxide Assay Kit, Calbiochem, Bad Soden, Germany.
The results presented are representative for three independent experiments.

Flow cytometric detection of oxidative DNA damage (oxy-DNA)

The presence of oxidised DNA (by a fluorescent probe, directly binding to 8-oxoguanine as the major oxidative DNA product) was indicated by a green/yellow fluorescence that could be detected using a flow cytometry system. In Figure 86 a partial augmentation (occurring as a shoulder on the right side of the signal, see arrow Figure 86 of FL-1 fluorescence intensity), indicating the presence of oxidised DNA, was observed for the RF-exposed signal (green) in contrast to sham-exposed signal (blue). Additionally, RF-exposed cells showed a significant shift to the left as compared to sham-exposed cells. Table 16 shows the data for the quantification of ROS levels using oxyDNA-FITC conjugate to stain 8-oxoGuanosine residues on oxidatively damaged DNA of HL-60 cells. RF-field exposure of HL-60 cells induced a mean increase of oxidative DNA damage of 21.7 ± 2.0 %.

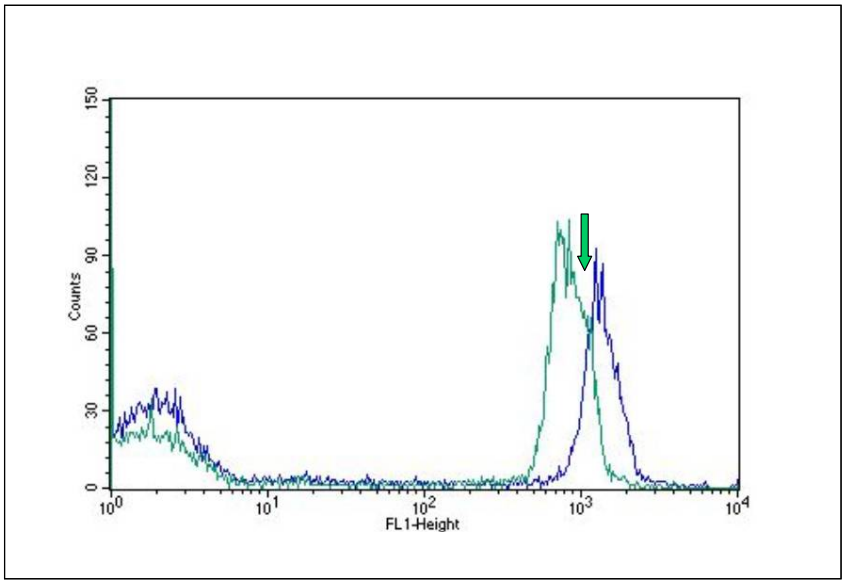

Figure 86. Flow cytometric detection of ROS levels using oxyDNA-FITC conjugate to stain 8-oxoGuo residues on oxidatively damaged DNA of HL-60 cells. The diagram shows the signal of oxidatively damaged DNA of RF-field exposed cells (green line) compared to sham-exposed cells (blue line). One representative histogram plot out of four independent experiments is shown. A partial augmentation (shoulder at the right side of the signal, indicated by arrow) of FL-1 fluorescence intensity was observed for the RF-exposed signal in contrast to sham-exposed signal.

Table 16. Quantification of ROS levels of HL-60 cells after exposure to RF-field (1800 MHz, continuous wave, SAR 1.3 W/kg) for 24h using oxyDNA-FITC conjugate to stain 8-oxoGuo residues on oxidatively damaged DNA.

No. of experiment	% augmentation of fluorescence signal of RF-field exposed cells (area under curve AUC of shoulder at the right side of the signal)
1	21.38
2	24.44
3	19.80
4	20.98
mean ± SD	21.65 ± 2.0

0.75×10^6 HL-60 cells/dish were sham- or RF-field exposed for 24 h. oxyDNA-FITC was used to stain 8-oxoGuo residues on oxidatively damaged DNA using the oxyDNA assay from Calbiochem-Novabiochem GmbH, Bad Soden, Germany. Oxidatively damaged DNA was quantified by determination of the area under the curve (AUC) of the shoulder at the right side of the signal fluorescence intensity (see arrow Figure 83) in RF-field exposed cells * Significant difference between the median of fluorescence intensity of RF-field exposed cells and sham-exposed cells at $P<0.05$ (n=4, Student's t-test, two-sided).

Oxidative DNA damage measured by DHR123 and flow cytometry

Cellular production of ROS was determined by measuring the rhodamine fluorescence of HL-60 cells, incubated in growth medium containing 5 µmol/l dihydrorhodamine 123 (DHR123) for 24h at 37°C. DHR123 is a non-fluorescent reduced Rhodamine 123 (Rh123) derivative that is freely permeable through cell membranes. Intracellular oxidation converts DHR123 to the fluorescent Rh123, which is retained intracellularly by the mitochondrial potential.

Figure 87 displays the overlay fluorescence histograms for RF-field exposed cells (1800 MHz, continuous wave, SAR 1.3 W/kg), compared to sham-exposed cells after simultaneous incubation with DHR123 for 24h. The figure shows that, in RF-field exposed cells, the fluorescence intensity signal shifts to the right in comparison to the signal of sham-exposed cells. In contrast, treating cells with 100 µmol/l H_2O_2 resulted in an even more pronounced shift of fluorescence signal. These shifts indicate enhanced fluorescence intensities and thereby increased production of intracellular ROS during RF-field exposure or H_2O_2 treatment of HL-60 cells.

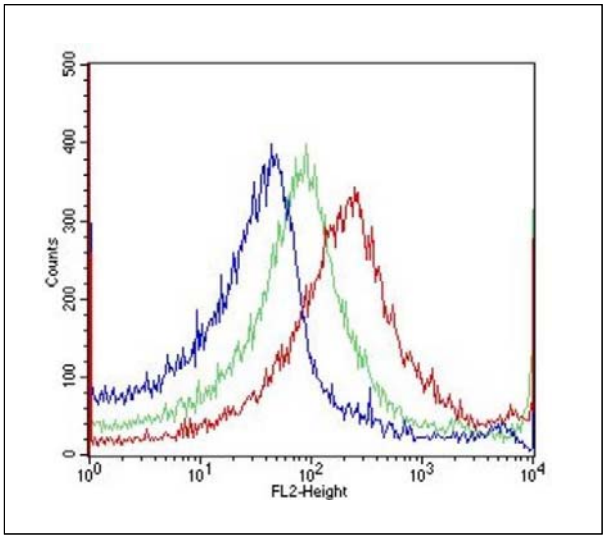

Figure 87. Fluorescence histograms for RF-field exposed (1800 MHz, continuous wave, SAR 1.3 W/kg, 24h) and sham-exposed HL-60 cells simultaneous treated with 5 µmol/l dihydrorhodamine 123 (DHR123). Blue line represents sham-exposed sample, green line represents RF-field exposed sample and red line represents H_2O_2-treated positive control (100 µmol/l for 1 hour). DHR123 reacts with intracellular ROS to form fluorescent Rh123, which is then retained by the mitochondria, enabling a flow cytometric assessment of cellular oxidant production.

By means of the DHR123 flow cytometry detection assay the shift of the signal can be quantified by determining the medians of the fluorescence intensities and the increase in rhodamine fluorescence for each population compared to sham, expressed in percent (Table 17). The data show that there is no difference in the level of oxidatively damaged DNA for control cells and sham-exposed HL-60 cells, expressed as the median of fluorescence intensity. The median values for control cells were 41.8 ± 5.8 and for sham-exposed cells 39.9 ± 8.5 (n=3). The values for the positive control (H_2O_2, 100 µmol/l, 1h) were 230.6 ± 100.3. In contrast, exposing cells to RF-fields resulted in a significant increase in median (75.5 ± 19.2; P<0.05, n=3). The percentage increase of rhodamine fluorescence for RF-field exposed cells compared to sham-exposed cells is 17.8 ± 9.7%, that of H_2O_2-treated cells 31.9 ± 12.4% (Table17).

Table 17. Detection and quantification of ROS levels with Dihydrorhodamine 123 after exposure to RF-field (1800 MHz, continuous wave, SAR 1.3 W/kg, 24 h), compared to control, sham-exposed and H_2O_2-treated HL-60 cells. For quantitative measurement the shift in median and the increase of fluorescence intensity was evaluated.

No. of exp.	Median of fluorescence intensity [units]				% increase of rhodamine 123 fluorescence relative to sham-exposure [a]	
	control	sham-exposed	RF-field exposed	H_2O_2-treated	RF-field exposed	H_2O_2-treated
1	39.95	30.51	95.60	149,89	28.98	43.12
2	37.18	42.17	57.26	199.02	12.35	18.53
3	48.26	46.98	73.65	342.89	11.97	33.91
mean	41.8 ± 5.8	39.9 ± 8.5	75.5 ± 19.2 *	230.6 ± 100.3	17.8 ± 9.7	31.9 ± 12.4

[a] differences of rhodamine 123 fluorescence (AUC, area under curve) of cells exposed to RF-field or those treated with H_2O_2 was determined and the values were plotted as percentage increase relative to sham-exposure.
* Significant difference between the median of RF-exposed cells to the median of sham-exposed cells and the median of RF-exposed cells to that of control cells at P<0.05 (Student's t-test, two-sided).

Lipid peroxidation

Lipid peroxidation was measured using the colorimetric Lipid Peroxidation Assay Kit, Calbiochem, Bad Soden, Germany. Malondialdehyde (MDA) and 4-hydroxy-2(E)-nonenal (4-HNE), products of lipid peroxidation, were estimated spectrophotometrically at 586 nm after reaction with a chromogenic reagent at 45°C. The absorbance values obtained for the samples were compared with a standard curve of known concentrations of MDA / 4-HNE (1 - 20 µmol/l). For MDA and 4-HNE the amounts of lipid peroxidation markers in all experiments and samples were below 1 µmol/l. Table 18 shows that there is no difference in the level of lipid peroxidaton for RF-field exposed HL-60 cells, compared to control and sham-exposed cells (n=3).

Table 18. Lipid peroxidation (LPO) in HL-60 cell homogenates after exposure to RF-field (1800 MHz, continuous wave, SAR 1.3 W/kg, 24h), compared to control and sham-exposed cells.

Group	amount of (MDA + HNE) [µmol/l]		
	exp. 1	exp. 2	exp. 3
control	< 1.0	< 1.0	< 1.0
sham	< 1.0	< 1.0	< 1.0
RF-field	< 1.0	< 1.0	< 1.0

Lipid peroxidation was measured using the colorimetric Lipid Peroxidation Assay Kit from Calbiochem, Bad Soden, Germany. Malondialdehyde (MDA) and 4-hydroxy-2(E)-nonenal (4-HNE), products of lipid peroxidation, were estimated spectrophotometrically at 586 nm in an aliquot corresponding to 6 x 10^5 cells after reaction with a chromogenic reagent at 45°C. The results presented are means of three independent experiments.

Antioxidant enzyme activities

RF-EMF did not affect antioxidant enzyme activities of HL-60 cells (SOD and GPx activity).

To screen the possible effect of RF-EMF on endogenous antioxidant enzyme activity, the activities of superoxide dismutase (SOD) and glutathione peroxidase (GPX) were determined in the HL-60 cells that were exposed to RF-fields (1800 MHz), continuous wave, SAR 1.3 W/kg for 24h. Positive controls as indicated in the assays by the manufacturer were included in the analysis.

Superoxide dismutase (SOD) activity

Superoxide dismutase (SOD) activity of cell homogenates was determined using the Superoxide Dismutase Assay Kit from Calbiochem, Bad Soden, Germany. The data in Table 19 show SOD activities in HL-60 cells after exposure to RF-field (1800 MHz, continuous wave, SAR 1.3 W/kg, 24h), compared to control and sham-exposed cells. For an amount of 4 x 10^5 cells, in neither treatment group the detection limit of 0.2 U/ml SOD activity was exceeded. The results presented are means of two independent experiments. Concludingly, no in vitro effect of RF-field exposure on SOD activity was detected for the exposure conditions tested.

Table 19. Superoxide dismutase (SOD) activity in HL-60 cell homogenates after exposure to RF-field (1800 MHz, continuous wave, SAR 1.3 W/kg, 24h), compared to control and sham-exposed cells.

Group	SOD_{525} activity [U/ml]	
	exp. 1	exp. 2
control	< 0.2	< 0.2
sham	< 0.2	< 0.2
RF-field	< 0.2	< 0.2

Superoxide dismutase (SOD) activity of cell homogenates was determined using the Superoxide Dismutase Assay Kit from Calbiochem, Bad Soden, Germany. The SOD-mediated increase in the rate of autooxidation of the reaction mixture was utilized to yield a chromophore with maximum absorbance at 525 nm. SOD activity was measured in an aliquot corresponding 4 x 10^5 cells (n=2). Detection limit for SOD activity is 0.2 U/ml.

Glutathione peroxidase (GPx) activity

Glutathione peroxidase (GPx) activity of cell homogenates was determined using a cellular Glutathione Peroxidase Assay Kit, Calbiochem, Bad Soden, Germany. The data in Table 20 show the GPx activity in HL-60 cells after exposure to RF-field (1800 MHz, continuous wave, SAR 1.3 W/kg, 24h), compared to control and sham-exposed cells. For an amount of 1 x 10^6 cells, in neither treatment group the detection limit of 5.6 mU/ml GPx activity was exceeded. The results presented represent two independent experiments. Concludingly, no in vitro effect of RF-field exposure on GPx activity was detected for the exposure conditions tested.

Table 20. Glutathione peroxidase (GPx) activity in HL-60 cell homogenates after exposure to RF-field (1800 MHz, continuous wave, SAR 1.3 W/kg, 24h), compared to control and sham-exposed cells.

Group	GPx activity [mU / ml]	
	exp. 1	exp. 2
control	< 5.6	< 5.6
sham	< 5.6	< 5.6
RF-field	< 5.6	< 5.6

Glutathione peroxidase (GPx) activity of cell homogenates was determined in two independent experiments using the cellular Glutathione Peroxidase Assay Kit from Calbiochem, Bad Soden, Germany.
Cell homogenisate of 1 x 10^6 cells is added to a 1050 µl of a solution containing glutathione (GSH, 1mmol/l), GSH reductase (0.4 U/ml) and NADPH. The reaction is initiated by the addition of 350 µl of the diluted organic peroxide t-butyl hydroperoxide and the absorbance at 340 nm was recorded over a period of 5 minutes. The rate of decrease in the absorbance is directly proportional to the GPx activity in the cell homogenisate. Detection limit for GPx activity is 5.6 mU/ml.

Summarising, the endogenous antioxidant enzyme activities of HL-60 cells (SOD and GPx activity) were not altered by RF-field exposure compared to sham-exposure using the conditions of the assays described above. This screening approach revealed, that the analysis of antioxidant enzyme activities does not show enough methodological sensitivity for the amounts of ROS to be generated by RF-field exposure of HL-60 cells.

Indirect genotoxicity by modulation of cellular toxifying and detoxifying capacities

The generation of genotoxic effects through RF-EMF was inhibited by ascorbic acid.

In a further series of experiments it was examined, whether ascorbic acid as a free radical scavenger and inhibitor of reactive oxygen species is capable to inhibit MN induction and DNA damage by co-administration to RF-field-exposure (continuous wave, SAR 1.3 W/kg, 24h). The inhibition of micronuclei induction and Comet formation was measured by use of the cytokinesis-block in vitro Micronucleus assay and the Comet assay. In both tests systems, ascorbic acid effectively reduced the RF-field induction of micronuclei and DNA damage (Figures 85 and 86).

Figure 88 displays the inhibition of MN induction induced by RF-fields (continuous wave, SAR 1.3 W/kg, 24h) and simultaneous treatment of cells with ascorbic acid (AA, 10 µmol/l) for 24h. MN frequencies for sham-exposed and RF-field exposed cells were 4.1 ± 0.2 and 11.6 ± 1.9 expressed as MN / 1000 BNC. After co-incubation of sham-exposed and RF-exposed HL-60 cells with ascorbic acid (AA, 10 µmol/l) for 24h the frequencies were 4.3 ± 0.4 and 4.8 ± 1.9. The MN frequency for the incubator control was 3.4 ± 0.4. Data show, that ascorbic acid inhibits RF-field associated MN induction significantly (n=3, P<0.05). The inhibition resulted in an induction by factor 1.08 compared to sham.

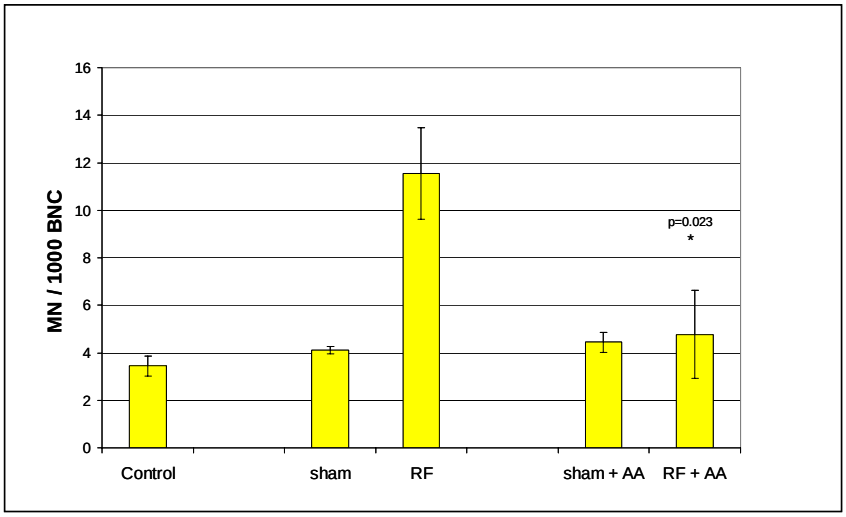

Figure 88. Effect of ascorbic acid (AA, 10 µmol/l) on RF-field (1800 MHz, continuous wave, SAR 1.3 W/kg, 24h) induced MN frequencies in HL-60 cells, compared to control and sham-exposed cells. Each bar represents the mean ± SD of results obtained in at least three independent experiments. Significant differences between RF-field exposure and sham-exposure with co-administration of AA is given by * P<0.05 (Student's t-test, two-sided).

Figure 89 displays the inhibition of DNA damage induced by RF-fields (continuous wave, SAR 1.3 W/kg, 24h) and simultaneous treatment of cells with ascorbic acid (AA, 10 µmol/l) for 24h. The values of Olive Tail Moment for sham-exposed and RF-field exposed cells were 0.9 ± 0.1 and 2.0 ± 0.2. After co-incubation of sham-exposed and RF-field exposed HL-60 cells with ascorbic acid (AA, 10 µmol/l) for 24h the values were 1.0 ± 0.1 and 1.2 ± 0.03. The OTM for the incubator control was 0.8 ± 0.05. Data show, that ascorbic acid inhibits the RF-field induced DNA damage significantly (n=3, P<0.01). The inhibition resulted in an induction by factor 1.2 compared to sham. Additionally, no induction of cytotoxicity (trypan blue test), no alteration of cell medium pH value and no influence on cell growth or cell cycle progression was observed for ascorbic acid alone and for co-administration of ascorbic acid together with RF-field exposure over 24h.

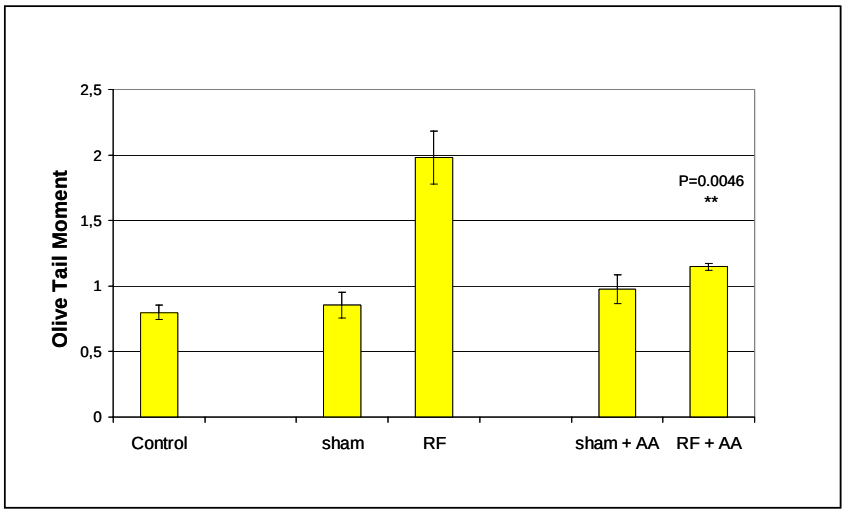

Figure 89. Effect of ascorbic acid (AA, 10 µmol/l) on RF-field induced Comet formation in HL-60 cells (1800 MHz, continuous wave, SAR 1.3 W/kg, 24 h), compared to control and sham-exposed cells. Each bar represents the mean ± SD of results obtained in at least three independent experiments. Significant differences between RF-field exposure and sham-exposure with co-administration of AA is given by ** P<0.01 (Student's t-test, two-sided).

Concludingly, this observed inhibition of genotoxicity by ascorbic acid supports the hypothesis that the effect of RF-field on genomic integrity may be explained by the generation of free oxygen radicals.

3.2.1.2 Human fibroblasts and granulosa cells of rats (Participant 3)

RF-EMF generated DNA strand breaks in human fibroblasts and in granulosa cells of rats.

The influence of RF-EMF exposure on the generation of DNA strand breaks in cells of two different tissues (human fibroblasts, rat granulosa cells) was evaluated using alkaline and neutral Comet assay. Four different sets of exposure conditions were tested: continuous (1800 MHz, 2 W/kg), intermittent (5 min on/10 min off, 1800 MHz, 2 W/kg), pulse modulation (1800 MHz, 2 W/kg, amplitude 217 Hz, 5 min on/10 min off) and talk modulation (1800 MHz, 1.2 W/kg, DTX 66%, GSM basic 34%, continuous). Different exposure duration was applied (4, 16 and 24 hours).

An elevation of Comet assay levels in exposed cells compared to sham-exposed controls could be detected in each of these experiments, even at continuous exposure (Figure 90). This elevation became significant at 16 hours of exposure, but no significant differences between 16 and 24 hours could be detected. At intermittent, pulse modulation and talk modulation Comet assay levels were significantly higher than at continuous exposure. Human fibroblasts and granulosa cells responded equally to RF-EMF, albeit the latter exhibited higher basal and higher end levels (Figure 91). The Comet factors with neutral Comet assay were similar, albeit lower (Figures 92, 93). Dose response investigations with human fibroblasts, which were exposed intermittently (5 min on/10 min off) for 24 hours, revealed a dose dependent increase of the Comet tailfactor beginning already at a SAR of 0.3 W/kg with a peak level at 1.0 W/kg (Figure 94).

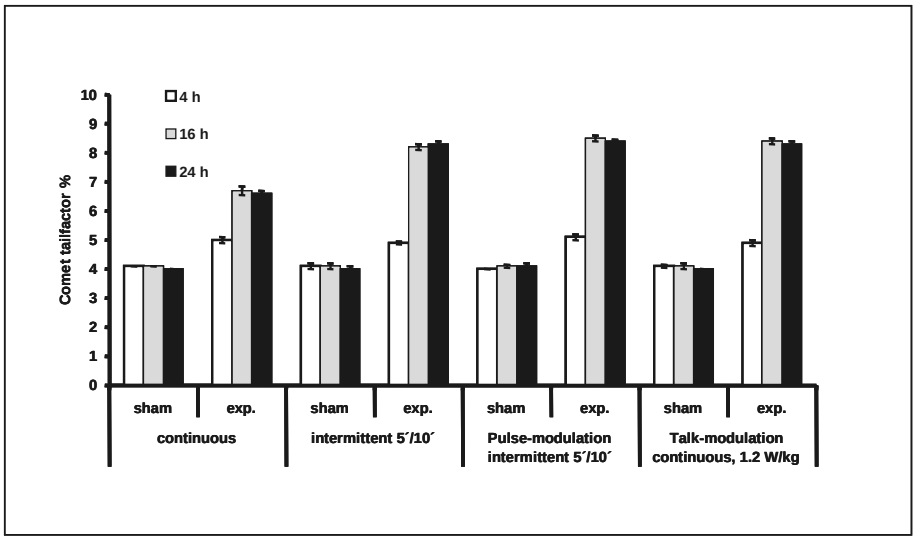

Figure 90. Influence of exposure time and of different exposure conditions on formation of DNA single and double strand breaks in human fibroblasts determined with Comet assay under alkaline conditions (cell strain ES 1, 1800 MHz, SAR 2 W/kg).

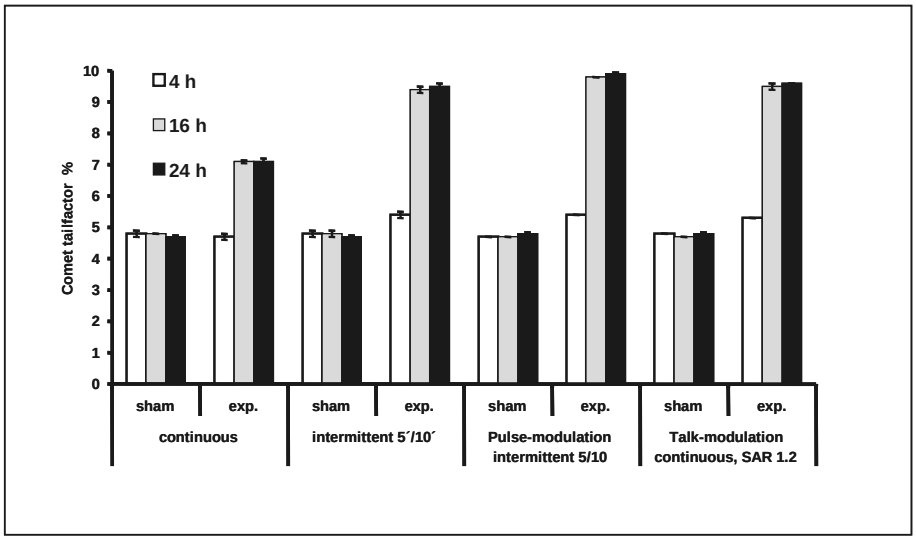

Figure 91. Influence of exposure time and of different exposure conditions on formation of DNA single and double strand breaks in granulosa cells determined with Comet assay under alkaline conditions.

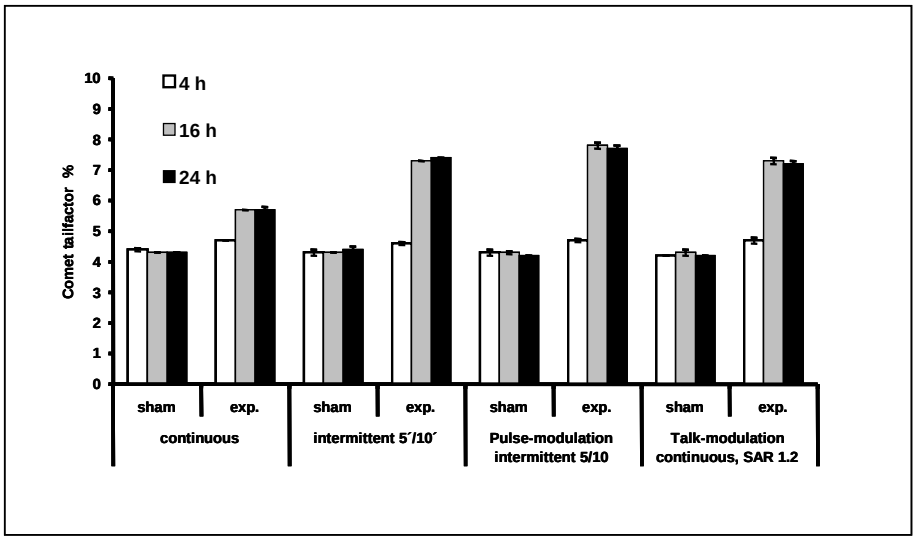

Figure 92. Influence of exposure time and of different exposure conditions on formation of DNA double strand breaks in human fibroblasts determined with Comet assay under neutral conditions (cell strain ES 1, 1800 MHz, SAR 2 W/kg).

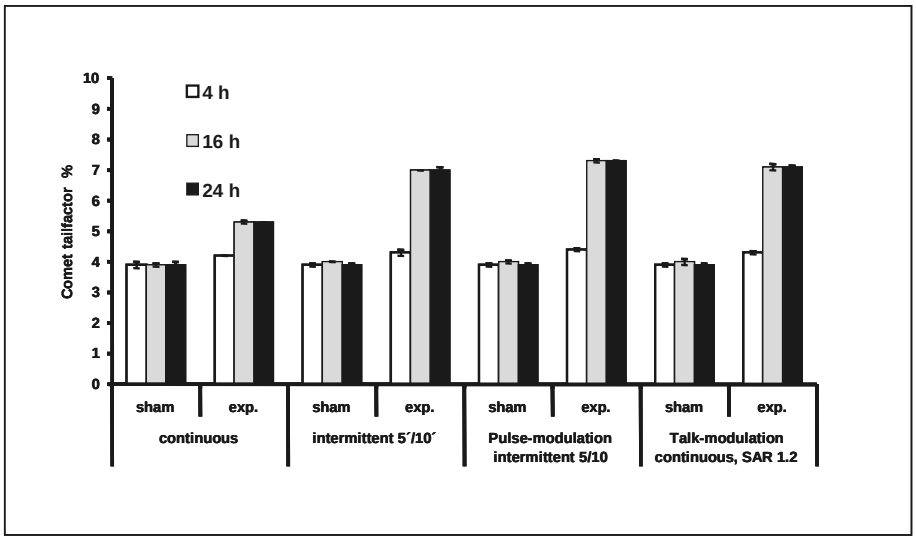

Figure 93. Influence of exposure time and of different exposure conditions on formation of DNA double strand breaks in granulosa cells determined with Comet assay under neutral conditions (1800 MHz, SAR 2 W/kg).

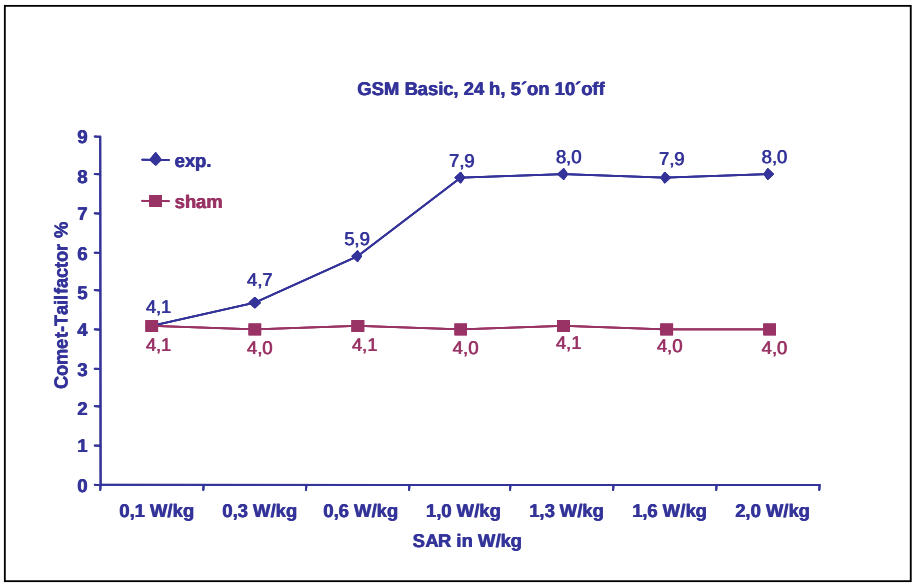

Figure 94. Dose dependent increase of DNA single and double strand breaks in human fibroblasts determined with the Comet assay under alkaline conditions

RF-EMF generated chromosomal aberrations in human fibroblasts.

Since we could demonstrate an induction of DNA strand breaks in human fibroblasts after RF-EMF exposure and due to the results of chromosome aberrations upon ELF-EMF exposure, we also evaluated the chromosome aberrations after RF-EMF exposure (GSM basic 1950 MHz, 1 W/kg, 5 min on/10 min off, 15 hours). These preliminary experiments (500 metaphases scored) revealed in RF-EMF exposed fibroblasts a 10-fold increase in chromosome gaps, a 4-fold increase in chromosome breaks and very high incidences of dicentrics and acentric fragments (Table 21).

Table 21. Percentage of chromosomal aberrations induced by RF-EMF exposure (GSM basic 1950 MHz, 1 W/kg, 5 min on/10 min off, 15h) in cultured human fibroblasts[a]

types of aberration	RF-exposed (% ± SD)	sham-exposed (% ± SD)	p-value[b]
chromosome gaps	57.5 ± 2.1 %	4.8 ± 1.6 %	< 0.001
chromosome breaks	8.1 ± 0.7 %	1.7 ± 0.1 %	< 0.001
dicentric chromosomes	4.5 ± 0.7 %	---	
acentric fragments	1.5 ± 0.7 %	---	

[a] a number of 1,000 metaphases were scored in each of five independent experiments. Results are expressed as percentage chromosomal aberrations per cell.
[b] Significant differences (p<0.05) as compared to sham-exposed controls using Student's t-test for independent samples

RF-EMF induced micronuclei in human fibroblasts.

Cultured human fibroblasts were exposed to RF-EMF (GSM basic 1950 MHz, 15h, 2 W/kg) and micronuclei frequencies were evaluated. These results showed an induction of micronuclei in RF-EMF exposed fibroblasts (Figure 95a). The observed increase in micronucleus frequencies was about 20-fold compared to sham exposed cells or non-exposed controls, but not as high as in bleomycin (10 µg/ml, 17h) treated cells, which were used as positive controls.

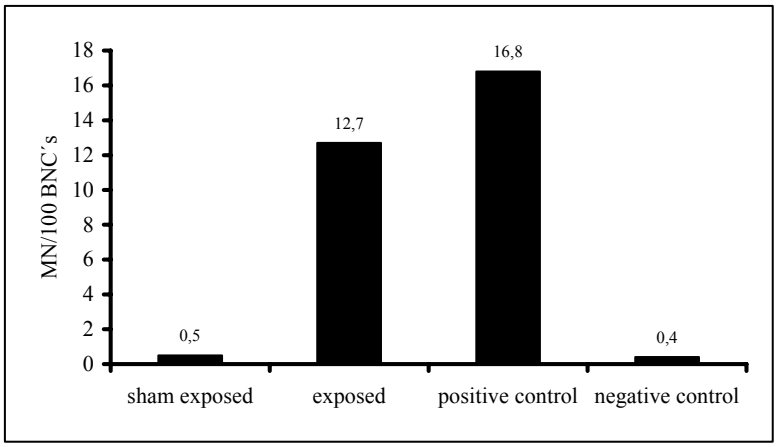

Figure 95. Micronucleus frequencies of RF-EMF exposed (GSM basic 1950 MHz, 15h, 2 W/kg) cultured human fibroblasts and control cells. Bleomycin-treated cell were used as a positive control.

Results on the influence of RF-EMF on the mitochondrial membrane potential were inconsistent.

Evaluating changes in the mitochondrial membrane potential after RF-EMF exposure (GSM basic 1950 MHz, 1 W/kg, 5 min on/10 min off, 15h) using JC-1, revealed a significant decrease in the mitochondrial membrane potential in one experiment, which could not be reproduced..

3.2.1.3 Mouse embryonic stem cells (Participant 4)

RF-EMF affected double-strand DNA break induction in ES cell derived neural progenitors immediately after exposure.

We studied the possible effects of RF-EMF on the integrity of DNA strands in differentiating ES cell from EB outgrowths. Two schemes were applied: (1) For RF-EMF exposure (GSM signal 217-Hz, 1.71 GHz, 1.5 W/kg, intermittency 5 min on/30 min off, 6h), the percentage of primary DNA damage was measured in the alkaline and neutral Comet assay immediately after the RF-EMF exposure at the stage of neural differentiation (4+4d - 4+6d) and 18 hours after the RF-EMF exposure. No differences in the induction of single-strand breaks as measured by the alkaline Comet assay were observed 0 and 18 hours after exposure. The tailfactor was slightly, but significantly increased in the neutral Comet assay immediately after exposure ($p<0.05$) (Table 26). In the second set of experiments, the same RF-EMF exposure conditions were applied for 48 hours instead of 6 hours, and the alkaline Comet assay was done immediately after exposure, while the neutral Comet assay was done 24 or 48 hours post exposure. However, no significant differences were observed in the induction of single- or-double DNA strand breaks between sham-exposed or EMF exposed neural progenitors after prolonged exposure (48h).

3.2.1.4 Summary (Participant 1)

Our data indicate a genotoxic action of RF-EMF in various cell systems. This conclusion is based on the following findings:

- RF-EMF exposure was able to induce DNA single and double strand breaks as well as an increase in micronuclei in HL-60 cells (3.2.1.1).
- The DNA damage generated by RF-EMF in HL-60 cells was dependent on the time of exposure, the field strength and the type of RF-EMF signals (3.2.1.1).
- The DNA damage in HL-60 cells probably resulted from an increase in free oxygen radicals induced during RF-EMF exposure (3.2.1.1).
- RF-EMF exposure at a SAR value between 0,3 and 2,0 W/kg produced DNA single and double strand breaks in human fibroblasts and in granulosa cells of rats dependent on the exposure time and the type of signals (3.2.1.2).

- RF-EMF exposure at a SAR value of 2 W/kg caused an increase in chromosomal aberrations in human fibroblasts demonstrating that the DNA repair was not error-free (3.2.1.2).
- RF-EMF exposure at a SAR value of 1,5 W/kg caused a slight, but significant increase in DNA double strand breaks in neural progenitor cells stemming from mouse embryonic stem cells (3.2.1.3).

3.2.2 Cell proliferation and cell differentiation

3.2.2.1 Human neuroblastoma cell line NB69 and neural stem cells (NSC) (Participant 5)

RF-EMF did not affect growth or viability of NB69 neuroblastoma cells and neural stem cells (NSC).

NB69 cells were exposed at day 3 postplating to GSM-Basic over a 24-hour period. After exposure, the cells were left to grow in the absence of field for an additional 24 hour lapse (5 days postplating). The field exposure was applied alone or in combination with bFGF. As it is shown in Figure 96, the GSM-Basic signal alone did not affect significantly cell growth or cell viability. The morphological analysis did not show significant differences between exposed and control groups, either (data not shown). The treatment with bFGF alone induces differentiation in NB69 cells, which exhibit significant increases in the number and the extension of processes per cell and in the cell size (see 3.2.4.2). An equivalent response was obtained after exposure to the combined treatment with bFGF plus GSM-Basic.

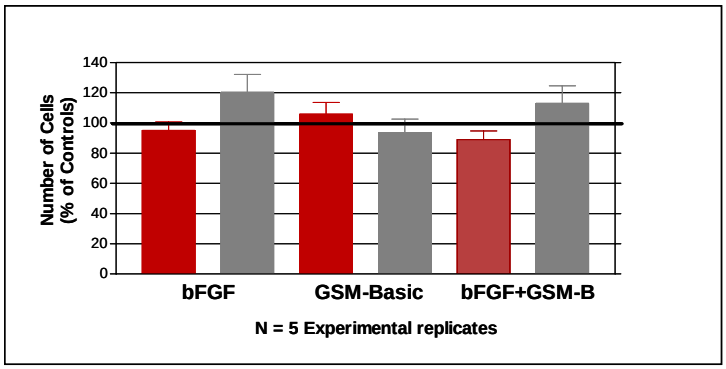

Figure 96. Number of living (red) and dead (grey) cells after a 24-h exposure to GSM-Basic signal followed by 24 additional hours of incubation in the absence of the RF-EMF. No significant changes were observed in the exposed samples when compared to the respective controls

NS cells were exposed at day 2 postplating to GSM-Basic over a 24-hour period. After exposure, the cells were left to grow in the absence of field for an additional 48-hour lapse (5 days postplating). At the end of this period, the samples were studied for cell growth and/or cell viability. The treatment did not affect cell growth (Figure 97A) and did not induce significant changes in the cells' morphology (data not shown). However, the cell size in the exposed samples was observed to be slightly, but not significantly augmented when compared to the respective controls (Figure 97B; image analysis of 60 microscope fields per condition of a total of 4 experimental replicates). The observed, slight reductions in the percent of dead cells, and in the increase of the cells' size after exposure to the GSM-Basic signal (Figure 97) could be due to an enhancement of the cell attachment to the substrate in the exposed samples. Such an attachment was microscope observed, though not image-analysis quantified (data not shown).

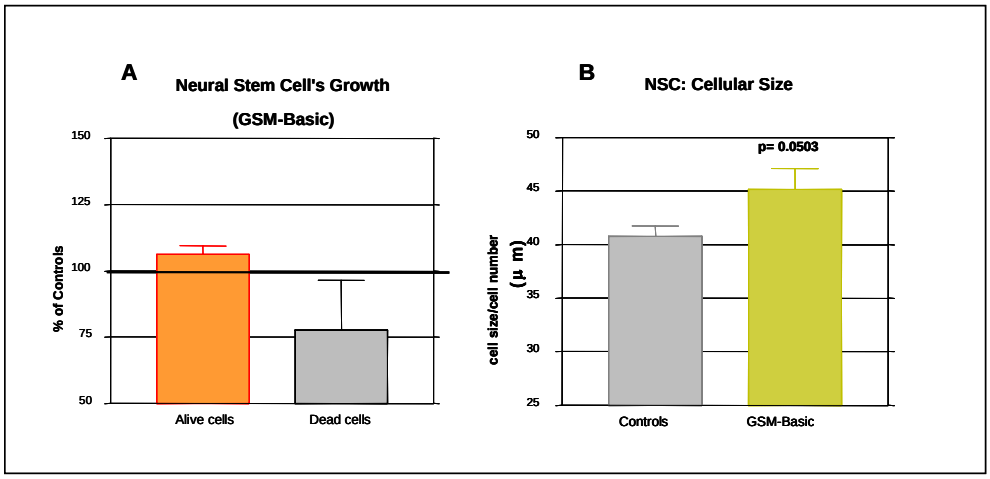

Figure 97. (A) Number of living and dead cells after a 21-h exposure to GSM-Basic signal followed by 48 additional hours of incubation in the absence of RF-EMF (5 days postplating). No significant changes were observed, even though a small reduction of dead cells occurs in the exposed samples. (B) The cell size in the exposed samples was observed to be slightly, but not significantly augmented when compared to the respective controls.

RF-EMF may affect the expression of FGF receptors in NB69 human neuroblastoma cells and in neural stem, potentially influencing cellular differentiation.

See 3.2.4.2

RF-EMF affected the differentiation of neural stem cells (NSC), but not of neuroblastoma cells (NB69).

The aim of the study was to determine whether the exposure of neural stem cells (NSC) to GSM-1800 signals (GSM-Basic signal, 21-hours, 5 min on/10 min off) can influence the evolution of the phenotypic differentiation at the middle term (6 additional days after exposure). As described in the methodology, the cells were exposed to RF-EMF at day 2 postplating. After the 21-hour exposure, the cells were grown for 6 additional days in the absence of the GSM stimulus. At the end of this period, the cells were immunostained with O1 for mature oligodendrocyte identification, GFAP for astrocytes and ß-tubulin III for neurons. All experiments and analysis were conducted following blind protocols. The data (N= 5 experimental replicates) indicate that the GSM-Basic signal promotes marked morphological changes in differentiating oligodendrocytes and astrocytes derived from NSC (Figure 98).

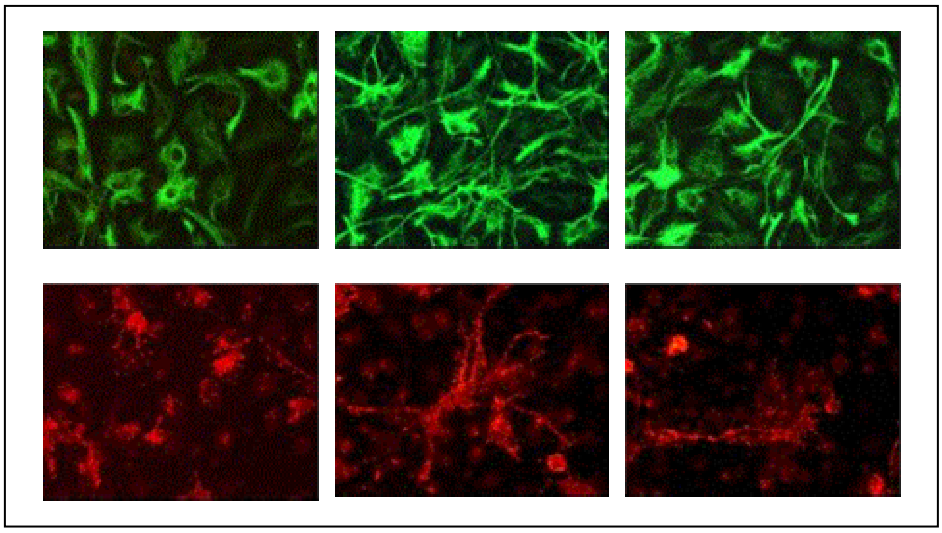

Figure 98. Photomicrographs of neural stem cells progeny. Astrocytes labelled with GFAP (green) and oligodendrocytes labelled with O1 (red) immunostaining: A, Control; B, and C, exposed to the GSM-Basic signal. The exposure increases cell extension in astrocytes and oligodendrocytes.

Similar experiments have been carried out to evaluate the phenotypic differentiation of NB69 cells treated with the above GSM-signal and exposure conditions, in the presence or absence of RA. As described in the methodology, the cells were exposed to the field at day 3 postplating, during a 24-hour period, and then grown for 2 additional days in the absence of GSM exposure. After that, the cells were analysed for expression of mature neuronal cell marker ß-tubulin III, and for tyrosine hydroxylase (TH) marker. Exogenous, basic fibroblast growth factor was used as a positive control. The data show that the neuronal outgrowth of NB69 cells (Figure 99) and the percent of TH+ cells seem not to be altered by the exposure to the GSM-Basic signal. Only the treatment with bFGF promoted the neuronal microtubules network in these cells.

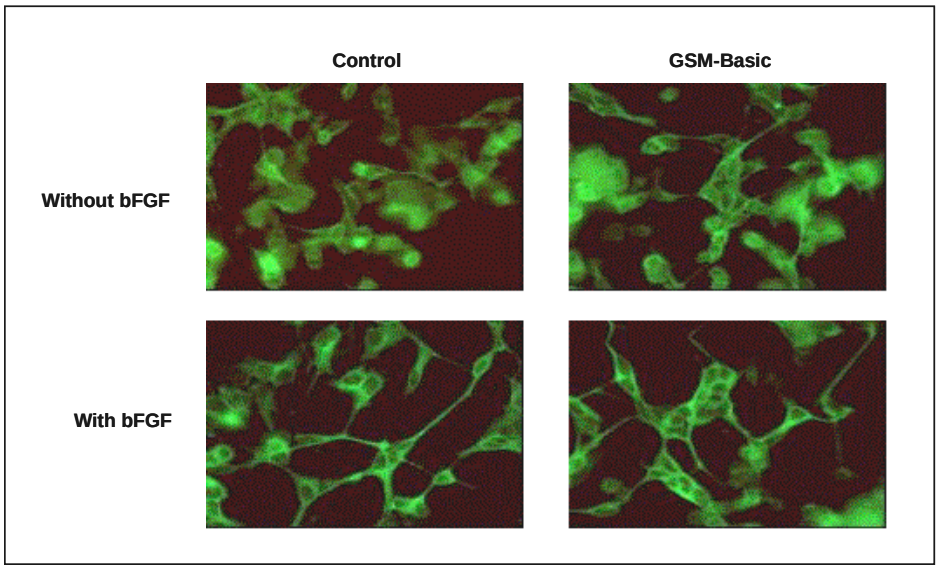

Figure 99. Photomicrographs of NB69 cells analysed 3 days after the exposure and/or incubation in the presence or absence of bFGF. Cells stained with anti-beta-tubulin antibody. The neuronal outgrowth of NB69 cells seems not to be altered by the exposure to the GSM-Basic signal. However, the treatment with bFGF promotes the neuronal microtubules network in these cells.

3.2.2.2 Human lymphocytes and thymocytes (Participant 8)

RF-EMF did not affect proliferation, cell cycle and activation of human lymphocytes.

The experiments with RF-EMF were performed at SAR 1,4-2,0 W/kg using different RF modulations or time exposure. Studies on cell proliferation were performed discriminating CD4+CD28+/- and CD8+CD28+/-lymphocytes subpopulation. Cells were exposed to Talk modulated RF-EMF (2 W/kg) and two intermittent types of exposure were applied: 1) 10 min on/20 min off for 44 hours; 2) 2 hours on/22 hours off for 72 hours. We performed experiments with cells from 6 donors using the former approach, from 11 donors using the latter approach. All cells were acquired and analysed after 72 hours and 120 hours of culture. A small increase (3%) of proliferating CD8+CD28+ T lymphocytes was observed in exposed cells both at 72 hours and 120 hours of culture. Since the differences observed are similar to the calculated standard error, we considered this effects not relevant. In Tables 22 and 23 data related to proliferating and not proliferating cells subsets after 72 hours and 120 hours of culture, respectively, are reported.

Table 22. T lymphocytes subsets exposed to talk modulated RF-EMF 2 hours on/22hours off for 72 hours. Data are reported as mean (% ± s.e.) of all experiments performed

Lymphocyte subsets	Sham % ± se	RF % ± se	p
P CD4+CD28+	30.7 ± 2	28.2 ± 2	ns
P CD4+CD28-	0.9 ± 0.4	0.7 ± 0.3	ns
NP CD4+CD28+	13.0 ± 2	12.4 ± 2	ns
NP CD4+CD28-	1.8 ± 0.9	0.8 ± 0.3	ns
P CD8+CD28+	19 ± 2	21 ± 2	0.042
P CD8+CD28-	7.9 ± 3	7.7 ± 3	ns
NP CD8+CD28+	8.0 ± 1	9.3 ±1	ns
NP CD8+CD28-	1.1 ± 0.2	1.0 ± 0.4	ns

P = proliferating; NP = non proliferating; ns = not significant

Table 23. T lymphocytes subsets exposed to Talk modulated RF-EMF 2 hours on/22 hours off for 72 hours and analysed at 120 hours of culture. Data are reported as mean (% ± s.e.) of all experiments performed

Lymphocyte subsets	Sham % ± se	RF % ± se	p
P CD4+CD28+	61.0 ± 2	62.1 ± 2	ns
P CD4+CD28-	0.60 ± 0.07	0.80 ± 0.11	ns
NP CD4+CD28+	9.3 ± 0.2	8.7 ± 0.2	ns
NP CD4+CD28-	1.4 ± 0.1	1.72 ± 0.11	ns
P CD8+CD28+	32 ± 4	35 ± 4	0.048
P CD8+CD28-	5.4 ± 3	4.3 ± 2	ns
NP CD8+CD28+	5.4 ± 0.7	4.7 ± 0.9	ns
NP CD8+CD28-	0.9 ± 0.3	0.8 ± 0.3	ns

P = proliferating; NP = non proliferating; ns = not significant

Cell cycle analysis was performed in PBMCs exposed at three RF-EMF modulations and in the case of Talk signal also PBMCs from old donors were analysed. In all the cases observed no differences were found between exposure and control cells. Some slight differences (1-2%, sometimes increase and sometimes decrease) were observed when analysis of activation markers on CD4+ and CD8+ T lymphocytes were performed on both young and old donors. Since the effects were really small, we

performed from 5 up to 8 replications of T lymphocyte phenotypical analysis, using cells from the same donor.

Results obtained from replications did not confirm the data previously obtained, thus suggesting that such small significant effects must be considered at the noise level of the statistical analysis. Moreover, we performed a more sophisticated analysis on fluorescence intensity in order to verify if the number of molecular markers could be changed in RF exposed cells in comparison with sham exposed cells. We found that in T helper lymphocytes from elderly, but not from young donors, and exposed to Talk modulated RF-EMF, CD95 molecules shifted significantly their fluorescence from bright to dim, as reported in Figure 96. This effect means that in the exposed cells the number of molecular markers on membrane surface was slightly decreased (around 9%).

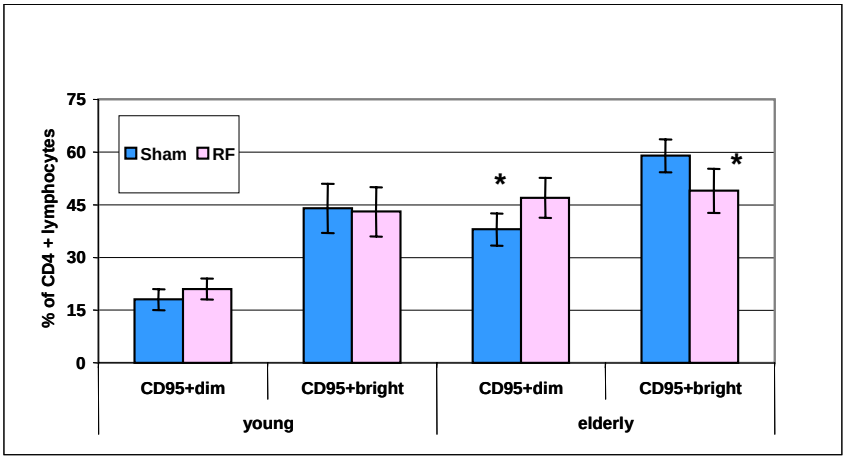

Figure 100. Analysis of fluorescence brightness of proliferating CD4+CD95+ from 10 young and 8 elderly donors, after sham and talk modulated RF-EMF exposure (2W/kg). * = $p < 0.05$. Data are represented as mean ± s.e.

RF-EMF (DTX) may inhibit the production of IL-1beta in human lymphocytes, but did not affect the production of IL 6.

The results obtained showed no significant differences between cells sham-exposed or differently modulated RF-EMF exposed, except in the case of IL-1beta. Indeed, we found a decrease of IL-1beta production (around 13%) in CD3-stimulated PBMCs exposed to DTX modulated RF-EMF in comparison with sham-exposed cells. As demonstrated in Figure 101, the decrease observed was statistically significant on 6 experiments performed. This result was not found when PBMCs were exposed to Talk modulated RF-EMF or using the other stimulus.

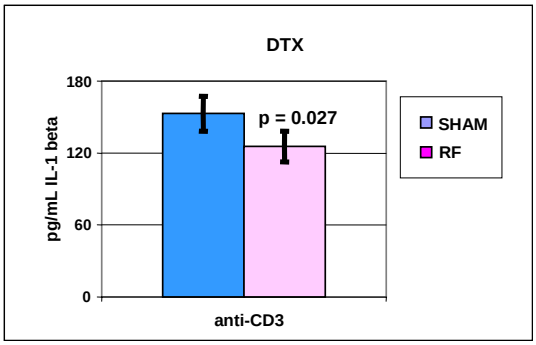

Figure 101. Effect of DTX modulated RF (SAR 1.4 W/kg) on IL-1 beta production in CD3-stimulated PBMCs.

RF-EMF did not affect thymocyte differentiation.

HTOC were performed in order to assess *in vitro* phenotypical differentiation and apoptotic phenomena due to negative selection, which usually occurs in vivo inside the thymus. Thus, different subsets of thymocytes were analysed such as CD71+CD4-CD8-, CD3-/+CD4+CD8+, abTCR-/+CD4+CD8+, gdTCR-/+CD4-CD8-, CD3+CD4+CD8-, CD3+CD4CD8+, abTCR+CD4+CD8-, abTCR+ CD4-CD8+ cells. Each population represents a different phase of development, which was monitored before the exposure and at the end of culture, in presence or absence of RF-EMF. Thymocyte apoptosis was assessed with two different methods, in the same conditions, but the data obtained from 6 human thymus on thymocyte differentiation and apoptosis did not suggest positive results on both the endpoints. Actually, a small increase (4%) of double positive thymocytes (CD4+CD8+) was found in RF-EMF-exposed cultures in comparison with sham-exposed tissue fragments. Also in this case the effect is of the order of the standard error thus we consider these results irrelevant.

3.2.2.3 Human promyelocytic cell line HL-60 (Participant 2)

RF-EMF did not affect the cell cycle of HL-60 cells as shown by flow cytometric analysis.

See 3.2.1.1

RF-EMF did not affect the growth behaviour of HL-60 cells with respect to growth velocity and DNA synthesis.

See 3.2.1.1

Indicators for HL-60 cell growth were the proliferation rate, reflected by the cellular doubling time, and the synthesis of the enzyme thymidine kinase (TK). The enzyme thymidine kinase plays an important role in DNA synthesis. It has been well established that the cellular activity of thymidine kinase is correlated with the growth rate of cells (Johnson et al. 1982). Its relation to the cell cycle has been shown in previous studies (Chang 1990; Kit 1976; Pelka-Fleischer et al. 1987; Piper et al. 1980).

Cellular doubling time

Cellular growth behaviour with respect to growth velocity was assessed by determination of the cellular doubling time. Cellular doubling time of HL-60 cells following RF-field exposure (1800 MHz, 24h) for different SARs (continuous wave, 0.2, 1.0, 1.3, 1.6, 2.0 and 3.0 W/kg) and different signal modulations (continuous wave, C.W., 5 min on/10 min off, GSM-217Hz, GSM-Talk) was compared to controls and sham-exposure. No alteration of the cellular doubling time was observed for any of the different SARs or signal modulations tested (Figures 101, 102). The value of the doubling time for the control was 20.8 ± 2.8 h. Calculation of the average HL-60 doubling time after exposure to all SAR levels tested revealed a value of 22.0 ± 3.8 h (n=21) versus that for all sham-exposed cells: 21.6 ± 4.5 hours (n=21). On the other hand the calculation of the average HL-60 doubling time after exposure to all signal modulations tested at SAR = 1.3 W/kg revealed a value of 21.3 ± 4.2 h (n=14) versus that for all sham-exposed cells: 21.7 ± 4.5 h (n=14).